Modelling method to evaluate the thermo-regulating behaviour of micro-encapsulated PCMs coated fabric

SIDDIQUI MUHAMMAD OWAIS RAZA
BALOCH ZEHRA
NOORANI MUHAMMAD USAMA

IQBAL KASHIF
ZUBAIR MUHAMMAD
SUN DANMEI

ABSTRACT – REZUMAT

Modelling method to evaluate the thermo-regulating behaviour of micro-encapsulated PCMs coated fabric

Micro-encapsulated Phase Change Materials (MicroPCMs) have been widely used to enhance the thermal comfort of the clothing; they can be applied to fabric by various techniques including the coating process. Phase change material (PCM) has a unique property of latent heat that can absorb and release energy over a constant temperature range which enhances the thermal comfort of the clothing microenvironment. PCM textile structures are used in making smart textiles and thermo-regulated garments. An advanced modelling technique was successfully established to develop a finite element model of woven fabrics coated by MicroPCMs, the developed model was used to simulate and predict the effective thermal conductivity and thermal resistance.

Keywords: MicroPCMs, thermo-regulating, latent heat, FEM

Metodă de modelare pentru evaluarea comportamentului de termoreglare a țesăturii acoperite cu materialele cu schimbare de fază micro-încapsulate

Materialele cu schimbare de fază micro-încapsulate (MicroPCM) au fost utilizate pe scară largă pentru a spori confortul termic al îmbrăcămintei; pot fi aplicate pe materialul textil prin diferite tehnici, inclusiv prin procesul de acoperire. Materialul cu schimbare de fază (PCM) are o proprietate unică de căldură latentă care poate absorbi și elibera energie într-un interval constant de temperatură, ceea ce sporește confortul termic al micromediului îmbrăcămintei. Structurile textile PCM sunt folosite la realizarea de textile inteligente și articole de îmbrăcăminte cu termoreglare. O tehnică avansată de modelare a fost stabilă cu succes pentru a dezvolta un model cu elemente finite al țesăturilor acoperite cu MicroPCM, modelul dezvoltat a fost folosit pentru a simula și a preconiza conductivitatea termică efectivă și rezistența termică.

Cuvinte-cheie: MicroPCM, termoreglare, căldură latentă, FEM

INTRODUCTION

The demands for functional clothing increased with the growth of textile technology. The production of garments with comfort properties is worth considering [1]. One of the categories of clothing comfort is thermal comfort which mainly depends on the ability of the fabric to transmit heat and moisture from the body to the surroundings [2]. Phase change technology has been widely used to protect the thermal balance of the body and keep constant body temperature even if the physical activity or outer environmental condition changes. Textile products having thermal storage and regulation property can be manufactured by incorporation of phase change material to textiles [3].

In the early 1980s, thermo-regulating textile clothing was developed under the National Aeronautics and Space Administration (NASA) research program by using PCM. The effect of PCMs on the heat transfer behaviour of textiles has been investigated by many researchers [1–13]. Lamb and Duffy-Morris [4] studied the cooling rate, the permeability of fabrics and factors which influence the effectiveness of fabrics containing phase change materials in improving insulation. They designed a rotating arm device through which heat loss through fabrics with and without PCM when a controlled amount of air is passed through it was monitored. It was concluded that a combination of PCM treated cotton fabric inside with polyester felts was used and the heat loss was nearly zero for some time.

Pause [5] studied the effect of the application of PCM for the development of heat and cold insulating membrane structures. The tests were carried out where basic thermal resistance and dynamic thermal resistance were measured separately, and the results were compared for the original membrane material, membrane material coated with foam and their different concentration. The test results showed that the dynamic thermal insulation is increased as the quantity of Microencapsulated Phase Change Materials (MicroPCMs) increased.

Kim and Cho [6] coated a fabric with MicroPCMs of octadecane, the effect of curing temperature and time on heat storage/release, durability and temperature sensing properties were studied and comparisons

were made between the treated and untreated fabrics. They concluded that as the concentration of MicroPCMs increased thermal storage or release also increased. Moreover, the treated fabric would be able to provide a better cooling effect than the untreated.

Ghali et al. [7] studied the effect of PCMs on body heat loss when environment condition changes from hot to cold in a numerical three-node ventilation model. When a PCM is incorporated in the fabric the sensible heat loss from the skin decreases. They concluded that the heating time depends on the amount of PCMs encapsulated in the fabric, the ventilation frequency, and the outdoor environmental temperature.

Li and Zhu [2] developed a mathematical model that takes account of the simultaneous heat and moisture transfer in porous textiles with PCM). The coupled heat and moisture transfer processes in porous textiles were simulated with different amounts of PCM using the finite volume method. For mathematical formulation, the mass balance of the vapour and liquid moisture, and the energy balance were considered. By specifying the initial and the boundary conditions, they calculated the distributions of temperature, moisture concentration, and water content in the fibres for different amounts of PCM in porous textiles. They computed temperature changes at the fabric surface during heat and moisture transfer into porous textiles based on theoretical predictions.

Ying et al. [8] conducted a series of experiments to establish a method to specify the effects of micro-PCM incorporated fabrics. The computed temperature changes at fabric surfaces were compared with experimental measurements and consistency between the experimental observations and the computational results were found. The analysis illustrates the complex multiple coupling effects among different moisture transport processes, as well as the heat transfer process, and there is reasonable agreement between the predictions and the measurements.

Li and Li [9] developed a mathematical model to predict the heat and moisture transfer behaviour of a permeable membrane incorporated with PCMs. The fibre hygroscopicity effect on heat and moisture transfer was investigated and the heat absorbing and releasing rate, distributions of temperature, moisture concentration and water content in the fibres with MicroPCMs were analysed. The ability of a PCMs fabric to react to the moisture content of the air by absorbing or releasing water vapour was investigated. It was found that the changes in environmental effects on fabric hygroscopicity due to the PCMs microcapsules took more time for temperature variation in the fabric.

Bendkowska and Wrzosek [10] studied the thermo-regulating properties of MicroPCMs coated nonwoven fabrics. Microcapsules of n-Octadecane and n-eicosane were applied using pad-mangle and screen-printing technique. Thermal properties such as thermal storage and thermal resistance were determined under steady-state condition whereas thermal performance was studied under transient condition. Results showed that microcapsules presented in the interstitial spaces between the fibres whereas in the case of printed technique MicroPCMs formed a layer on one side of the nonwovens. All nonwovens with MicroPCMs exhibited a lower TRF value in the whole range of frequencies of heat flux changes compared to the reference nonwoven. This is due to the increase in nonwoven thermal capacitance resulting from the incorporation of MicroPCMs. There is a reduction in the thermal resistance of non-ovens resulting from the incorporation of MicroPCMs into the nonwoven structure. In the case of nonwoven without PCMs, there is a greater amount of trapped air, which has a very low thermal conductivity and is, therefore, a good insulator. Due to applying microcapsules to the nonwoven structure, the proportion of air is reduced, leading to the lowering of thermal resistance under steady-state conditions. The second important factor is the way of MicroPCMs distribution in the fibrous structure, the position of the MicroPCMs layer was proved to be of great importance for the thermoregulating properties of the printed nonwoven samples. In general, the heat control effect of a garment treated with MicroPCMs is determined by the quantity and the storage capacity of the MicroPCMs.

Yoo et al. [12] investigated the effect of the number and position of the PCMs treated fabric in the four-layer garments by using the Human Clothing-Environment (HCE) simulator. Garments consisted of different layer of fabrics. The temperature differences between garments with different layers of PCMs treated fabric were examined. It was found that with PCMs in the inner layer, which is in contact with skin, is more suitable for the thermal regulating effect. Alay et al. [1] investigated the thermal comfort properties of the fabrics treated with MicroPCMs under steady-state condition. MicroPCMs were applied to cotton and cotton/polyester blend fabrics. The thermal conductivity of treated fabrics decreases as compared to the untreated fabric.

In this work, a Novel Modelling technique is developed to evaluate the thermo-regulating behaviour of MicroPCMs coated fabrics via Finite Element Analysis (FEA) using commercial software Abaqus/CAE. Unit cell models of MicroPCMs coated woven fabric has been created, a novel modelling method has been established to simulate and predict the effective thermal conductivity and thermal resistance of MicroPCMs coated fabrics in a single unit cell model. The predicted effective thermal conductivity and thermal resistance of MicroPCMs coated fabrics have been compared with the previously developed method [13] to validate the model.

MATERIALS

A Nomex® III plain-woven fabric was coated at both sides with MicroPCMs, the coating mixture was applied through the screen coating technique, then dried and cured after the coating process. The fabric specifications are shown in table 1. The physical properties of Microcapsules are shown in table 2.

FABRIC SPECIFICATIONS	
Specifications	Nomex® III Fabric
Areal density (g/m^2)	170
Warp/Weft sett (per inch)	59/59
Warp/Weft yarn linear density (Tex)	33.3/33.3

PHYSICAL PROPERTIES OF MICRO PCMS	
Capsule composition	85–90 wt.% PCM
Core material	n-octadecane
Shell material	Melamine formaldehyde
Particle size (µm)	17–20
Melting point (ºC)	28.2
Heat of fusion (J/g)	180–195
Specific gravity	0.9

The materials used for the core and shell of the Microcapsules are n-octadecane and melamine formaldehyde, respectively.

METHODOLOGY

A unit cell model of MicroPCMs coated composite fabric has been developed to evaluate the effective thermal conductivity by finite element method. The developed unit cell model of coated composite fabric consists of four sections i.e., the woven fabric section, MicroPCMs section which is submerged inside the binder section and the air-fluid matrix section. Scanning Electron Microscope images were inspected, for the establishment of geometrical unit cell models of MicroPCMs coated composite fabrics. It was revealed that the capsules were only present at the surface of the fabric. The steps to develop a finite element model follow: (i) develop a model of MicroPCMs then analyse it; (ii) develop a unit cell model of uncoated fabric; (iii) develop a unit cell model of coated fabric; (iv) the above models were merged to form a final model which was then analysed to compute the effective thermal conductivity of the coated fabric. The technique used to develop a finite element unit cell model of coated composite fabric is shown in figure 1. While analysis of model certain presumptions has been taken into consideration: (i) heat transfer through convection and radiation phenomena is neglected; (ii) no variation in the density of the PCM with temperature change; (iii) no internal heat generation in the model. For analysis, the parts were meshed using tetrahedral shaped four-node elements.

The seed size of the elements was optimized. The temperature specified boundary conditions were applied. The model was simulated under transient condition. It is visible from temperature contours that MicroPCMs act as conductive material and heat transfer takes place from shell to core as shown in figure 2. Latent heat of fusion was calculated using
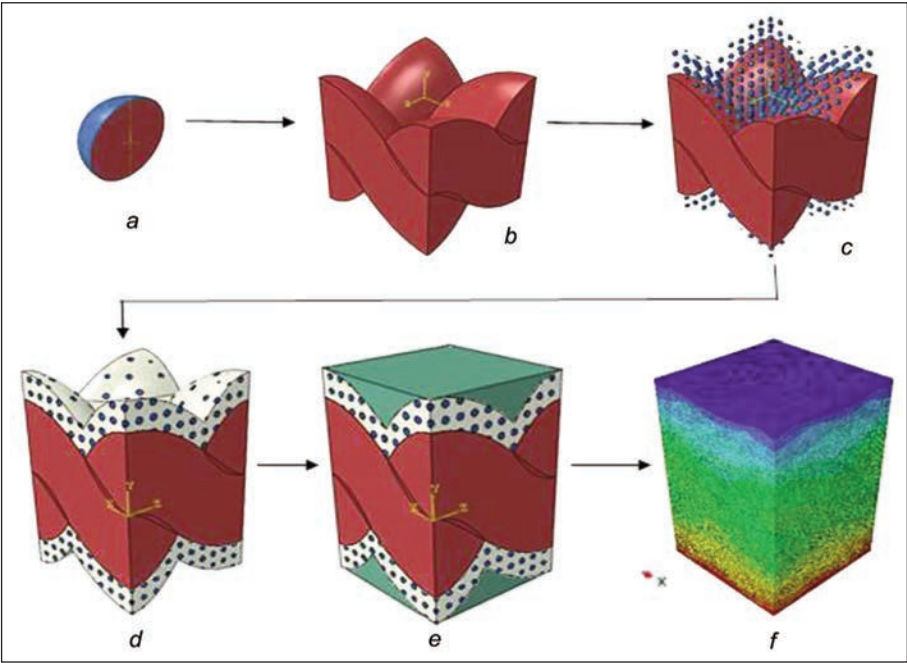
Fig. 1. Stages of modelling: *a* – model of Micro-PCMs; *b* – unit cell model of woven fabric only; *c* – unit cell model of woven fabric with Micro-PCMs; *d* – unit cell model of woven fabric with Micro-PCMs and binder; *e* – unit cell model of woven fabric with Micro-PCMs, binder and air; *f* – heat flow through the unit cell of MicroPCMs coated Nomex® III fabric
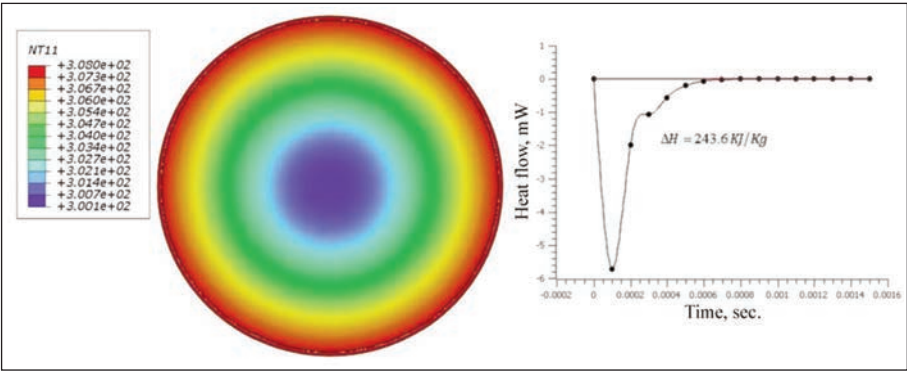
Fig. 2. Temperature contour of MicroPCMs

Table 3

THERMO-PHYSICAL PROPERTIES OF MICRO-PCMS			
Property	n-Octadecane [2]	Melamine formaldehyde [14]	Acrylic binder
Density (kg/m^3)	779	1500	1080
Specific heat (kJ/kg·K)	1.9 (solid) 2.2 (liquid)	1.2	2.4
Thermal conductivity (W/m·K)	0.4 (solid) 0.3 (liquid)	0.5	0.155 [15]
Latent heat of fusion (kJ/kg)	238.76	-	-
Melting point (°C)	28.2	-	-

post-processing data from the model and compared with the latent heat value of fusion provided by the manufacturer.

Model of MicroPCMs

In the FE model, the shell (formaldehyde) and core (octadecane) of MicroPCMs were considered as two separate parts. Both parts were assembled using surface to surface contact interaction property. Material properties were assigned to both parts separately. Thermo-physical properties of MicroPCMs shown in table 3, were used as material properties for finite element analysis.

Model of uncoated and coated fabric

The unit cell model of plain-woven fabrics was produced by taking the actual geometric parameters of fabric which are listed in table 4. The following parameters of the fabrics were needed for the geometric model of the fabric: warp/weft yarn spacing (W_{as}/W_{fs}), fabric thickness (t) and width of the warp/weft yarn (W_{ad}/W_{fd}), and yarn cross-sectional shape. Yarn spacing was determined using warp and weft set. The thickness of the fabric was determined through the FAST-1 compression meter. The appropriate force of 2 gf/cm^2 or 0.196 KPa was applied on the surface area of 10 cm^2. SEM was used to obtain the yarn cross-sectional shape.

Table 4

MEASURED GEOMETRIC DIMENSIONS OF UNIT CELL MODELS	
Dimensions	Nomex® III Fabric
(Wa$_s$/Wf$_s$) (mm)	0.431/0.431
(Wa$_d$/Wf$_d$) (mm)	0.337/0.337
t (mm)	0.5
Total length of the unit cell (mm)	0.862
Total width of the unit cell (mm)	0.862
Unit cell volume (mm^3)	0.3715

After the generation of the uncoated fabric model being a base layer, a layer of MicroPCMs was created on top of the fabric which was submerged inside the layer of binder as a coating layer of the fabric. The coating layer contains 5% MicroPCMs which is homogeneously distributed among the binder. A layer of air is also created above the layer of coating. All the layers were then merged together forming a unit cell model of MicroPCMs coated composite fabric. To mesh the unit cell model of MicroPCMs coated composite fabric 4-node linear tetrahedral element (DC3D4) has been used. It is the most suitable mesh element enabling completely mesh the unit cell model. It was examined that further refinement cannot change the results of mesh density.

Analysis of the model

It is important to consider the nature of the material for thermal analysis via FEA. Textile fibres are special orthotropic material. To find out the effective thermal conductivity of yarns thermal properties of fibres used are listed in table 5.

Table 5

FIBRE PROPERTIES	
Specifications	Nomex® III Fibre [16–20]
ρ_f (kg/m^3)	1380
K_{fa} (W/m·K)	1.3
K_{ft} (W/m·K)	0.13
C_{pf} (J/kg·K)	1200

The yarn is orthotropic in nature due to this reason of orthotropic nature of the yarn, the thermal conductivity of yarn in both axial (K_{ya}) and transverse direction (K_{yt}) are to be calculated. The thermal conductivity can be determined through equation 1 and equation 2 are listed in table 6.

$$K_{ya} = K_{fa}V_{fy} + K_{air}(1 - V_{fy}) \quad (1)$$

$$K_{yt} = \frac{K_{ft}K_{air}}{V_{fy}K_{air} + (1 - V_{fy})K_{ft}} \quad (2)$$

where K_{fa} is the thermal conductivity along the fibre axis, K_{ft} is the thermal conductivity perpendicular to the fibre's axis, K_{air} is the thermal conductivity of air and V_{fy} is the yarn fibre volume fraction.

To determine the effective thermal conductivity of the unit cell model of MicroPCMs coated composite fabric, two boundary conditions were specified: one was the temperature of the hot surface, and the other was

Table 6

THERMAL CONDUCTIVITY OF YARN IN THE WOVEN FABRICS				
Yarn	**Thermal conductivity in the axial direction, K_{ya} (W/m·K)**		**Yarn thermal conductivity in the transverse direction, K_{yt} (W/m·K)**	
	Warp	Weft	Warp	Weft
Nomex® III Fibre	0.5356	0.5356	0.0382	0.0382

the temperature of cold surface assuming all other surfaces of the unit cell as insulated, shown in figure 3. This temperature difference causes heat flow through the unit cell as shown in figure 4.
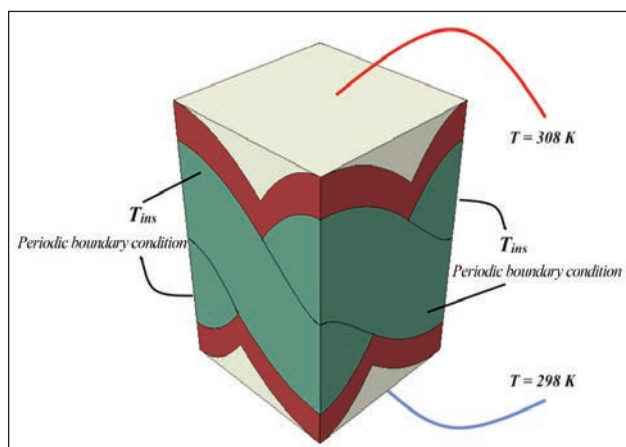
Fig. 3. Boundary conditions

Equations 3 and 4 are used to calculate the effective thermal conductivity (K_z) and thermal resistance (R_z) of the composite fabric model.

$$K_z = Q_z \frac{t}{\Delta T_z} \quad (3)$$

$$R_z = \frac{t}{K_z} \quad (4)$$

where Q_z is the overall heat flux, is the thickness of the unit cell and is the temperature in the z-direction. To obtain K_z, Q_z needs to be calculated first by the following mean. Define the surface and then add the following lines:
*Section Print, Name = Section_name, Surface = Surface_name, freq = 1
SOH, SOAREA

$$Q_z = \frac{SOH}{SOAREA} \quad (5)$$

where SOH and SOAREA are built-in keywords in Abaqus/CAE that provide the value of the total section heat flux and the total surface area of the unit cell respectively. These values are then used in equation 5, equation 3 and equation 4 respectively.

After performing all the above calculations, the predicted effective thermal conductivity of the unit cell model of MicroPCMs coated composite fabric of Nomex® III is 0.08154 W/m·K.

Validation of model

The model was validated by using a two-step model which has already been validated by experimental results by Siddiqui and Sun [13]. Two finite element models were developed to determine the effective thermal conductivity MicroPCMs coated composite fabric. A unit cell model of coating that is MicroPCMs and binder was developed and analysed. The results from the coating model were used as input property for the second model which is a unit cell model of MicroPCMs coated composite fabric as shown in figure 5. The effective thermal conductivity of MicroPCMs coated Nomex® III fabric from the two-step and one-step model is found to be 0.08278 W/m·K. and 0.08154 W/m·K, respectively. The mean absolute error between the two models is 1.498%.

Furthermore, the thermo-regulating behaviour of PCMs coated composite fabric is analysed by comparing the heat flow through the thickness of the coated fabric as shown in figure 6, where transient analysis was used by applying temperature specified boundary conditions. Fabric without MicroPCMs reaches the highest heat flow Q_{max} very quickly, whilst the MicroPCMs coated composite fabric reaches the same level of heat flow but with much delayed time. With the increase of MicroPCMs applied, the time for the coated fabric to reach the highest level of heat flow increases. The increased PCMs in a fabric would improve the thermal comfortability of wear, but it would reduce flexibility. Therefore, a compromise between wear comfortability and flexibility needs to be considered, so as the amount of PCMs to be applied on fabric. This delay in heat flow is contributed by the phase change effect and latent heat contained in PCM, and the effect prolongs as the amount of MicroPCMs contained in the fabric increases. Such a thermal regulating zone created by MicroPCMs means that the temperature is arrested for some time because of the phase change effect. It is clearly evident from the enlarged view in figure 6 that the fabric containing 5% of MicroPCMs only reaches 60% of the maximum heat flow whilst the fabric without PCM reaches the maximum heat flow at the same time interval.

These parameters were also reported useful to determine the thermal protective efficiency of fabrics containing PCM elements according to Hes and Lu [21]. They studied the effect of heat flow through fabric with and without PCM by using PC Tester, it was found that the heat flow through PCM containing fabric was much lower, only half of the maximum heat
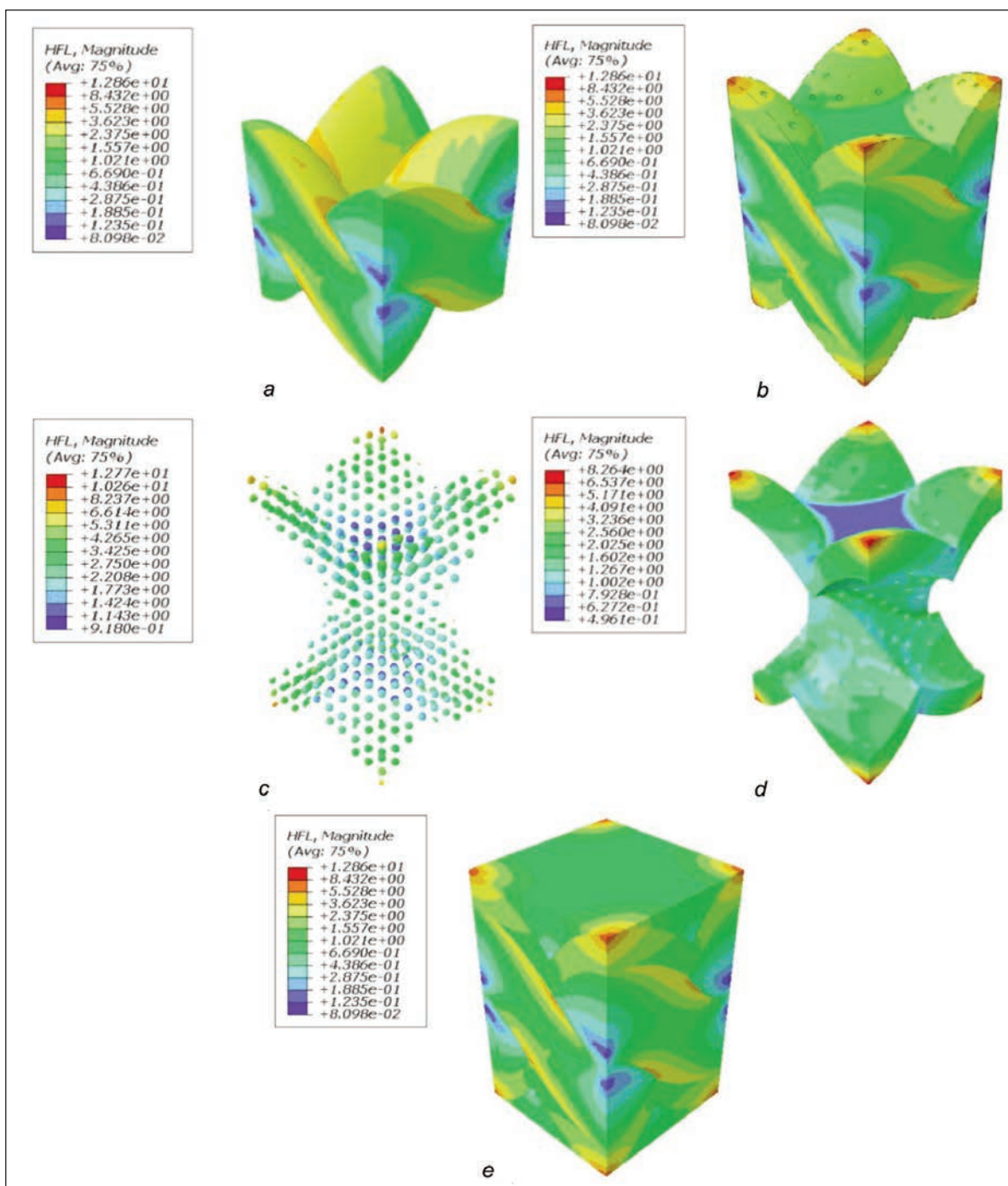
Fig. 4. Heat flux contours: *a* – unit cell model of woven fabric only; *b* – unit cell model of woven fabric with binder; *c* – unit cell model of Micro PCMs; *d* – unit cell model of binder only; *e* – heat flow through the unit cell of MicroPCMs coated Nomex® III fabric

flow rate through the fabric without PCM. In other words, PCM containing fabric had double thermal protection than the one without. As discussed above the highest thermal protection achieved is 1.67 times as shown in figure 6. This is caused by the much slower heat flow in the fabric containing PCM, attributed to the effect of heat accumulation needed for PCM to accomplish phase change. This thermal protection can be increased (even many times) depending on the amount of PCM to be applied onto fabric for a specified end-use application.

CONCLUSIONS

In this research, a modelling technique has been established to evaluate the thermo-regulating behaviour of MicroPCMs coated Nomex® III woven fabric via finite element analysis. The orthotropic nature of the fibre, fibre orientation, accurate yarn cross-sectional shape, and fibre volume fraction of the fabric was considered for thermal analysis in order for the developed models to provide more realistic thermal properties of the MicroPCMs coated fabrics. The small mean absolute error (1.498%) shows the applicability of the developed technique for the
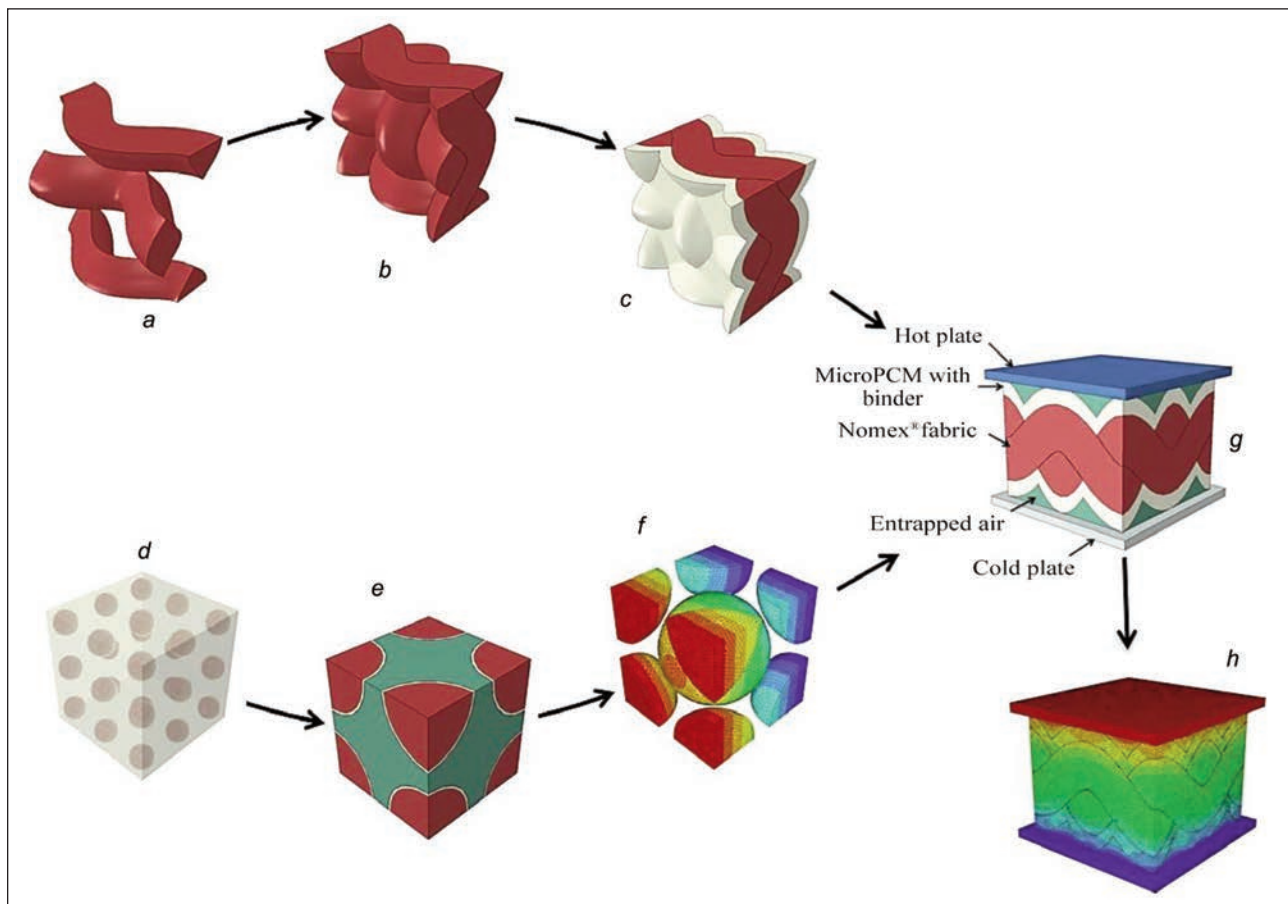
Fig. 5. Stages of modelling: *a* – model of yarn; *b* – unit cell model of woven fabric only; *c* – unit cell model of woven fabric with coated material; *d* – binder and MicroPCMs composite; *e* – unit cell model of binder and Micro-PCMs composite; *f* – simulated temperature profile of fabric composite [13]
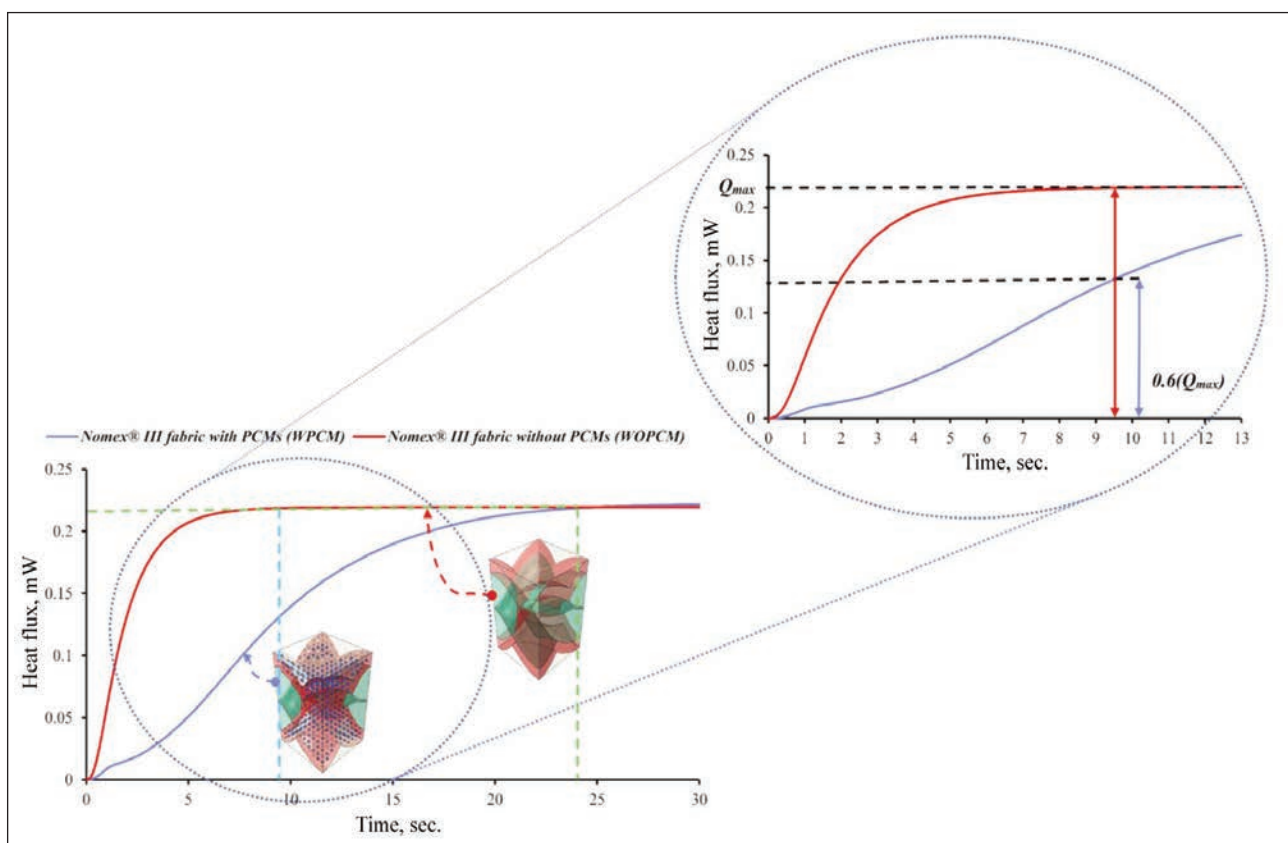
Fig. 6. Evaluation of PCM efficiency by comparing the heat flow behaviour through coated with and without MicroPCMs

prediction of thermal conductivity of MicroPCMs coated composite fabric. The model is capable of predicting the effect of thermo-regulating behaviour at various levels of MicroPCMs coating. The validated model is used to evaluate the thermo-regulating behaviour of coated with and without MicroPCMs which is useful in determining the amount of phase change materials to protect the wearer against extreme weather conditions. Furthermore, the established novel simulation method from this research can be used to determine the thermo-regulating behaviour of fabrics treated using different PCM in the core of Microcapsules by applying various temperature boundary conditions according to the applications and specific temperature environment.

ACKNOWLEDGEMENTS

REFERENCES

[1] Alay, S., Alkan, C., Göde, F., *Steady-state thermal comfort properties of fabrics incorporated with microencapsulated phase change materials,* In: Journal of the Textile Institute, 2012, 103, 7, 757–765, https://doi.org/10.1080/00405000.2011.606982

[2] Li, Y., Zhu, Q., *A model of heat and moisture transfer in porous textiles with phase change materials*, In: Textile Research Journal, 2004, *74*, 5, 447–457, https://doi.org/10.1177/004051750407400512

[3] Mondal, S., *Phase change materials for smart textiles–An overview*, In: Applied thermal engineering, 2008, 28, 11–12, 1536–1550, https://doi.org/10.1016/j.applthermaleng.2007.08.009

[4] Lamb, G.E., Duffy-Morris, K., *Heat loss through fabrics under ventilation with and without a phase transition additive*, In: Textile Research Journal, 1990, 60, 5, 261–265, https://doi.org/10.1177/004051759006000503

[5] Pause, B., *Development of heat and cold insulating membrane structures with phase change material,* In: Journal of Coated Fabrics, 1995, 25, 1, 59–68, https://doi.org/10.1177/152808379502500107

[6] Kim, J., Cho, G., *Thermal storage/release, durability, and temperature sensing properties of thermostatic fabrics treated with octadecane-containing microcapsules,* In: Textile Research Journal, 2002, 72, 12, 1093–1098, https://doi.org/10.1177/004051750207201209

[7] Ghali, K., Ghaddar, N., Harathani, J., Jones, B., *Experimental and numerical investigation of the effect of phase change materials on clothing during periodic ventilation,* In: Textile Research Journal, 2004, 74, 3, 205–214, https://doi.org/10.1177/004051750407400304

[8] Ying, B.A., Li, Y., Kwok, Y.L., Song, Q.W., *Mathematical modeling heat and moisture transfer in multi-layer phase change materials textile assemblies,* In: 2009 International Conference on Information Engineering and Computer Science IEEE, 2009, 1–4, https://doi.org/10.1109/ICIECS.2009.5364248

[9] Fengzhi, L., Yi, L., *A computational analysis for effects of fibre hygroscopicity on heat and moisture transfer in textiles with PCM microcapsules*, In: Modelling and Simulation in Materials Science and Engineering, 2007, 15, 3, 223, https://doi.org/10.1088/0965-0393/15/3/003

[10] Bendkowska, W., Wrzosek, H, *Experimental study of the thermoregulating properties of nonwovens treated with microencapsulated PCM*, In: Fibres & Textiles in Eastern Europe, 2009, 17, 5, 87–91

[11] Onofrei, E., Rocha, A.M., Catarino, A., *Textiles integrating PCMs–A review*, In: Buletinul Institutului Politehnic din Iasi, 2010, 60, 2, 99–107.

[12] Yoo, H., Lim, J., Kim, E, *Effects of the number and position of phase-change material-treated fabrics on the thermoregulating properties of phase-change material garments*, In: Textile Research Journal, 2013, 83, 7, 671–682, https://doi.org/10.1177/0040517512461700

[13] Siddiqui, M.O.R., Sun, D., *Computational analysis of effective thermal conductivity of microencapsulated phase change material coated composite fabrics*, In: *Journal of Composite Materials*, 2015, 49, 19, 2337–2348, https://doi.org/10.1177/0021998314545193

[14] Martienssen, W., Warlimont, H. (Eds.), *Springer handbook of condensed matter and materials data,* In: Springer Science & Business Media

[15] Efanova, V.V., Shut, N.I., *Thermal conductivity and kinetics of polymerization of an acrylate polymer coating*, In: Journal of Engineering Physics and Thermophysics, 1994, 66, 2, 164–171, https://doi.org/10.1007/BF00862717

[16] Futschik, M.W., Witte, L.C., *Effective thermal conductivity of fibrous materials,* In: Asme-Publications Htd, 1994, 271, 123–123

[17] Willians, S.D., Curry, D.M., *Thermal Protection Materials: Thermophysical Property Data*, In: NASA Reference Publication 1289, National Aeronautics and Space Administration, Scientific and Technical Information Program, 1993

[18] Futschik, M.W., *Analysis of effective thermal conductivity of fibrous materials,* In: MS thesis. Department of Mechanical Engineering, University of Houston, USA, 1993

[19] Torvi, D.A., *Effective thermal conductivity of fibrous materials,* In: PhD thesis. Department of Mechanical Engineering, University of Alberat, Canada, 1997

[20] Song, G., *Modeling thermal protection outfits for fire exposures,* In: PhD thesis. Fiber and Polymer Science, North Carolina State University, USA, 2002

[21] Hes, L., Lu, B.I., *Using a Thermal Simulator to Determine the Amount of Time that Humans are Thermally Protected by Fabrics Containing Phase Change Materials,* In: Research Journal of Textile and Apparel, 2004, 271, 2, 8, 51–56

Authors:

SIDDIQUI MUHAMMAD OWAIS RAZA[1], BALOCH ZEHRA[1], NOORANI MUHAMMAD USAMA[1], IQBAL KASHIF[2], ZUBAIR MUHAMMAD[3], SUN DANMEI[4]

[1]NED University of Engineering & Technology, Department of Textile Engineering, University Road, 75270, Karachi, Pakistan

[2]National Textile University, Department of Textile Engineering, Sheikhupura Road, 37610, Faisalabad, Pakistan

[3]North Carolina State University, Wilson College of Textiles, 1020 Main Campus Drive, Raleigh, 27606, NC, USA

[4]Heriot-Watt University, School of Textiles & Design, TD1 3HF, Galashiels, UK

Corresponding author:

SIDDIQUI MUHAMMAD OWAIS RAZA
e-mail: orazas@neduet.edu.pk

Selected barrier properties of some disposable protective coveralls in wet state

LUBOS HES
OLGA PARASKA

HASAN M. MALIK
NAVEED M. AKHTAR

ABSTRACT – REZUMAT

Selected barrier properties of some disposable protective coveralls in wet state

Certain types of disposable protective clothing should protect its user against liquids including water; therefore, the knowledge of their thermophysiological and barrier properties in wet state is important, as moisture mostly deteriorates comfort-related barrier properties of clothing, namely its water vapour permeability and thermal insulation. However, papers on comfort-related barrier properties are almost missing, as testing of these properties in wet state is very uneasy, due to long times of testing of these properties in standard commercial instruments. If the testing time exceeds 15 to 30 minutes, the sample gets dry and the testing is practically impossible. In the study, a special testing instrument is presented, which enables to measure water vapour permeability and thermal resistance of wetted fabrics within a few minutes, thus making possible the determination of these parameters with satisfactory precision. By means of this unique instrument and other instruments, water vapour permeability, air permeability and hydrostatic resistance of 6 wetted protective coveralls were determined. The main finding of the study is that due to the absorbed moisture, the effective relative water vapour permeability of the studied clothing gets substantively reduced, as well as their air permeability.

Keywords: protective clothing, water vapour, air permeability, hydrostatic resistance, wet state

Selecția proprietăților de barieră ale unor salopete de protecție de unică folosință în stare umedă

Anumite tipuri de echipamente de protecție de unică folosință ar trebui să-și protejeze utilizatorul împotriva lichidelor, inclusiv a apei; prin urmare, cunoașterea proprietăților lor termofiziologice și de barieră în stare umedă este importantă, deoarece umiditatea deteriorează în mare parte proprietățile de barieră legate de confort ale îmbrăcămintei, și anume permeabilitatea la vapori de apă și izolarea termică. Cu toate acestea, lucrările despre proprietățile de barieră legate de confort aproape lipsesc, deoarece testarea acestor proprietăți în stare umedă este foarte dificilă, din cauza timpilor lungi de testare a acestor proprietăți utilizând instrumentele standard comercializate. Dacă timpul de testare depășește 15 până la 30 de minute, proba se usucă și testarea este practic imposibilă. În studiu este prezentat un instrument special de testare, care permite măsurarea permeabilității la vapori de apă și a rezistenței termice a țesăturilor umede în câteva minute, făcând astfel posibilă determinarea acestor parametri cu o precizie satisfăcătoare. Cu ajutorul acestui instrument unic și a altor instrumente, au fost determinate permeabilitatea la vapori de apă, permeabilitatea la aer și rezistența hidrostatică a 6 salopete de protecție în stare umedă. Principala concluzie a studiului este că, datorită umidității absorbite, permeabilitatea relativă efectivă la vapori de apă a îmbrăcămintei studiate se reduce substanțial, precum și permeabilitatea lor la aer.

Cuvinte-cheie: îmbrăcăminte de protecție, vapori de apă, permeabilitate la aer, rezistență hidrostatică, stare umedă

INTRODUCTION

Disposable protective clothing is frequently used for protecting the wearer from sprayed pesticides, liquid dyestuffs, blood, detergents etc. and their specific barriers properties are naturally systematically tested and evaluated. Along with the mentioned barrier properties, there are also barrier properties influencing the thermophysiological comfort of protective clothing, such as its thermal resistance (insulation) and water vapour (WV) permeability [1]. Thermal insulation of clothing should protect its wearer from cold and clothing with high WV permeability should provide cooling of the wearer in a hot environment by intensive evaporation of his sweat. Thus, in recent decades, more attention is paid to the development

of protective clothing with optimum thermal resistance, with the highest possible WV permeability and also with certain hydrostatic resistance (resistance against penetration of pressured water) [2–6]. However, the published papers on the evaluation of thermo-physiological properties of protective clothing are focused on testing these properties in laboratory conditions, it means without additional wetting. However, protective clothing is worn not only in dry state, but very often in wet state, and the knowledge of transfer properties of the used fabrics in wet state is important, as higher moisture content mostly reduces water vapour permeability and thermal resistance of any fabrics [7, 8]. However, papers on thermal comfort properties of disposable protective clothing in wet state are very rare [7–9], as standard

instruments for the determination of water vapour permeability (gravimetric testers and common Skin models) do not allow to measure this parameter of fabrics in wet state, as the testing time mostly exceeds 30 minutes. Within this time, the wetted tested fabric gets almost dry and the WVP results are not reliable.

Therefore, the main and only objective of this study is to demonstrate the possibility of experimental determination of thermal comfort-related barrier properties of selected protective clothing in a wet state.

Protective coveralls analysed in the study are one-piece garments, commonly worn by mechanics, oil industry workers, painters, insulation installers, agricultural technicians and laboratory and cleanroom workers. Keeping in view the working environment, such personnel generally need disposable, one-time-use coveralls, which, along with the required barrier properties bringing specific protection, ensure certain thermophysiological comfort of their user in wet state also.

In this study, air permeability, water vapour permeability hydrostatic resistance and water repellence of six protective clothing were experimentally investigated, particularly in wet state. Dry measurements were executed for comparison only; therefore the results of measurements on dry fabrics are not discussed. All

the protective garments were made of very thin thermal bonded nonwovens, resulting in their very low thermal resistance. Therefore, the thermal properties of the overalls were not analysed in this study, even if the related special testing procedure is available [8]. It is important to note, that the objective of this study is not a systematic analysis of barrier properties of commercial protective overalls, it is just probably the first published analysis of the effect of the fabric moisture on the selected properties of this group of protective clothing. Therefore, the description of the structure and composition of the tested overalls is limited.

MATERIALS AND METHODS

In order to study the barrier properties of disposable protective clothing, six types of protective clothing were obtained from the local market for the study [10]. The basic specifications of these clothing are given in table 1, whereas their shapes are shown in figure 1. In order to avoid any commercial aspects of this study, the overalls are characterized by code names only.

The data of square mass in brackets present the limits of the 95% confidence interval. Mean pore diameter was determined optically. However, the determination

Table 1

SOME CHARACTERISTICS OF PROTECTIVE OVERALLS USED IN THE STUDY [10]					
Sample code: PP or PE + square mass (g/m^2)	Related standard	Composition	Structure	Mean pore diameter (µm)	Laminated foil
PP 65 (64.2 – 65.9)	EN 943-1	PP + PE	Nw* therm.bond	0.00	Yes
PE 44 (43.2 – 44.5)	EN 14605	Tyvek micro	Fs* therm.bond	7.49	Yes, porous
PE 43 (42.0 – 43.4)	EN 14605	Tyvek micro	Fs* therm.bond	322.00	Yes, porous
PP 41 (40.5 – 41.9)	EN 943-1	PP	Nw* therm.bond	71.94	No
PP 37 (36.6 – 37.7)	EN 14605	PP	Nw* therm.bond	100.80	No
PP 32 (31.3 – 32.3)	EN 13982-1	PP	Nw* therm.bond	163.50	No

Note: Nw means nonwovens, Fs is the nonwoven layer consisting of flash spun fibres, PP means polypropylene, PE is polyethene

PP 65   PE 41   PP 43   PE 44   PP 37, PP 32

Fig. 1. Various types of protective overalls [9]

of the geometrical porosity was not meaningless, due to the lamination and thermal bonding by a calender with a structured surface. It was found, that the sample PP 65 which is also laminated with the nonporous PE foil on the face side, exhibits the highest hydrostatic and wear resistance.

Measuring methods and instruments

Wetting of the samples

The samples were first kept at standard laboratory conditions for 24 hours and then weighted, in order to determine their reference square mass. Then, the samples were immersed for 6 hours in a large volume of distilled water with 1% of special detergent to get their full saturation by the liquid. Then, the samples were dried with towels in a stepwise manner on both sides and each sample was carefully weighed before each measurement. Due to the small size of the samples (12 cm × 12 cm), this method offers quite uniform moisture distribution, as verified at least 10 times [7]. Simulated sweat was not used in this case, as the salt causes corrosion of the hotplate in the used Skin model.

Air permeability

Air permeability can be characterized by the rate of volumetric airflow Q in m^3/s or derived units, passing perpendicularly through a known area A in m^2 under a prescribed air pressure drop Δp in Pa between two surfaces of material with thickness H in m. The airflow should respect the following Darcy law either at a fixed pressure drop or at a fixed airflow rate Q (K is the permeability and μ means the viscosity):

$$Q/A = K \cdot \Delta p \cdot \mu^{-1} \cdot H^{-1} \qquad (1)$$

Permeability of the studied samples was determined according to the ISO 9237 by means of the FX 3300 instrument (TEXTEST) at the pressure drop 200 Pa. Each sample was measured 10 times.

WV permeability

As regards the testing of WV permeability of wet clothing, these data are rare [6–9] as this unique parameter cannot be determined by any widely used gravimetric WV permeability testing method [11]. Standard Skin model-based WV permeability or resistance testers are too slow, to keep the sample wet during the testing. Therefore, there are no standards on WV permeability of clothing in wet state. Thus, the PERMETEST fast Skin model is probably the only tester, which enables reliable determination of WV permeability and thermal resistance [11, 12] of fabrics in wet state.

The PERMETEST commercial instrument used in this study enables the determination of relative *WVP* [%] and evaporation resistance *Ret* in m^2Pa/W of dry and wet fabrics within 3–5 minutes. The measuring head of this small Skin Model is covered by a semi-permeable foil, which avoids the liquid water transport from the measuring system into the sample. Cooling flow caused by water evaporation from the thin porous layer is recorded by a special sensing system and evaluated by a computer. The results are

treated statistically [11]. The PERMETEST testing does not require the preparation of samples of any special dimensions; the testing is non-destructive [4]. Following the ISO 11092 Standard, the measurement results can be expressed in terms of water vapour resistance R_{et} in m^2Pa/W, from the relationship:

$$R_{et} = C \cdot (p_{wsat} - p_{wo}) \cdot (q_o^{-1} - q_s^{-1}) \qquad (2)$$

where q_s and q_o mean non-calibrated heat loses of the wetted measuring head in a free state and covered by a sample. The values of water vapour partial pressures p_{wsat} and p_{wo} in Pa in this equation represent the water vapour saturate partial pressure valid for the temperature of the air in the measuring laboratory t_o (22–25°C), and the partial water vapour pressure in the laboratory air. The constant C will be determined by the already mentioned calibration procedure. Special hydrophobic polypropylene reference fabric for this purpose is delivered with the instrument.

Besides the water vapour resistance, also the relative water vapour permeability of the textile sample P_{wv} can be determined by the instrument, where $P_{wv} = 100\%$ presents the permeability of free surface. This practical parameter is given by equation 3.

$$P_{wv} (\%) = 100 \cdot q_s/q_o \qquad (3)$$

However, the determination of WV permeability of wet fabrics by Skin models is quite complicated. As it can be seen in figure 2, total cooling flow from the wet fabric consist of cooling flow $q_{fab,surf}$ which is given by the moisture evaporation from the surface of the wet fabric (dashed line) and cooling flow q_{skin} caused by the sweat evaporation from the skin. When the investigated wet fabric is placed directly on the porous measuring surface of the PERMETEST tester, then the Skin model sensing head records the sum of both cooling flows, q_{tot}. The new measurement principle involves another measuring step, depending on covering the wet porous surface of the tester with a thin non-permeable foil. In the following step, the wet sample is placed again in the instrument, but this time over this non- permeable foil, which stops moisture transfer from the skin. Thus, the instrument measures the cooling flow $q_{fab,surf}$ only, which is given by the moisture evaporation from the surface of the wet fabric. The difference between the q_{tot} and the $q_{fab,surf}$ then presents the effective
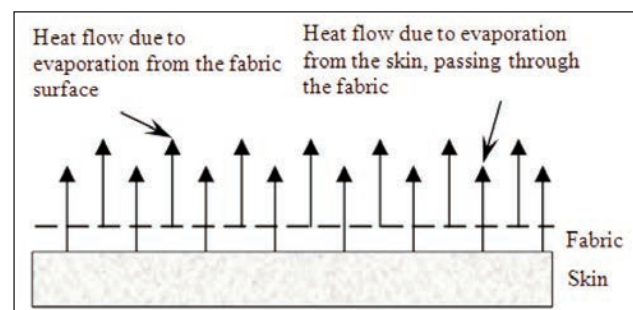
Fig. 2. Cooling effect from the wet fabric surface and passing from the skin through the wet fabric [6]

relative WV permeability of the proper samples – see the theory in [4]. The clothing wearer will feel the negative effect of the reduced WV permeability in cases when there is a gap between the wet outer fabric and the skin, as indicated in figure 2 [4, 12].

Hydrostatic resistance

Hydrostatic resistance, also called "water column", was determined by the SDL ATLAS tester "M018", according to the ISO 811 standard. The resistance to passage of water through the circular fabric specimen of area 100 cm^2 mounted on a hydrostatic head was measured. Water was forced to penetrate through the fabric due to steadily increasing pressure and reading was taken when water penetrated the fabric. The mean pressure of water was measured by the height of water column in centimetres.

EXPERIMENTAL RESULTS

Air permeability of the studied protective clothing

Examples of the structure of the studied samples are presented in figure 3. The dry state tests in figure 4 follow that clothing without the laminated foil and with lower areal density exhibits higher air permeability as compared to denser clothing, due to more open spaces per unit fabric area. In porous laminated fabrics PE44FP and PE43FP made of Tyvek the air permeability also increases with a decrease

in fabric density. However, laminated fabrics without open pores are practically impermeable for air.

Figure 5 indicates a weak inverse relationship between air permeability and moisture content of the fabrics. The variation coefficient of air permeability of dry samples extended from 8% to 10%. The PE65 and PE44 fabrics are practically impermeable for air. Preparing fabrics of the same moisture level is very time consuming, thus avoiding repeated measurements on wetted samples and creating the error bars.

Water vapour permeability of the studied protective clothing

Water permeability (WV) test results of fabrics in dry state as shown in figure 6 indicate that WV permeability increased with the decrease of the areal density of the fabrics. Similarly, the evaporation resistance steadily decreased with a decrease in the areal density of the tested fabrics. The samples without lamination foil expressed very little evaporation resistance as compared to samples with lamination.
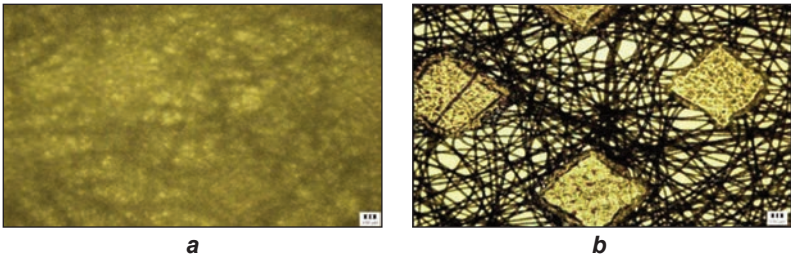
Fig. 3. Amplified picture of thermally bonded (calendered) samples: *a* – PP 65 (front); *b* – PP 37 (backside)
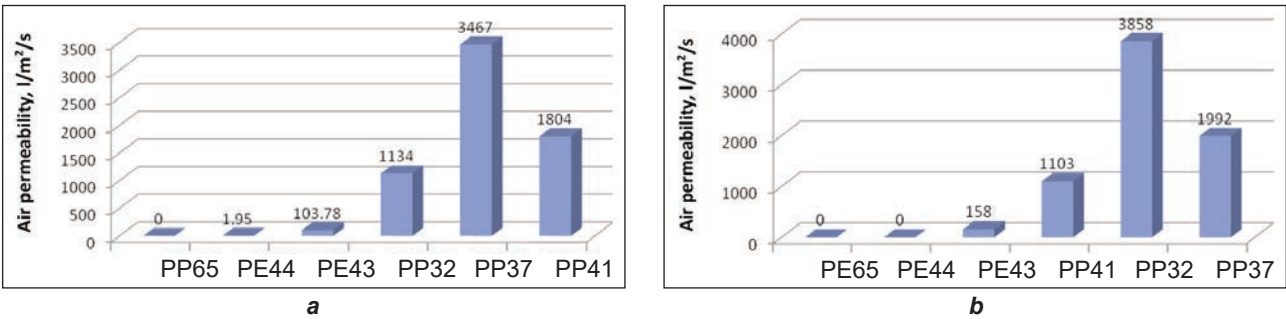
Fig. 4. Air permeability of samples: *a* – fabric relative moisture 50%; *b* – in dry samples
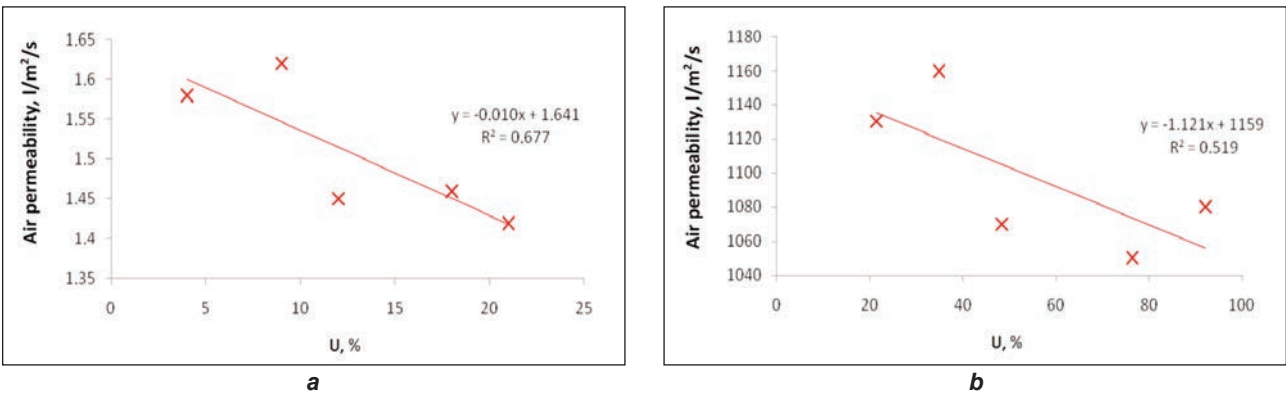
Fig. 5. Air permeability of fabrics at various levels of the relative moisture content U: *a* – PE43; *b* – PP32

Higher water vapour permeability enables higher evaporation cooling, thus offering higher thermal comfort to a wearer (figure 7).

The variation coefficient of PP 65, PE 44 and PE 43 samples was about 11%, whereas CV of other samples was 1.1% – 2.8% only.

Effective relative water vapour permeability ERWVP was calculated for all studied samples (bottom red line) as the function of the relative moisture related to the ultra-dry sample. Top blue lines indicate the total cooling flow from the wet fabric q_{tot} and the green medium line presents the cooling flow $q_{fab,surf}$ from the wet fabric surface (figure 8). As preparing fabrics with the same moisture level is practically impossible,

the measurements were not repeated. Therefore, the error bars are not presented in the diagrams.

Error bars are missing again, as preparing fabrics with the same moisture level is practically impossible and repeated measurements are not achievable.

Hydrostatic resistance test results

The hydrostatic resistance test results (figure 9) in fact also involve wet state of the tested fabrics. From the experiments follows, fabrics with higher areal density showed higher hydrostatic resistance (higher values of water column height). Similarly, the laminated samples also showed higher hydrostatic resistance.

Statistical treatment of the results is missing, as during the measurement of hydrostatic resistance the fabric samples are destroyed.

Evaluation of results

The study follows, that half of the investigated protective coveralls are practically impermeable for air, as their apparent "pores" caused by thermal calandering with outstanding segments (figure 3) are not open. On the other hand, the air permeability of the resting protective fabrics at the 50% fabric humidity

Fig. 6. Relative WV permeability (in blue) and evaporation resistance R_{et} [m²Pa/W] of dry samples
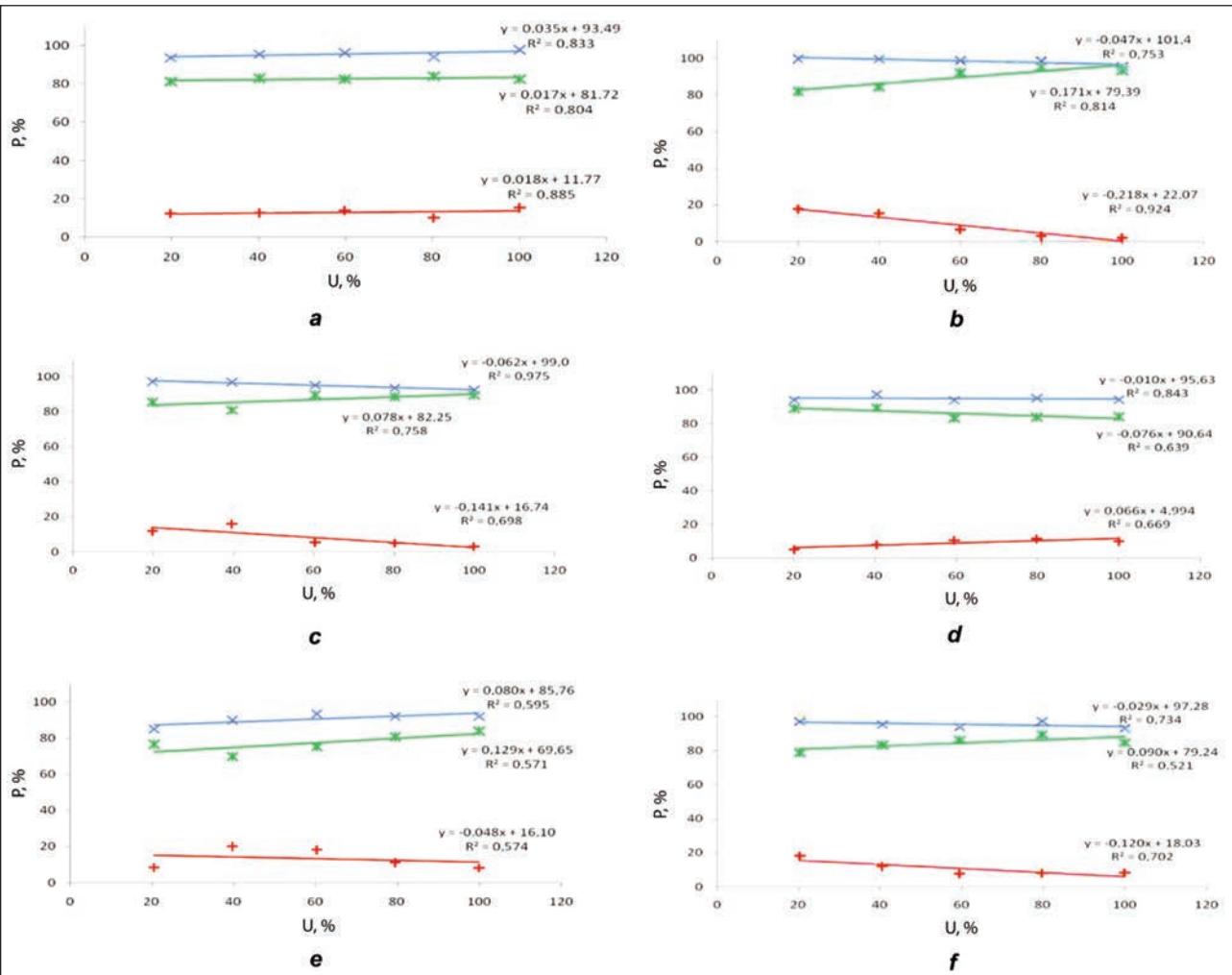
Fig. 7. Relative WV permeability of the sample: *a* – PP65; *b* – PE44; *c* – PE43; *d* – PP41; *e* – PP37; *f* – PP32
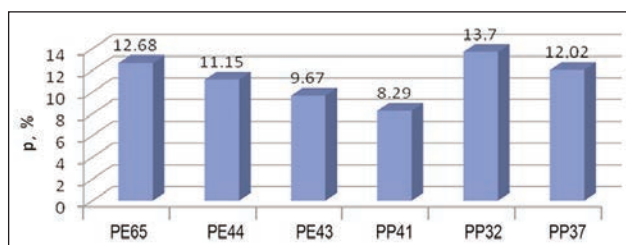
Fig. 8. ERWVP of all samples at their 50% relative moisture
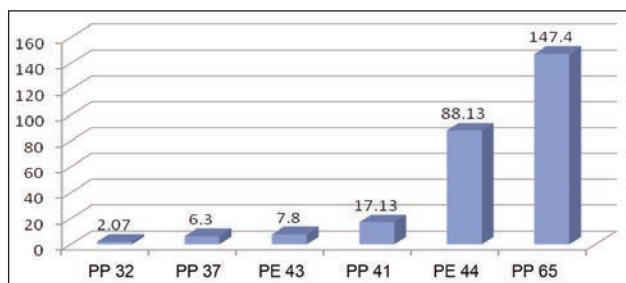
Fig. 9. Hydrostatic resistance of the studied protective coveralls in centimetres of the water column

level was almost the same as their air permeability in dry state.

Regarding the very important parameter of thermophysiological comfort, water vapour permeability, all materials are permeable for water vapour, but in dry state, fabrics made of PP were almost 2 times more permeable than PE (Tyvek) based fabrics. The relative WV permeability of the protective fabrics made of PP fibres was even excellent, but contrary to this (as expected), their hydrostatic resistance was very low. The presence of water in the tested samples reduced their effective WV permeability significantly, which might cause wearing discomfort to their user.

CONCLUSIONS

Protective clothing must offer to its wearer optimum thermal resistance, the highest possible WV permeability and also with certain hydrostatic resistance, namely under real conditions of its use. One of these conditions which deteriorate the wearing comfort of protective clothing is the liquid moisture absorbed in fabrics. As stated in the presented paper, standard testing instruments mostly do not allow reliable testing of the effect of moisture on the thermophysiological comfort of clothing.

In this study, a special testing instrument was presented, which enables to measure water vapour permeability and thermal resistance of wetted fabrics within a few minutes. By means of this unique instrument and other instruments, water vapour permeability, air permeability and hydrostatic resistance of 6 wetted protective coveralls were determined. The main finding of the study is that due to the absorbed moisture, the effective relative water vapour permeability of the studied clothing gets substantively reduced, as well as their air permeability. Thus, using the coveralls tested in the study under real conditions of their use characterised by elevated moisture content would certainly cause a seriously reduced level of their wearing comfort and would influence negatively the performance of the user. It is important to emphasise that the mentioned findings, even if practically perceived and understood, was in this paper probably the first time characterized quantitatively.

The above-demonstrated possibility of quantitative evaluation of thermophysiological comfort of protective clothing in wet state should enable an advanced design of this clothing with higher water vapour and air permeability even under real wearing conditions. The research in this area will continue.

REFERENCES

[1] Lee, S., Obendorf, S.K., *Barrier effectiveness and thermal comfort of protective clothing materials.* In: J. Text. Inst., 2007, 98, 2, 87–98

[2] Yanmei, L., Charlotte, C., Susan, A., Jintu, F.A., *Comparative Study of Disposable Agriculture Coveralls Based on Wearer Trials,* In: Curr. Trends Fashion Technol. Text. Eng., 2017, 1, 552–555

[3] Midha, V.K., Dakuri, A., Midha, V., *Studies on the properties of nonwovens surgical gowns*, In: J. Industrial Textiles, 2013, 43, 2, 174–190

[4] Choi, J.W., Lee, J.Y., Kim, S.Y., *Evaluation of the Thermal Properties of Disposable Coveralls for Railroad Carriage Maintenance Workers*, In: J. Korea Soc. Clothing and Text., 2008, 28, 1175–1185

[5] Kopitar, D., Rogina-Car, B., Skenderi, Z., *Thermo-Physiological Comfort and Microbial Properties of Different Textile Raw Materials and Structures,* In: Functional Textiles and Clothing, (ed. By Majumdar, A., Gupta, D., Gupta, S.) Springer, Singapore, 2019, 285–294

[6] Paraska, O., Rak, T., Rotar, D., Radek N., *The research on the effect of compositions of ecologically safe substances on the hygienic properties of textile products,* In: Eastern-European Journal of Enterprise Technologies, 2019, 10, 97, 43–49

[7] Hes, L., Bogusławska-Baczek, M., *Analysis and experimental determination of effective water vapour permeability of wet woven fabrics,* In: J. of TATM, 2014, 8, 41–48

[8] Mangat, M.M., Hes, L., Bajzik, V., *Thermal resistance models of selected fabrics in wet state and their experimental verification,* In: Text. Res. J., 2015, 85, 200–210

[9] Ren, Y.J., Ruckman, J., *Water vapour transfer in wet waterproof breathable fabrics*, In: J. Ind. Text., 2003, 32, 165–175

[10] Zimova, M., Hes, L., *Report on protective disposable coveralls.* Research report, TU Liberec, Faculty of Textiles, 2013

[11] Hes, L., Tesinova, P., *Imperfections of gravimetric methods for the measurement of water vapour permeability of fabrics,* In: Book of Abstracts, Aachen – Dresden Internat. Textile Conf., Dresden, 2010
[12] Hes, L., Araujo, M., *Simulation of the Effect of Air Gaps between the Skin and a Wet Fabrics on Resulting Cooling Flow,* In: Text. Res. J., 2014, 84,1488–1497

Authors:

LUBOS HES[1], OLGA PARASKA[2], HASAN M. MALIK[3], NAVEED M. AKHTAR[3]

[1]Faculty of Textile Engineering, Technical University of Liberec,
Studentska 2, 46117, Czech Republic
e-mail: lubos.hes@gmail.com

[2]Faculty of Technology and Design, Khmelnytskyi National University,
11, Instytuts'ka str., Khmelnytskyi, 29016, Ukraine

[3]School of Textile and Design, University of Management and Technology,
Lahore, 54 770, Pakistan
e-mail: std.dean@umt.edu.pk

Corresponding author:

OLGA PARASKA
e-mail: olgaparaska@gmail.com

The improvement of bactericidal properties and change of colour characteristics of knitted materials at using nanosilver and carboxymethyl starch

BEKTURSUNOVA AINUR
BOTABAYEV NURZHAN

YERKEBAI GANI
NABIEV DONYOR

ABSTRACT – REZUMAT

The improvement of bactericidal properties and change of colour characteristics of knitted materials at using nanosilver and carboxymethyl starch

The availability of bactericidal knitted cotton fabrics by processing a biodegradable bactericidal nano composition containing nanoparticles of silver and Na-carboxymethyl starch is studied in this work. The nanocomposite based on Na-carboxymethyl starch and silver nanoparticles were successfully fixed on the surface of knitted cotton fabrics through the formation of links between carboxymethyl groups of carboxymethyl starch and nanosilver, as well as air interlacing between nano composition and material. The analysis of the change in the colour of knitted cotton fabrics after processing them with a solution of the nano composition of silver and Na-carboxymethyl starch showed the stability of the colouristic indicators of the colour during antibacterial treatment.
Knitted cotton fabrics treated with the developed nano composition exhibit high antibacterial activity towards gram-positive fungal cultures of Bacillus subtilis, Staphylococcus aureus, and gram-negative Pseudomonas aeruginosa. Consistency of colour and the presence of bacteriostatic properties after repeated washing of knitted cotton fabrics confirms the stability of the antimicrobial properties of reusable fabrics.

Keywords: *nano composition, antibacterial activity, Suprem fabric, Interlock fabric, natural component*

Îmbunătățirea proprietăților bactericide și modificarea caracteristicilor de culoare ale tricoturilor prin utilizarea nano-argintului și a amidonului carboximetilic

În această lucrare este studiată posibilitatea obținerii tricoturilor bactericide din bumbac, prin procesarea unui nano-compozit bactericid biodegradabil care conține nanoparticule de argint și amidon Na-carboximetil. Nanocompozitul pe bază de amidon de Na-carboximetil și nanoparticule de argint a fost fixat cu succes pe suprafața tricoturilor din bumbac prin formarea de legături între grupările carboximetil ale amidonului carboximetil și nano-argint, precum și prin intercalarea aerului dintre nanocompozit și materialul textil. Analiza modificării culorii tricoturilor din bumbac după prelucrarea lor cu o soluție de nanocompozit de argint și amidon Na-carboximetil, a arătat stabilitatea indicatorilor coloristici în timpul tratamentului antibacterian.
Tricoturile din bumbac tratate cu nanocompozitul dezvoltat prezintă activitate antibacteriană ridicată față de culturile fungice gram-pozitive de Bacillus subtilis, Staphylococcus aureus și Pseudomonas aeruginosa gram-negative. Rezistența culorii și prezența proprietăților bacteriostatice după spălarea repetată a tricoturilor din bumbac confirmă stabilitatea proprietăților antimicrobiene ale materialelor textile reutilizabile.

Cuvinte-cheie*: nanocompozit, activitate antibacteriană, tricot Suprem, tricot Interlock, componentă naturală*

INTRODUCTION

Cotton fibres are the most widespread for the production of knitted materials with bactericidal properties [1]. As it is known, cotton is the most susceptible to microbial action [2]. In addition, natural fibres also have a varied retention period of microbes [3]. In this direction, the leading position is occupied by the antimicrobial processing of knitted fabrics [4, 5]. Antimicrobial materials made of cotton, linen, woollen, synthetic and silk fibres are widely used in the production of medical dressings [6, 7], napkins [8, 9], sanitary-hygienic products [10, 11], underclothing and bed linen [12, 13], hosiery [14, 15], as well as protective clothing at working with causative pathogens of dangerous infections [16].

The situation with the coronavirus COVID-19 showed the need to intensify work on the production of high-quality safe knitted fabrics with bactericidal properties [17–19]. Analysis of the latest advances in science in this direction shows that silver nanoparticles are often used for the antibacterial processing of knitted materials [20–22]. Today there are many methods of the synthesis of silver nanoparticles, but most of them are based on toxic reagents (derivatives of ammonia, glycerol, and others), used either to stabilize the resulting nanoparticles [23, 24] or to reduce silver ions [25, 26]. At the same time, it is necessary to exclude using toxic substances in the synthesis of bactericidal compounds applied for antibacterial

processing of knitted fabrics to use nanoparticles that ensure safety for the consumer [27–30].

Based on the foregoing, the purpose of the research was the formation of stabilized silver nanoparticles safe for humans in a solution of Na-carboxymethyl starch (NaCMS), the production of bactericidal knitted materials by processing the resulting nano composition, as well as the study of the effect of antimicrobial treatment on the bactericidal and physico-mechanical properties of the obtained materials.

The choice of NaCMC is due to the fact that it is widely used in the textile industry due to its biodegradability, has gel-forming, sorption and other biological properties, and is also a natural, environmentally friendly component that does not cause irritation to human skin [31].

EXPERIMENTAL PART

Materials

KnThe knittedotton fabric of the styles "Suprem" and "Interlock" (manufacturer of Uzbekistan) was chosen for research. "Suprem" is a bleached knitted fabric with, a surface density of 80 g/m^2. Suprem is considered one of the types of stockinette structure (figure 1, *a*), recognized as the thinnest among cotton jerseys (manufacturer Uzbekistan) [32]. "Interlock" knitted fabric is dyed brown with the reactive dye Orange 2R from "BEZEMA CHT Switzerland AG", surface density 120 g/m^2, dimensional stability, has a low level of stretching (manufacturer Uzbekistan). Interlock in weaving, the concept of the front and backside is absent (figure 1, *b*). It possesses good heat-shielding properties. Both canvases are 100% cotton. The choice of cotton knitted fabric for obtaining antibacterial materials with bactericidal properties based on nanosilver and carboxymethyl starch in our research was due to the fact that the knitted weave provides the greatest flexibility and softness of the fabric, and it has also high adsorption capacity, capillarity, air permeability, which contributes to the creation of the basis of products with antibacterial finishing for household and medical purposes.

Front	Backside	
a		*b*
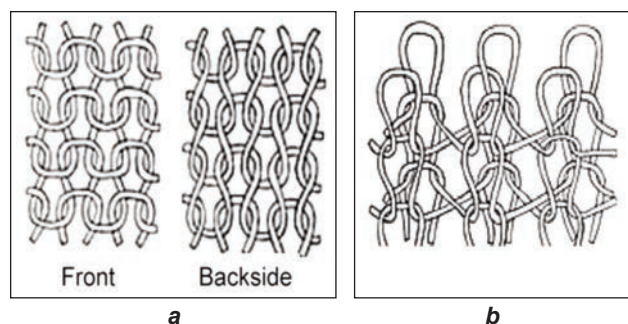
Fig. 1. Knitted weaving: *a* – supreme (stockinette stitch); *b* – interlock

Chemically pure silver nitrate (JSC "Reakhim", GOST 1277-75) was used to obtain the nanocomposite. All chemical substances were used as purchased, without any further purification or processing. NaCMS

produced by LLP "Khlopkoprom-cellulose" (manufactured of Kazakhstan), the mass fraction of NaCMS of 99.6% (ST LLP 40936697-004-2015) was used as a reducing agent.

The reduction of silver ions and synthesis of silver nanoparticles

The method of reduction of silver ions using NaCMS and ultraviolet radiation was used in this work.

Photochemical reduction of silver ions in the Ag$^+$CMS$^-$ structure to nanoparticles was carried out by irradiating them with an RDS-250-3 ultrahigh-pressure mercury-quartz ball lamp.

Ultrasonic dispersers of the UVRP-1, U-4.2 brands were used to recover dispersions of silver nanoparticles.

The synthesis of nanoparticles was carried out by reducing silver ions in an aqueous solution of NaCMS under the combined action of ultraviolet radiation with a wavelength of 280–400 nm and ultrasonic waves with a frequency of 1.7 MHz.

The reaction proceeds according to the following equation:

$$R-COO^- + Ag^+ \xrightarrow{h\nu} R-COO:Ag^0 \qquad (1)$$

$$R-COO^- + Ag^0 + e \rightarrow R-COO^-:Ag^0 \qquad (2)$$

$$R-COO^-:Ag^0 + Ag^+ \xrightarrow{h\nu} R-COO:Ag_2^0 \qquad (3)$$

$$R-COO^-:Ag_2^0 \xrightarrow{h\nu} R-COO:Ag_n^0 \qquad (4)$$
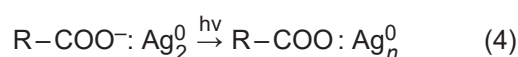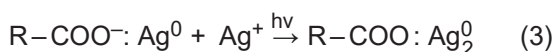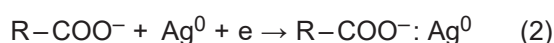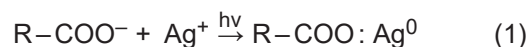
Due to the presence of negatively charged ions (COO–) in the carboxymethyl group, carboxymethyl starch interacts with silver cations, linking them into a strong complex (1), reducing them under the influence of UV directly in this complex (2), and stabilize sequentially formed during synthesis small charged clusters and silver nanoparticles (3) [33, 34]. Thus, the entire process of nanoparticle formation from the initial cation to the final state particle proceeds in direct contact with the polymer matrix [35].

Recovering of aqueous composite solution

50 ml of water was poured into the container, 0.5 g of NaCMS was added and it was stirred with a mechanical stirrer for 10 min, then 50 ml of 0.50% (1.0%) solution of silver nitrate was added into this solution and it was stirred until a homogeneous solution for 15–20 minutes to get an aqueous composite solution containing 0.500 mass % of NaCMS and 0.15 mass % (0.30 mass %) of silver nanoparticles. The resulting solution was subjected to ultrasonic dispersion and ultraviolet radiation for 15 minutes.

Processing of knitted fabrics

The processing of knitted fabrics in order to avoid deformation of their structure was carried out by the method of aerosol application of the solution. 100 ml of the obtained composite solution of silver nanoparticles (100% application) was sprayed onto 100 g of

knitted material by aerosol method, after which the material was subjected to ultraviolet radiation for 15 min. After radiation, the treated material was dried in a model 202-OE drying oven at 120°C to a residual moisture content of 6%.

Diagnostics and testing of knitted materials

The electron microscopy was carried out using a JEOL JSM–6490 LV scanning electron microscope with an accelerating voltage from 0.3 to 30 kV to evaluate the surface morphology of the fibres of knitted fabrics and the sizes of nanoparticles.

The study of the antibacterial activity of knitted fabrics treated with the nanocomposite composition Ag^+CMS^- was carried out in accordance with the international standard ISO 20743:2007 "Textiles – Determination of the antibacterial activity of antibacterial finished products".

The change in the colour characteristics of knitted fabrics after antibacterial treatment with Ag^+CMS^- nano composition was tested on the laboratory colourimeter according to the method [36] in standard radiation D_{65} [37]. Color characteristics were determined by the CIELAB formula, recommended by the Commission internationale de l'éclairage (CIE) [38].

The breaking load and elongation of the strip were determined on the tensile testing machine of the RT-250 type according to GOST 8847-85.

The resistance to abrasion of materials was determined on the IT-3M, TI-1 or TI-1M devices by the number of abrasion cycles before the destruction of the fabric according to GOST 12739-85. The method is based on determining the resistance of the knitted fabric to abrasion by the number of revolutions of the device heads until the destruction of the elementary sample.

The moisture content of knitted fabrics was determined according to GOST 8845-87. The principle of determining moisture content was that a certain amount of knitted fabric was dried to constant weight, and the amount of moisture in the studied knitted fabric was found from the difference between the initial weight and the weight of the dry residue.

The capillary test was determined according to GOST 3816-81 (ISO 811-81) "Textile fabrics. Methods of determination of hygroscopic and water-repellent

properties". The essence of the method is to determine the height of the capillary rise of fluid in the fabric. Wet processing of knitted fabrics was carried out in accordance with ISO 6330:2012 "Textiles – Domestic washing and drying procedures for textile testing.

RESULTS AND DISCUSSION

Surface morphology of dyed knitted fabrics treated with Ag carboxy-methyl-starch (AgCMS) nano composition

The surface morphology of the fibres of knitted fabrics modified with the AgCMS nano composition was determined in a scanning electron microscope by scanning electron microscope analysis of figure 2.

The scanning electron microscopy results show that the treatment of knitted fabrics with the nanocomposite composition AgCMS (figure 2, *a* and *b*) leads to a uniform distribution of almost spherical Ag agglomerates on the surface of the fabrics, mainly with sizes of about 10–40 nm. A large number of Ag nanoparticles are visible on the surface of the knitted fabrics, which indicates the successful fixation of AgCMS. Larger agglomerates with sizes from 10 to 120 nm are formed on the surface of knitted fabrics at treating with colloidal silver without the addition of carboxymethyl starch (figure 2, *c*). The absence of carboxymethyl starch led to the agglomeration of Ag particles and the formation of larger silver clusters. These results showed the role of carboxymethyl starch in the reduction of nanosilver and its ability to stabilize the AgCMS system.

The conditions for the implementation of the recovery method and the results of testing the antibacterial activity of knitted fabrics treated with the developed nanocomposite solution AgCMS are presented in table 1 and figure 3, respectively.

The presented results indicate (figure 3) that knitted fabrics treated with the developed nanocomposite solution Ag^+CMS^- have high antimicrobial activity towards gram-positive fungal cultures of Bacillus subtilis (5.5–6.9), Staphylococcus aureus (5.8–7.0) and gram-negative Pseudomonas aeruginosa (5.6–.6). It can also be seen that with an increase in the silver content in the cloth twice, the antibacterial activity increases by only 0.7–1.2 units. Control samples treated with colloidal silver without reduction with

a   b   c
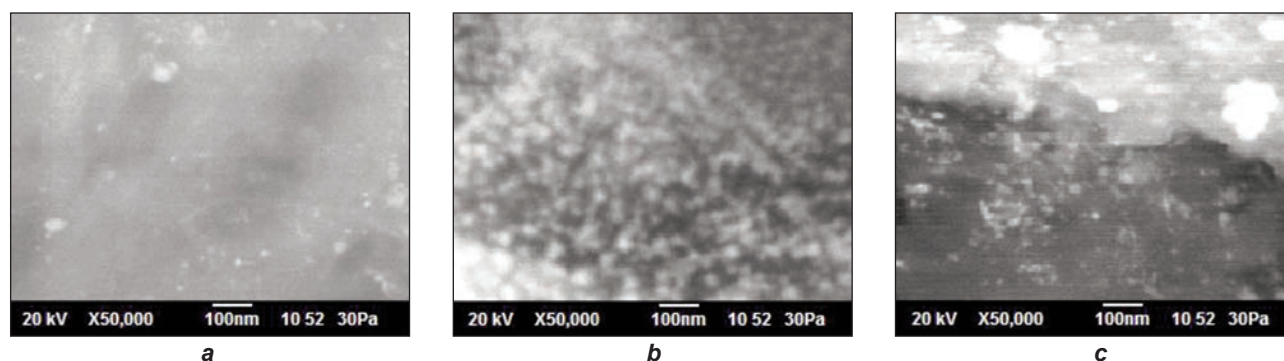
Fig. 2. Scanning electron microscopy of knitted fabric fibres modified with AgCMS nano composition; the processing of textile fabric: *a* – CMS – 0.5 wt.% and Ag – 0.15 wt. %; *b* – CMS – 0.5 wt. % and Ag – 0.30 wt. %; *c* – Ag – 0.15 wt. %

Table 1

№ samples	Knitted materials	Concentration of NaCMS in solution (wt.%)	Concentration of silver salt in solution (wt.%)	Concentration of silver nanoparticles on the material (wt.%)
		CONDITIONS OF THE IMPLEMENTATION OF THE RECOVERY METHOD OF NANO COMPOSITE KNITTED MATERIALS		
1	Suprem (white)	absent	0.25	0.15
2	Suprem (white)	0.500	0.25	0.15
3	Suprem (white)	0.500	0.50	0.30
4	Interlock (brown)	absent	0.25	0.15
5	Interlock (brown)	0.500	0.25	0.15
6	Interlock (brown)	0.500	0.50	0.30

Fig. 3. The value of the antibacterial activity of knitted fabrics modified with a solution of Ag^+CMS^-:
1,2,3 – Suprem; 4,5,6 – interlock

carboxymethyl starch have almost half the antibacterial effect in relation to all selected fungi. From the obtained data, it follows that the developed nanocomposite solution AgCMS, proposed for antibacterial processing of knitted materials, has a depressing effect in relation to the selected fungi and therefore, meet the requirements for cellulose materials directed to the manufacture of sanitary-hygienic and technical purpose.

The research of the effect of treatment with a solution of the AgCMS nanocomposite on the colcolouror characteristics of bleached and dyed knitted fabrics is shown in figures 4 and 5.

Figures 4, b and 5, b show that the colour changes slightly at using bleached and coloured knitwear with a solution containing 0.15% Ag. The material acquires a slightly greyish colour, that is, it darkens a little at processing bleached knitwear with a solution containing Ag – 0.30% (figure 4, b). The change can also be seen visually at processing coloured knitwear with a solution containing Ag – 0.30% (figure 4, c). This is due to the fact that silver particles introduced into the nano composition system can affect the structure and properties of light-gamma dyes. The colour characteristics of knitted fabrics were used adopted by the International Commission on Lighting in the CIE L *a* b* colour space to clarify the effect of the AgCMS nano composition.

The results of colorimetric studies of changes in the colour characteristics of fabric after bactericidal finishing with nanoparticles of silver and carboxymethyl starch are shown in table 2.

According to the data in table 2, the original Suprem fabric was white with a high-value L* and insignificant a* and b* values. The values of lightness L* of the treated fabric decreased slightly from 95.51 to 94.01. After treatment with a nanocomposite of silver and CMS. The L* value also decreased slightly at processing a painted fabric. The discolouration of knitted
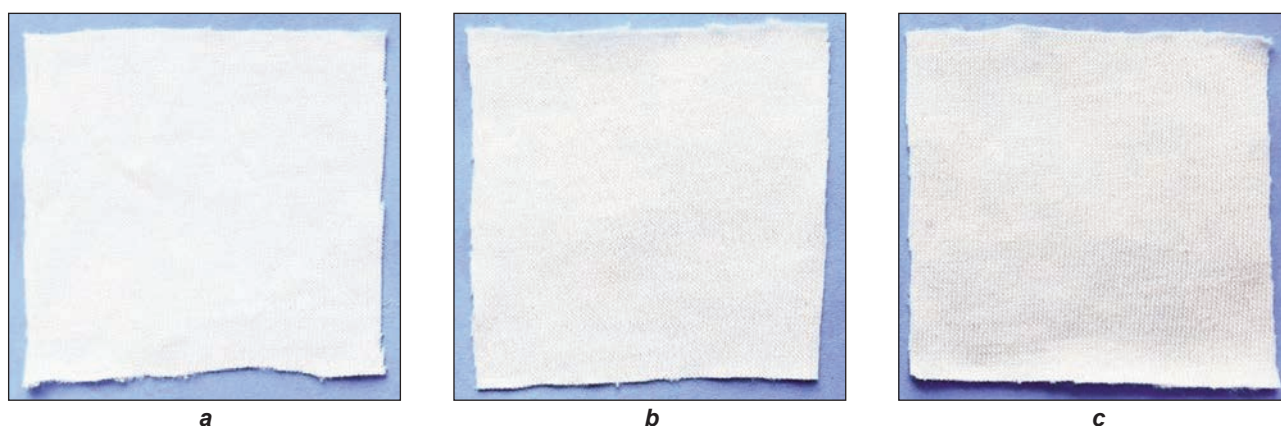
Fig. 4. Photographs of bleached knitwear "Suprem", before and after treatment with a nanocomposite solution AgCMS:
a – original sample without treatment; b – treated with a solution containing CMS – 0.5 wt.% and Ag – 0.15 wt. %;
c – treated with a solution containing CMS – 0.5 wt. % and Ag – 0.30 wt. %
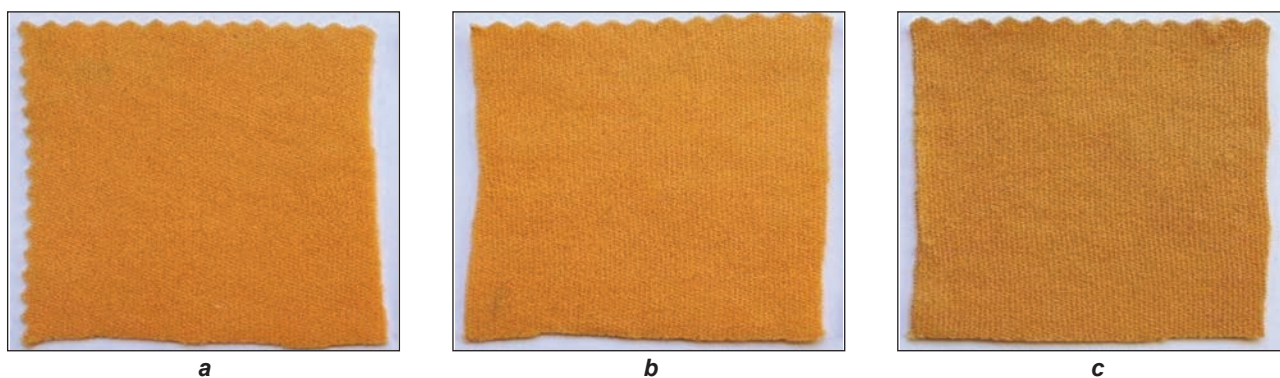
Fig. 5. Photographs of knitted fabric "Interlock", dyed brown before and after processing with nanocomposite solutions AgCMS: *a* – original sample without processing; *b* – treated with a solution containing CMS – 0.5 wt. % and Ag – 0.15 wt. %; *c* – treated with a solution containing CMS – 0.5 wt. % and Ag – 0.30 wt. %

Table 2

COLOUR COORDINATES AND REFLECTION SAMPLES COEFFICIENT

№ samples	Name of the material	Samples	Brightness L*	Coordinates	
				a*	b*
1	Suprem (white)	original	95.51	2.75	−9.37
2	Suprem (white)	0.5% CMS+0.15%Ag	95.25	2.06	−10.59
3	Suprem (white))	0.5% CMS +0.30%Ag	94.01	2.94	−10.96
4	Interlock (brown)	original	73.08	24.72	33.63
5	Interlock (brown)	0.5% CMS +0.15%Ag	72.41	24.27	33.13
6	Interlock (brown)	0.5% CMS +0.30%Ag	68.92	21.06	29.38

fabrics depends on the content of Ag nanoparticles. The colour characteristics of both the white and the dyed fabric did not change significantly with Ag content of 0.15% in the knitted fabric. The analysis of the change in the colour of cotton knitted fabrics carried out in this work after treatment with a solution of the nano composition of silver and AgCMS showed the stability of the colouristic indicators of colour during antibacterial treatment and proved the effectiveness of the proposed nano composition used in the bactericidal treatment of sanitary and hygienic and household products.

Further, the operational and hygienic properties of the initial and processed by the nanocomposite knitted fabrics were investigated. We have determined the following indicators: breaking force on the loop stitches, extensibility, stretching property in width and abrasion resistance from the performance properties that affect the service life of knitted products. The results of testing the operational characteristics of the initial and prototypes of knitted fabrics treated with the AgCMS nanocomposite solution are shown in table 3.

Table 3

CHARACTERISTICS OF KNITTED FABRICS TREATED WITH NANO COMPOSITE SOLUTION AgCMS AND WITHOUT TREATMENT (FABRICS TREATED WITH SOLUTION CONTAINING 0.5%CMS+0.15%Ag)

Type of treatment	Name of knitted fabric	Quality indicators			
		Breaking load on the buttonhole posts (H)	Extensibility (mm)	Stretchability in width (%)	Abrasion resistance (turns)
AgCMS	Suprem	105	11 ±1	65	27
AgCMS	Interlock	156	6 ± 1	32	54
Without treatment	Suprem	100	12±1	66	24
Without treatment	Interlock	147	6±1	35	45
Requirements of GOST 28554-90		Not less than 80	-	I – from 0 till 40 II–from 41 till 100 III – above 100	common15–30 fast 31–60 extra fast 61 and more

Table 4

HYGIENIC CHARACTERISTICS OF KNITTED FABRICS TREATED WITH NANO COMPOSITE SOLUTION AgCMS (0.5%CMS+0.15%Ag) AND WITHOUT TREATMENT					
Type of treatment	**Name of knitted fabric**	**Quality indicators**			
		Breaking load on the buttonhole posts (H)	**Extensibility (mm)**	**Stretchability in width (%)**	**Abrasion resistance (turns)**
AgCMS	Suprem	161	44	8,2	6.6
AgCMS	Interlock	163	48	9,0	7.0
Without treatment	Suprem	157	41	8,0	6.5
Without treatment	Interlock	158	47	8,8	7.0

According to table 3, samples of knitted fabric treated with nanocomposite solution of AgCMS, in comparison with samples without treatment, have greater strength and resistance to abrasion, and according to other indicators, at the level of standard requirements. It is possible that carboxymethyl starch, being a polymer component of nanocomposite solution sprayed onto a knitted fabric, forms polymer films on its surface, which increase tensile strength and abrasion resistance.

The test results of characteristics affecting the hygienic properties of knitted materials samples treated with the AgCMS nanocomposite solution are shown in table 4.

The results of table 4 show that samples of knitted fabric treated with nanocomposite solution of AgCMS, compared to samples without treatment, have higher capillarity, fluid loss and porosity. This confirms that the processing of knitted fabric with

developed nanocomposite solution AgCMS has a beneficial effect on the hygienic properties of knitted fabric. The improvement in the hygienic properties of knitted fabrics can be explained by the fact that the carboxymethyl starch used in the composition of the nanocomposite solution is a hygroscopic polymer. At processing knitted fabric with the developed composition, reticulated polymer structures are formed on its surface, which lead to an increase in the hygienic characteristics of the materials under study.

The test results of the effect of the number of washings on the antibacterial activity of knitted fabrics treated with the nanocomposite solution AgCMS are shown in figure 6.

It was found that a sufficiently high antimicrobial activity retention, slightly decreasing only after the tenth wash in a washing solution as a result of the study of the resistance of knitted fabrics treated with
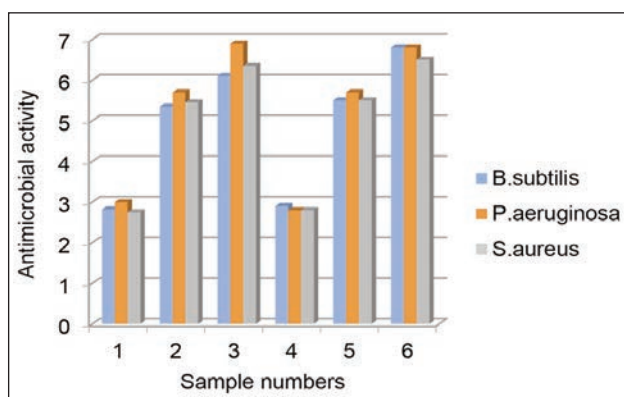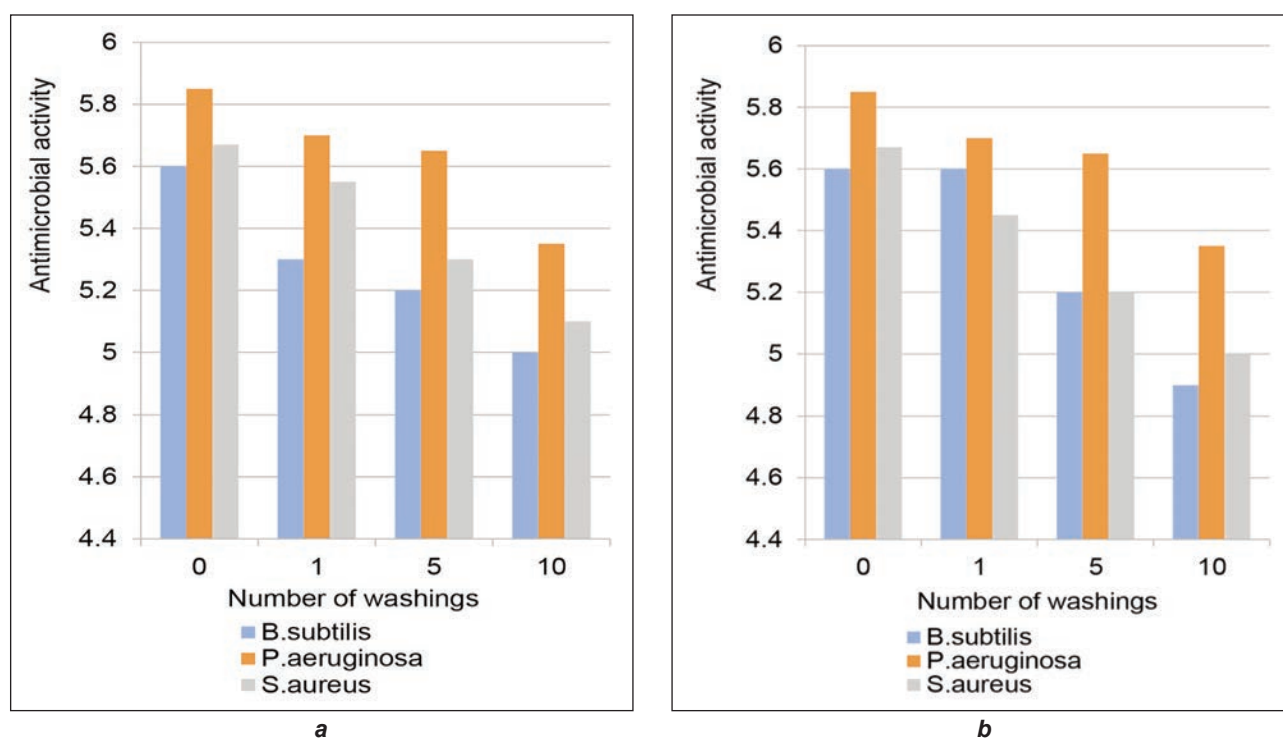

Fig. 6. The effect of the number of washings on the value of the antibacterial activity of knitted fabrics modified with solution of AgCMS: a – suprem; b – interlock

a nanocomposite solution of AgCMC to wet treatments (figure 6, *a* and *b*). The stability of the antimicrobial properties of reusable fabric was proved by the presence of bacteriostatic properties after multiple washes**.**

CONCLUSIONS

The studies have shown that the usage of NaCMS in the developed composition makes it possible to obtain stable systems of silver nanoparticles in the knitted fabric with a sufficient distribution of nanoparticles in size. The stability of nanoparticles is achieved due to the fact that NaCMS, binding with silver particles, creates a charged shell around them, preventing aggregation.

It has been shown that cellulose knitted fabrics treated with the developed nanocomposite solution of AgCMS have high antimicrobial activity towards gram-positive fungal cultures of *Bacillus subtilis*, *Staphylococcus aureus* and gram-negative *Pseudomonas aeruginosa*. The stability of colour indicators of dyeing during antibacterial treatment proved the effectiveness of the proposed nano composition. The discolouration of knitted fabrics depends on the content of Ag nanoparticles.

It was found that the treatment with the developed composition has a beneficial effect on the consumer and hygienic properties of the knitted material. The improvement in the hygienic properties of knitted fabrics can be explained by the fact that the carboxymethyl starch used in the composition of the nanocomposite solution is a hygroscopic polymer. At processing knitted fabric with the developed composition, reticulated polymer structures are formed on its surface, which lead to an increase in the hygienic characteristics of the materials under study.

The knitted fabrics exhibit excellent antibacterial properties and excellent washing resistance. After 10 wash cycles, the resulting fabrics still showed excellent bacterial resistance against fungal cultures of *Bacillus subtilis, Staphylococcus aureus* and *Pseudomonas aeruginosa*. The stability of the antimicrobial properties of reusable fabric was proved by the invariability of colour and the presence of bacteriostatic properties after repeated washing.

It should be noted that the composition formulation includes natural components, which makes it possible to recommend the developed composition based on silver nanoparticles for processing sanitary and hygienic products and knitted materials in order to impart bactericidal properties to them.

REFERENCES

[1] Zhang, Y.Y., Xu, Q.B., Fu, F.Y., Liu, X.D., *Durable antimicrobial cotton textiles modified with inorganic nanoparticles*, In: Cellulose, 2016, 23, 5, 2791–2808, http://doi.org/10.1007/s10570-016-1012-0

[2] Shanmugasundaram, O.L., *Application of nanotechnology to textile finishing*, In: Textile Review, 2009, 11, 135–139

[3] David, T.W., David, D.M., Hughs, S.E., Cobb, D.R., *Microbial census and cotton bale moisture during a 6-month storage*, In: Beltwide Cotton Conferences, 2004, 2425–2431

[4] Pachiayappan, K.M., Prakash, C., Kumar, V., *Influence of process variables on antimicrobial properties of cotton knitted fabrics*, In: Journal of Natural Fibers, 2018, 17, 3, 313–325, http://doi.org/10.1080/15440478.2018.1492487

[5] Antonova, M.V., Krasina, I.V., Ilyushina, S.V., *Methods of imparting antibacterial properties to textile fibers,* In: Bulletin of the Technological University, 2014, 17, 18, 56–63

[6] Kim, T.-S, Cha, J.-R., Gong, M.-S., *Facile procedure for producing silver nanocoated cotton gauze and antibacterial evaluation for biomedical applications*, In: Fibers and Polymers, 2017, 18, 3, 453–459, http://doi.org/10.1007/s12221-017-6831-6

[7] Dzhanpaizova, V.M., Myrkhalykov, Zh.U., Tashmenov, R.S., Kaplunenko, V.G., Togatayev, T.U., Orymbetova, G.E., *The study of the optimal concentration of silver citrate solution to impart antibacterial properties to medical gauze,* News of Higher Educational Institutions, In: Textile Industry Technology, 2016, 3, 133–137

[8] Melnikova, O.A., Petrov, A.Yu., Samkova, I.A., *Medical napkin for external usage*, R.U. Patent 2519662, 2014

[9] Xu, Q.B., Wu, Y.H., Zhang, Y.Y., Fu, F.Y., Liu, X.D., *Durable antibacterial cotton modified by silver nanoparticles and chitosan derivative binder*, In: Fibers and Polymers, 2016, 17, 11, 1782–1789, http://doi.org/10.1007/s12221-016-6609-2

[10] Trapeznikov, A., Diankova, T., Fjodorova, N., *Antimicrobial and Antifungal Finishing of Cotton Materials*, In: Programme and abstracts of XXIII Congress of IFATCC, 2013, 143

[11] Moryganov, A.P., Dymnikova, N.S., *Functional textile materials based on cellulosic fibers for medical, sanitary-hygienic and cosmetic purposes*, In: Modern achievements of chemical technology in the production of textiles, synthesis and usage of chemical products and dyes: report All-russian scientific-practical conference with international participation, 2019, 6–7

[12] Gu, J., Yuan, L., Zhang, Z., Yang, X., Luo, J., Gui, Z., Chen, Sh., *Non-leaching bactericidal cotton fabrics with well-preserved physical properties, no skin irritation and no toxicity*, In: Cellulose, 2018, 25, 9, 5415–5426, http://doi.org/10.1007/s10570-018-1943-8

[13] Nikitina, L.L., Kanayeva, N.S., Gavrilova, O.E., Gerkina, O.Yu., *The usage of synthetic polymers in hosiery production. Review of modern developments*, In: Bulletin of the Technological University, 2016, 19, 7, 72–76

[14] Ageyeva, A.A., Sytsko, V.E., *Features of the formation of competitive assortment of hosiery*, In: Youth in science and entrepreneurship: collection of scientific articles of the VII international forum of young scientists, 2018, 242–244

[15] Khammatova, V.V., *The production of trial amount of samples of nanostructured textile materials for the manufacture of special-purpose clothing with increased hydrophobic and hygienic properties*, Russian market of technical textiles and nonwovens: science and production in modern conditions: collection of reports of participants of the 1st International Scientific practical symposium, 2016, 127–132

[16] Sportelli, M.C., Izzi, M., Kukushkina, E.A., Hossain, S.I., Picca, R.A., Ditaranto, N., Cioffi, N., *Can Nanotechnology and Materials Science Help the Fight against SARS-CoV-2?*, In: Nanomaterials, 2020, 10, 802–814

[17] Roberto, M.C., *Here's how nanoparticles could help us get closer to a treatment for COVID-19*, Available at: https://news.northeastern.edu/2020/03/04 [Accessed on November 2020]

[18] Shestakov, M., *The SB RAS intends to produce masks with silver and a vaccine against COVID-19*, Available at: https://nsk.rbc.ru/nsk/31/03/2020/5e829f819a794707bc1b7009 [Accessed on November 2020]

[19] Ru, J., Qian, X., Wang, Y., *Roberto of cotton fabric with silver nanoparticles stabilized by nanoliposomes*, In: Cellulose, 2018, 25, 9, 5443–5454, http://doi.org/10.1007/s10570-018-1953-6

[20] Naseeb, U., Sohail, Y., Zamir, A., Lin, L., Qufu, W., *Mechanically robust and antimicrobial cotton fibers loaded with silver nanoparticles: synthesized via chinese Holly plant leaves*, In: International Journal of Textile Science, 2014, 3, 1A, 1–5

[21] Velmurugan, P., Shim, J., Kim, H.W., Lim, J.-M., Kim, S.A., Seo, Y.-S., Kim, J.-W., Kim, K., Oh, B.-T., *Bio-functionalization of cotton, silk, and leather using different in-situ silver nanoparticle synthesis modules, and their antibacterial properties*, In: Research on Chemical Intermediates, 2020, 46, 2, 999–1015, http://doi.org/10.1007/s11164-016-2481-3

[22] Meng, M., He, H.W., Xiao, J., Zhao, P., Xie, J.L., Lu, Z.S., *Controllable in situ synthesis of silver nanoparticles on multilayered film-coated silk fibers for antibacterial application*, In: Journal of Colloid and Interface Science, 2016, 461, 369–375, http://doi.org/10.1016/j.jcis.2015.09.038

[23] Ravilova, A.F., Antonova, M.V., Krasina, I.V., *Comparison of the antibacterial effect of various drugs on cotton fabric*, In: Bulletin of the Technological University, 2017, 20, 20, 74–76

[24] Silvestri, D., Wacławek, S., Venkateshaiah, A., Krawczyk, K., Sobel, B., Padil, V.V.T., Černík, M., Varma, R.S., *Synthesis of Ag nanoparticles by a chitosan-poly(3-hydroxybutyrate) polymer conjugate and their superb catalytic activity*, In: Carbohydrate Polymers, 2020, 232, 115806, http://doi.org/10.1016/j.carbpol.2019.115806

[25] Petrova, L.S., Malysheva, K.A., Odintsova, O.I., Vladimirtseva, E.L., *Influence of the type of reducing agent on the properties of synthesized silver nanoparticles*, In: Science in the modern information society, 2016, 2, 98–101

[26] Balamurugan, M., Saravanan, S., Soga, T., *Coating of green-synthesized silver nanoparticles on cotton fabric*, In: Journal of Coatings Technology and Research, 2017, 14, 3, 735–745, http://doi.org/10.1007/s11998-016-9894-1

[27] Petrova, L.S., Lipina, A.A., Zaitseva, A.O., Odintsova, O.I., *The usage of silver nanoparticles to impart bactericidal properties to textile materials*, In: Proceedings of higher educational institutions. Textile industry technology, 2018, 378, 6, 81–85

[28] El-Sheikh, M.A., *A novel photosynthesis of carboxymethyl starch-stabilized silver nanoparticles*, In: Scientific World Journal, 2014, 1–11, 514563, http://doi.org/10.1155/2014/514563

[29] Dymnikova, N.S., Erokhina, E.V., Kuznetsov, O.Yu., Moryganov, A.P., *Research of the influence of the substantivity of silver-containing preparations to cellulose material on its biological activity,* In: Russian Chemical Journal, 2017, 61, 2, 3–12

[30] Zhushman, A.I., *Modified starches*, Moscow: Pishchepromizdat, 2007

[31] Kudryavin, L.A., Shalov, I.I., *Fundamentals of knitwear production technology,* Moscow: Legprombytizdat, 1991

[32] Oksigenler, B.L., Turayeva, N.N., Yunusov, Kh.E., Sarymsakov, A.A., Rashidova, S.Sh., *The mechanism of the influence of ultraviolet irradiation on the growth and properties of silver nanoparticles in polymer solutions*, In: Republican scientific-practical conference. Actual problems of chemistry, physics and technology of polymers, 2009, 82–85

[33] Sergeev, G.B., *Nanochemistry*, Moscow: MSU, 2003

[34] Yunusov, K.E., Sarymsakov, A.A., Atakhanov, A.A., Ashurov, N.Sh., Rashidova, S.Sh., *Physicochemical studies of cotton cellulose and its derivatives containing silver nanoparticles*, In: Chemistry of natural compounds, 2011, 47, 370–373

[35] Instruction sheet, *Computer color matching system operation and maintenance manual*, Korea industrial technology ODA, 2012, 79

[36] Shashlov, A.B., Uarova, R.M., Churkin, A.V., *Fundamentals of lighting engineering*, Moscow: MSUP Publishing House, 2002

[37] Gorbunova, E.V., Chertov, A.N., *Typical calculations for the colorimetry of radiation sources*, St. Petersburg: ITMO University, 2014

[38] Pool Ch., Owens F., *Nanotechnology*, Moscow: Technosphere, 2005

Authors:

BEKTURSUNOVA AINUR[1], BOTABAYEV NURZHAN[1], YERKEBAI GANI[1], NABIEV DONYOR[2]

[1]M. Auezov South Kazakhstan State University, High School of Textile and Food Engineering,
Tauke Khan Avenue, 5, 160012, Shymkent, Kazakhstan

[2]Tashkent Institute of Textile and Light Industry, Department of Technology Textile Industry,
Shokhjakhon street, 5, 100100, Tashkent, Uzbekistan
e-mail: nabievdonyor@rambler.ru

Corresponding author:

BEKTURSUNOVA AINUR
e-mail: ainurbektursunova@yandex.kz

Random forest-based physical activities recognition by using wearable sensors

ZHANG JUNJIE
CAI SHENGHAO

XU JIE
YUAN HUA

ABSTRACT – REZUMAT

Random forest-based physical activities recognition by using wearable sensors

Physical activity recognition (PAR) is a topic worthy of attention. In order to improve the practicality of wearable sensors for recognition, in this study, we propose an approach to create a classifier of PAR based on the collected data. At first, we discuss how features extracted from the accelerometer and gyroscope contribute to distinguish different activities, including walking, walking upstairs, walking downstairs, sitting, standing, laying, and also provide an analytical method employed for this purpose. Then, a supervised machine learning method, random forest algorithm, is adopted to create a classifier to recognize physical activities based on the extracted features. Lastly, the performances of the constructed classifier are evaluated and compared with other methods. The performance evaluation shows the classifier trained by random forest algorithm are better than other algorithms, and its overall recognition rate reaches 93.75%. In addition, our approach also has strong potential for applications in smart textiles.

Keywords: physical activities recognition, random forest, smart textiles, features analysis

Recunoașterea activităților fizice prin algoritmul arborilor decizionali utilizând senzorii purtabili

Recunoașterea activității fizice (PAR) este un subiect demn de atenție. Pentru a îmbunătăți caracterul practic al senzorilor purtabili pentru recunoaștere, în acest studiu, propunem o abordare pentru a crea un clasificator al PAR pe baza datelor culese de către aceștia. La început, discutăm despre modul în care caracteristicile extrase din accelerometru și giroscop contribuie la distingerea diferitelor activități, inclusiv mersul pe jos, urcarea, coborârea, poziția așezat, statul în picioare, poziția culcat și, de asemenea, oferă o metodă analitică folosită în acest scop. Apoi, o metodă de învățare automată supravegheată, algoritmul arborilor decizionali, este adoptată pentru a crea un clasificator care să recunoască activitățile fizice pe baza caracteristicilor extrase. În final, performanțele clasificatorului construit sunt evaluate și comparate cu alte metode. Evaluarea performanței arată că acest clasificator antrenat de algoritmul arborilor decizionali este mai performant decât alți algoritmi, iar rata sa de recunoaștere globală ajunge la 93,75%. În plus, abordarea noastră are și un potențial puternic pentru aplicații în textilele inteligente.

Cuvinte-cheie: recunoașterea activităților fizice, arbori decizionali, textile inteligente, analiza caracteristicilor

INTRODUCTION

Wearable technologies and smart textiles have gained popularity in recent years, especially for constant supervision of human health or rehabilitation. Some of the related works focused on monitoring body parameters (e.g., blood pressure and heart rate) [1], while some others were absorbed in body posture recognition [2]. By means of wearable technology, another topic worthy of attention is physical activity (e.g., standing, sitting and walking) recognition (PAR), which can also be illustrated as one measure of biomechanical or biomedical tasks of our population as well as body posture [2]. For instance, suggested bending ranges of the human spine are varied with physical activities, hence, whether the spine bending angle is appropriate should be considered together with the physical activity at that time.

In order to recognize the physical activity, various approaches have been proposed in the past decades, and most of them were realized by conducting vision computing [3]. Obviously, visual-based recognition is not suitable for wearable products. Some other works based on audio [4] or radio [5] technologies own potentials for applying to smart textiles, but environment or multi-sensors dependent characteristics discourage users from participating in the PAR [6]. Single or few sensors based wearable technology should be a good choice for PAR with advantages of low-cost, low-energy and low-complexity, and it is most likely to be integrated into textiles. Some previous research utilized an independent accelerometer [7] or a set of accelerometers and gyroscopes embedded in the smartphone [8] with some supervised machine learning algorithms to realize recognition. From the works, we can find that data acquisition by a set of accelerometers and gyroscope, which can be integrated into smart textiles, do contribute to PAR, but data analysis methods can still be improved to promote recognition rates.

In this study, we proposed a new alternative that combines features reduction and random forest algorithm to analyse data from the work of Anguita et al. [8],
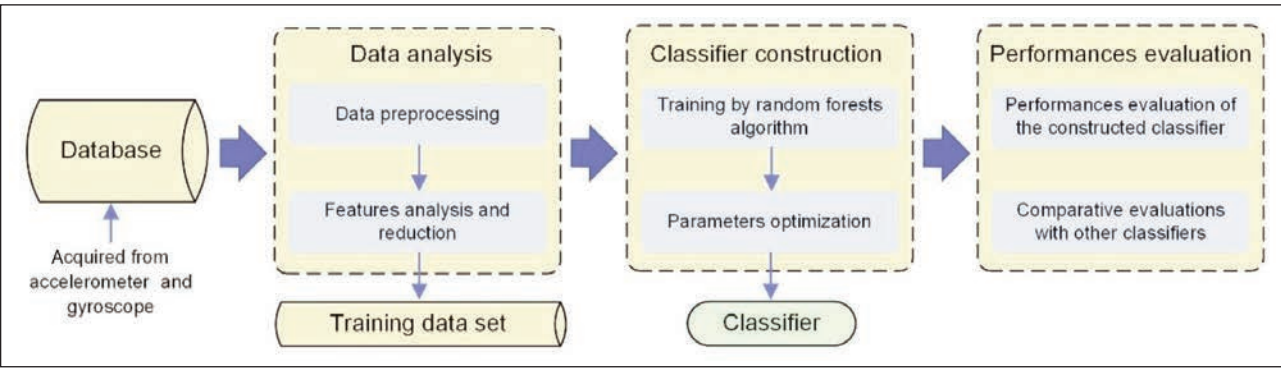
Fig. 1. The flowchart of the proposed methodology

which aims to create a more effective classifier for PAR and improve practicality of wearable accelerometer and gyroscope for PAR. The flowchart of the proposed methodology is shown in figure 1. At first, numerous features extracted from the database are analysed for capabilities of distinguishing different activities (including walking, walking upstairs, walking downstairs, sitting, standing, laying), and the principal features with main contributions to PAR are explored. Then, a supervised machine learning method, random forest (RF) algorithm, is adopted to create a classifier to recognize physical activities based on the extracted features. Lastly, the performances of the constructed classifier are evaluated and compared with other methods to demonstrate the effectiveness of our approach.

BACKGROUND OF RANDOM FOREST

Random forest, which is a variant of the decision tree-based bagging technique [9], is commonly used for regressions, classifications and cluster problems [10]. The main idea of RF is generating results by a simple unweighted average over a series of independently decision trees [11] that are trained based on samples by sampling with replacement and features by sampling without replacement, as shown in figure 2, and the steps are listed as follow.
1. Randomly draw n sets of samples from the data set with replacement, and the number of samples in each set is the same with original data set. Meanwhile, m features in each set are randomly selected from all features without replacement, and features in different sets may be different.
2. Decision trees are grown, based on the corresponding drawn samples and features, in the light of the minimum Gini index as below.

$$I_G(t_{x(x_i)}) = 1 - \sum_{j=1}^{M} f(t_{x(x_i)}, j)^2 \qquad (1)$$

where $f(t_{x(x_i)}, j)$ denotes the proportion of samples that belongs to the leaf j while node t has the value x_i.
3. The classifier is built on the so-called forest, that is composed of the grown decision trees, by unweighted voting as below

$$\overline{T}(x) = \frac{1}{N} \sum_{k=1}^{N} T_k \qquad (2)$$
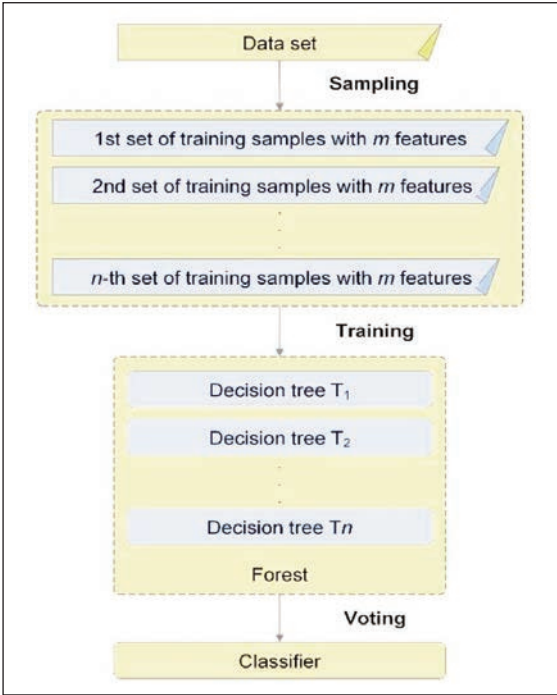
Fig. 2. The flowchart of random forest

where T_k indicates the k-th decision tree.

FEATURES ANALYSIS

Data acquisition and pre-processing

In this study, the adopted human activity recognition data set was created by Anguita et al. [8]. All data, in terms of 3-axial linear acceleration and 3-axial angular velocity at a constant rate of 50 Hz, came from the accelerometer and gyroscope embedded in smartphones worn on the waist by 30 volunteers, who are in an age bracket of 19–48 years. The collected data went through a transformation process, including noise filtering, time-domain analysis and frequency domain analysis, and 35 kinds of signals were obtained as listed in table 1. Then, a set of 561 features were estimated from these signals by conducting a series of mathematical operations listed in table 2. For examples, body acceleration signals in X direction ('tBodyAcc-X' in table 1) can be averaged ('mean()' in table 2) to generate a feature named 'tBodyAcc-mean()-X'.

Table 1

	DESCRIPTION FOR OBTAINED SIGNALS	
Code	**Name**	**Descriptions**
0-2	tBodyAcc-XYZ	X,Y,Z-dimensional time domine signals of body linear acceleration
3-5	tGravityAcc-XYZ	X,Y,Z-dimensional time domine signals of acceleration of gravity
6-8	tBodyAccJerk-XYZ	X,Y,Z-dimensional time domain signals of body linear jerk
9-11	tBodyGyro-XYZ	X,Y,Z-dimensional time domain signals of body angular velocity
12-14	tBodyGyroJerk-XYZ	X,Y,Z-dimensional time domain signals of body angular jerk
15	tBodyAccMag	Magnitude of three-dimensional time domine signals of body linear acceleration was calculated by conducting Euclidean norm
16	tGravityAccMag	Magnitude of three-dimensional time domine signals of acceleration of gravity was calculated by conducting Euclidean norm
17	tBodyAccJerkMag	Magnitude of three-dimensional time domine signals of body linear jerk was calculated by conducting Euclidean norm
18	tBodyGyroMag	Magnitude of three-dimensional time domine signals of body angular velocity was calculated by conducting Euclidean norm
19	tBodyGyroJerkMag	Magnitude of three-dimensional time domine signals of body angular jerk was calculated by conducting Euclidean norm
20-22	fBodyAcc-XYZ	X,Y,Z-dimensional frequency domine signals of body linear acceleration
23-25	fBodyAccJerk-XYZ	X,Y,Z-dimensional frequency domain signals of body linear jerk
26-28	fBodyGyro-XYZ	X,Y,Z-dimensional frequency domain signals of body angular velocity
29-31	fBodyGyroJerk-XYZ	X,Y,Z-dimensional frequency domain signals of body angular jerk
32	fBodyAccMag	Magnitude of three-dimensional frequency domine signals of body linear acceleration was calculated by conducting Euclidean norm
33	fBodyAccJerkMag	Magnitude of three-dimensional frequency domine signals of body linear jerk was calculated by conducting Euclidean norm
34	fBodyGyroMag	Magnitude of three-dimensional frequency domine signals of body angular velocity was calculated by conducting Euclidean norm
35	fBodyGyroJerkMag	Magnitude of three-dimensional frequency domine signals of body angular jerk was calculated by conducting Euclidean norm

Table 2

	DESCRIPTION FOR SIGNAL OPERATORS	
Code	**Name**	**Descriptions**
1	mean( )	Mean value
2	std( )	Standard deviation
3	mad( )	Median absolute deviation
4	max( )	Largest value in array
5	min( )	Smallest value in array
6	sma( )	Signal magnitude area
7	energy( )	Energy measure. Sum of the squares divided by the number of values.
8	iqr( )	Interquartile range
9	enntropy( )	Signal entropy
10	arCoeff( )	Autoregresion coefficients with Burg order equal to 4
11	correlation( )	Correlation coefficient between two signals
12	maxInds( )	Index of the frequency component with the largest magnitude
13	meanFreq( )	Weighted average of the frequency
14	skewness( )	Skewness of the frequency domain signal
15	kurtosis( )	Kurtosis of the frequency domain signal
16	bandsEnergy( )	Energy of a frequency interval within the 64 bins of the FFT of each window
17	angle( )	Angle between to vectors

Meanwhile, human activities were also recorded by video, which were utilized for labelling acquired data. 10297 items of activities were labelled and classified into six categories in terms of laying (1944 items), standing (1906 items), sitting (1777 items), walking (1722 items), walking upstairs (1542 items), walking downstairs (1406 items). In a word, there are 10297 items of labelled activities with 561 features for descriptions in the data set.

Features analysis and reduction

More features would boost the potential for discriminating different physic activities, but they also increase the computational load. In order to reduce computational load without decreasing the ability of PAR, the validity of features was verified at first, and useless features were eliminated.

In the verification, histograms were utilized to visualize descriptive characteristics of the features for different activities. Abscissa and ordinate in the histogram respectively indicate the normalized value of the selected feature and a corresponding number of activities, while different types of activities are discriminated by colours. From the histograms of some features, we can find that distributions of some types of activities are significantly different from others, and it means these types of activities can be recognized by the features. For example, as shown in figure 3, the feature "angle(X,gravityMean)" is particularly suitable for distinguishing 'laying' from other activities, and the feature "fBodyAcc-entropy()-X" can be used for distinguishing between static activities (i.e., "sitting",

"standing" and "laying") and dynamic activities (i.e., "walking", "walking upstairs" and "walking downstairs"). By contrast, some features are hardly utilized for recognition due to similarities of different distributions in the histograms, some distributions are so similar that the corresponding feature cannot own the ability of recognition, such as the features "fBodyBodyGyroJerkMag-kurtosis()" and "fBodyBody GyroMag-skewness()" in figure 4. The similarity of any two distributions in the histogram of a feature be quantitatively measured by equation 3.

$$S = \frac{\sum_{i=1}^{N}\left[(H_1(i) - \overline{H}_1) \cdot (H_2(i) - \overline{H}_2)\right]}{\sqrt{\sum_{i=1}^{N}(H_1(i) - \overline{H}_1)^2 \cdot \sum_{i=1}^{N}(H_2(i) - \overline{H}_2)^2}} \quad (3)$$

where denotes the number of activities (i.e., ordinate value) corresponding to the *i*-th bin (range of abscissa value are divided into *N* bins) in the distribution 1, and $\overline{H}$ is the mean values calculated as below.

$$\overline{H} = \frac{\sum_{i=1}^{N} H_1(i)}{N} \quad (4)$$

In equation 3, *S* approaching 1 indicates the greater the correlation between the two distributions, and if *S* is negative, it indicates that the feature has a strong ability to distinguish between the two distributions. Thus, by pairwise comparison of the distributions caused by six types of activities in the histogram of a feature, we can generate the confusion matrix of similarities for judging the ability of PAR of the feature, as shown in figure 3 and 4. After analysis, 64 features were eliminated because of low contributions to PAR.

a

b
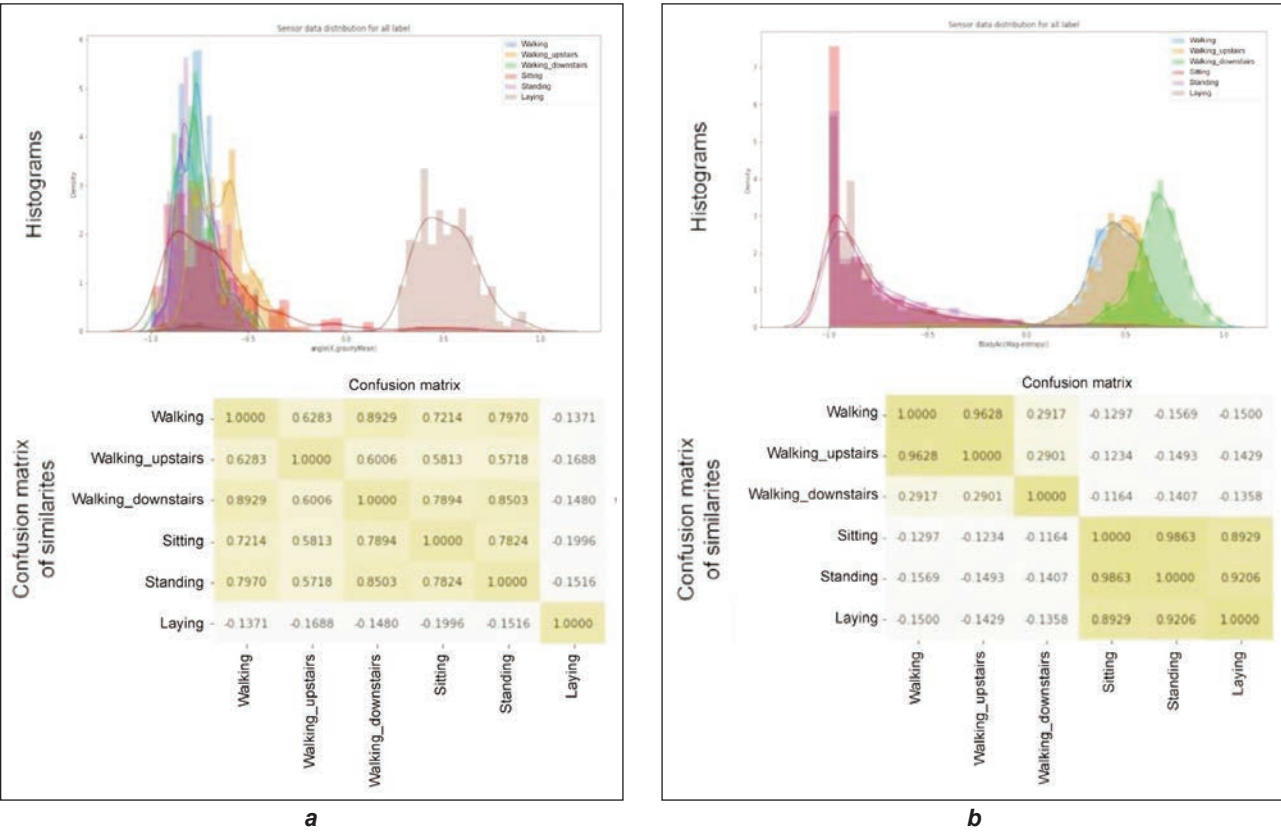
Fig. 3. Histograms and confusion matrix of similarities of the features with high contributions to PAR, including:
a – angle(X,gravityMean); *b* – fBodyAcc-entropy()-X
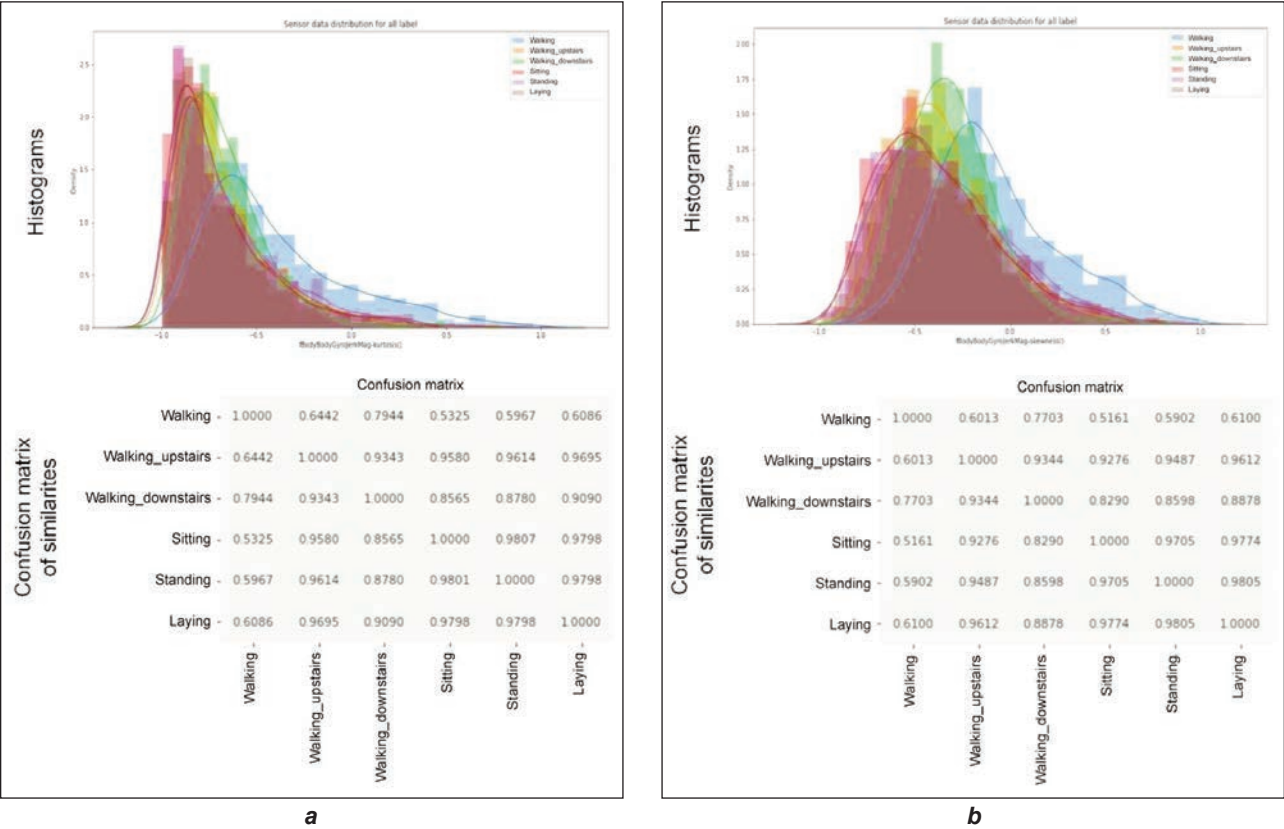
Fig. 4. Histograms and confusion matrix of similarities of the features with low contributions to PAR, including:
a – fBodyBodyGyroJerkMag-kurtosis(); *b* – fBodyBodyGyroMag-skewness()

CLASSIFIER CONSTRUCTION AND EVALUATION

In the construction of the classifier, at first, the obtained data set is divided into a training subset and test subset according to the ratio of 7:3. Next, based on the training subset, parameters of random forest algorithm were optimized to generate a classifier for PAR. Then, the performance of the classifier was evaluated based on test subset. Finally, a comparison experiment with other commonly used classifiers, including support vector machines (SVM) [12], k-nearest neighbour classification(KNN) [13], multilayer perceptron (MLP) [14] and quadratic discriminant analysis (QDA) [15], was conducted. The detailed descriptions are given in the following subsections.

Classifier training by random forest

The classifier for PAR was trained by random forest algorithm based on training subset. During the training process, two important parameters, including the number of decision trees *n_tree*, and the max number of features used for growing a tree *max_features*, need to be determined. In usual, *max_features* is decided by "sqrt" or "log2", in other words, *max_features* can be square root or base 2 logarithm of total number of features, and which one is better needs to be compared. The optimal value of *n_tree* can be achieved by traversing possible values. Thus, as shown in figure 5, we have plotted curves that reflect
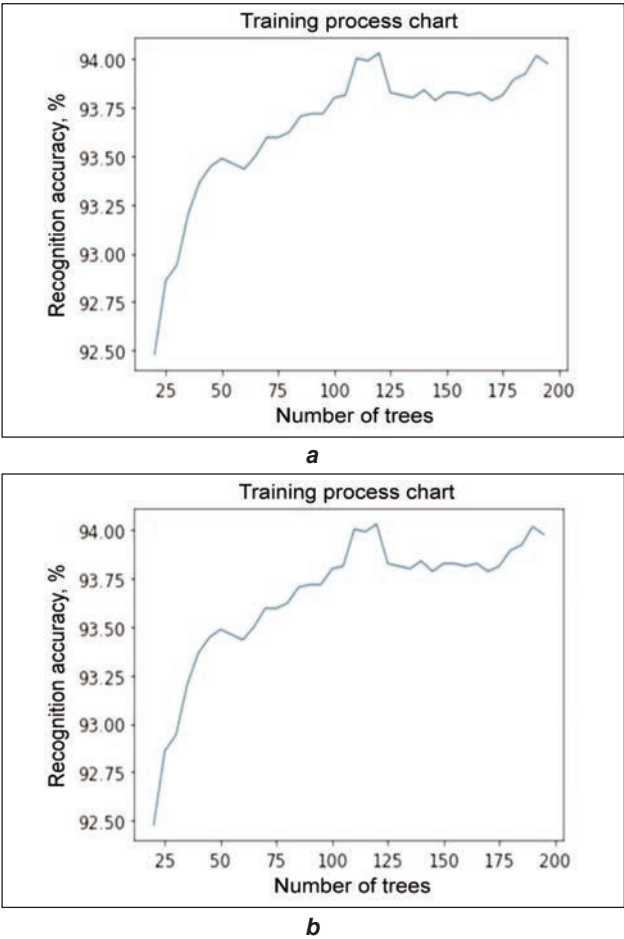
Fig. 5. Iteration curves of training by random forest with different max_features decided by: *a* – "log2"; *b* – "sqrt"

the training accuracy varies with the *n_tree* respectively under the *max_features* determined by "sqrt" and "log2".

RECOGNITION RATES OF THE ACTIVITIES		
Labels	Number of samples	Recognition rate (%)
Laying	537	100
Standing	533	97.00
Sitting	490	89.80
Walking	496	97.58
Walking upstairs	471	92.57
Walking downstairs	420	83.09
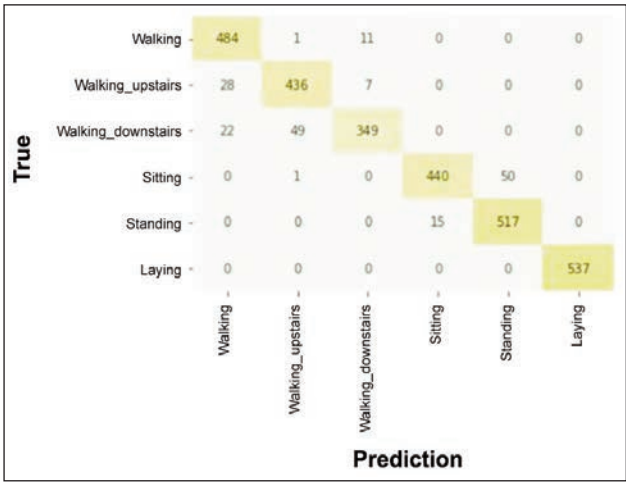
Fig. 6. Confusion matrix of prediction performance

COMPARISON RESULTS OF CLASSIFIERS TRAINED BY DIFFERENT ALGORITHMS					
Indicator	RF	SVM	KNN	MLP	QDA
Recognition rate	93.34%	91.49%	87.37%	89.57%	78.78%

From the curves, we can find that the best recognition rate is 94.03% corresponding to *n_tree* =120 on the conditions of *max_features* decided by "log2", while the best recognition rate is 93.24% corresponding to *n_tree* = 125 on the conditions of *max_features* decided by "sqrt". Obviously, the curve from figure 5, *a* can achieve better result than curve from figure 5, *b*. Thus, the optimized parameters can be determined as follow: *n_tree* = 125; *max_features* = round($\log_2 497$) = 9, where 497 derives from that 561 (total number of features) subtracts 64 (eliminated features).

Performance evaluation

Through the application of the trained classifier on the test subset, we find that the overall recognition rate of the classifier reached 93.75%, of which the recognition rates for the six physical activities are listed in table 3, and more details are presented by the confusion matrix as shown in figure 6.

The test results show that the classifier has achieved a good recognition rate for dynamic activities, static activities, and single-type activity. Among them, the trained classifier has the best ability to recognize "laying", and the recognition rates of "standing", "walking" and "walking upstairs" are all above 90%, while the recognition rate of "sitting" is approximate to 90%. Although the recognition rate of "Walking downstairs" is only 83.09%, it is still at a relatively high level. In addition, the recognition rate of the classifier on the test subset is close to the recognition rate on the training subset, which indicates the trained classifier has a strong generalization ability.

In order to further evaluate the performances of the classifier, we compare the current classifier with the classifiers trained by other common algorithms, including SVM, KNN, MLP and QDA, based on the same training set. The comparison result is listed in table 4.

From the results, it is easy to find that the classifier trained by random forest has better performances than others.

CONCLUSIONS

In order to improve the practicality of wearable accelerometers and gyroscopes for physical activities recognition, we have proposed an approach that combines features reduction and random forest algorithm to boost the recognition rate. The test has shown the classifier trained by random forest algorithm are better than other algorithms, and its overall recognition rate reaches 93.75% which means this kind of scheme has strong feasibility.

In addition, wearable accelerometers and gyroscopes can be integrated into smart textiles, some examples were created by other researchers [16, 17], which means our approach has strong potential for applications in smart textiles. It is worth mentioning that data and features for recognitions should be different if wearable sensors are embedded in the smart textiles placed on different parts of the body, but we think our approach can still deal with them and achieve a good result.

Therefore, in the future, works can be focused on the following aspects.

1. Make a series of wearable sensors embedded in smart textiles and collect more data from them to prove the feasibility of applications in smart textiles and further improve the recognition rate of the classifier.

2. Pay attention to recognize other physical activities besides the six existing ones, such as running and jumping.

REFERENCES

[1] Quandt, B.M., Scherer, L.J., Boesel, L.F., Wolf, M., Bona, G.L., Rossi, R.M., *Body-Monitoring and Health Supervision by Means of Optical Fiber-Based Sensing Systems in Medical Textiles,* In: Advanced Healthcare Materials, 2015, 4, 3, 330–355

[2] Abro, Z.A. , Zhang, Y.F. , Chen, N.L., Hong, C.Y. , Lakho, R.A. , Halepoto, H., *A novel flex sensor-based flexible smart garment for monitoring body postures,* In: Journal of Industrial Textiles, 2019, 49, 2, 262–274

[3] Jalal, A., Kim, Y.H., Kim, Y.J., Kamal, S., Kim, D., *Robust human activity recognition from depth video using spatiotemporal multi-fused features,* In: Pattern Recognition, 2017, 61, 295–308

[4] Chahuara, P., Fleury, A., Vacher, M., *On-line human activity recognition from audio and home automation sensors: comparison of sequential and non-sequential models in realistic smart homes,* In: Journal of Ambient Intelligence & Smart Environments, 2016, 8, 4, 399–422

[5] Wang, S., Zhou, G., *A review on radio-based activity recognition,* In: Digital Communications & Networks, 2015, 1, 1, 20–29

[6] Voicu, R.A., Dobre, C., Bajenaru, L., Ciobanu, R.I., *Human physical activity recognition using smartphone sensors,* In: Sensors, 2019, 19, 3, 458

[7] Mannini, A., Sabatini, A.M., *Machine learning methods for classifying human physical activity from on-body accelerometers,* In: Sensors, 2010,10, 2, 1154–1175

[8] Anguita, D., Ghio, A., Oneto, L., Parra, X., Reyes-Ortiz, J.L., *A Public Domain Dataset for Human Activity Recognition Using Smartphones,* In: 21th European Symposium on Artificial Neural Networks, Computational Intelligence and Machine Learning, ESANN 2013, Bruges, Belgium, 24–26 April 2013, Available at: http://archive.ics.uci.edu/ml/datasets/Human+Activity+Recognition+Using+Smartphones [Accessed on January 27, 2021]

[9] Dietterich, T.G., *An experimental comparison of three methods for constructing ensembles of decision trees: bagging, boosting, and randomization,* In: Machine Learning, 2000, 40, 2, 139–157

[10] He, Z., Tran, K.-P., Thomassey, S., Zeng, X., Xu, J., Yi, C.H., *Modeling color fading ozonation of reactive-dyed cotton using the Extreme Learning Machine, Support Vector Regression and Random Forest,* In: Textile Research Journal, 2020,90, 7–8, 896–908

[11] Myles, A.J., Feudale, R.N., Liu, Y., Woody, N.A., Brown, S.D., *An introduction to decision tree modelling,* In: Journal of Chemometrics, 2004,18, 6, 275–285

[12] Andrew, A.M., *An introduction to support vector machines and other kernel-based learning methods*, In: Kybernetes, 2001, 32, 1, 1–28

[13] Kramer, O., *K-nearest neighbors,* In: Intelligent Systems Reference Library, 2013, 41, 2, 13–23

[14] Rynkiewicz, J., *Introduction to multilayer perceptron and hybrid hidden Markov models,* In: Lesage, C., Cottrell, M. (eds) Connectionist Approaches in Economics and Management Sciences. Advances in Computational Management Science, Springer, Boston, 2003, 6

[15] James, G., Witten, D., Hastie, T., Tibshirani, R., *An Introduction to Statistical Learning: With Applications in R*, Springer Texts in Statistics, 2013, 149–151.

[16] Younes, R., Hines, K., Forsyth, J., Dennis, J., Martin, T., Jones, M., *The design of smart garments for motion capture and activity classification*, In: Smart Textiles and their Applications, 2016, 627–655

[17] Li, M., Torah, R., Nunes-Matos, H., Wei, Y., Beeby, S., Tudor, J., Yang, K., *Integration and Testing of a Three-Axis Accelerometer in a Woven E-Textile Sleeve for Wearable Movement Monitoring,* In: Sensors*, 2020, 20, 18, 5033

Authors:

ZHANG JUNJIE[1], CAI SHENGHAO[1], XU JIE[2], YUAN HUA[3]

[1]Engineering Research Center of Hubei Province for Clothing Information, School of Mathematics and Computer Science, Wuhan Textile University, 430073 Wuhan, China

[2]School of Textile Science and Engineering, Wuhan Textile University, 430073 Wuhan, China

[3]Wuhan Textile and Apparel Digital Engineering Technology Research Center, School of fashion, Wuhan Textile University, 430073, Wuhan, China

Corresponding authors:

XU JIE
e-mail: jxu@wtu.edu.cn

YUAN HUA
e-mail: 2019009@wtu.edu.cn

Effect of washing and temperature on electrical properties of conductive yarns and woven fabrics

SULTAN ULLAH
HASSAN IFTIKHAR AHMED

SYED TALHA ALI HAMDANI

ABSTRACT – REZUMAT

Effect of washing and temperature on electrical properties of conductive yarns and woven fabrics

In our daily life, the temperature and washing parameters go unnoticed on the electrical properties of conductive yarns and woven fabrics. However, in many cases, these parameters play a crucial role in the use of conductive materials since they modify their electrical properties. It is critical to predict what this behaviour will be, as these washing and, in our temperature, parameters can improve or even deteriorate desirable properties in the materials, especially of sensors embedded textiles. The weight of the conductive samples was decreased up to 11% for silver-coated and 7.75% for gold-coated yarn after washing. The results suggest that the electrical resistance of yarns increases 1.6%, 8%, and 8.7% for silver-coated while 13%, 20%, and 21% increase in resistance value for gold-coated yarn after 1st, 2nd, and 3rd wash, respectively. The silver-coated yarn has better electrical conductance, and ageing does not affect the electrical resistance of both silver-coated yarns and fabrics till two washes and a slight change occurred after 3rd wash. The woven structure's mass per unit area decreases up to 7.69% and 3.7% for silver-coated and gold-coated samples, respectively. Woven samples conductivity for silver-coated structures decreased 95% and 98% for gold-coated structures.

Keywords: *conductive yarns, woven structures, electrical resistance, ageing, conductive textiles*

Influența ciclurilor de spălare și a temperaturii asupra proprietăților electrice ale firelor și țesăturilor conductive

În viața noastră de zi cu zi, temperatura și parametrii de spălare trec neobservați în ceea ce privește proprietățile electrice ale firelor și țesăturilor conductive. Cu toate acestea, în multe cazuri, acești parametri joacă un rol crucial în utilizarea materialelor conductive, deoarece modifică proprietățile electrice. Este esențial să preconizăm care va fi acest comportament, deoarece aceste spălări și la temperatura stabilită, pot îmbunătăți sau chiar deteriora proprietățile dorite ale materialelor, în special ale textilelor cu senzori integrați. După spălare, greutatea probelor conductive a fost redusă până la 11% pentru firele acoperite cu argint și 7,75% pentru firele acoperite cu aur. Rezultatele sugerează că rezistența electrică a firelor crește cu 1,6%, 8% și 8,7% pentru cele acoperite cu argint, în timp ce valoarea rezistenței pentru firele acoperite cu aur crește cu 13%, 20% și 21% după prima, a doua și a treia spălare. Firul acoperit cu argint are o conductanță electrică mai bună, iar îmbătrânirea nu afectează rezistența electrică atât a firelor cât și a țesăturilor acoperite cu argint, până la două spălări, iar după a treia spălare a avut loc o ușoară modificare. Masa structurii țesute per unitatea de suprafață scade până la 7,69% și, respectiv, 3,7% pentru probele acoperite cu argint și respectiv cu aur. Conductivitatea probelor țesute pentru structurile acoperite cu argint a scăzut cu 95% și 98% pentru structurile acoperite cu aur.

Cuvinte-cheie: *fire conductive, structuri țesute, rezistență electrică, îmbătrânire, textile conductive*

INTRODUCTION

Smart textiles or e-textiles are fibres, yarns, or fabrics that enable digital components such as batteries, light, and electronics to embed in them. Smart materials add a function to the textiles called e-textiles. This idea was generated in Japan for the first time in 1989. These are those categories of textiles having the ability to sense a change in environment and respond to them in a designed manner. This change in environment and the response both are electrical, thermal, chemical, or other bases. Smart textiles have extensive applications in the field of clothing. Smart clothing conveys, transmits, and drives the signals from one part of a structure into the other. Smart textiles are intelligent textiles that can sense and

react to environmental stimuli. E-textile system is fabricated by the development of electrical devices like sensors, energy harvesting, actuators, storage items, etc. [1]. Smart textiles interact with the environment and such e-textiles are existing in different shapes and compositions (woven, knitted, or non-woven) [2]. The term e-textiles representing the class of fabric structures that sense and respond to environmental changes and multifaceted surroundings for e-textiles is shown in figure 1.

Wet spinning and melt spinnings are the processes/methods of fibre preparation which is electrically conductive [4]. The type of materials, fibre configuration, and fibre arrangement are the main factors for determining the performance of smart textiles [5].

Textiles "Smart Clothing"	Electrical Engineering "Wearable Electronics'	Information Science "Wearable Computer"

Fig. 1. Multifaceted surroundings for smart textiles [3]

Conductive fibres may also have electrical as well as delivering good antimicrobial, anti-static, and electromagnetic shielding properties [6]. Conducting polymers/fibres made from the thermosetting materials (non-thermoplastic) at low temperatures, such as fibres degrade and cannot be remelted or reused. A materials/fibres electrical conductivity would be superior to the less dense fibres and vice versa [7]. The electrical properties of materials were once solely assigned within the scope of electronic engineering and science applications. Such properties have now been incorporated into smart textiles or e-textiles, and they are found crucial in certain types of fibres, yarns called electrically conductive yarns. There are several processes for producing electrically conductive yarns. In staple yarns, it is possible to spin short strands of regular yarns with metal yarns. However, the most important method to produce conductive yarn is coating a base yarn with metalized material. Such as coating silver on base polymer, including polyester or polyamide. They can also be produced from nanoparticles such as carbon nanotubes. The temperature (ageing process, physical properties of the structures changes due to heat/temperature factor and it's as important to benefit the textiles), and humidity are the key parameters in the use of materials since they change their electrical properties [8]. The high value-added textiles industry is facing huge problems for e-textiles washing especially. Water and detergent solution effects on silver-coated yarns. Conductive yarn surface damages more during washing with water as compared to the detergent solution [9]. The effects of yarn surface properties for conductive lines on electrical properties have excellent stability. Small pore size yarns have better electrical performance as compared to large pores [10]. Polyethene/multi-walled carbon nanotube coated polyester yarns are made into conductive woven/knitted fabrics. It was observed that these conductive yarns have the lowest electrical resistivity and stabilizing structure [11]. In recent years, the synthesis of lightweight, and flexible materials for electronic textile applications has been increased extensively. Materials like conductive copper wire E-yarn have been found similar application properties and failed after 25 cycles of washing. E-yarn containing Vectran which has high strength fail after more than 15 cycles of washing and tumble-drying. Silver coated were found the best among all conductive yarns due to their electrical properties and flexibility [12]. Features of the electrical charging and dissipation of charges in fabrics containing conductive yarns after washing. Electrical resistance and surface resistivity are the parameters whose values are sensitive to the number of conductive yarns in the fabrics. EMI shielding, lightweight batteries, and molecular electronic devices are made of conductive fabrics [13]. This work is carried out to investigate the effect of temperature and washing on electrical properties of conductive yarns and woven structures for many wearable electronics applications like textile-based sensors, garments, baby suits, military suits, smart socks, etc.

MATERIALS

Conductive polyester yarns plasma coated with gold and silver particles provided by SWICOFIL, Switzerland was used as weft yarns to save the yarn conductivity and breakage. The details of these conductive yarns are provided in table 1. All the conductive yarns provided by SWICOFIL were already coated with silver and gold using the plasma coating technique. Coating a filament yarn by the plasma coating method gives much better wear, a perfect level coating, and little to no conductivity fluctuation compared to usual techniques of coating yarn with metal.

8/1 Ne Polyester yarn was used as warp yarn and warping of 1.5 m was completed on a sample warping machine (CCI LUTAN 2.500). Polyester was chosen for warp yarn due to its low water absorption.

Table 1

SPECIFICATIONS OF CONDUCTIVE YARNS USED IN THE WEFT DIRECTION						
Sr. no.	Substrate	Count	Resultant/ measured dtex	Metal	Characteristic name (mg/m)	Electrical resistance (Ohm/cm)
S1	PET FDY*	dtex (150) f (48) (Z) (60) (pre-twist)**	174	Ag	2.5	5
S2	PET FDY	dtex 150 f 48 Z200 (60 pre; 140 post-twist)	176	Ag	2.7	3–5
S3	PET high ten.	dtex 440 f 96 S 80 rauh special construction	444	Ag	14	0.26
S4	PET FDY	dtex 150 f 48 S 60	172	Au	2.15	30

Note: *Fully drawn yarn; **count (value) number of filaments f (value) direction of twist (Z/S) (number of twists) (additional remarks).

DESIGN OF EXPERIMENT

The electrical properties of the sized yarn and the sized fabric were measured after each wash and subjected to ageing after each wash. A total of three washes was done. The weight of the yarn and fabric was measured before and after wash. The areal contraction was also measured. Four samples S1, S2, S3, S4 were weaved having the same weave design, material, and ends/inch and picks/inch. To produce the fabric samples, a semi-automatic loom as shown in figure 2, was used and four samples were prepared by the 4/1 satin weave method of 5 inches width and the length of each sample is 4 inches as shown in figure 2, *b*. 50 dents per inch reed were used.

a

b

Fig. 2. Graphical representation of: *a* – semi-automatic weaving loom used for sample preparation; *b* – sample top view

METHODOLOGY

Sizing of both yarns and fabrics was done. The major purpose of sizing is to increase the weave ability for fabric production. It also adds to the strength of warp yarn as well as increases the frictional resistance which results in less damage of warp yarn increasing the quality of the product. Later, size materials were not removed due to the possibility of fibre attack, fibre damage, and less variety of application methods. The sizing machine and warping machine details are shown in table 2. The sizing chemicals are shown in table 3.

Table 2

SIZING, AND WARPING MACHINE SPECIFICATIONS

Sr. no.	Name	Model	Manufacturer
1	Sizing machine	SS-5600	TAIWAN
2	Warping machine	LUTAN-2.500	TAIWAN

Table 3

CHEMICAL'S SPECIFICATIONS

Sr. no.	Name	Function	Manufacturer
1	PVA	To provide strength	Kuraray Co. Ltd Japan
2	Starch	Binding agent	Rafhan Pvt. Ind. Pakistan
3	Softener	To make yarn pliable	BASF Co. Ltd Pakistan

To size the given yarn samples, first, the size recipe was prepared by adding 50 grams of polyvinyl alcohol in 200 litres of water along with 2% starch. Then the recipe was fed to the single-end sizing machine. A 1000 meters length of sized yarn was produced. Washing of yarn was done manually at room temperature. The warm water of 40° was taken in a 100 ml beaker. 1 gram of detergent was added to the beaker. A yarn sample of 30 cm length was cut and added to the beaker. The water was stirred for 20 minutes. After that yarn could dry.

The fabric was washed by using NaOH detergent in the process for 40 minutes at 40°C having a speed of 25 cycles/min was done according to the standard: ISO 6330:2012 by wascator FOM71 CLS. Ageing (temperature) of samples was done after each wash. 1st ageing was done by placing the samples at room temperature for 24 hours. The second ageing is done after the second wash by the same procedure. But third ageing was done in the oven for 2 hours at 94°C temperatures.

To check the conductivity of the fabric samples before washing, we used a multimeter. The electrical resistance of single conductive yarn was measured using Keithley Source Measuring Unit 2450. This test procedure for measuring the resistance of yarns and woven fabrics was adapted according to standard AATCC 84 and AATCC 76, respectively. Resistance was noted down from 5 different places of the yarn and a mean value was calculated.

RESULTS AND DISCUSSION

The effect of temperature and hand washing on the electrical resistance of conductive yarn was measured as shown in table 4. The electrical resistance was measured after consecutive three washes. Ageing was done after each wash according to the procedure specified earlier. The results suggest that the electrical resistance of the yarn increases slightly after each wash. However, ageing does not affect the electrical resistance of conductive yarn. After washing

Table 4

Sr. no.	Sample	Electrical resistance specified by the manufacturer (Ohm/cm)	Actual measured electrical resistance (Ohm/cm)	Ageing after 1st wash (Ohm/cm)	Electrical resistance after 1st wash (Ohm/cm)	Ageing after 2nd wash (Ohm/cm)	Electrical resistance after 2nd wash (Ohm/cm)	Ageing after 3rd wash (Ohm/cm)	Electrical resistance after 3rd wash (Ohm/cm)
		EFFECT OF TEMPERATURE AND WASHING ON ELECTRICAL PROPERTIES OF CONDUCTIVE YARNS							
S1	Dtex 150 f48 z60 pre twist	5	5.5 ± 3.8	Unchanged	5.59 ± 4.9	Unchanged	6.01 ± 4.7	6.017 ± 5.2	6.03 ± 4.2
S2	Dtex 150 f48 z200 60 pre-140 pro twist	3–5	3–5 ± 2.7	Unchanged	3.3 ± 2.4	Unchanged	3.39 ± 2.1	3.41 ± 6.0	3.41 ± 2.9
S3	Dtex 440 f96 s80 rauh special construction	0.26	0.61 ± 2.5	Unchanged	0.65–0.75 ± 3.0	Unchanged	0.88 ± 4.1	0.91 ± 5.4	0.90 ± 4.4
S4	Dtex 150 f48 s60	30	30–40 ± 11.5	Unchanged	40.5 ± 12.34	Unchanged	44.1 ± 13.0	45.2 ± 11.4	44.3 ± 11.7

samples for the first time, the conductivity was measured. Conductivity check was followed by the second time wash of the samples to study the effects of washing.

All the sample's weight was measured on a digital weighing machine before and after wash as shown in table 5. The results suggest that the weight of the sample decreases by up to 11% after washing for silver-coated and 7.53% for gold-coated yarn.

The effect of temperature and washing on the electrical resistance of conductive fabric was measured as shown in table 6. After making woven conductive samples, the measured resistivity was insignificant. With a very high conductance, the minimum value of resistance remained 0.007 Ohm/cm^2 and the highest value was 0.02 Ohm/cm^2.

After the first wash, some of the conductive material was removed. But still, the fabric samples were conductive.

Table 5

Sr. no.	Sample	Mass before washing (g)	Mass after washing (g)	Percentage decrease (%)
	CHEMICAL'S SPECIFICATIONS			
S1	Dtex 150 f48 z60 pre twist	0.0185	0.00177	4.51
S2	Dtex 150 f48 z200 60 pre-140 pro twist	0.0240	0.0231	3.89
S3	Dtex 440 f96 s80 rauh special construction	0.0410	0.0369	11.11
S4	Dtex 150 f48 s60	0.0214	0.0199	7.53

Table 6

Sr. no.	Sample	Before wash resistivity (Ohm/cm^2)	After 1st wash resistivity (Ohm/cm^2)	Ageing after 1st wash (Ohm/cm^2)	After 2nd wash resistivity (Ohm/ cm^2)	Ageing after 2nd wash (Ohm/cm^2)	After 3rd wash resistivity (Ohm/cm^2)	Ageing after 3rd wash (Ohm/cm^2)
		EFFECT OF TEMPERATURE AND WASHING ON THE ELECTRICAL RESISTANCE OF WOVEN FABRICS						
S1	Dtex 150 f48 z60 pre twist	0.008	0.009	Unchanged	0.012	Unchanged	0.19	0.2
S2	Dtex 150 f48 z200 60 pre-140 pro twist	0.007	0.017	Unchanged	0.07	Unchanged	0.01	0.015
S3	Dtex 440 f96 s80 rauh special construction	0.0084	0.011	Unchanged	0.10	Unchanged	0.17	0.18
S4	Dtex 150 f48 s60	0.02	0.036	Unchanged	0.14	Unchanged	1.1	1.17

Table 7

		MASS PER UNIT AREA AND AREAL CONTRACTION BEFORE AND AFTER WASHES OF WOVEN FABRICS					
Sr. no.	Sample	Mass/area before washing (g/cm^2)	Mass/area after washing (g/cm^2)	Percentage decrease (%)	Mass/area before washing (g/cm^2)	Mass/area after washing (g/cm^2)	Contraction percentage (%)
S1	Dtex 150 f48 z60 pre twist	4.08	3.75	8.2	44.8	43.3	3.46
S2	Dtex 150 f48 z200 60 pre-140 pro twist	3.77	3.41	10.3	51.84	48.5	6.88
S3	Dtex 440 f96 s80 rauh special construction	3.67	3.25	7.69	56.6	52.7	7.09
S4	Dtex 150 f48 s60	3.047	3.47	3.7	49	47.7	2.72

As the minimum value of resistance remained 0.009 Ohm/cm^2 of sample S1 and the highest value was 0.036 Ohm/cm^2 of sample S4. The ageing after 1st wash did not affect the electrical resistance.

After the second wash, the value of resistance was increased, as it got washed. The minimum value was 0.012 Ohm/cm^2 of sample S1 and the maximum value was 0.14 Ohm/cm^2 of sample S4.

But the third wash decreased the sample's properties because a lot of conductive material was removed, and the fabric was considered still conductive. The minimum value of resistivity measured was 0.01 Ohm/cm^2 of sample S2 and the maximum 1.1 Ohm/cm^2 was of sample S4. The 3rd ageing was done by keeping the samples in the oven for 2 hours at an elevated temperature of 94°C. The results show that resistivity slightly increases by increasing the temperature of samples.

The fabric mass per unit area before wash and after three washes was measured and shown in table 7. The results suggest that a mass reduction of 10.3% maximum is attained after three washes. Whereas the maximum fabric area contraction of 7.09% is achieved. The woven samples after 3rd wash are shown in figure 3.

CONCLUSION

The effect of washing and temperature on the electrical properties of conductive yarns and fabric was measured. The fabric was constructed using
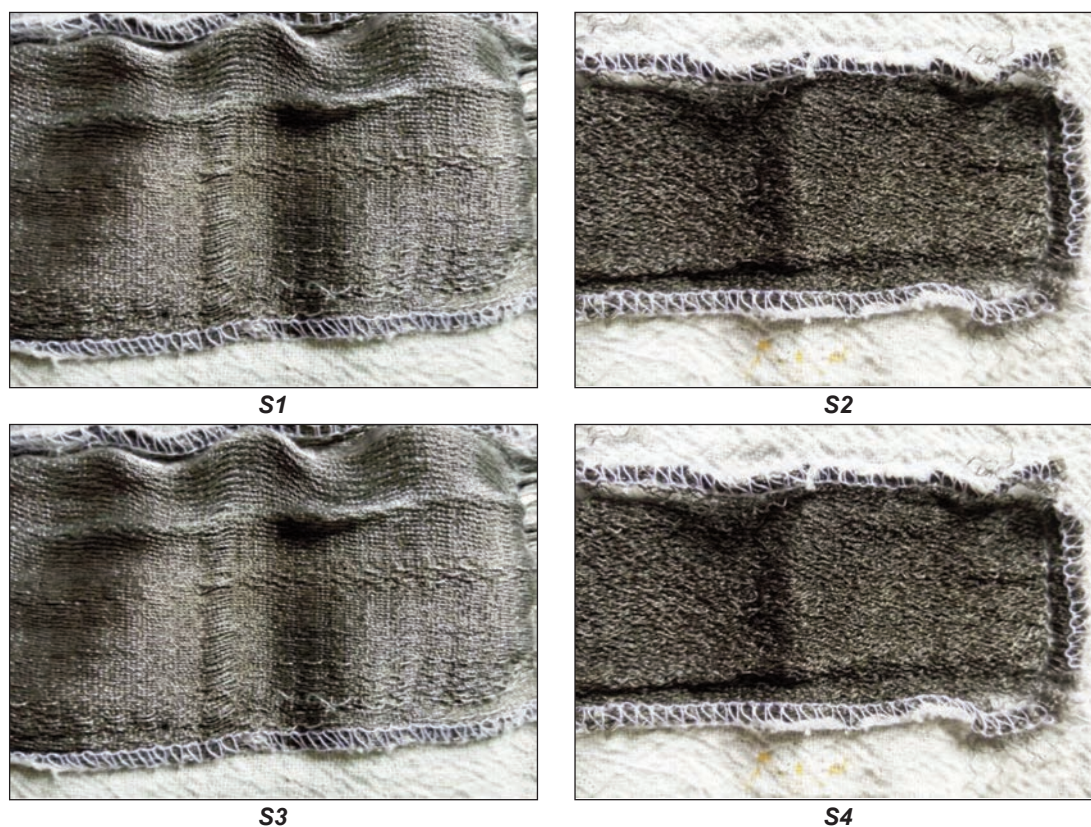
Fig. 3. Woven samples S1, S2, S3, and S4 after 3rd wash

polyester yarn as warp yarn and conductive yarn as weft yarn. Satin 4/1 weave was used for the construction of the fabric. The effect of washing on sized conductive yarn suggests that electrical resistance slightly increases, and the mass of the conductive yarn is reduced up to 11% showing conductive material is removed. The silver yarn is more conductive than gold-coated yarn. Out of four conductive fabric samples, the silver-coated sample S2 has excellent conductive properties. The rest samples also show good conductive properties but as far as conductivity is concerned, the fabric made from gold-coated yarns shows poor conductivity than fabric made from silver-coated yarns. The resistivity slightly increases after each wash. But the fabrics failed to retain and maintain the conductivity after three washes and are highly non-conductive suggesting the fabrics are wasted. The ageing after each wash does not affect electrical properties. However, ageing at an elevated temperature after the 3rd wash slightly increases the resistivity suggesting increasing the temperature of fabric decreases the conductivity of fabric. The fabric contracts after each wash and the mass per unit area are reduced after 3rd wash showing that conductive material is removed.

ACKNOWLEDGEMENT

REFERENCES

[1] Chatterjee, K., Tabor, T., Ghosh, T.K., *Electrically conductive coatings for fibre-based E-Textiles*, In: Fibers, 20197, 6, https://doi.org/10.3390/fib7060051

[2] Stoppa, M., Chiolerio, A., *Wearable electronics and smart textiles: A critical review,* In: Sensors (Switzerland), 2014, 14, 7, 11957–11992, https://doi.org/10.3390/s140711957

[3] Ghahremani Honarvar, M., Latifi, M., *Overview of wearable electronics and smart textiles*, In: J. Text. Inst., 2017, 108, 4, 631–652, https://doi.org/10.1080/00405000.2016.1177870

[4] Xue, P., Park, K.H., Tao, X.M., Chen, W., Cheng, X.Y., *Electrically conductive yarns based on PVA/carbon nanotubes,* In: Compos. Struct., 2007, 78, 2, 271–277, https://doi.org/10.1016/j.compstruct.2005.10.016

[5] Patel, P.C., Vasavada, D.A., Mankodi, H.R., *Applications of electrically conductive yarns in technical textiles*, In: IEEE Int. Conf. Power Syst. Technol. POWERCON, 2012, https://doi.org/10.1109/PowerCon.2012.6401374

[6] Raji, R.K., Miao, X., Boakye, A., *Electrical conductivity in textile fibers and yarns-review,* In: AATCC J. Res., 2017, 4, 3, 8–21, https://doi.org/10.14504/ajr.4.3.2

[7] Paiva, P., Carvalho, H., Catarino, A., Postolache, O., Postolache, G., *Development of dry textile electrodes for electromiography a comparison between knitted structures and conductive yarns*, In: Proc. Int. Conf. Sens. Technol. ICST, 2016, 3, 447–451, https://doi.org/10.1109/ICSensT.2015.7438440

[8] Torreblanca González, J., García Ovejero, R., Lozano Murciego, A., Villarrubia González, G., De Paz, J. F., *Effects of environmental conditions and composition on the electrical properties of textile fabrics*, In: Sensors, 2019, 19, 23, 5145, https://doi.org/10.3390/s19235145

[9] Ismar, E,. uz Zaman, S,. Tao, X,. Cochrane, C,. Koncar, V,. *Effect of water and chemical stresses on the silver coated polyamide yarns*, In: Fibers Polymer, 2019, 20, 12, 2604–2610, https://doi.org/10.1007/s12221-019-9266-4

[10] Hong, H., Hu, J,. Yan, X., *Effect of the basic surface properties of woven lining fabric on printing precision and electrical performance of screen-printed conductive lines*, In: Text. Res. J., 2020, 90, 11–12, 1212–1223, https://doi.org/10.1177/0040517519888251

[11] Lin, Z., Lou, C., Pan, Y., *Conductive fabrics made of polypropylene/multi-walled carbon nanotube coated polyester yarns: Mechanical properties and electromagnetic interference shielding effectiveness*, In: Compos. Sci. Technol., 2017, 141,74–82, https://doi.org/10.1016/j.compscitech.2017.01.013

[12] Hardy, D.A., Rahemtulla, Z., Satherasinghe, A., Shahidi, A., Oliveira, C., Anastasopoulos, I., Nashed, M. N., Kgatuke, M., Komolafe, A., Torah, R., Tudor, J., Hughes-Riley, T., Beeby, S., Dias, T., *Wash Testing of Electronic Yarn,* In: Materials, 2020, 13, 5, 1228, https://doi.org/10.3390/ma13051228

[13] Ahmad, S., Subhani, K., Rasheed, A., Ashraf, M., Afzal, A., Ramzan, B., *Development of conductive fabrics by using silver nanoparticles for electronic applications,* In: Journal of Electronic Materials, 2020, 49, 2, 1330–1337, https://doi.org/10.1007/s11664-019-07819-x

Authors:

SULTAN ULLAH, HASSAN IFTIKHAR AHMED, SYED TALHA ALI HAMDANI

National Textile University, Department of Weaving, Sheikhupura Road, Faisalabad 37610, Pakistan

Corresponding author:

SYED TALHA ALI HAMDANI
e-mail: hamdani.talha@ntu.edu.pk

Development and study of textile-based hydrogel wound dressing material

MICHAEL RODRIGUES   GOVINDHARAJAN THILAGAVATI

ABSTRACT – REZUMAT

Development and study of textile-based hydrogel wound dressing material

In this article, the developed textile-based hydrogel dressing is seen to be effective in terms of its exudates management capacity, strength, elongation and water vapours permeability. The usage of active antimicrobial and antibiofilm agent i.e., Usnic acid, has given it a broad-spectrum antimicrobial activity and antibiofilm property. The combination of these properties makes this dressing a better choice for the management of wounds especially chronic wounds that are infected with biofilm. The design of the experiment (BBD) used in this study is able to point at the optimal combination of the materials for the construction of such hydrogel dressings and understand the contribution of each factor used in the study.

Keywords: hydrogel, wound healing, knitted fabric, antimicrobial, biofilm, Usnic acid

Dezvoltarea și studiul pansamentului textil pe bază de hidrogel

În acest articol, pansamentul textil pe bază de hidrogel este considerat a fi eficient în ceea ce privește capacitatea de gestionare a exsudatelor, rezistența, alungirea și permeabilitatea la vapori de apă. Utilizarea unui agent antimicrobian activ și antibiofilm, adică acidul usnic, i-a conferit o activitate antimicrobiană cu spectru larg și proprietate antibiofilm. Combinația acestor proprietăți face din acest pansament o alegere mai bună pentru gestionarea rănilor, în special a rănilor cronice care sunt infectate cu biofilm. Designul experimentului (BBD) utilizat în acest studiu este capabil să indice combinația optimă a materialelor pentru realizarea unor astfel de pansamente pe bază de hidrogel și să elucideze contribuția fiecărui factor utilizat în studiu.

Cuvinte-cheie: hidrogel, vindecarea rănilor, tricot, antimicrobian, biofilm, acid usnic

INTRODUCTION

Skin is the largest organ in the human body. It plays a crucial role as a protective barrier from the external environment; prevent external noxious agents such as all type of microbes from getting inside the body. It also maintains the internal environment by the regulation of water and electrolyte balance and thermoregulation. It is crucial to keep the skin intact so that the designated functions of the skin are uncompromised. When the skin is damaged, due to any cause (mechanical injuries, ulcers, burns, neoplasm or surgical trauma) [1], there are chances of it getting infected. In that case, the body resources are wasted in fighting them.

With the advanced progress of technology, the old understanding of dry wound healing has shifted to become a new one. The new approach emphasizes the need for moist wounds for better healing. However, the moist and warm dressing may act as favourable conditions for Microbial proliferation. Bacteria and other organisms in the exudates have been studied to have an adverse effect on the wound healing process [1]. Microbial proliferation may lead to a prolonged inflammatory stage and cause infection. It may even lead to acute wounds getting converted to hard-to-heal chronic wounds. Chronic wounds are those that do not progress through a normal, orderly, and timely sequence of repair [2].

Further, prolonged infection in the wound would lead to biofilm formation. These are complex microbial colonies where the microorganisms synthesize and secrete a protective, thick and slimy matrix around them [3]. The heterogeneous communities of microbes grow in the matrix and keep spreading all over the wound. They are responsible to cause delays in the healing of wounds.

Biofilm is a major contributor to diseases that are characterized by an underlying bacterial infection and chronic inflammation e.g., periodontal disease, cystic fibrosis, chronic acne and osteomyelitis [4, 5]. Electron microscopy of biopsies from chronic wounds found that 60% of the specimens contained biofilm structures in comparison with only 6% of biopsies from acute wounds [6].

Since biofilms are reported to be a major factor contributing to multiple chronic inflammatory diseases, it is likely that almost all chronic wounds have biofilm communities on at least part of the wound bed.

The topical antiseptics that are effective on the colonies of microorganisms are not effective on the biofilms as the extra protective matrix does not allow the antiseptic to work. Thus, wound infected with biofilms needs very specific biofilm targeting substances to be able to take care of the infections.

In the present study, a wound dressing is developed that has intrinsic strength and stability of inert textile

material and it forms absorbent hydrogen dressing along with Usnic acid release which is a known antimicrobial and antibiofilm agent [7]. So, unlike the conventional hydrogel dressings, the reinforced textile dressing exhibits good strength and elongation properties that are conformable to the skin at the same time it is equally effective in exudates management of chronic wounds. The Box–Behnken design of experiment (BBD) [8] aims at understanding the best ratio of the raw materials in the construction of hydrogel dressing without limiting the antimicrobial and antibiofilm properties of the dressing.

MATERIALS AND METHODS

Sodium Alginate (SA) (MW, 20–40 kDa, CAS No. 9005-38-3), Pectin (PC) (MW, 30,000–100,000, CAS No. 9000-69-5), Usnic acids (CAS No. 79902-63-9) and Glycerol, used as a plasticizer). Phosphate Buffer (PBS) all from Sigma-Aldrich (UK). Ethanol and calcium chloride dehydrate from Swastik chemicals India). Distilled water was used in all experiments. The Polyester fibre used in the production of reinforced textile was procured from Reliance Industries, India. Knitted fabric specifications are as listed below:
• Fabric: Weft Knitted Interlock;
• Yarn: 44 DTex, number of filaments: 14;
• Machine gauge: 20, GSM: 30.
Polyester being a widely used, economical and relatively very Inert material for medical usage is the preferred material of choice. Figure 1 shows high-resolution images taken by an optical magnifying lens with the digital scale of the textile material used.

Dressing preparation

A schematic diagram representing the dressing and the cross-linking process is shown as graphical abstract in figure 2. Sodium Alginate (SA)-Pectin(PC) (1:1) composite dressings were prepared by solvent-casting method. In brief, SA and PC (1:1) were dissolved in distilled wate and then 50% (w/w) of the total dry polymer weight, glycerol was added with continuous stirring at 1000 rpm for 3 h at 40°C. Thereafter, 4 when a uniform gel (free of any undissolved particles or bubbles) was obtained, 20 ml of ethanolic Usnic Acid solution was added
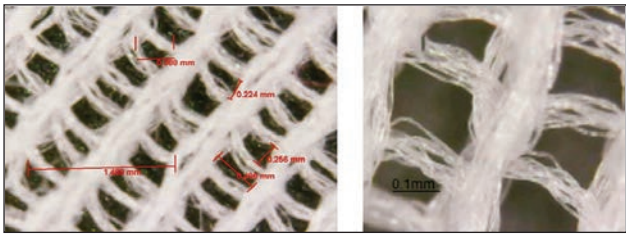
Fig. 1. Magnified image of the scaffolding fabric

to the gel. Next, 80 g of the gel was cast into a Specially designed tray along with the reinforcing fabric (figure 1). and dried in an oven at 45°C for 48 h. The dried films were uniform without any cracks or casting defects and had good flexibility required for a wound dressing application. The dressing did not curl at the edges due to the presence of reinforcing textile material in the structure. The obtained dried dressings on the reinforced fabric were labelled and stored in medical paper envelopes until further use. 15 different combinations were used to cast the dressings. Each combination was used in triplicate amounting to total of 45 dressings being formed [9].
It is only after the treatment of the dressing with calcium chloride the monovalent sodium ions are exchanged with divalent calcium ions whereby the calcium ion bounds two long chains together and forms a complex stable calcium alginate structure as schematically represented in figure 3. This figure shows a schematic diagram of the conversion of sodium alginate to calcium alginate.
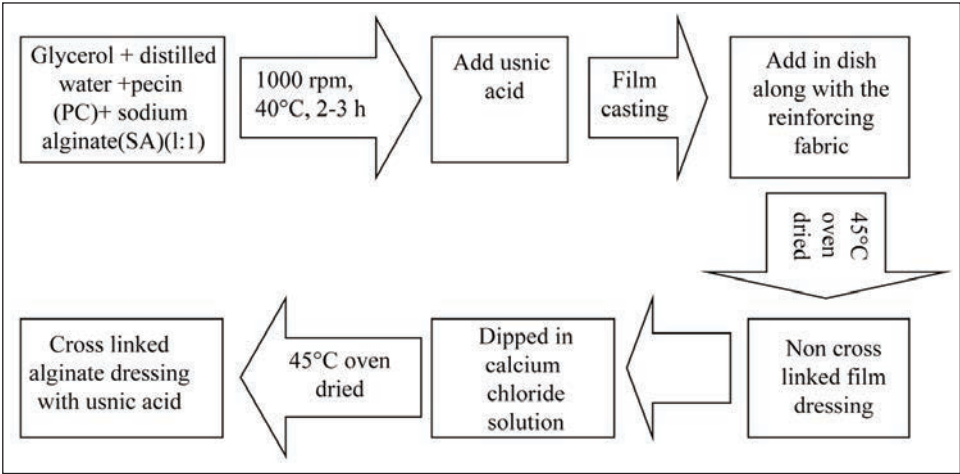
Fig. 2. Schematic representation of dressing preparation
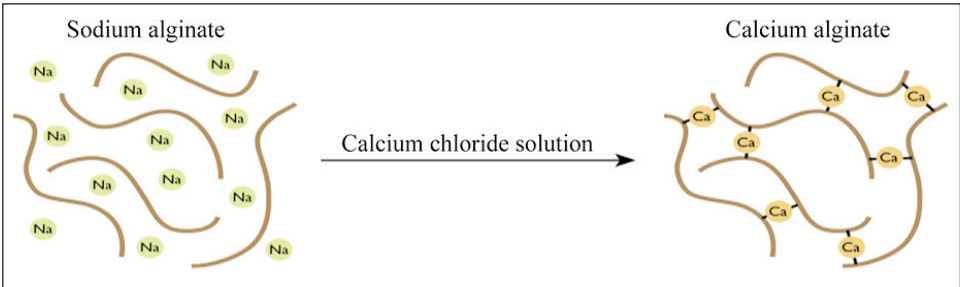
Fig. 3. Conversion of Sodium Alginate to Calcium Alginate

Preparation of cross-linked hydrogel dressing

The dressings were cross linked by immersing in 0.25% CaCl$_2$ for 1 min. Next, each dressing was rinsed by dipping in distilled water three times to remove the excess CaCl2 solution or cations that were not bound to the surface. The dressings were then immediately blot-dried using paper The dressings were then dried at room temperature for 12 h. Dried cross-linked dressings were then labelled and stored in medical grade paper envelops at room temperature until further use.

Experimental Design – Box and Behnken Design (BBD)

Design of experiment selected was Box and Behnken design for response surface curve. Here 3 factors at three different levels were studied for the various characteristics of the dressings. Thus 15 different combinations of the dressings work out for the study. The middle level combinations repeat for 3 times and thus effectively only 13 combinations need to be studied. Hence 13 combination of dressing material were used [8]. Table 1 shows the various levels of the three factors under study.

Table 1

BOX AND BEHNKEN DESIGN: FACTORS AND LEVELS			
Levels	**−1**	**0**	**+1**
X1(SA:PC) gram	16	20	24
X2(Glycerol) gram	5	10	15
X3 (Usnic Acid) gram	0.6	0.8	1.0

Methodology of evaluation

Appearance and thickness
Flexibility, colour, and transparency of the dressings were assessed visually. Thickness was evaluated using a digital calliper at 10 sites (Covering centre and edges).The mean was calculated along with its CV% (Coefficient of variation %). The sample specimens were conditioned at 25ºC and 50±5% RH (Relative Humidity) for 48 h prior to analysis.

Drug content uniformity test
To ensure the uniform distribution of drug (Usnic) within dressing, all drug-loaded samples of known mass (4 gm loaded with Usnic acid) were trimmed from random sites on different dressings marked in area as A, B, C, D and E respectively. The samples were placed in separate glass vials containing 40 ml of Phosphate buffer Solution (PBS) solvent. Vials were shaken at 50 rpm in a water bath for 4 h at 37°C, and then 10 ml of the sample solution was withdrawn. The sample solution was evaluated with Standard solutions of Usnic acid with by measuring transmittance at 290 nm by using a UV spectrophotometer (Agilent Technologies, Model-USA & G 6860 A). The transmittance of Usnic acid from the dressing samples was measured and the concentration of the Usnic acid was calculated based on the calibration curve.

In vitro release Kinetics
Extraction of dressing was done in PBS solution. PBS at pH 7.4 was used as the receptor medium. Dressings of 2.5 cm×2.5 cm, were used, which works to ~0.2 g/ml, mass/volume extraction ratio. The contents were continuously agitated (50 rpm) during extraction using incubator shaker at 37°C +/– 2°C for 24 h [10]. The test item and solvent controls were subjected to extraction conditions as described in the table 2.

After the completion of the extraction period, extracts were decanted to a container and were tested for their leachability using the UV–Vis spectrophotometer (Agilent Technologies, Model-USA & G 6860) at a wavelength of 290 nm.

Mechanical properties of the dressing
Tensile strength (TS) and percentage elongation at break (%E) of the dressings were determined by Zwick Roell, Model UTM 10KN according to the ASTM D 882-02 standard. The sample specimens were conditioned at 25°C and 50±5% RH for 48 h prior to analysis. Dressings were cut to dumbbell-shaped strips that were 30 mm long and 5 mm wide. The mechanical properties of specimens were measured by stretching the dressings at a crosshead speed of 50 mm/min to their breaking point [11]. At least five replicates from each type of dressing were used for this analysis. Tensile strength (TS) in N/mm^2, tensile strain at break (E) and Young's modulus were calculated based on the following equations:

$$TS = \text{Maximum load at break} / \text{Transverse section area} \quad (1)$$

$$E = \text{Extension of length at rupture} / \text{Initial length} \times 100 \quad (2)$$

$$\text{Youngs modulus} = \text{Tensile stress (TS)} / \text{Tensile strain (E)} \quad (3)$$

Table 2

PARAMETERS – IN VITRO RELEASE KINEMATICS			
Type of extract	**Quantity of Test Item (g)**	**Volume of Solvent added (ml)**	**Extraction conditions**
PBS pH 7.4, Solvent Control with known amount of USNIC Acid as 0.3,0.4,0.5 and 0.6 gpl	-	60	37±2ºC for 24 h drawn equally at 4 h, 8 h, 12 h, 16 h, 20 h and 24 h
PBS pH 7.4 Plus Test Item Extract	4	60	37±2ºC for 24 drawn equally at 4 h, 8 h, 12 h, 16 h, 20 h and 24 h

Water vapour transmission

In this test, a fixed amount (around 70 ml) of distilled water was taken in the containers that were holding the water at a constant temperature of 37°C +/– 2°C. The face of the containers was sealed by using the dressing without leaving any gaps by proper clamping. A cross blowing fan ensured the air velocity above the containers at a constant speed of 50 cm/sec. The containers were kept at constant temperature cabinets and were weighted at equal intervals of 4 h, 8 h, 12 h, 16 h, 20 h and 24 h. The amount of moisture loss across the dressing was evaluated by calculating the difference in weight of the containers over the period of time.

Triplicate measurements were run, and mean values were obtained. Water vapours transmission (WVT) over each interval was determined using the following equation:

$$WVT = W/S \qquad (4)$$

where W is the loss in weight of the container over the time interval and S is the exposed surface area of the dressing (m^2), WVT is expressed in $g/m^2/time$ interval. The study was conducted for 24 h to evaluate WVT as $g/m^2/24$ h.

Exudate's absorptivity and absorption profile

The artificial gelatine wound model method along with simulated wound fluid was used in this study. The study uses a similar method as used by K.H. Matthew et al. [12]. In this study, gelatine is used as the material that is mimicking the role of exudates laden wound tissues.

Each dressing was trimmed into a square shape of defined size then placed at the centre of the gelatine gel laden with simulated biofluid (in the Petri dish). The change in the diameter, cross-section area and weight of the dressings was recorded at predetermined time intervals of 4 h, 8 h, 12 h, 16 h, 20 h and 24 h. The test was performed in triplicate for each formulation and the mean value was used to calculate the expansion behaviour using the following equation:

$$\text{Percentage Exudates absorption AI (\%)} =$$
$$= (Ws - Wd)/Wd \times 100 \qquad (5)$$

where Ws and Wd are weights of the swollen wet dressing and dry dressing, respectively.

Evaluation of antimicrobial activity

The antimicrobial activity of the dressing was evaluated by using the quantitative method AATCC 100 (American Association of Textile Chemists and Colorists) [13]. The initial Inoculation chosen was 10^5 CFU/ml.

Here the test item pores with 1 ml +/– 0.1 ml of the inoculated microbial solution. Then the test item is transferred to 100 ml +/– 1 ml of 0.05% neutralizing, shacked vigorously and then made into serial dilutions with sterile water as per the timelines of the studies. This is then plated on a nutrient agar plate and incubated at 37°C for 24 hours. The material count is then taken and the number of bacterial count

reduction is expressed as the reduction percentage over the prior load incubated on the test item.

The positive control used was sterile nonwoven fabric dipped in 0.4% Benzalkonium Chloride (BKC). Eight challenge microorganisms were used and the test outcomes are as shown in table 3. The study was conducted at the lowest level of Usnic acid (0.6 grams in 20 ml).

Biofilm inhibition assay

The methodology used here was adapted from Luciano Giardino et al. [14] with some modifications. Biofilms of *Enterococcus faecalis* strain ATCC 29212 were generated on cellulose nitrate membrane filters. An overnight culture of *E faecalis* grown in broth, adjusted to 0.5 Mc Farlandscale,1×10^8 CFU/ml, was used. An aliquot of 20 microlitre *E faecalis* was seeded onto 2 cm × 2 cm cellulose nitrate membrane filters (0.22-micron pore diameter. which were placed on the surfaces of BHI agar plates. 10 membranes were used for each plate. Plates containing membranes were then incubated for 48 hours at 37°C in an aerobic atmosphere. The efficiency of the method for biofilm generation was observed in a pilot study visually. After incubation, membrane filters were removed aseptically from the agar plate and transferred carefully to avoid any disruption of the biofilm. The study material was then placed on each of the biofilms without leaving any contact gap. There was one plate for control and one for positive reference. The Reference plate was with a blank dressing formed without any Usnic acid content in it. The Plates thus formed were then incubated for 48 hours at 37°C in an aerobic atmosphere. After 48 hours the specimen was leached with PBS (Phosphate buffer) solutions in aseptic conditions and aliquots of each leach content was incubated for 48 hours to see if there is any bacterial growth. The Plates were compared with the blank plate which did not have Usnic acid content in the dressing.

RESULTS AND DISCUSSIONS

Appearance and thickness

Appearance and thickness results showed that the visual appearance of dressing was consistent over all the places. Measurement of thickness showed no major change in thickness within the combination. It was seen that proper stirring and settling of the material was vital to avoid any defects in the reinforcement of the textiles.

Drug content uniformity test

This study was done to demonstrate that the procedure and methods followed in the preparation of dressing were capable of ensuing uniform content of Usnic acid in the film. Any variation in uniformity of Usnic acid in the dressing may cause variation in the dosage of it in the wound.

Results of this study showed that the drug (Usnic acid) was uniformly distributed in the dressing at different areas. The effect of the variables like SA:PC

concentration or Glycerol concentration was not seen to affect the uniformity of Usnic acid in the dressing. It was fairly consistent among dressings of specified combinations.

In vitro release Kinetics

The in vitro release kinetics study done on the dressing for different time durations showed that the Usnic acid release in the phosphate buffer solution kept on increasing with time for all dressing combinations. The release rate was higher upto 16 h which flattened by around 24 h for the majority of the dressings as shown in figure 4. This figure shows in vitro release kinetics of each experimental run that is indicated by experiment number as per the BBD experimental design explained earlier.

The results show that the dressings show full swelling in around 4 hours of time and after that, the entrapped Usnic acid is released from the structure. The release proceeds fairly for around 24 hours of time. Figure 5 shows the In vitro release of Usnic acid compared over each time zone of the study.

From figure 6, it is clear that for a given concentration of Usnic acid the release of Usnic acid increases with the amount of glycerol concentration and decreases with the amount of SA:Pectin concentration. This is seen to be true for all levels of Usnic acid concentrations. In other words, a lower level of SA: Pectin gives good release characteristics to the dressing especially at higher concentrations of glycerol.

This can be explained by the fact that glycerol being a plasticizer helps in reducing the compact packing of the molecular chains of the Alginate and Pectin and hence release of the entrapped Usnic acid is easier. The lower levels of SA:Pectin also makes the dressings thinner and hence more prone to leaching of Usnic acid in extraction solvent like PBS.

Mechanical properties of the dressing

An ideal wound dressing is expected to have sufficient strength, elongation and flexural rigidity that it may encounter when used on the wound as a primary or secondary dressing.

The tensile properties of the dressing show that the dressings were having varying levels of elongation at break (figure 7). Significant variation was seen in values of tensile modulus and stress at 6% strain (which represents low levels of stretching that the dressing is eventually expected to experience when used on the skin as a wound dressing) This can be attributed to varying composition levels of the SA:PC ratio and Glycerol. The amount of Usnic acid was not seen to have any significant impact on the tensile properties of the dressing.
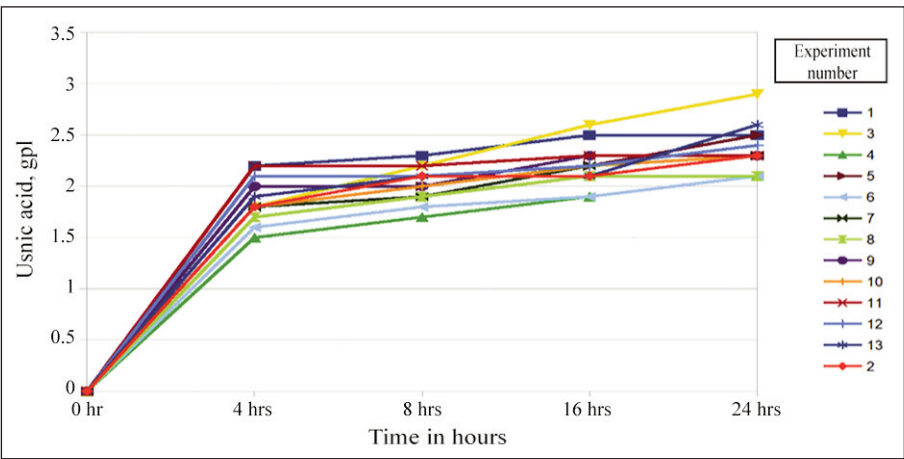
Fig. 4. In vitro release of Usnic acid from the dressing over a period of time
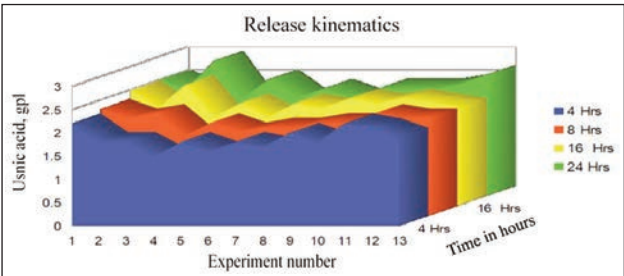
Fig. 5. In vitro Release of Usnic acid compared over each time zone
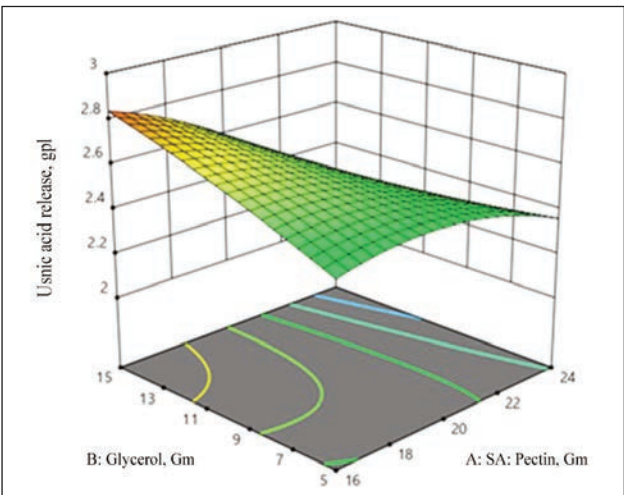
Fig. 6. Effect of SA:PC and glycerol levels on the In vitro release of Usnic acid
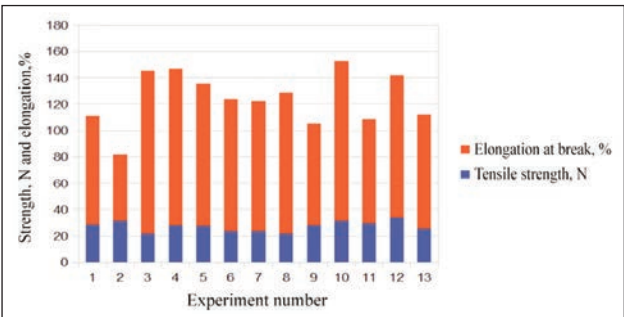
Fig. 7. Strength and elongation of dressing materials
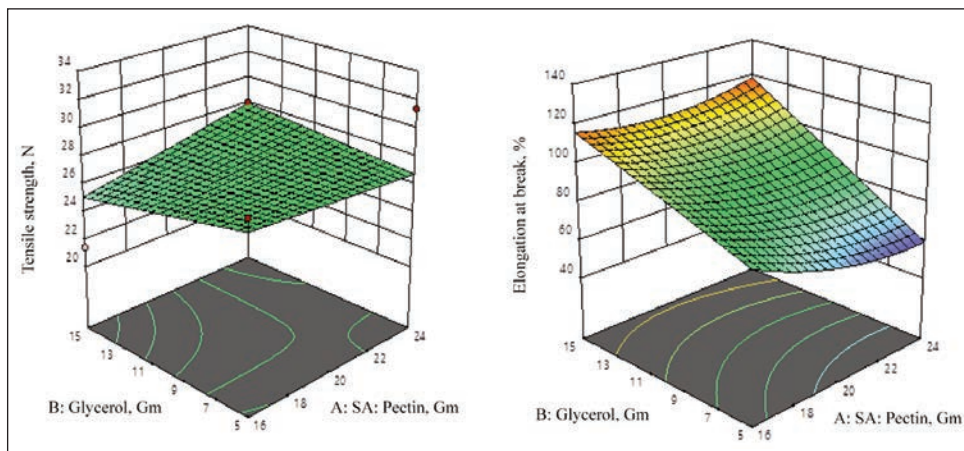
Fig. 8. Effect of SA:PC and glycerol levels on the tensile strength and elongation at break

the study considerably impacted the performance of the dressing for this property. This can be attributed to the fact that the thickness of the dressings across all combinations was almost the same with no significant difference and MVT rate is more linked with the path the vapour takes to pass through the structure (figure 10).

It was seen that the tensile strength of the dressings drops slightly with the increasing amount of glycerol. A higher amount of SA:Pectin combination gives slightly better strength especially at lower glycerol concentrations. The effect is found to be fairly the same with different levels of Usnic acid. The reason for the lower strength at a higher concentration of glycerol is due to the increased flexibility of the dressings. Stiffer dressings are seen to break at lower strength compared to the more flexible dressings.

Figure 8 shows that the elongation at break for the dressings is sensitive to the amount of glycerol content. The higher the content of glycerol, the higher is the elongation, especially so when the SA:Pectin content is lower. This can be attributed to the fact that plasticizing effect is achieved by the presence of more glycerol in the dressing.

Water vapour transmission

Moisture vapours transmission (WVT) across the dressings under the experimental conditions show that moisture vapours transmissions across the dressings for all combinations were good and fairly consistent over each time zone of the study. This is a very important characteristic of a wound dressing. A good wound dressing material should not lock vapours from the wound and create a condition of exudates locking in the wound (figure 9).

The experimental analysis shows that the dressings had 350 grams per square meter per 24 h or more of the WVT levels. And none of the variable factors in

Fig. 10. Water vapour transmission per 24 hours for the dressing materials

Exudate's absorptivity and absorption profile

The exudates absorption property of dressing was seen to be rapidly increasing from 4 to 8 hours of the study and thereafter the absorption stabilizes (figure 11). This is seen more so in combinations containing higher glycerol contents. This is due to the saturation of the hydrogel in the dressing. Experimental analysis shows that exudates absorption is higher when SA:PC is Low and Glycerol is higher and also at a higher level of SA: PC level when Glycerol is low (figure 12).

The reason for the former effect can be attributed to the more porous content of the dressing with higher glycerol content helping for exudates absorption and retention. The latter effect can be attributed to the content of a more solid mass of SA:PC causing more exudates absorption, though a bit slower than the one containing more Glycerol.

Fig. 9. Water vapour transmission studied over each time zone
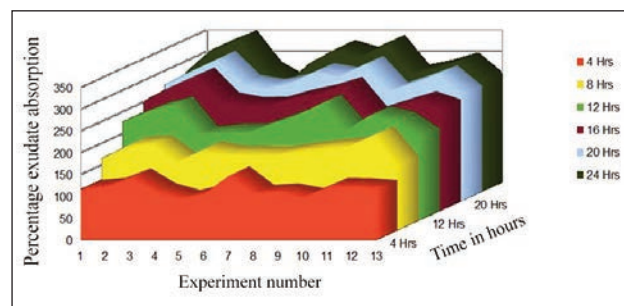
Fig. 11. Percentage exudate's absorption study over each time zone
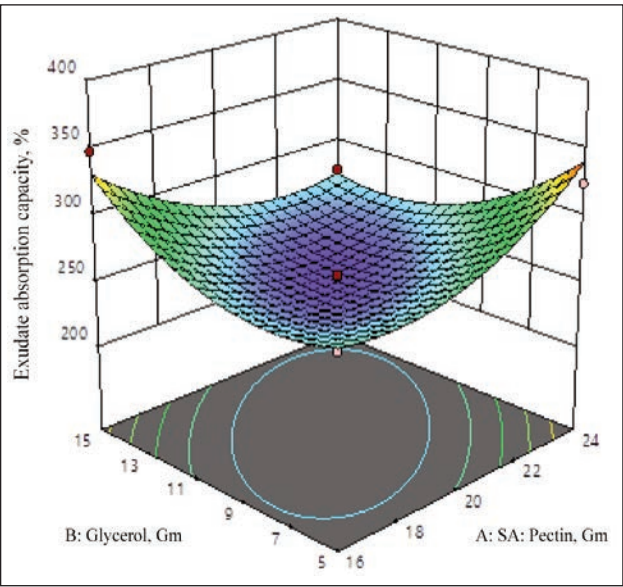
Fig. 12. Effect of SA:PC and glycerol levels on the exudate's absorption of dressing

Evaluation of antimicrobial activity

Results in table 3 show that the dressing was effective against a broad range of microbes including gram-positive, gram-negative bacteria and fungi/yeast. Table 3 summarizes the reduction in microbial count in 8 hours and 24 hours.

With these efficacy tests, it can be inferred that the developed dressing material can be used for infected wounds that have polymicrobial co-infections.

Biofilm inhibition assay

In this study, it was found that the plate with no Usnic acid dressing had bacterial growth on the plates, whereas all the other study plates demonstrated excellent biofilm inhibition. In this study, it can be seen that the presence of Usnic acid is able to nullify the bacteria even in the biofilm and hence after incubation none of the plates containing Usnic acid showed bacterial growth. Thus, it can be concluded that the lowest amount of Usnic acid used in the experimental study was sufficient enough to take care of bacterial growth in the form of biofilm and hence the formulation can be used very effectively in the development of wound care dressing that can be used in managing chronic wound conditions (figure 13). The drug release studies have shown that the Usnic acid is released significantly in the first 4 hours during swelling and there is the presence of drug for 24 hours in the swelling atmosphere. This will ensure that the biofilms are targeted by the presence of Usnic acid and its residual antimicrobial action will help in reducing the microbial load on the wound significantly.

CONCLUSION

The developed textile-based hydrogel dressing is seen to be effective in terms of its exudates management capacity, Strength, elongation and Water vapours permeability. The usage of active antimicrobial and antibiofilm agent, Usnic acid, has given it a broad-spectrum antimicrobial activity and antibiofilm property. The combination of these properties makes this dressing a better choice for the management of chronic wounds. The design of the experiment used in this study is able to point at the optimal combination of the materials for the construction of such hydrogel dressings and understand the contribution of each factor used in the study.

Table 3

ANTIMICROBIAL ANALYSIS OF DRESSING WITH LOWEST USNIC ACID CONTENT			
Sr. no.	Test organisms	% Reduction in	
		8 hours	24 hours
1	Staphylococcus aureus ATCC 6538	99.90	99.99
2	Listeria monocytogenes ATCC 19115	99.90	99.99
3	Enterococcus faecalis ATCC 29212	99.90	99.99
4	Escherichia coli ATCC 25922	99.90	99.99
5	Pseudomonas aeruginosa ATCC 15442	99.90	99.99
6	Klebsiella pneumoniae ATCC 4352	99.90	99.99
7	Candida albicans ATCC 10231	90.00	99.90
8	Aspergillus niger ATCC 6275	90.00	99.90
9	Positive Control	100.00	100.00
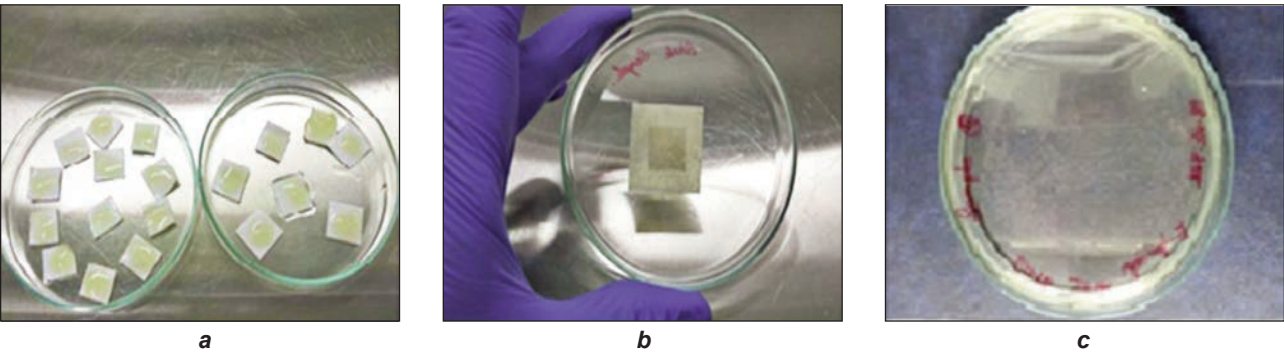
Fig. 3. Stages in biofilm inhibition assay study: *a* – biofilm on Nitrocellulose base; *b* – dressing placed on the biofilm; *c* – incubated plate for bacterial count

The disadvantage associated with the current hydrogel dressings is that the gels after swelling are too weaker to be removed and disintegrates, whereas the current approach makes it possible to be handled easily. The dressing developed can be cut into rope form also and used as wound well-filling material which later can be easily removed once laden with exudates. This will ensure good debridement of chronic wounds, which is essential in the management of chronic wounds.

REFERENCES

[1] Daood, U., et al., *A quaternary ammonium silane antimicrobial triggers bacterial membrane and biofilm destruction*, In: Scientific Reports, 2020, 10, 10970, https://doi.org/10.1038/s41598-020-67616-z

[2] Bowers, S., et al., *Chronic Wounds: Evaluation and Management*, In: American Family Physician, 2020, 2, 101, 3,159–166

[3] Stoodley, P., Sauer, K., Davies, D.G., Costerton, J.W., *Biofilms as complex differentiated communities*, In: Annual Review of Microbiology, 2002, 2, 56, 1, 187–209, https://doi.org/10.1146/ annurev.micro.56.012302.160705

[4] Hall-Stoodley, L., Stoodley, P., *Evolving concepts in biofilm infections*, In: Cell Microbiology, 2009, 11, 7,1034–43, https://doi.org/10.1111/j.1462-5822.2009.01323.x

[5] Costerton, J.W., Stewart, P.S., Greenberg, E.P., *Bacterial biofilms: a common cause of persistent infections*, In: Science,1999, 284, 5418, 1318–1322, https://doi.org/ 10.1126/science.284.5418.1318

[6] James, G.A., Swogger, E., Wolcott, R., et al., *Biofilms in chronic wounds*, In: Wound Repair and Regeneration ,2008,16, 1, 37–44, doi/10.1111/j.1524-475X.2007.00321.x

[7] Francolini, I., et al., *Usnic acid, a natural antimicrobial agent able to inhibit bacterial biofilm formation on polymer surfaces*, In: Antimicrobial Agents and Chemotheraphy, 2004, 48, 11, 4360–4365, https://doi.org/10.1128/ AAC.48.11.4360-4365.2004

[8] Sergio, L.C., et al., *Box-Behnken design: An alternative for the optimization of analytical methods*, In: Analytica Chimica Acta, 2007, 597, 2, 179–186, https://doi.org/10.1016/j.aca.2007.07.011

[9] Masoud, R., et al., *Optimization, characterization, and in vitro assessment of alginate-pectin ionic cross-linked hydrogel film for wound dressing applications*, In: International Journal of Biological Macromolecules, 2017, 97, 131–140, https://doi.org/10.1016/j.ijbiomac.2016.12.079

[10] Anuja, A., Roli, P., *Swelling and drug release kinetics of composite wound dressing*, In: Indian Journal of Fibre & Textile Research, 2018, 43, 3, 104–111

[11] Zaman, H., et al., *Physico-mechanical properties of wound dressing material and its biomedical application*, In: Journal of the Mechanical Behavior of Biomedical Materials, 2011, 4, 7, 1369–1375, https://doi.org/10.1016/ j.jmbbm.2011.05.007

[12] Matthews, K.H., et al., *Lyophilised wafers as a drug delivery system for wound healing containing methylcellulose as a viscosity modifier*, In: International Journal of Pharmaceutics 289, 2005, 51–62, https://doi:10.1016/ j.ijpharm.2004.10.022

[13] Wiegand, C., et al., *In vitro assessment of the antimicrobial activity of wound dressings: influence of the test method selected and impact of the pH*, In: Journal of Materials Science: Materials in Medicine, 2015, 26, 18, 5343, https://doi.org/10.1007/s10856-014-5343-9

[14] Giardino, L., et al., *Comparative Evaluation of Antimicrobial Efficacy of Sodium Hypochlorite, MTAD, and Tetraclean Against Enterococcus faecalis Biofilm*, In: Journal of Endodontics, 2007, 33, 7, 852–855, https://doi.org/10.1016/ j.joen.2007.02.012

Authors:

MICHAEL RODRIGUES, GOVINDHARAJAN THILAGAVATI

PSG College of Technology, Department of Textile Technology,
Post Box No. 1611, Peelamedu Coimbatore, 641004, India
e-mail: thilagapsg@gmail.com

Corresponding author:

MICHAEL RODRIGUES
e-mail: mbrodrigues2000@gmail.com

Investigating the nexus between safety training, safety rules and procedures, safety performance and protection against hazards in Pakistani construction companies considering its impact on textile industry

MUHAMMAD AWAIS-E-YAZDAN   CRISTI SPULBAR
ZURAIDA HASSAN   RAMONA BIRAU
ABDULLAH EJAZ   NARCIS EDUARD MITU

ABSTRACT – REZUMAT

Investigating the nexus between safety training, safety rules and procedures, safety performance and protection against hazards in Pakistani construction companies considering its impact on textile industry

The main aim of this research paper is to examine the linkage between safety training, safety rules and procedures, safety performance and protection against hazards in Pakistani construction companies related to its effects on the textile industry. The primary responsibility of the organization is to provide a safe workplace to the workers where workers do their work safely. The current study examines the relationship between safety training, safety rules & procedures and safety performance. A total of 450 workers from 15 companies participated in the study. A questionnaire survey was used to collect the data. The findings revealed that both safety training and safety rules and procedure were significantly and positively associated with safety compliance. The results propose that construction companies should give proper training to their worker in order to avoid any bad incidents. Similarly, adequate safety rules and procedures are essential for a safer work environment. The textile industry is a very important sector in Pakistan with a significant impact on employment and the labour market.

Keywords: *safety training, safety rules and procedures, safety performance, construction companies, workers protection, textile sector*

Examinarea conexiunii dintre instruirea în materie de siguranță, regulile și procedurile privind securitatea în muncă, performanța în materie de siguranță și protecția împotriva pericolelor în companiile de construcții din Pakistan, având în vedere impactul acesteia asupra industriei textile

Obiectivul principal al acestei lucrări de cercetare este de a investiga legătura dintre instruirea în materie de siguranță, regulile și procedurile privind securitatea în muncă, performanța în materie de siguranță și protecția împotriva pericolelor în companiile de construcții din Pakistan, având în vedere efectele generate asupra industriei textile. Responsabilitatea principală a organizației este de a oferi angajaților un loc de muncă adecvat în care lucrătorii își desfășoară activitatea în condiții de siguranță. Studiul de cercetare actual examinează relația dintre instruirea în materie de siguranță, regulile și procedurile de siguranță și performanța în materie de siguranță. Un total de 450 de lucrători din 15 companii au participat la studiu. Pentru colectarea datelor a fost folosit ca instrument de cercetare chestionarul. Rezultatele empirice au arătat că atât instruirea în materie de siguranță, cât și regulile și procedurile de siguranță au fost asociate în mod semnificativ și pozitiv cu respectarea/conformarea în materie de siguranță. De asemenea, rezultatele sugerează ca firmele de construcții să ofere o instruire adecvată lucrătorilor proprii pentru a evita orice incident cu urmări negative. În mod similar, regulile și procedurile adecvate de siguranță sunt esențiale pentru un mediu de lucru mai sigur. Industria textilă este un sector foarte important în Pakistan, cu un impact semnificativ asupra ocupării forței de muncă și a dinamicii pieței muncii.

Cuvinte cheie: *instruire în materie de siguranță, reguli și proceduri de siguranță, performanță în materie de siguranță, companii de construcții, protecția lucrătorilor, sectorul textil*

INTRODUCTION

Today, there are numerous occupational accidents at the workplace and it is the obligation of the organizations to give a safer workplace to the employees. An occupational accident is defined as an occurrence arising from the course of work, which results in non-fatal or fatal injury [1]. Similarly, an occupational accident is unexpected and unintentional and can result in one or more workers suffering an injury, disease or death [2].

According to Iqbal et al. [3], the textile industry represents "one of the oldest industries in Pakistan" but sustainable development of this sector involves financial and technological investments. Toprak and Anis [4] investigated the impact of the textile industry on the environment and identified certain factors such as discharge chemical loads, energy waste, air pollution, huge chemical and water consumption, solid dissipation and odour emergence. Rempel et al. [5] argued that textile reinforcements do not corrode in contradistinction to ordinary steel reinforcements.

Moreover, Bick et al. [6] discussed low wages of workers and limited working conditions considering the fact that both environmental and social costs related to the textile manufacturing sector are very scattered. Memon et al. [7] argued that the textile industry is an essential pillar of economic growth in Pakistan while the leading components are the following: clothing and garments, readymade fabrics, weaved apparel, twisting sector and chemical processing sector.

Pakistan, which is a developing country, is part of the group of lower-middle-income economies, with a GNI per capita from USD 1036 to USD 4045 [8].

The fact is documented by giving an example of the US, where the expenditure of occupational injuries reached up to $990 million and the expenses may further increase as additional damages occur in other industries. Thus, organizations with a safe work environment have numerous benefits both direct and indirect [9]. Direct one is related to workers who are influenced by occupational injuries and accidents and the organization which bears unnecessary loss [10].

Similarly, indirect relates to families of the employees, insurers, society and consumers [9].

Poor performance relating to occupational safety and health leads to the immeasurable human cost of injuries and fatalities as well as great financial loss of an organization and country. For example, according to the International Labour Organization [11], there were 2.78 million deaths across the globe. Similarly, more than 7500 people die every day, 6500 from work-related diseases and 1000 from occupational accidents. Some of the worst occupational accidents include, the Flixborough Works of Nypro (UK) Limited experienced an extensive vapour cloud blast in which 36 employees were injured and 28 employees were killed [12]. Another accident occurred in Bhopal, India, killing 3,800 people. This accident in India caused major injuries and health-related problems because of the leakage of methyl isocyanate chemicals [13]. Moreover, an effusion occurred at Buncefield Oil Storage Depot in which there were no deaths but 43 people were injured [14].

Due to the huge amount of cost involved in occupational injuries and accidents as discussed above many countries and entities started taking interest in this problem [15]. Economic and workforce loss occur because of occupational injuries and accidents. Companies suffer from direct costs which include death claims, medical fee, legal fee, expenses for safety and health and appliances damage [16]. Similarly, indirect cost also occurs which is sometimes remarkably higher, because indirect costs include disturbance in quality and productivity, employee's replacement costs, insurance costs and training costs [17]. While both direct and indirect costs are involved, quick action must be taken to stop the occurrence of occupational injuries and accidents. The actions may be the scientific and systematic type to examine that what are the factors that contribute to occupational injuries and accidents so that effective practices and measures can be implemented.

Construction industry faces similar occupational injuries and accidents. Occupational safety and health are significant with respect to the unique nature of working conditions which turn construction workers prone to accidents. As compared to other industries construction industries have a high rate of workplace accidents [18]. The construction industry employed hardly 10% of the working population but contributes 30% of lethal accidents over the European Union (EU), furthermore in the United States (US) it contributes 22% of all deadly accidents among 7% of working persons [19]. According to Haadir and Panuwatwanich [20], up to 25% of accidents arise in the construction industry of the United Kingdom, similarly 40% in Japan and 50% in Ireland construction industries. In the light of literature, specifically, the construction workers working on construction sites have a 1 in 300 chance of killing at the workplace. The ratio of other major illnesses, paralysis and being disabled are very high as compared to other nature of works [21].

These types of injuries consume 4% of the world's GDP [18]. The developing countries, like India, Sri Lanka and Pakistan, are labour extensive countries that involved 2.5–10 times as many individuals per task [22]. Moreover, in certain Asian economies, most of the population actually has no entrance to quality health care facilities [23]. If we talk about construction injuries in Pakistan it is going higher and higher [22]. The situation is very bad and it needs some sort of precautions that reduce this higher rate (16.28%) of injuries and accidents at the worksites [11].

Therefore, the present study comes up with the contribution to the body on the knowledge that if the top-level management provides appropriate training and apply basic safety rules & procedure then construction injuries and accidents can be reduced.

LITERATURE REVIEW

Safety performance

The degree which explains the level of safety within an organization is called safety performance. It is also known as the annual number of injuries and accidents which describe the safety level of an organization [24]. Similarly, Kohli [25] argued that it is a set of regulations that are used to improve workplace safety. The definitions themselves give the directions for the reduction of workplace injuries and accidents. Safety performance is attached to injuries and accidents rates hence, this study aims to reduce the injuries and accidents at construction sites.

Previous studies argued that safety performance is directly associated with injuries rates [26, 27] and it is evident that it leads to the success of the organizations. In this study, safety performance is determined by a factor named safety compliance. Safety compliance is actual rules set by the organization. In addition, it refers to the regulations which are directed by the top management in order to reduce workplace unsecure incidents which leads to accidents [28]. Hence, safety compliance is mandatory to be followed

on construction sites in order to avoid any dangerous incident.

Safety training

Training refers to the actions taken by individuals in order to work safely in the organization. The organization which takes adequate work from their workers should train their employees. It is a factor that updates an individual during work time. Goldstein [29] argued it is the attribute that leads to a safer work environment. On the other hand, the importance of ESG factors, which include social, environmental, economic and corporate governance aspects is significant considering the impact on sustainable economic growth [30]. Thus, everyone at the workplace should be trained and able to control any hazard at the workplace. Moreover, safety training is the adequate knowledge that allows the worker to behave safely in order to avoid any uncomfortable situation [31]. Therefore, we propose the following hypothesis:
H1: Safety training is significantly related to safety performance.

Safety rules and procedures

Rules are expectations and procedures which are set by any organization in order to maintain the decorum of the organization. According to Vinodkumar and Bhasi [28], these are well-established procedures in order to maintain the safety of an organization. Lu & Yang [32] argued that these are the actions that we can perform at the workplace. Similarly, it refers to the action from which an organization do accountabilities and manage future goals. Numerous studies are evident about the association between safety rules & procedures and safety performance [28, 32, 33]. Safety rules & procedures play an important role in safety-related outcome therefore we propose that:
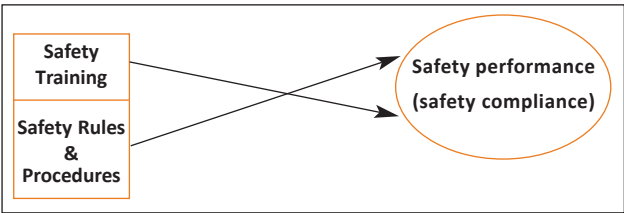
Fig. 1. Research framework

H2: Safety rules & procedures is significantly related to safety performance.

DATA COLLECTION AND RESEARCH METHODOLOGY

The target population of this study are the construction workers from different construction companies operating in Punjab, Pakistan. The reason behind selecting Punjab is that most numbers of the companies are established here. Moreover, Punjab is progressing in order to give employment to individuals coming from other areas. Data was collected personally through self-administered questionnaires.

450 workers from 15 companies participated in the study. The objective of the study was mentioned on the first page of the questionnaires to avoid any inconvenience. The response rate was 83%. The sample consists of (75%) males and (25%) females. The majority of the respondents were married (85%). Similarly, the majority of the respondents were young (91.3%) with less than 40 years of age.

The main questionnaire included the item of safety training, safety rules & procedures and safety performance. The questionnaire was divided into two sections. Section one consists of the demographics whereas section two consists of the items of the variables used in this study (table 1). The questionnaire

Table 1

MEASURING INSTRUMENT OF THE STUDY [28]	
Protocols	**Items**
Safety performance (Safety compliance)	1. I use all necessary safety equipment's to do my job. 2. I carry out my work in a safe manner. 3. I follow correct safety rules and procedures while carrying out my job. 4. I ensure the highest levels of safety when I carry out my job. 5. Occasionally due to lack of time, I deviate from correct and safe work procedures. 6. Occasionally due to over-familiarity with the job, I deviate from correct and safe work procedures. 7. It is not always practical to follow all safety rules and procedures while doing a job.
Safety training	1. My company gives comprehensive training to the employees in workplace health and safety issues. 2. Newly recruits are trained adequately to learn safety rules and procedures. 3. Safety issues are given high priority in training programs. 4. I am not adequately trained to respond to emergency situations in my workplace 5. Management encourages the workers to attend safety training programs. 6. Safety training given to me is adequate to enable me to assess hazards in the workplace
Safety rules & procedures	1. The safety rules and procedures followed in my company are sufficient to prevent incidents from occurring. 2. The facilities in the safety department are not adequate to meet the needs of my company. 3. My supervisors and managers always try to enforce safe working procedures. 4. Safety inspections are carried out regularly. 5. The safety procedures and practices in this organization are useful and effective.

was adapted from the study of Vinodkumar and Bhasi [28]. Questionnaire's items were measured by a 5-point Likert scale ranging from (1) strongly disagree to (5) strongly agree. Moreover, regression and correlation analysis were incorporated to find the safety performance (safety compliance) of the workers working in construction. Table 2 presents the Cronbach Alpha value which states that the questionnaire is suitable for data analysis [34].

Table 2

CRONBACH ALPHA			
Constructs	**Items**	**Cronbach Alpha**	**Source**
Safety performance (Safety compliance)	7 Items	0.81	Vinodkumar and Bhasi [28]
Safety training	6 Items	0.79	Vinodkumar and Bhasi [28]
Safety rules & procedures	5 Items	0.77	Vinodkumar and Bhasi [28]

Table 2 showed the Cronbach Alpha value of the variable used in the study. Similarly, it also illustrates the sources and number of items incorporated in the study. The following paragraphs will examine the correlation and validity analysis. Table 3 illustrates the mean, standard deviation and average variance extracted of the construct used in this study. If take the average the construction workers showed agreement on all variables used in the study. Hence, it showed the importance and the construction companies should follow these protocols (safety training; safety rules & procedures). Pearson correlation was applied in this study. The correlation of the variable used in this study was at a satisfactory level.

Table 3

DESCRIPTIVE, CORRELATION ANALYSIS, CONVERGENT AND DISCRIMINANT VALIDITY						
Protocols	**Mean**	**SD**	**AVE**	**1**	**2**	**3**
Safety training	4.75	0.92	0.56	**0.74**		
Safety rules & procedures	4.15	0.81	0.52	0.32**	**0.72**	
Safety compliance	3.88	1.03	0.75	0.37*	0.57**	**0.86**

Note: the square root of AVE is provided bold (Diagonal); * p < 0.01; ** p < 0.05.

For convergent validity table 3 presents the value of AVE. Each vale of AVE is greater the 0.5 which depicts that all value is satisfactory for convergent validity and goodness of fit of the model.

EMPIRICAL RESULTS AND DISCUSSIONS

The results showed that both variables (safety training and safety rules & procedures) have been associated with safety performance in the order of safety compliance. Both variables used in the current study are highly significant and positively related to safety compliance. Hence, safety training and safety rules & procedures (β = 0.381 and 0.337 p < 0.000) were found significant and positive with safety compliance. Therefore, all hypotheses in the present study were supported. The result showed that the construction management should provide appropriate training and apply necessary rules & procedures in order to avoid any bad incident which leads to injuries. In other words, safety training and safety rules & procedures are significantly important for construction sites to be safe from accidents. The result is consistent with the previous study which also put a positive impact on safety compliance [28, 35] which give evidence that both variables of the study are important in accordance with safety compliance (table 4).

Table 4

REGRESSION RESULTS WITH PATH COEFFICIENTS			
Relationships	**Coefficients**	**P-Value**	**Decision**
Safety training → Safety compliance	0.381	0.000	Supported
Safety rules & Procedures → Safety Compliance	0.337	0.000	Supported

CONCLUSIONS

The present study provides appropriate benefits relating to construction workers. Although, this research has certain limitations. Firstly, the present study measured safety performance with safety compliance. It can be measured with other dimensions of safety performance (e.g., safety participation & risky behaviour) in future. Secondly, this study focuses only on the workers which are from the Punjab, province of Pakistan. Thus, the findings are only limited to the particular region. Studies can be done on the other provinces of Pakistan in order to increase the generalizability of the results. Thirdly, this study measured only safety training and safety rules & procedures as an antecedent of the safety performance other antecedents can also be incorporated in future. Fourthly, this study targeted the employees of the construction companies. Further studies should include the workers of the other industries like sugar, textile and fertilizers industries. Lastly, this study followed the quantitative method. The studies in future should adopt qualitatively or mixed modes of studies for advanced understanding.

The textile industry is an essential sector and these aspects must be taken into account in order to achieve sustainable development. On the other hand, Spulbar et al. [36] argued that an extreme event, such as a global financial crisis or COVID-19 pandemic is a rare and highly unpredictable event, but very difficult to anticipate and forecast. Memon et al. [7] have highlighted various issues affecting the textile industry of Pakistan such as frail infrastructure,

obsolete technology, adverse law and order situation and lack of investment. The current study represents the new direction in the area of safety management. The present study gives evidence on the association between safety training, safety rules and procedures and safety compliance in a developing country. Whereas, most of the studies were conducted in developed economies. Hence, this study is evidence that safety training and safety rules and procedures do influence safety compliance in developing nations like Pakistan.

Therefore, it is expected that the current study fill the gap relating to safety performance literature. Furthermore, this study determined the direct relationship between safety training, safety rules and procedures and safety compliance. For our future research study, it can also be tested with the help of introducing mediators or moderators.

REFERENCES

[1] Papazoglou, L.A., Aneziris, O., Konstandinidou, M., Giakoumatos, L., *Accident sequence analysis for sites producing and storing explosives*, In: Analysis and Prevention, 2009, 41, 1145–1154

[2] Visser, E., Pijl, Y.J., Stolk, R.P., Neeleman, J., Rosmalen, J., *Accident proneness, does it exist? A review and meta-analysis*, In: Accident Analysis and Prevention, 2007, 39, 556–564

[3] Iqbal, M.S., Shaikh, F.M., Mahmood, B., Shafiq, K., *Development of Textile Industrial Clusters in Pakistan*, In: Asian Social Science, 2010, 6, 11, 123–140, ISSN 1911-2017, E-ISSN 1911-2025, https://doi.org/10.5539/ass.v6n11p123

[4] Toprak, T., Anis, P., *Textile industry's environmental effects and approaching cleaner production and sustainability, an overview*, In: Journal of Textile Engineering & Fashion Technology, 2017, 2, 4, 429–442, https://doi.org/10.15406/jteft.2017.02.00066

[5] Rempel, S., Ricker, M., Hegger, J., *Safety Concept for Textile-Reinforced Concrete Structures with Bending Load*, In: Applied Sciences, 2020, 10, 20, 7328, https://doi.org/10.3390/app10207328

[6] Bick, R., Halsey, E., Ekenga, C.C., *The global environmental injustice of fast fashion*, In: Environmental Health, 2018, 17, 92, https://doi.org/10.1186/s12940-018-0433-7

[7] Memon, J.A., Aziz, A., Qayyum, M., *The Rise and Fall of Pakistan's Textile Industry: An Analytical View*, In: European Journal of Business and Management, 2020, 12, 12, ISSN 2222-1905 (Paper), ISSN 2222-2839 (Online)

[8] Hayat, M.A., Ghulam, H., Batool, M., Naeem, M.Z., Ejaz, A., Spulbar, C., Birau, R., *Investigating the Causal Linkages among Inflation, Interest Rate, and Economic Growth in Pakistan under the Influence of COVID-19 Pandemic: A Wavelet Transformation Approach*, In: Journal of Risk and Financial Management, 2021, 14, 6, 277, https://doi.org/10.3390/jrfm14060277

[9] Mossink, J.C.M., de Greef, M., *Inventory of socioeconomic costs of work accidents*, Bilbao: Office for Official Publications of the European Communities, 2002

[10] Haslam, C., O'Hara, J., Kazi, A., Twumasi, R., Haslam, R., *Proactive occupational safety and health management: Promoting good health and good business*, In: Safety Science, 2016, 81, 99–108

[11] Pakistan Bureau of Statistics, *Labor Force Survey (2014–2015)*, Government of Pakistan Statistics Division, 2014–2015, Available at: http://www.pbs.gov.pk/sites/default/files//Labour%20Force/publications/lfs2014_15/t33-pak.pdf [Accessed on July 2021]

[12] Vaidogas, E.R., Juocevičius, V., *Sustainable development and major industrial accidents: the beneficial role of risk-oriented structural engineering*, In: Technological and Economic Development of Economy, 2008, 14, 4, 612–627

[13] Broughton, E., *The Bhopal disaster and its aftermath: a review*, In: Environmental Health, 2005, 4, 1, 1–6

[14] Johnson, D.M., *The potential for vapour cloud explosions–Lessons from the Buncefield accident*, In: Journal of Loss Prevention in the Process Industries, 2010, 23, 6, 921–927

[15] Rikhardsson, P.M., Impgaard, M., *Corporate cost of occupational accidents: an activity-based analysis*, In: Accident Analysis & Prevention, 2004, 36, 2, 173–182

[16] Pessemier, W., *Improving Safety Performance by Understanding Perceptions of Risk and Improving Safety Management Systems*, Public Entity Risk Institute, 2008

[17] Buckle, P.W., Devereux, J.J., *The nature of work-related neck and upper limb musculoskeletal disorders*, In: Applied Ergonomics, 2002, 33, 3, 207–217

[18] Ahmed, I., Shaukat, M.Z., Usman, A., Nawaz, M.M., Nazir, M.S., *Occupational health and safety issues in the informal economic segment of Pakistan: a survey of construction sites*, In: International Journal of Occupational Safety and Ergonomics, 2017, 1–11

[19] Chuks, O.K., Uchenna, O.P., *Appraising the influence of cultural determinants of contruction workers safety perception and behaviour in Nigeria*, In: International Journal of Engineering and Medical Science Research, 2013, 1, 1, 11–24

[20] Al Haadir, S., Panuwatwanich, K., *Critical success factors for safety program implementation among construction companies in Saudi Arabia*, In: Procedia Engineering, 2011, 14, 148–155

[21] Ho, D.C.P., Ahmed, S.M., Kwan, J.C., Ming, F.Y.W., *Site safety management in Hong Kong*, In: Journal of Management in Engineering, 2000, 16, 6, 34–42

[22] Azhar, S., Choudhry, R.M., *Capacity building in construction health and safety research, education, and practice in Pakistan*, In: Built Environment Project and Asset Management, 2016, 6, 1, 92–105

[23] Qaiser Gillani, D., Gillani, S.A.S., Naeem, M.Z., Spulbar, C., Coker-Farrell, E., Ejaz, A., Birau, R., *The Nexus between Sustainable Economic Development and Government Health Expenditure in Asian Countries Based on Ecological Footprint Consumption*, In: Sustainability, 2021, 13, 6824, https://doi.org/10.3390/su13126824

[24] Siu, O.L., Phillips, D.R., Leung, T.W., *Safety climate and safety performance among construction workers in Hong Kong: The role of psychological strains as mediators*, In: Accident Analysis & Prevention, 2004, 36, 3, 359–366

[25] Kohli, S., *Safety Management System*, Bangalore International Airport Limited: Karnataka, India, 2007

[26] Fabiano, B., Currò, F., Pastorino, R., *A study of the relationship between occupational injuries and firm size and type in the Italian industry*, In: Safety Science, 2004, 42, 7, 587–600

[27] Oliver, A., Cheyne, A., Tomás, J.M., Cox, S., *The effects of organizational and individual factors on occupational accidents*, In: Journal of Occupational and Organizational Psychology, 2002, 75, 4, 473–488

[28] Vinodkumar, M.N., Bhasi, M., *Safety management practices and safety behaviour: Assessing the mediating role of safety knowledge and motivation*, In: Accident Analysis & Prevention, 2010, 42, 6, 2082–2093

[29] Goldstein, I.L., *Training in work organizations*, In: Annual Review of Psychology, 1980, 31, 1, 229–272

[30] Meher, B.K., Hawaldar, I.T., Mohapatra, L., Spulbar, C., Birau, R., *The Effects of Environment, Society and Governance Scores on Investment Returns and Stock Market Volatility*, In: International Journal of Energy Economics and Policy, 2020, 10, 4, 1–6, https://doi.org/10.32479/ijeep.9311

[31] Abdullah, N.A.C., Spickett, J.T., Rumchev, K.B., Dhaliwal, S.S., *Assessing employees' perception on health and safety man agement in public hospitals*, In: International Review of Business Research Papers, 2009, 5, 4, 54–72

[32] Lu, C.S., Yang, C.S., *Safety leadership and safety behavior in container terminal operations*, In: Safety science, 2010, 48, 2, 123–134

[33] Prussia, G.E., Brown, K.A., Willis, P.G., *Mental models of safety: do managers and employees see eye to eye?*, In: Journal of Safety Research, 2003, 34, 2, 143–156

[34] Hair, E., Halle, T., Terry-Humen, E., Lavelle, B., Calkins, J., *Children's school readiness in the ECLS-K: Predictions to academic, health, and social outcomes in first grade*, In: Early Childhood Research Quarterly, 2006, 21, 4, 431–454

[35] Subramaniam, C., Shamsudin, F.M., Zin, M.L.M., Ramalu, S.S., Hassan, Z., *Safety management practices and safety compliance in small medium enterprises*, In: Asia-Pacific Journal of Business Administration, 2016

[36] Spulbar, C., Trivedi, J., Birau, R., Tenea, C.A., Ejaz, A., *Estimating volatility spillovers, dynamic causal linkages and international contagion patterns between developed stock markets: An empirical case study for USA, Canada, France and UK*, In: Annals of the „Constantin Brâncuşi" University of Târgu Jiu, Economy Series, „Academica Brâncuşi" Publisher, 2019, 3, 44-62

Authors:

MUHAMMAD AWAIS-E-YAZDAN[1], ZURAIDA HASSAN[2], ABDULLAH EJAZ[3],
CRISTI SPULBAR[4], RAMONA BIRAU[5], NARCIS EDUARD MITU[4]

[1]College of Business, Universiti Utara Malaysia, Malaysia (UUM), 06010 Sintok, Kedah Darul Aman, Malaysia
e-mail: awais.yazdan@gmail.com

[2]College of Business, Universiti Utara Malaysia, Malaysia (UUM) 06010 Sintok, Kedah Darul Aman, Malaysia
e-mail: h.zuraida@uum.edu.my

[3]Department of Anthropology, Economics and Political Science, MacEwan University, Canada and
Augustana Campus – University of Alberta, Canada
e-mail: ejazabdullah03@gmail.com

[4]University of Craiova, Faculty of Economics and Business Administration Craiova, Romania
e-mail: cristi_spulbar@yahoo.com, mitunarcis@yahoo.com

[5]C-tin Brancusi University of Targu Jiu, Faculty of Education Science, Law and Public Administration, Romania

Corresponding author:

RAMONA BIRAU
e-mail: ramona.f.birau@gmail.com

Impact of ultraviolet radiation on thermal protective performance and comfort properties of firefighter protective clothing

ADNAN MAZARI
FUNDA BUYUK MAZARI
JAWAD NAEEM

ANTONIN HAVELKA
PARASHANT MARAHATTA

ABSTRACT – REZUMAT

Impact of ultraviolet radiation on thermal protective performance and comfort properties of firefighter protective clothing

In this study, the impact of ultraviolet radiation is studied on thermal protective performance and clothing comfort properties of firefighter protective clothing. Firefighter clothing assembly consists of the outer shell, moisture barrier and thermal barrier. In this research, two different outer shells were utilized. Outer shell O1 consists of inherently fire-retardant fibres mainly consisting of Conex (Nomex) and firefighter assembly having Conex as the outer shell was called specimen A. On the other hand, clothing arrangement which employed Proban coated outer layer (O2) was termed as specimen B. Both specimens were evaluated for tensile testing, air permeability, radiant heat transmission machine, bending moment and water vapour resistance before and after exposure to ultraviolet radiation. The tensile strength value of outer shell O2 was higher than that of O1 before and after exposure to UV radiation. Tensile strength values of both outer shells O1 and O2 decline after exposure to ultraviolet radiation. Air permeability values of both outer shell O1 and O2 increase after being exposed to ultraviolet radiation. It was noted that specimen A has better thermal protective performance as compared to specimen B, before and after exposure to UV radiation. Also, radiant heat transmission index RHTI 24 values were greater for specimen A as compared to specimen B, before and after exposure to UV radiation. Moreover, bending moment values for both outer shell O1 and O2 decline after being subjected to UV radiation. Furthermore, Water vapour resistance values of outer shell O1 and outer shell O2 enhance after exposure to ultraviolet radiation.

Keywords: thermal protective performance (TPP), ultraviolet radiation (UV), radiant heat transmission index (RHTI 24)

Influența radiațiilor ultraviolete asupra performanței de protecție termică și proprietăților de confort ale îmbrăcămintei de protecție pentru pompieri

În acest studiu, s-a analizat influența radiațiilor ultraviolete asupra performanței de protecție termică și proprietăților de confort vestimentar ale îmbrăcămintei de protecție pentru pompieri. Ansamblul de îmbrăcăminte pentru pompieri este format din stratul exterior, barieră de umezeală și barieră termică. În această cercetare au fost utilizate două straturi exterioare diferite. Stratul exterior O1 este format din fibre ignifuge în mod inerent constând în principal din Conex (Nomex), iar ansamblul vestimentar al pompierilor având Conex ca strat exterior a fost numit proba A. Pe de altă parte, îmbrăcămintea care a folosit stratul exterior acoperit cu Proban (O2) a fost denumită proba B. Ambele probe au fost evaluate pentru rezistența la tracțiune, permeabilitatea la aer, transmiterea căldurii radiante, rezistența la încovoiere și rezistența la vapori de apă înainte și după expunerea la radiații ultraviolete. Valoarea rezistenței la tracțiune a stratului exterior O2 a fost mai mare decât cea a stratului O1, înainte și după expunerea la radiații UV. Valorile rezistenței la tracțiune ale ambelor straturi exterioare O1 și O2 scad după expunerea la radiații ultraviolete. Valorile permeabilității la aer, atât ale stratului exterior O1 cât și ale stratului O2, cresc după expunerea la radiații ultraviolete. S-a observat că proba A are o performanță de protecție termică mai bună în comparație cu proba B, înainte și după expunerea la radiații UV. De asemenea, valorile indicelui de transmitere a căldurii radiante RHTI 24 au fost mai mari pentru proba A în comparație cu proba B, înainte și după expunerea la radiații UV. În plus, valorile rezistenței la încovoiere atât pentru stratul exterior O1, cât și pentru stratul O2 scad după ce au fost supuse la radiații UV. Mai mult, valorile rezistenței la vapori de apă ale stratului exterior O1 și ale stratului exterior O2 se îmbunătățesc după expunerea la radiații ultraviolete.

Cuvinte-cheie: performanță de protecție termică (TPP), radiații ultraviolete (UV), indice de transmitere a căldurii radiante (RHTI 24)

INTRODUCTION

Firefighter clothing is a multilayer garment that is manufactured from high-performance fibres. In multilayer firefighter protective clothing, there are normally three layers i.e., outer shell, moisture barrier and thermal barrier. The outer shell consists of those materials which don't burn or degrade on having contact with heat and flame. A moisture barrier is a microporous membrane that is impermeable to water but permeable to water vapours. The thermal barrier supports the body of a firefighter by blocking the amount of heat from reaching the firefighter's body [1]. The primary purpose of this firefighter protective

garment is to protect the body of firefighter clothing from hazardous working atmospheres like flash fire, chemical spillage and radiant heat flux density [2–5]. The location of firefighters' bodies and kinds of action performed by firefighters are contingent on exposure of multilayer protective clothing to different conditions. It is almost impossible to comprehend the useful life of firefighter clothing assembly. In general, normally 10 years are given to firefighter protective clothing. After this tenure, this multilayer clothing is not applicable for utility as it did not comply with National Fire Fighter Protective Clothing, NFPA 1851 standard [6]. The pertinent element in weathering is sunlight [7]. The interaction of sunlight with organic polymers caused irreversible changes and polymer degradation due to photo-oxidation caused brittleness and reduction in textile strength parameters. There are two conditions that are essential for the light of a specific wavelength to cause deterioration of polymers. Firstly, a polymer must be able to absorb light rays. Secondly, the energy of light must be strong enough to break chemical bonds. The ageing of chemicals takes place through three main reactions i.e., breakage of chain, cross-linking and depolymerisation. Chain breaking leads to the polymer ageing process [8]. Scission of the chain is seldom accompanied by oxidation, causing self-sustained procedure inculcating production of extremely reactive free radicals. Weathering can take place naturally and artificially [9]. Firefighter protective clothing is generally made from high-performance fibres which are made from combination meta-aramid and para-aramids. The high-performance fibres are inherent absorbers of ultraviolet light. UV light causes degradation in these fibres due to primary photoreactions resulting in the breakage of the main chain bond. Para-aramids fibres (Kevlar) have a more ordered crystalline structure than meta-aramid fibres.

Mechanical properties of multilayer protective clothing play a pivotal role in the performance of firefighter protective clothing. In recent years, it has been found that high-performance fibres can absorb ultraviolet radiation and suffer photolytic deterioration instigated by crucial photo reactions causing the scission of main chain bonds. In the case of polyaramids, photo-oxidation is very acute. The factors that impact the protective performance of firefighter clothing are thermal exposure, washing, moisture absorbing, laundering and abrasion [10–14].

In this study impact of artificial weathering of ultraviolet radiation on thermal protective performance and comfort properties of firefighter protective clothing was investigated. Two different outer shells Nomex and Proban coated outer layers were utilized. At first, tensile strength, air permeability, radiation heat flux density, bending moment and water vapour resistance values were evaluated. Afterwards, these specimens were exposed to ultraviolet radiation in Atlas weathering machine UV 340 for continuous thirteen days and later on aforementioned properties were also calculated.

EXPERIMENTAL WORK

Materials

All specimens were provided by Vochoc Company, Czech Republic. Two different combinations were made from these specimens. Each specimen consists of an outer shell layer, moisture barrier and thermal barrier. The specification of materials is mentioned in table 1 and the combination of specimens is revealed in table 2.

Outer shell 1 (O1) is made from a combination of inherently flame-resistant materials like meta-aramids and para-aramids. Outer shell 2 (O2) is Proban coated cotton/polyester fabric. Two different

Table 1

SPECIFICATION OF SAMPLES						
Sample no.	Name of sample	Code	Material specification	Weave design	Thickness	GSM (g/m²)
1	Outer shell (1)	O(1)	70% Conex, 23% Lenzing FR, 5% Twaron, 2% Beltron	Rip stop weave	0.44±0.01	225±2.1
2	Outer shell (2)	O(2)	79% Proban, 20% polyester and 1% antistatic	Twill	0.6±0.01	260±2.2
3	Moisture Barrier	MB	Face fabric, 50%/50% Kermel/viscose FR, PTFE membrane	Non-woven	0.55±0.01	120±1.8
4	Thermal Barrier	TB	Thermo: Para Aramid Inner futter: 50% Meta aramid, 50% viscose	Non-woven	1.8±0.02	200±2.3

Chemical degradation occurs more easily within disordered regions, which in para-aramids is only a small fraction of polymer and hence less susceptible to photodegradation [9–16]. Carlsson et al. [17] mentioned that stability in para-aramids is more as compared to meta-aramids are due to enhanced conjugation and delocalization of absorbed energy through the enol form of the amide group.

Table 2

COMBINATION OF SPECIMEN				
Sample no.	Fabric assembly	Fabric code	GSM (g/m²)	Thickness (mm)
1	O(1)+MB+TB	A	545±2.1	2.79±3.1
2	O(2)+MB+TB	B	580±2.9	2.95±2.9

outer shells were selected to compare thermal protective performance and thermal comfort properties of firefighter protective clothing before and after exposure to Ultraviolet light.

CHARACTERIZATION OF SPECIMEN

Weathering machine

Weathering of outer shell O1 and outer shell O2 was performed in artificially accelerated weathering chambers (Atlas Weathering machine UV 340) for 13 days of continuous exposure nearly equal to 6.6 years of firefighter clothing exposure to UV radiation in natural conditions of utility [9]. ASTM G154-06 standard was used. According to this standard, test specimens (outer shells) were exposed to fluorescent Ultraviolet light under controlled conditions. The approximate wavelength of absorbed Ultraviolet radiation was maintained around 340 nm and energy distribution in the form of spectral irradiance was 0.89 W/m^2/nm.

Evaluation of tensile strength

Tensile strength was evaluated from a tensile testing machine called Tensile Testometric M350-5CT as per EN ISO 13934-1 standard.

Evaluation of air permeability

Air permeability tester FX 3300 Labotester III (Textest Instruments) was employed to evaluate air permeability as per CSN EN ISO 9237 standard. The test pressure was kept at 200 pascals on an area of 20 cm^2 (l/m^2/sec).

Evaluation of radiation heat flow through tested fabrics

The X637 B machine utilizes ISO 6942 standard to evaluate the transmission of heat through the textile substrate or material assembly. The size of the specimen was 230 mm × 80 mm and shall be taken from the area more than 20 mm away from the edge of the textile substrate and must be free from defects. Specimens were conditioned for at least 24 hours at a temperature of (20±2)°C and had a relative humidity of (65±2)%. The room in which the test was performed must be freed from any current of air. The temperature of the room was maintained between 15°C and 35°C. The results are mentioned in the form of radiant heat transmission index ($RHTI$ 12 and $RHTI$ 24) and the percentage heat transmission factor (percentage $TF\,Q_o$) and transmitted heat flux density Q_c. Three specimens are required for testing at each level of heat flux density. A schematic diagram of the radiant flux density machine is shown in figure 1 [15]. Incident heat flux density is evaluated from the following equation [15]:

$$Q_o = \frac{C_p R M}{a A} \qquad (1)$$

where A is the area of the copper plate in m^2, a – the absorption coefficient of the painted surface of the calorimeter, M – the mass of copper plate in kg, C_p –

the specific heat of copper 0.385 (kJ/Kg^{o}C), R – rate of rise of the calorimeter temperature in the linear region in °C/s.

The transmitted flux density, Q_c in kW/m^2 is evaluated by the following equation:

$$Q_c = \frac{M C_p}{A} \times K \qquad (1)$$

$$K = \frac{12}{(RHTI\,24 - RHTI\,12)} \qquad (3)$$

where K is the mean rate of escalation of the calorimeter temperature in °C/s in the region between a 12°C and 24°C rise, $RHTI$ 12 is threshold time in seconds, when the temperature of the calorimeter increases in 12°C, $RHTI$ 24 is threshold time in seconds, when the temperature of calorimeter increases in 24°C.

Percentage age heat transmission factor, Percentage $TF\,Q_o$ for incident heat flux density level is explained by equation 4 [15]:

$$TF\,Q_o\,(\%) = 100 \cdot \frac{Q_c}{Q_o} \qquad (4)$$

Evaluation of bending resistance moment

TH-4 (Tuhomer) device was employed to calculate the bending moment of firefighter clothing specimen. This device measures the bending moment of firefighter clothing specimen according to CSN 80 0858 standard. The specimen was cut into 5 cm × 2.5 cm.

Evaluation of water vapour resistance

Water vapour resistance Ret (m^{2}Pa/W) and relative water vapour permeability ($RWVP$ %age) under steady-state conditions was evaluated by Permetest (non-destructive method) which was developed by Sensora company as per ISO 11092 standard.

Evaluations are based on the principle of heat flux sensing. The test was carried out under isothermal conditions; the temperature of the measuring head was regulated at room temperature. When water passed through the measuring head, some amount of heat is lost due to evaporation. The equipment determines the evaporation of the "uncovered" head as well as that of the head when sheltered with the test fabric. The full test is accomplished when the exchange of water from the measuring head to the atmosphere reaches a steady-state (usually within two to three minutes).

Relative water vapour permeability ($RWVP$) (or relative cooling effect) is the relative heat flow responsible for the cooling of the body:

$$RWVP\,(\%) = \frac{q_v}{q_o} \cdot 100 \qquad (5)$$

where q_v is the heat flow in W/m^2, passing through the measuring head covered by the sample, and q_o is the heat flow passing through the uncovered measuring head in W/m^2.

Plan of experimental work is shown in figure 2.
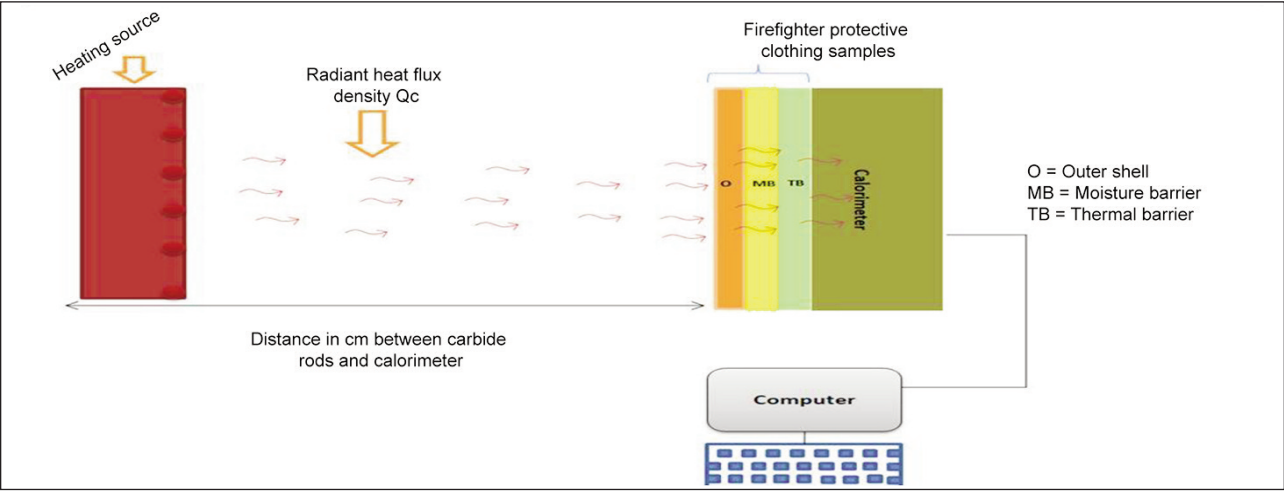
Fig. 1. Schematic diagram of radiant heat flux density machine
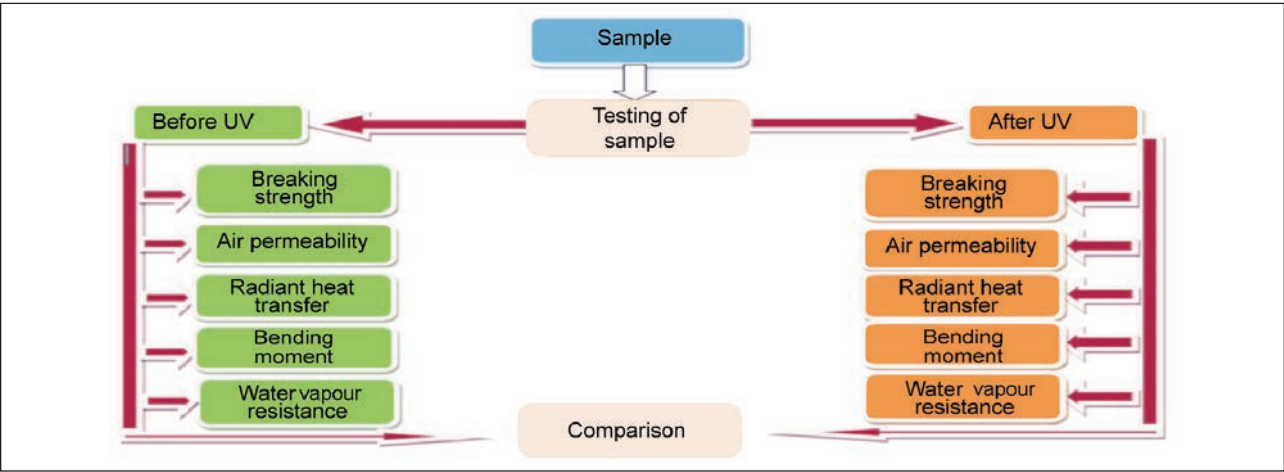
Fig. 2. Schematic diagram of experimental work

RESULTS AND DISCUSSION

Evaluation of tensile strength

It can be seen from figure 3, that the tensile strength of outer shell O1 was more before exposure to ultra-violet radiation. This clearly indicates that exposure to UV radiation impacts the mechanical properties of fibres by decreasing the strength of fibres which might be due to a decline in the breaking strength of fibres and as a result, there was a 13.06% decline in tensile strength after exposure to UV radiation. A similar pattern of tensile strength was observed in figure 4 for outer shell O2. However, the decline in breaking strength of the O2 shell was 9.67%.

After exposure to UV radiation, there was a considerable decline in the strength of outer shell O1 and O2. This indicates that there was deterioration in fibres due to which their breaking strength is decreased and as a result, the breakage of fibres takes place at low force.
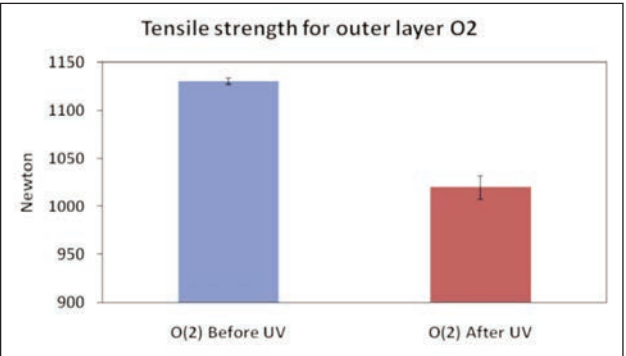
Fig. 3. Tensile strength of outer layer 1 before and after UV exposure
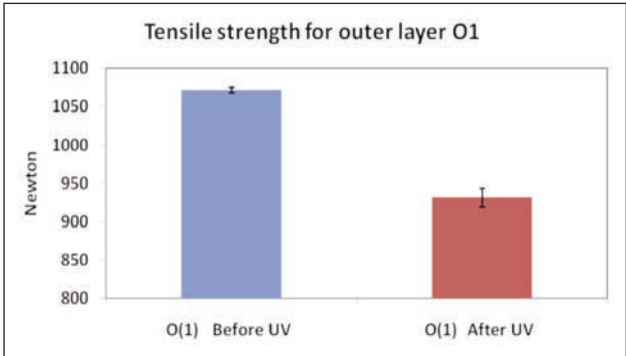
Fig. 4. Tensile strength for outer layer 2 before and after UV exposure

Evaluation of air permeability

It can be witnessed from figure 5 that there was a considerable decline in air permeability values for both specimen and outer shell O2. This might be due to fact that damage of fibres after exposure to UV radiation might further close the air gapes between fibres due to which less amount of air was passed through both outer shells. It was also witnessed that air permeability values of outer shell O1 were more as compared to outer shell O2 which might be due to the high thickness of outer shell O2.
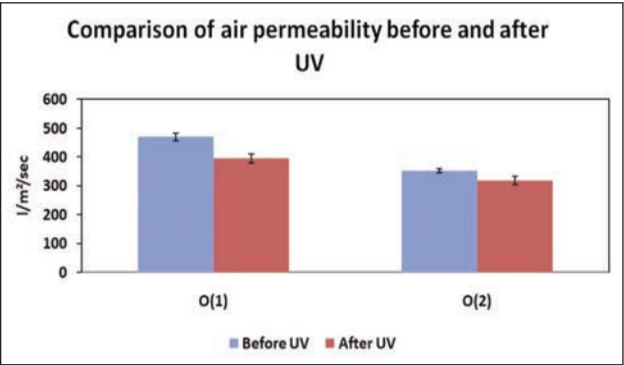
Fig. 5. Air permeability values before and after exposure to UV

After exposure to UV radiation in the outer shell, there was a 15.8 % decline in air permeability values in the case of outer shell O1. However, in the scenario of outer shell O2, there was a 9.67% decline in air permeability values.

Evaluation of radiation heat flow through tested fabrics

A perusal of table 3 reveals that specimen A has lower transmitted heat flux density values as compared to specimen B. The lesser the value of transmitted heat the better will be thermal protective performance as less amount of heat is transmitted towards the calorimeter. It is also evident from greater values for radiant heat transmission factor RHTI 24 which means the rate of rise of 24 degree centigrade is greater for specimen A as compared to specimen B.

However, it was witnessed from table 3 that after exposure to UV radiation, transmitted heat flux density values of both specimens A and B respectively have

increased. This might be due to the deterioration of constitutional fibres present in the fabric layer.

It is evident from figure 6 that before exposure to UV radiation, the pattern of the curve was flat. However, after exposure to UV radiation, the flatness of the curve decreases and it becomes slightly steep. This is a clear indication of a decline in thermal protective performance after exposure to UV radiation due to which lower values of RHTI 24 were acquired. Till the first 3 seconds, both curves are superimposed over each other. Later on, the curve of specimen A before exposure to UV radiation starts to slacken and the gaps between the two curves go on increasing till the end of the experiment.

A perusal of figure 7 reveals that the curve of specimen B before UV radiation exposure was much flat as compared to the curve of specimen B after exposure. Till the first three seconds, both curves superimposed each other. Later on, the curve before exposure started to become flat and the gap between
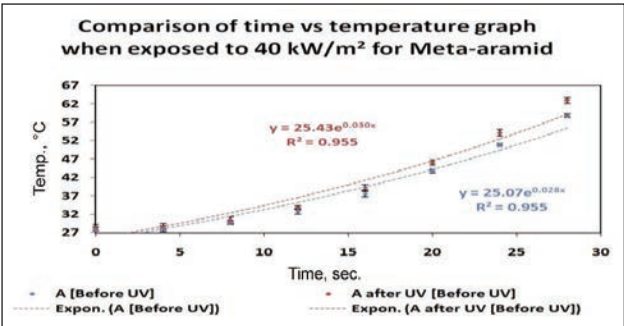
Fig. 6. Time vs temperature graph when exposed to UV for specimen A before and after UV exposure
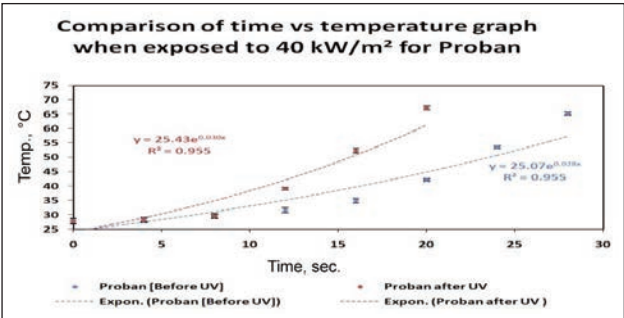
Fig. 7. Time vs temperature graph when exposed to UV for specimen B before and after UV exposure

Table 3

Sample no.	Name of material	Incident heat flux density Q_o (kW/m²)	UV exposure	RHTI12 (sec)	RHTI24 (sec)	RHTI24 − RHTI12 (sec)	Transmitted heat flux density Q_c (kW/m²)	Percentage TF Q_o
			INCIDENT HEAT FLUX DENSITY, TRANSMITTED HEAT FLUX DENSITY AND PERCENTAGE TRANSMISSION FACTOR					
1	A	40	Before UV	17.4	24.31	6.9	9.71	24
2	B			19.15	23.4	4.25	15.67	39
3	A	40	After UV	17.0	23.6	6.6	10.089	25
4	B			16.3	19.9	3.6	18.48	46.2

curves started to increase till the end of the experiment. This clearly depicts there was a decrease in thermal protective performance after exposure to UV radiation.

It can be witnessed from figures 6 and 7, the gap between curves of specimen B before and after UV radiation was much greater than the gap between curves of specimen A before and after UV radiation.

The greater the thickness of the fabric, the lesser the amount of heat passed through the fabric. However, the constituent fibre and construction of fabric and porosity also plays important role in the thermal protective performance of firefighter protective clothing. It is evident from figure 8, that specimen A has a larger value of time for rise of 24°C (RHTI 24) as compared to specimen B. This clearly indicates the better thermal protective performance of specimen A as compared to specimen B. RHTI 24 sec value of specimen A was greater than that of specimen B by 2.92%. This might be due to the fact that specimen A consist of Nomex fibre which are inherently flame resistant. Specimen B is coated with flame retardant chemical Proban on a mixture of cotton and polyester.

The decrease in thermal protective performance is a clear indication of a decrease in thermal protective behaviour of specimen because of structural changes or deterioration of outer shell of specimen B due to the swift rate of decomposition of cellulosic fibres as the incident temperature at the surface of specimen for Q_o of 40 kW/m^2 is 495°C. Consequently, specimen A had better thermal protective behaviour.
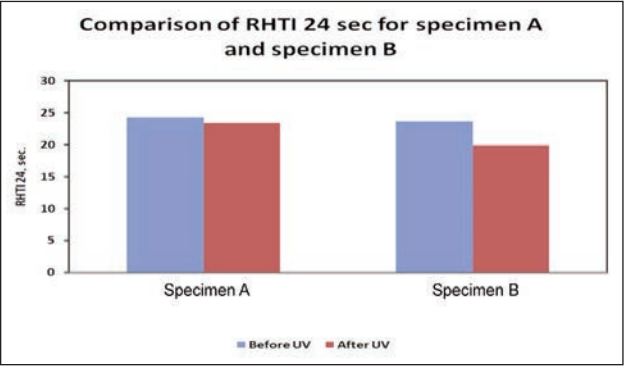
Fig. 8. Comparison of Radiant Heat Transmission Index RHTI 24 sec

It can be seen from figure 8, that in the case of specimen A, the decline in RHTI 24 sec before and after UV radiation was 3.74% when exposed to 40 kW/m^2. However, the declining percentage in specimen B was 15.67%. This clearly indicates that transmission of heat flow in the specimen takes place in a greater amount of time. The rate of heat flow in specimen A occurs at a slower rate as compared to specimen A. In consequence, specimen A has greater thermal protective performance as compared to specimen B.

Evaluation of bending resistance moment through tested fabrics

It can be noted from figure 9 that after exposure to ultraviolet (UV) radiation, there was a negligible
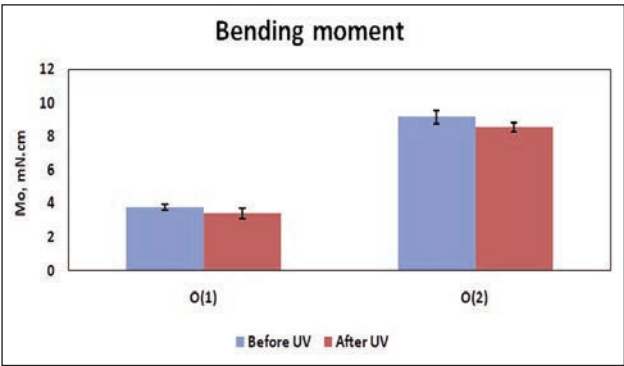
Fig. 9. Bending resistance moment values before and after UV

decline in bending moment values of both outer shell O1 and outer shell O2. Bending moment is related to the flexibility of fibres.

The greater the bending moment values, the greater will be the force required to bend the fibre. After exposure to UV radiation, there was a considerable decline in the strength of fibres as witnessed from the textile strength tester, due to which less amount of force was required to bend the fibres. In the case of outer shell O1, there was a 9.785 t decline in bending moment values after UV radiation exposure. Also, there was a 6.95% decline in bending moment values for outer shell O2 after being subjected to UV radiation.

Evaluation of water vapour resistance

The breathability of the textile substrate is related to the water vapour permeability of the fabric. The greater the water vapour permeability, the better will be comfort property of the fabric. Permeation of water vapour is one the most important aspect of the textile substrate. The greater the water vapour permeability, the lesser will be water vapour resistance values. If the permeation of water vapour is not good, it may accumulate inside the fabric and may cause an uncomfortable feeling.

It can be witnessed from figure 10 that water vapour resistance of both outer shells enhanced after exposure to UV radiation which might be due to degradation of constituent fibres which might be able to block the flow of water vapour through the exposed fabric to UV radiation. There was a 10% enhancement in water vapour resistance for outer shell O1 after exposure to
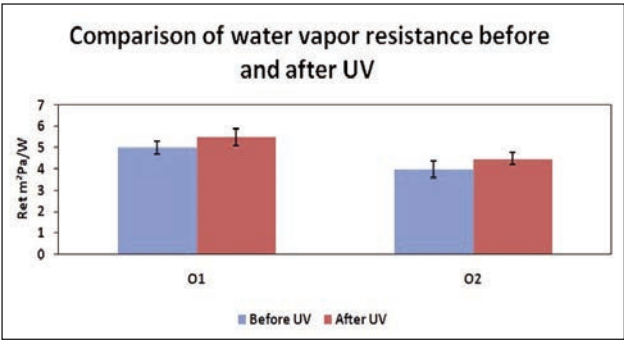
Fig. 10. Comparison of water vapor resistance before and after exposure to UV

ultraviolet radiation. In the case of O2, there was a 12.5% increment in water vapour resistance values when subjected to ultraviolet radiation.

CONCLUSION

It can be witnessed that the breaking strength of both outer shells declines after exposure to ultraviolet radiation. In the case of outer shell O1, there was a 13.06% decline in tensile strength after exposure to UV radiation and for outer shell O2, the decline in breaking strength of the O2 shell was 9.67%. Air permeability values of outer hell O1 was higher than air permeability values of outer shell O2. After exposure to UV radiation in the outer shell, there was a 15.8% decline in air permeability values in the case of outer shell O1. In the case of outer shell O2, there was a 9.6% decline in air permeability values. However, air permeability values of both specimens increase after exposure to UV radiation because of the deterioration of fibres.

Specimen A delivers better thermal protective performance as compared to specimen B. Radiant heat transmission index of both specimens A and B declines after exposure to UV radiation. RHTI 24 sec values of specimen A were greater than that of specimen B by 2.92%. For specimen A, there was a 3.74% decline in RHTI 24 sec before and after UV radiation when exposed to 40 kW/m². Whereas, the declining percentage in specimen B was 15.67%. Bending moment values of both outer shell O1 and O2 decline when subjected to UV radiation. This might be due to the loss of strength in fibres. Outer shell O1 depicts a 9.78% decline in bending moment values after UV radiation exposure. However, in the case of outer shell O2, a 6.95% decline in bending moment values was witnessed after being subjected to UV radiation. Water vapour resistance of both outer layers increases after being exposed to UV radiation. For outer shell O1, there was a 10% increment in water vapour resistance values after exposure to ultraviolet radiation. For outer shell O2, there was a 12.5% improvement in water vapour resistance values when subjected to ultraviolet radiation.

ACKNOWLEDGEMENT

REFERENCES

[1] Nayak, R., Houshyar, S., Padhye, R., *Review: Recent trend and future scope in protection and comfort of firefighter's personal protective clothing,* In: Fire science Reviews, 2014, 3, 4, 1–19

[2] Keiser, C., Rossi, R.M., *Temperature analysis for prediction of steam formation and transfer in multilayer thermal protective clothing at low level thermal radiation*, In: Text. Res. J*., 2008, 78, 1025–1035

[3] Naeem J, Mazari A, Akcagun E, Kus Z, Havelka A; Analysis of thermal properties, water vapor resistance and radiant heat transmission through different combinations of firefighter protective clothing, Journal of Industria Textilia, vol 69(6), 2018, page: 458–465

[4] Naeem, J., Mazari, A., Havelka, A., *Review: Radiation heat transfer through firefighter protective clothing,* In: Fib. and Text. East. Euro*., 2017, 25, 65–74

[5] Naeem, J., Mazari, A., Akcagun, E., Kus, Z., *Review: SiO$_2$ aerogels and its applications in firefighter protective clothing*. In: Industria Textila, 2018, 69, 1, 50–54, http://doi.org/10.35530/IT.069.01.1399

[6] Standard on *Selection, Care and Maintenance of Structural Firefighting and Proximity Fire-Fighting Protective Ensembles*, In: NFPA 1851, National Fire Protection Association, Quincy, Massachusetts, 2008

[7] Wall, M.J., Frank, G.C., *A study of the spectral distribution of sun-sky and Xenon-arc radiation in relation to the degradation of some textile yarns,* In: Text. Res. J., 1971, 41, 32–38

[8] Arrieta, C., David, E., Patricia, D., Vu-Khanh, T., *Thermal aging of a blend of high performance fibers,* In: J. of App. Poly Sci, 2010, 115, 3031–3039

[9] Shonali, N., Rick, D., Siang, P., Joannie, C., *Accelerated Weathering of Firefighter Protective Clothing: Delineating the Impact of Thermal, Moisture, and Ultraviolet Light Exposures,* In: NIST Technical Note 1746, 2012, 1–32

[10] Blais, P., Carlsson, D.J., Parnell, R.D., Wiles, D.M., *High Performance Fibers. Part II: Limitations: Photo-and Thermal Degradation,* In: Canadian Textile Journal*, 1973, 90, 93–96

[11] Carlsson, D.J., Gan, L.H., Paranell, R.D., Wiles, D.M., *The photodegradation of Poly (1,3-Phenylene Isophtalamide) films in air, Part B,* In: J. Pol. Sc., 1973, 11, 683–688

[12] Mazari, F.B., Mazari, A., Kremenakova, D., Huang, J. Effect of UV-weathering on flex fatigue of plastic optical fiber, *Industria Textila*, 2015, 66 (4), pp. 171–175.

[13] Brown, J.R., Browne, N.M., Burchill, P.J., Egglestone, G.T., *Photochemical ageing of Kevlar 49,* In: Text. Res. J., 1983, 53, 4, 214–219

[14] Said, M.A., Dingwall, B., Gupta, A., Seyam, A.M., Mock, G., Theyson, T., *Investigation of ultraviolet resistance of high strength fibers,* In: Advances In Space Research*, 2006, 37, 2052–2058

[15] Meb, G.W., Gmb, H.P., *Combustion behavior Test equipment*, Berlin, 2002

[16] Houshyar, S., Padhye, R., Ranjan, S., Steve, T.S., Nayak, R., *The impact of ultraviolet light exposure on the performance of polybenzidimazole and polyaramid fabrics: Prediction of end-of-life performance*, In: J. of Indus. Text., 2018, 48, 77–86

[17] Carlsson, D.J., Gan, L.H., Wiles, D.M., *The photolysis of fully aromatic amides,* In: Canadian Journal of Chemistry, 1975, 53, 2337–2344

[18] ASTM G 154-06: *Standard Practice for Operating Fluorescent Light Apparatus for UV Exposure of Non-metallic Materials*, 2006

Authors:

ADNAN MAZARI[1], FUNDA BUYUK MAZARI[1], JAWAD NAEEM[2], ANTONIN HAVELKA[1],
PARASHANT MARAHATTA[1]

[1]Technical University of Liberec, Faculty of Textile Engineering, Department of Clothing,
Studentska 2, Husova, 1402/2, Liberec, Czech Republic

[2]National Textile University, Pakistan, School of Engineering and Technology, Department of Textile Technology,
Sheikhupura Road, Faisalabad, Pakistan

Corresponding author:

ADNAN MAZARI
e-mail: adnan.ahmed.mazari@tul.cz

Effectiveness of electromagnetic shielding in the case of electromagnetic shields based on ferromagnetic materials

RALUCA MARIA AILENI
CRISTIAN MORARI

DOINA TOMA
LAURA CHIRIAC

ABSTRACT – REZUMAT

Effectiveness of electromagnetic shielding in the case of electromagnetic shields based on ferromagnetic materials

This paper presents a study concerning the effectiveness of electromagnetic shielding of textile structures coated with ferromagnetic materials. For this scientific approach, 6 experimental models of composites-based fabrics with electromagnetic properties were made by applying paste/dispersion based on polymeric matrices (polyvinyl alcohol (PVA), polyvinylpyrrolidone (PVP)), copper microparticles (Cu), nickel (Ni), aluminium (Al), silver (Ag), and graphene oxide (GO) using classical deposition (immersion, scraping) and ultrasonic technologies. The effectiveness of electromagnetic shielding has been evaluated using a coaxial cell model TEM 2000, oscilloscope model MDO 3102, power amplifier Model SMX5, signal generator type E8257D. The measurements were performed in the frequency range 0.1 MHz – 1 GHz and power 30 W. from all samples, the samples based PVA-Ni and PVA-Ni-Al exhibit pronounced surface conductivity and increased effectiveness of electromagnetic shielding for low and high frequencies.

Keywords: composites, textile, electromagnetic shielding, resistance, conductive, nickel, aluminium

Eficacitatea ecranării electromagnetice în cazul ecranelor electromagnetice pe bază de materiale feromagnetice

Această lucrare prezintă un studiu privind eficacitatea ecranării electromagnetice a ecranelor realizate din materiale textile cu acoperiri feromagnetice. Pentru acest demers științific, au fost realizate 6 modele experimentale de compozite pe bază de țesături cu proprietăți electromagnetice obținute prin aplicarea pastei/dispersiei pe bază de matrici polimerice (alcool polivinilic (PVA), polivinilpirolidonă (PVP)), microparticule de cupru (Cu), nichel (Ni), aluminiu (Al), argint (Ag) și oxid de grafen (GO)), prin intermediul tehnologiilor clasice de depunere (imersie, raclare) și tehnologiilor bazate pe ultrasunete. Eficacitatea ecranării electromagnetice a fost evaluată utilizând o celulă coaxială model TEM 2000, un osciloscop model MDO 3102, un amplificator de putere Model SMX5, un generator de semnal tip E8257D. Măsurătorile au fost efectuate în intervalul de frecvență 0,1 MHz – 1 GHz și putere 30 W. Dintre toate probele analizate, probele pe bază de PVA-Ni și PVA-Ni-Al prezintă o conductivitate ridicată și eficiență crescută a ecranării electromagnetice pentru frecvențe joase și înalte.

Cuvinte-cheie: compozite, textil, ecranare electromagnetică, rezistență, conductiv, nichel, aluminiu

INTRODUCTION

Numerous researches present different techniques starting from numerical simulation [1] and experimental development of the electromagnetic shields. Materials such as iron, cobalt and nickel are ferromagnetic materials having a positive susceptibility to the magnetic field and are commonly used for non-volatile information storage in tapes, hard drives. Different studies show intensive research in the synthesis of the nanostructures-based iron-nickel [2–4] using different techniques such as electrodeposition [3], integration of the metal particles in silicone [5, 6] or polymethacrylate matrix [7], plastic or metal matrix [8], low-density polyethene composite [9] or carbides [10]. Another versatile technique consists of using arc thermal spray deposition [11]. However, the coating of the textile materials with metals integrated into dispersions, paste [11–13] can lead to obtaining a material with good electromagnetic interference shielding effectiveness [14, 15]. Another challenge is to use carbon materials [14, 15] or conductive polymers [16] for electromagnetic shielding. However, an intense concern is to use nano or micro-structured composites based on copper and nickel [14] or aluminium.

EXPERIMENTAL PART

In the experimental part, we developed 23 experimental samples using cotton fabric (BBC) 100% with different structures (e.g., plain weave, twill, panama) with electroconductive properties based on classical technologies for thin-film deposition by scraping and immersion/ultrasonic technologies using the polymeric matrix (PVA, PVP), copper (Cu) or nickel (Ni), aluminium (Al) or silver (Ag) microparticles and graphene oxide (GO). To evaluate the effectiveness of electromagnetic shielding (SEdB) 6 functionalized fabrics (M1-M6) were selected and cut in the form of discs (figure 1) to the required dimensions and drilled
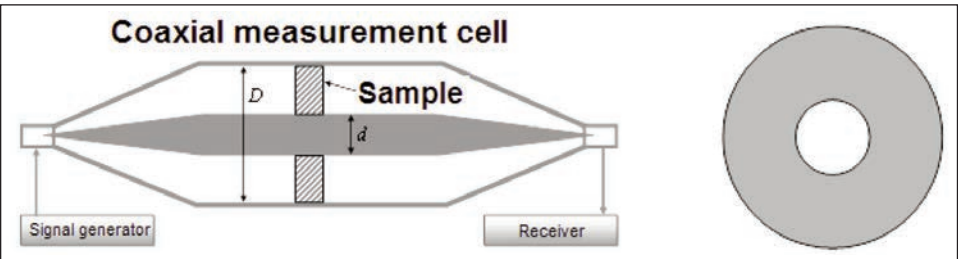
Fig. 1. Measurement assembly and shape of the measurement samples

The Schelkunoff equation 1 was used to evaluate the effectiveness of electromagnetic shielding:

$$SE_{dB} = 10 \log_{10} \frac{P_1}{P_2} \quad (1)$$

where: P_1 in dB is the signal strength detected in the absence of the electromagnetic screen; P_2 in dB is the signal strength detected in the presence of the electromagnetic screen.

The SE_{dB} is given by the difference between the signal level measured without a sample and the signal level measured with a sample mounted inside the measuring cell, both measured in dB (according to the IEEE Standard 299-2006). The tests were based on the ASTM ES7-83 standard.

Figure 3 shows the efficiency of electromagnetic attenuation depending on the values set for the frequency in the range 0.1 MHz – 1 GHz. From the series of experiments subjected to testing, the U4 and U5 samples proved to be effective. The results of

Fig. 2. Ag-contoured samples to measure the effectiveness of electromagnetic attenuation

in the centre to be mounted in the TEM cell measuring (outer diameter of 100 mm and inner diameter of 30 mm). After the discs were cut, a layer of silver-based conductive paint was applied to the edges of the samples to ensure proper electrical contact with the measuring cell (figure 2). The tests were performed at a temperature of 22°C and a humidity of 40%. For the investigation of the attenuation of the electromagnetic screens, the following specific equipment was used (from the endowment of INCDIE ICPE-CA): coaxial cell model TEM 2000; Tektronix oscilloscope model MDO 3102; power amplifier Model SMX5; signal generator type E8257D. The measurements were performed in the frequency range 0.1 MHz – 1 GHz (table 1).

Fig. 3. Graphical representation of electromagnetic attenuation efficiency vs. frequency

Table 1

PHYSICO-MECHANICAL AND ELECTRICAL PROPERTIES OF THE SAMPLES

Sample no.	PVA	PVP	GO	Ni	Ag	Cu	Al	Water	Rs* (Ω)	M** (g/m²)	δ*** (mm)
M0	-	-	-	-	-	-	-	x	10^{12}	518	1.36
M1	x	-	-	x	-	x	-	x	10^7	623.2	1.424
M2	-	x	x	-	-	-	-	x	10^{10}	671	1.51
M3	-	x	-	-	x	-	-	x	10^{10}	656	1.59
M4	x	-	-	x	-	-	-	x	10^3	834	1.71
M5	x	-	-	-	x	-	-	x	10^3	608	2.096
M6	x	-	-	x	-	-	x	x	10^3	769.6	3.878

Note: *Rs – Surface resistance, **M – Mass, ***δ – Thickness.

Frequency (MHz)	Electromagnetic shielding efficiency (SEdB)					
ELECTROMAGNETIC SHIELDING EFFICIENCY (SEDB)						
	Sample M1	Sample M2	Sample M3	Sample M4	Sample M5	Sample M6
0.1	0.6	0	0	22.7	0	17.7
0.2	0.4	0	0	22.4	0	17.7
0.3	0.4	0.1	0	22.5	0	17.7
0.5	0.4	0	0	22.5	0	17.6
1	0.6	0.1	0	22.7	0	17.8
5	0.5	0	0	**22.9**	0.1	18.1
10	0.6	0.1	0	22.7	0	18.3
50	0.5	0.2	0	21.1	0.1	18.1
100	0.4	0	0.2	19.9	0	18.4
200	0.4	0	0	17.3	0	17.6
300	0.2	0	0	15.5	0	17.6
400	0.4	0	0.1	14.9	0	18.1
500	0.7	0	0.4	14.1	0	17.9
600	0.3	0	0	13.9	0.1	19
700	1.2	0.7	0.6	14.6	0	**20.8**
800	0.3	0	0	12.6	0.1	17.9
900	0	-	0.1	12.4	0.1	18.1
1000	0.4	-	0.2	12.8	0.3	18.7

the electromagnetic attenuation efficiency are presented in table 2.

Figure 4 presents the topographic analysis of the surface of the textiles on the basis of the optical microscopy with the digital camera, magnification (60×), the surface of the initial fabric M_0 (without metallic microparticles) (figure 4, *a*) and the surface of the fabrics metallic microparticle and GO (figures 4, *b–g*).

The surface resistance investigation was performed using a resistance meter with built-in parallel electrodes and we obtained a surface resistance of $10^3 \ \Omega$

for samples M_4–M_6, which indicates the composite based on microparticles of Ni, Al and Cu present pronounced surface conductivity and can be used to develop electromagnetic shields.

RESULTS AND DISCUSSIONS

From the experimental samples of 3D composite based on polymer matrices with electromagnetic properties for electromagnetic screens, experimental models U_3 and U_5 obtained by immersion and ultrasound were selected because they show a uniform electrical conductivity over the entire surface after
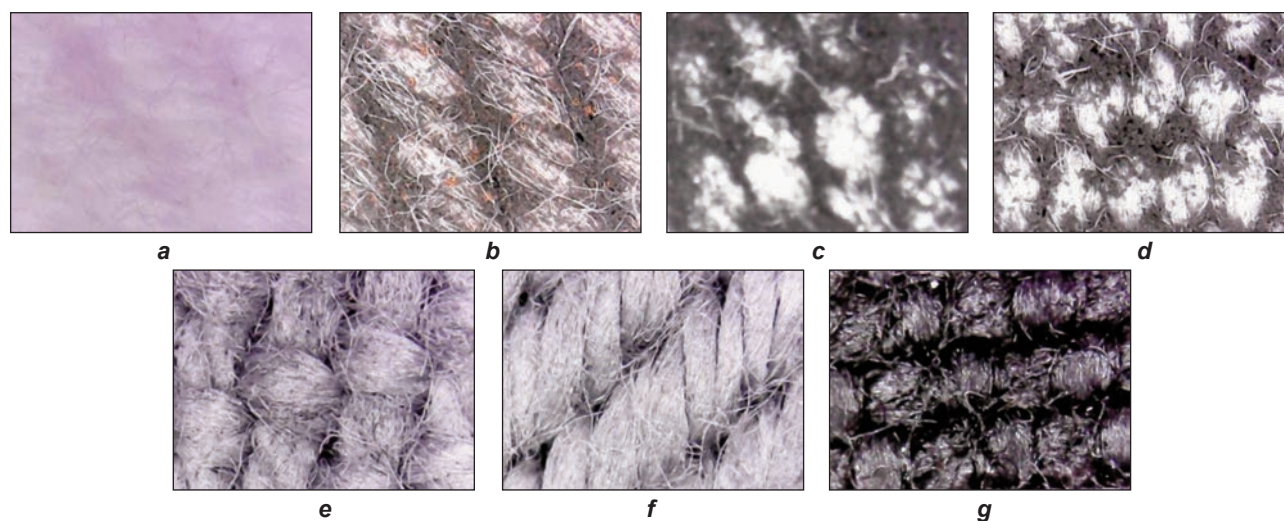
Fig. 4. Topographic analysis of the surface of the textiles based on the optical microscopy: *a* – fabric without microparticles submitted; *b* – Sample M1; *c* – Sample M2; *d* – Sample M3; *e* – Sample M4; *f* – Sample M5; *g* – Sample M6

drying and crosslinking, low surface resistance ($Rs = 10^3$ Ω) and have the highest electromagnetic efficiency.

Following the electromagnetic effectiveness and surface resistance tests, we observed that:

• Between the efficiency of the electromagnetic shielding and surface resistance of the obtained samples, it is an indirect relationship of dependence.

• Experimental tests performed by scraping off the conductive paste-based Ni and/or Al show surface resistance values similar to those obtained for samples made by immersion/ultrasound in dispersions based on PVA and Ni and Al microparticles (M4, M6).

• The efficiency of electromagnetic shielding in the case of screens based on Ni microparticles (M4 test) is higher than the efficiency of shielding in the case of electromagnetic screens based on Al and Ni (M6 test) at low frequencies (0.1–325 MHz).

• The efficiency of electromagnetic shielding in the case of screens based on Al and Ni microparticles (sample M6) is higher than the efficiency of shielding

in the case of Ni-based screens (sample M4) at high frequencies (326 MHz – 1 GHz).

For parameters such as electrical surface resistance, the thickness (δ), mass (M), and electromagnetic shielding efficiency (S1 for 5 MHz frequency and S2 for 700 MHz frequency) have been developed a multivariate analysis.

In figures 5–10 are presented the 3D representations of the electrical resistance (Rs) in the function of the thickness (δ), mass (M), electromagnetic shielding efficiency at 5 MHz (S1) and electromagnetic shielding efficiency at 700 MHz (S2) using MATLAB software. For experimental parameters (Rs, M, δ, S1, S2) was performed an analysis of the correlation coefficient Pearson between Rs and M, δ, S1, S2:

$$r_{xy} = \frac{\frac{1}{n} \sum (x - \overline{x})(y - \overline{y})}{s_x s_y} \qquad (2)$$

where x, y represent the individual values of the variables x and y; $\overline{x}$, $\overline{y}$ represent the arithmetic mean of all the values of x, y; s_x, s_y represents the standard deviation of all values x and y.
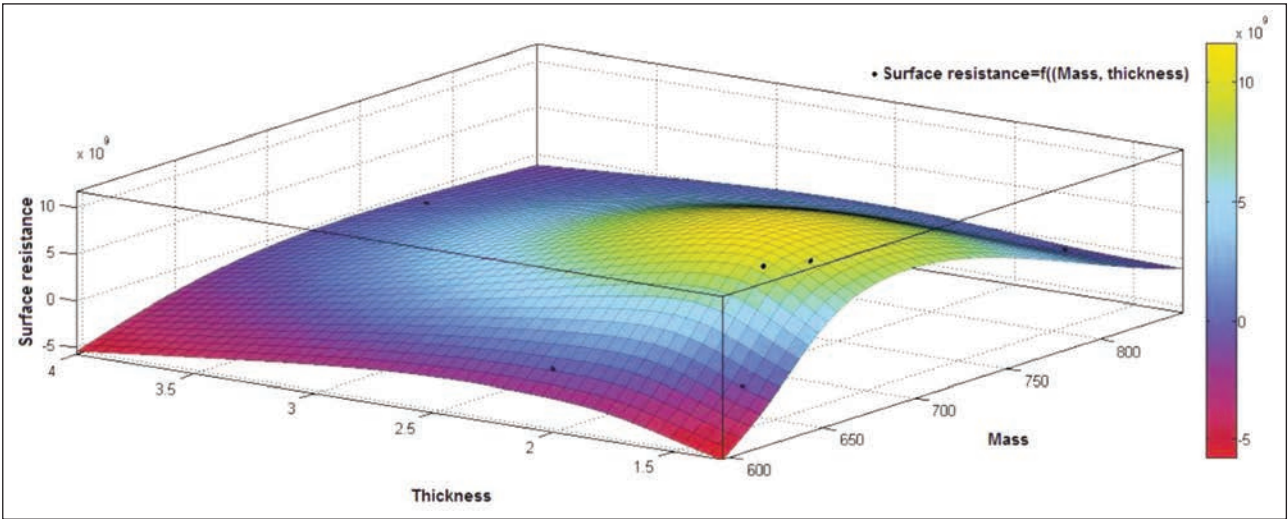
Fig. 5. 3D representation of the surface resistance according to the mass (M) and thickness (δ), Rs = f(M, δ))
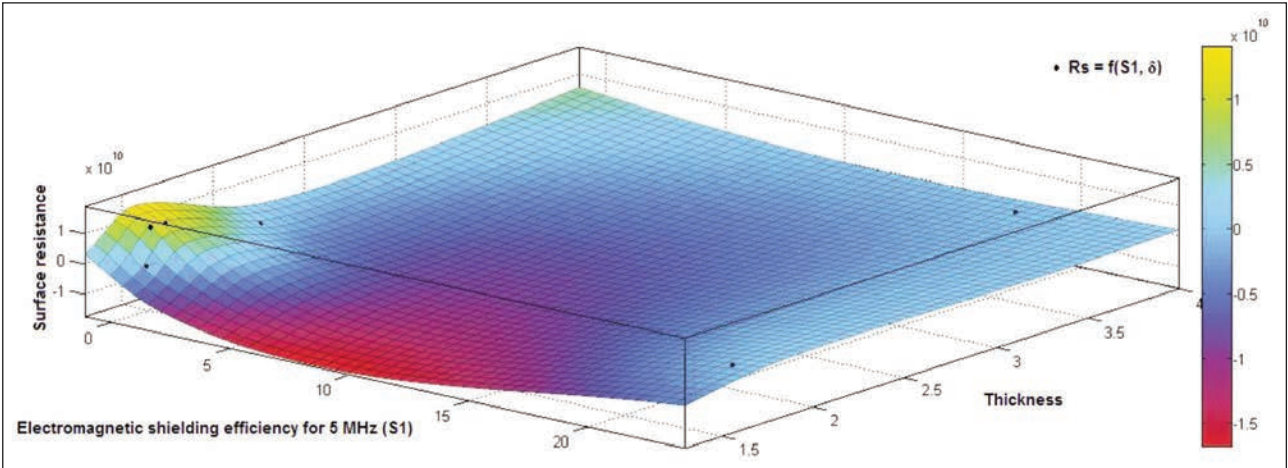
Fig. 5. 3D representation of the surface resistance (Rs) according to the electromagnetic shielding efficiency at 5 MHz (S1) and thickness (δ), Rs = f(S1, δ)
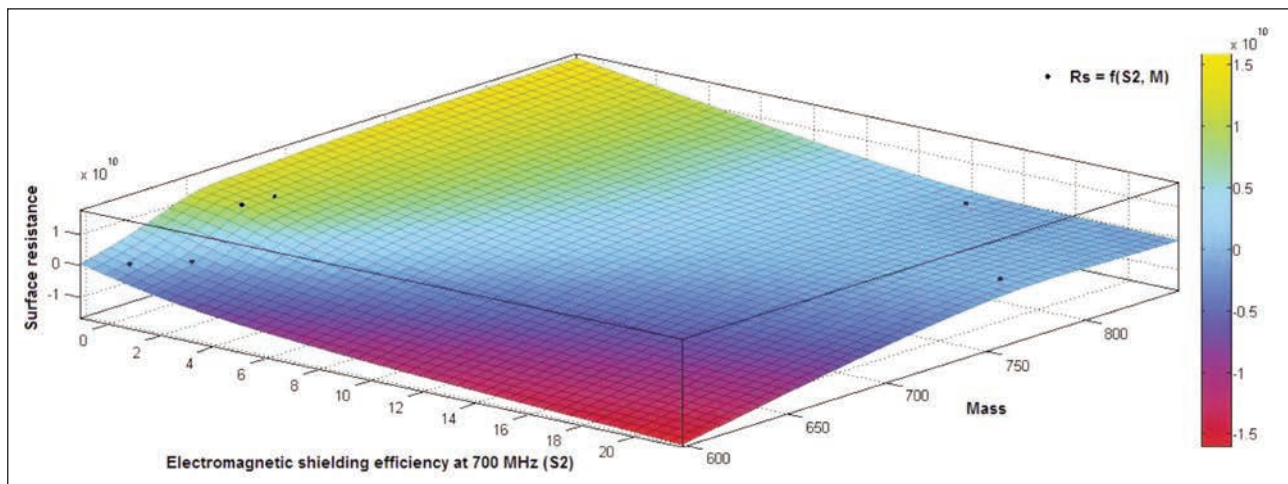
Fig. 7. 3D representation of the surface resistance (*Rs*) according to the electromagnetic shielding efficiency at 700 MHz (*S2*) and mass (M), *Rs* = *f*(*S2*, *M*)
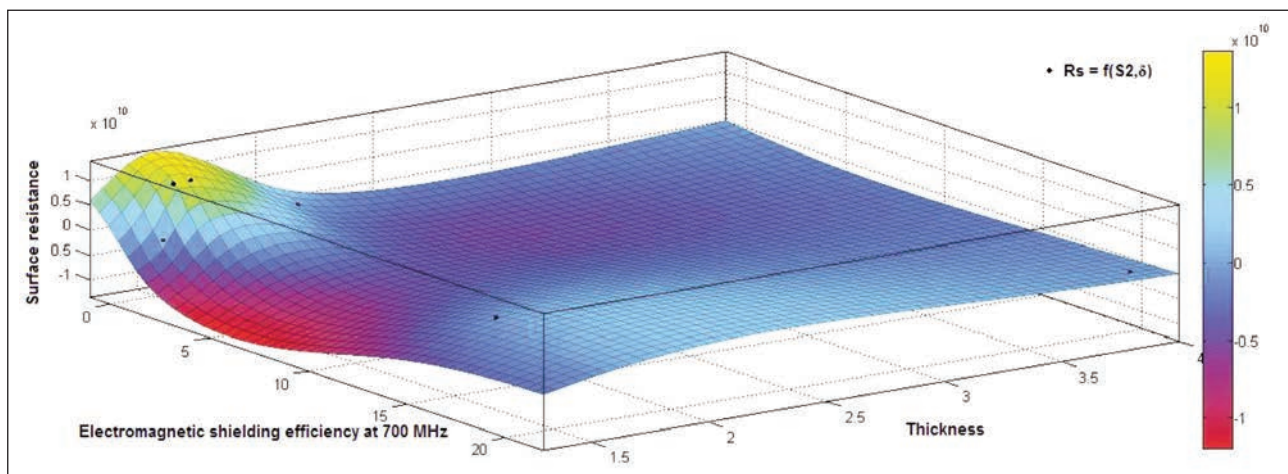
Fig. 8. 3D representation of the surface resistance (*Rs*) according to the electromagnetic shielding efficiency at 700 MHz (*S2*) and thickness (δ), *Rs* = *f*(*S2*, δ)
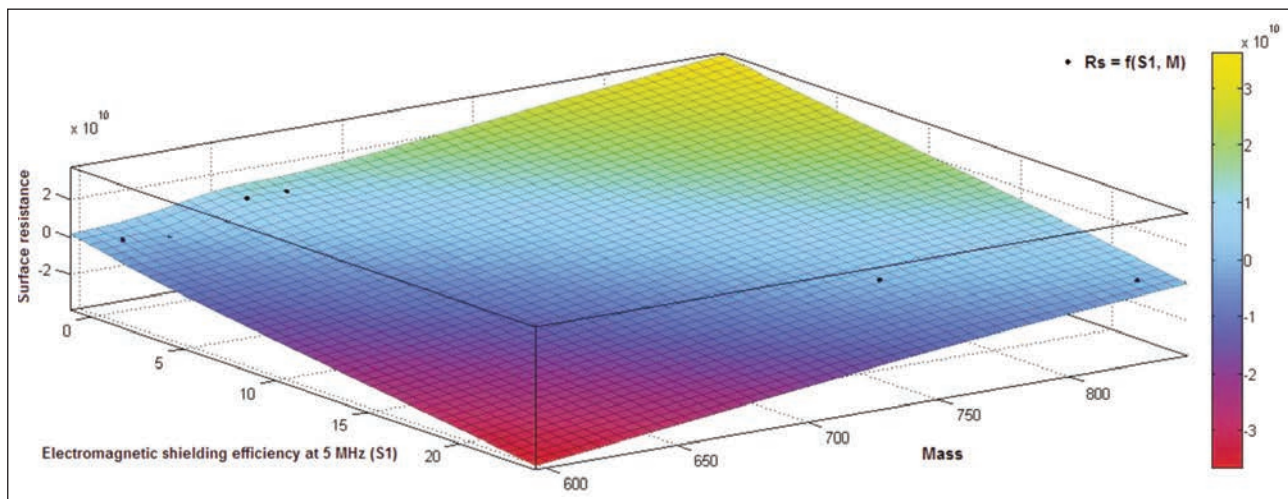
Fig. 9. 3D representation of the surface resistance (*Rs*) according to the electromagnetic shielding efficiency at 5 MHz (*S1*) and mass (M), *Rs* = *f*(*S1*, *M*)

$$r_{R_SM} = \begin{vmatrix} 1.0000 & -0.2623 \\ -0.2623 & 1.0000 \end{vmatrix} \Leftrightarrow$$

$$\Leftrightarrow r12_{R_SM} = r21_{R_SM} = -0.2623$$

(3)

$$r_{R_S\delta} = \begin{vmatrix} 1.0000 & -0.4027 \\ -0.4027 & 1.0000 \end{vmatrix} \Leftrightarrow$$

$$\Leftrightarrow r12_{R_S\delta} = r21_{R_S\delta} = -0.4027$$

(4)
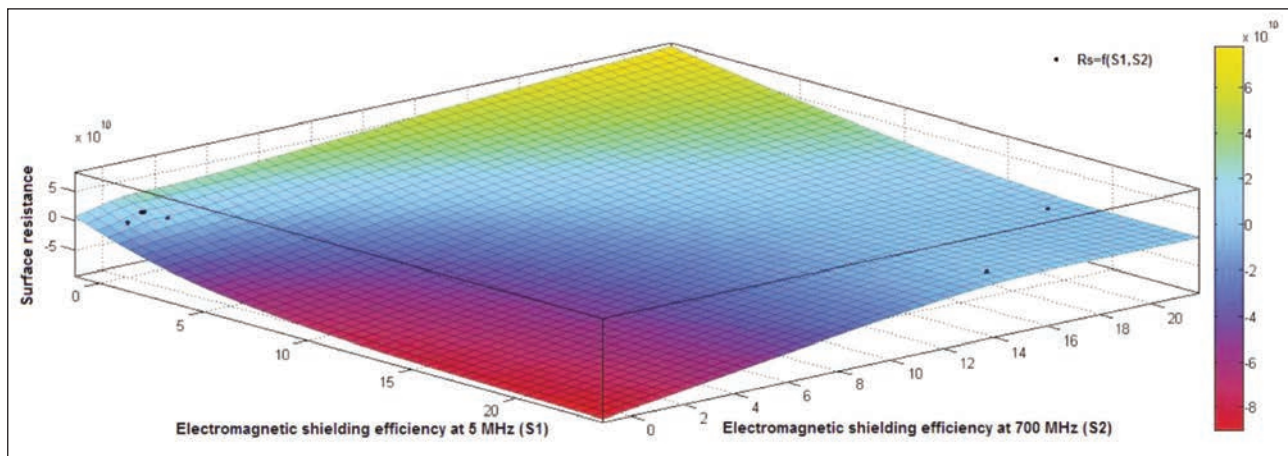
Fig. 10. 3D representation of the surface resistance (Rs) according to the electromagnetic shielding efficiency at 5 MHz ($S1$) and electromagnetic shielding efficiency at 700 MHz (S2), $Rs = f(S1, S2)$

$$r_{R_S S1} = \begin{vmatrix} 1.0000 & -0.5061 \\ -0.5061 & 1.0000 \end{vmatrix} \Leftrightarrow$$
$$\Leftrightarrow r12_{R_S S1} = r21_{R_S S1} = -0.5061$$

(5)

$$r_{R_S S2} = \begin{vmatrix} 1.0000 & -0.4858 \\ -0.4858 & 1.0000 \end{vmatrix} \Leftrightarrow$$
$$\Leftrightarrow r12_{R_S G} = r21_{R_S G} = -0.4858$$

(6)

Analysing the values of the correlation coefficients $r_{R_S M}$ (equation 3), $r_{R_S \delta}$ (equation 4), $r_{R_S S1}$ (equation 5), and $r_{R_S S2}$ (equation 6) which are all negative, it can be observed that between the surface resistance (Rs) and other parameters (mass, thickness, electromagnetic shielding efficiency at 5 MHz ($S1$) and electromagnetic shielding efficiency at 700 MHz ($S2$)), it is a negative inverse proportionality relationship, and this indicates that the increase of the mass or thickness with conductive coatings will generate the decreasing of the surface resistance, and obvious an increasing of the surface conductance and electromagnetic shielding efficiency. On the other side, it is evident the surface resistance and electromagnetic shielding efficiency are in an inverse proportionality relationship.

CONCLUSIONS

In conclusion, polymeric 3D composites obtained based on PVA-Ni, PVA-Ni-Al conductive pastes can be used to make electromagnetic screens for low or high frequencies.

Based on the analysis of the Pearson correlation coefficient, we can appreciate that mass, thickness and electromagnetic shielding efficiency are in inverse dependence relationship with the surface resistance. However, to obtain good electromagnetic shielding efficiency we should reduce the surface resistance. However, in this paper, the paramagnetic property of the nickel was evident and had an important contribution in shielding at different frequencies.

ACKNOWLEDGMENTS

REFERENCES

[1] Bavastro, D., Canova, A., Giaccone, L., Manca, M., *Numerical and experimental development of multilayer magnetic shields*, In: Electric power systems research, 2014, 116, 374–380.

[2] Krajewski, M., Tokarczyk, M., Stefaniuk, T., Słomińska, H., Małolepszy, A., Kowalski, G., Ślawska-Waniewska, A., *Magnetic-field-induced synthesis of amorphous iron-nickel wire-like nanostructures*, In: Materials Chemistry and Physics, 2020, 246, 122812

[3] Sreedeviamma, D. K., Remadevi, A., Sruthi, C. V., Pillai, S., Peethambharan, S. K., *Nickel electrodeposited textiles as wearable radar invisible fabrics*, In: Journal of Industrial and Engineering Chemistry, 2020, 88, 196–206

[4] Pandey, R., Tekumalla, S., Gupta, M., *EMI shielding of metals, alloys, and composites*, In: Materials for Potential EMI Shielding Applications, 2020, 341–355

[5] Wanying, L., Qin, W., Qi, S., Yinxiang, L., *Preparation of CF/Ni-Fe/CNT/silicone layered rubber for aircraft sealing and electromagnetic interference shielding applications*, In: Chinese Journal of Aeronautics, 2021

[6] Turczyn, R., Krukiewicz, K., Katunin, A., Sroka, J., Sul, P.*, Fabrication and application of electrically conducting composites for electromagnetic interference shielding of remotely piloted aircraft systems*, In: Composite Structures, 2020, 232, 111498

[7] Li, J., Wang, A., Qin, J., Zhang, H., Ma, Z., Zhang, G., *Lightweight polymethacrylimide@ copper/nickel composite foams for electromagnetic shielding and monopole antennas*, In: Composites Part A: Applied Science and Manufacturing, 2020, 140, 106144

[8] Tugirumubano, A., Vijay, S.J., Go, S.H., Kwac, L.K., Kim, H.G., *Characterization of electromagnetic interference shielding composed of carbon fibers reinforced plastics and metal wire mesh based composites*, In: Journal of Materials Research and Technology, 2019, 8, 1, 167–172

[9] Vaid, K., Rathore, D., Dwivedi, U.K., *Electromagnetic interference of nickel ferrite and copper ferrite filled low-density polyethylene composite*, In: Journal of Composite Materials, 2020, 54, 30, 4799–4806

[10] Shahzad, F., Alhabeb, M., Hatter, C.B., Anasori, B., Hong, S.M., Koo, C.M., Gogotsi, Y., *Electromagnetic interference shielding with 2D transition metal carbides (MXenes),* In: Science, 2016, 353, 6304, 1137–1140

[11] Jang, J.M., Lee, H.S., Singh, J.K., *Electromagnetic Shielding Performance of Different Metallic Coatings Deposited by Arc Thermal Spray Process*, In: Materials, 2020, 13, 24, 5776

[12] Geetha, S., Satheesh Kumar, K.K., Rao, C.R., Vijayan, M., Trivedi, D.C*., EMI shielding: Methods and materials – A review*, In: Journal of Applied Polymer Science, 2009, 112, 4, 2073–2086

[13] Palanisamy, S., Tunakova, V., Hu, S., Yang, T., Kremenakova, D., Venkataraman, M., Militky, J., *Electromagnetic Interference Shielding of Metal Coated Ultrathin Nonwoven Fabrics and Their Factorial Design*, In: Polymers, 2021, 13, 4, 484

[14] Chung, D.D.L., *Electromagnetic interference shielding effectiveness of carbon materials,* In: Carbon, 2001, 39, 2, 279–285

[15] Li, R., Wang, S., Bai, P., Fan, B., Zhao, B., Zhang, R*., Enhancement of electromagnetic interference shielding from the synergism between Cu@ Ni nanorods and carbon materials in flexible composite films,* In: Materials Advances, 2021, 2, 2, 718–727

[16] Chiguma, J., Jones Jr, W.E., *Template-Free Synthesis of Aligned Polyaniline Nanorods/Tubes and Copper/Copper Hydroxide Nanowires for Application as Fillers in Polymer Nanocomposites*, In: Advances in Materials Physics and Chemistry, 2018, 8, 01, 71

Authors:

RALUCA MARIA AILENI[1], CRISTIAN MORARI[2], DOINA TOMA[1], LAURA CHIRIAC[1]

[1]National Research Development Institute for Textiles and Leather,
16, Lucretiu Patrascanu Street, 030508 Bucharest, Romania

[2]INCDIE ICPE-CA, 313 Splaiul Unirii, Bucharest, Romania

Corresponding author:

RALUCA MARIA AILENI
e-mail: raluca.aileni@incdtp.ro

ANCOVA analysis of penetration force on Kevlar fabrics used for ballistic protective equipment

IONUT DULGHERIU
SAVIN DORIN IONESI
MANUELA AVADANEI
LILIANA HRISTIAN

EMIL CONSTANTIN LOGHIN
LILIANA BUHU
IRINA IONESCU

ABSTRACT – REZUMAT

ANCOVA analysis of penetration force on Kevlar fabrics used for ballistic protective equipment

The paper aims to highlight the existence of significant differences between the variation of the penetration force of three groups of fabrics used for ballistic protective equipment in the function of the deformation arrow, using the ANCOVA mathematical model with a nominal independent variable and a quantitative independent variable. The model included: the dependent variable (Y) – the variation of the penetration force T(N); nominal independent variable – fabric group; quantitative independent variable – deformation arrow, Δl(mm). This paper analyses the effect of the nominal independent variable and the quantitative independent variable on the penetration force variation, using the ANCOVA model. From the results obtained, through Tests of Be-tween-Subjects Effects, it is observed that the effect of the nominal independent variable "fabric group" is significant and also the effect of the covariate "deformation arrow" is significant. Interpreting the value of Sig < 0.05, it can be concluded that there are significant differences between the variation of the penetration force deformation (alternative hypothesis H1 is accepted). This technique can be used later to model the physical and mechanical properties of fabrics and to select the most appropriate fabrics to meet the requirements of a particular field of use.

Keywords: ANCOVA model, deformation arrow, penetration force, Kevlar fabrics

Analiza forței de străpungere a țesăturilor din Kevlar folosite pentru echipamente de protecție balistică utilizând modelul ANCOVA

Lucrarea și-a propus să evidențieze existența diferențelor semnificative dintre variația forței de străpungere a unor grupe de țesături destinate confecționării echipamentelor de protecție balistică în funcție de săgeata de deformare, utilizând modelul matematic ANCOVA cu o variabilă independentă nominală și o variabilă independentă cantitativă. În cadrul modelului au fost incluse: variabila dependentă (Y) – variația forței de străpungere T(N); variabila independentă nominală – grupa de țesături; variabila independentă cantitativă – săgeata de deformare, Δl(mm). Această lucrare studiază efectul variabilei independente nominale și a variabilei independente cantitative asupra variației forței de străpungere, utilizând modelul ANCOVA.

Din rezultatele obținute, prin intermediul Tests of Between-Subjects Effects, se observă că efectul variabilei indepen-dente nominale "grupa de țesături" este semnificativ și de asemenea, efectul covariabilei "săgeata de deformare" este semnificativ. Interpretând valoarea Sig < 0,05, se poate concluziona că între variația forței de străpungere există diferențe semnificative în funcție de grupele de țesături studiate și săgeata de deformare (se acceptă ipoteza alternativa H1). Această tehnică poate fi folosită ulterior pentru modelarea proprietăților fizico-mecanice ale țesăturilor și pentru selectarea celor mai adecvate țesături privind satisfacerea cerințelor unui anumit domeniu de utilizare.

Cuvinte-cheie: modelul ANCOVA, săgeata de deformare, forța de străpungere, țesături Kevlar

INTRODUCTION

Ballistic protection products simultaneously impose two contradictory requirements: ballistic performance requires a large mass and volume of the product, but at the same time the product must be light and comfortable to wear. The factors that are influencing the energy absorption characteristics of ballistic protection systems depend on the properties of the constituent materials, the design parameters of the textile material, the number of layers of textile material, the density of the material and the impact conditions, such as projectile mass, impact velocity and projectile geometry.

In the last decades, a significant research effort has been made to study the ballistic impact mechanisms of bulletproof vests reinforced with textile structures. The traditional method of improving ballistic characteristics is to increase the number of layers [1–7] or, for some applications, to stitch the layers together with an orthogonal pattern or bias pattern [8–10]. The ballistic performance of bulletproof vests/equipment is influenced by different factors, such as the design and structure of textile/non-textile layers, their

number, thickness, specific mass and nature of the raw material [11–15].

In order to improve the ballistic performances of the bulletproof equipment's, the computational analysis or the mathematical modelling of the different relevant factors/characteristics are frequently used, among which the most important ones are the penetration resistance and the deformation arrow [16–20]. The mechanisms of energy absorption at ballistic speeds are important in ballistic protection [21, 22]. The primary factors that determine the weight needed to stop a projectile are the specific energy absorption, determined by the tenacity and elongation, and the sonic velocity of fibres, determined by the specific modulus, indicating the area of the fabric to be involved in stopping the projectile [23]. Typical bulletproof vests are made from multiple layers of woven fabric, with the degree of protection being increased as the number of fabric layers increases [24]. These layers are assembled into a 'ballistic panel', which is then inserted into the 'carrier', which is constructed from conventional garment fabrics such as nylon or cotton. The ballistic panel may be permanently sewn into the carrier or maybe removable [25]. Although the overall finished product looks relatively simple in construction, the ballistic panel can be very complex. Even the manner in which the ballistic panels are assembled into a single unit can differ from one product to another [26, 27].

In the constructive technological design of ballistic/bulletproof vest, it is important to know under what conditions the layer structure has maximum/minimum deformation, at what value of the penetration force and what pressure is transmitted to the body during impact. The number and nature of the layers of material in the bulletproof vest directly determine the level of protection provided (according to the NIJ standard), the parameters of comfort, the production of possible traumas or shocks on the human body.

In the present paper, the variation of the penetration force and the corresponding elongation for several variants of Kevlar fabric groups were analysed, using the ANCOVA method.

MATERIALS AND METHODS

The combination of layers chosen for the manufacture of individual ballistic protection equipment must primarily ensure the protection of the body against the action of risk factors, low-level trauma and comfort parameters. Kevlar is a material whose manufacture imposes high costs. The need to use a large number of layers has highlighted the need to combine it with other materials when conditions of use allow. The study included the use of Kevlar layers (5 layers) and their combination with 1 or 2 metallic gauze layers, tested for penetration force and deformation arrow. The tested ballistic packages have the structure and characteristics presented in the table1. Ballistic performance of the three variants of Kevlar/metallic gauze materials was tested in the Testing Laboratory for Ballistic and Pyrotechnic Protection

Table 1

BULLETPROOF STRUCTURES VARIANTS

Variants	Structure
G1	5 layers of Kevlar
G2	5 layers of Kevlar + 1 layer of metallic gauze
G3	5 layers of Kevlar + 2 layers of metallic gauze

(LIPBP) within the Scientific Research Centre for Defense CBRN and Ecology in accordance with the NIJ 01.01 04/2000 standard, using the 9 mm Jericho weapon.

Experimental research was performed on the Marshall Stability Tester. Following the tests performed, the values recorded for the penetration force and the deformation arrow were introduced as variables in the ANCOVA mathematical model.

ANCOVA is a statistical procedure that enables one to compare groups on some quantitative dependent variable while simultaneously controlling for quantitative independent variables [28, 29]. Thus, ANCOVA combines both qualitative and quantitative independent variables. ANCOVA is used because the inclusion of the covariate in the model can increase power to detect group differences and the precision of estimates [30, 31]. With respect to the design, ANCOVA models explain the dependent variable by combining categorical (qualitative) independent variables with continuous (quantitative) variables [32, 33]. The ANCOVA method belongs to a larger family of models called GLM (Generalized Linear Models), as well as Linear Regression and Variance Analysis (ANOVA), with applications in different fields: medicine, psychology, sociology, engineering [34]. AN-COVA checks the correlation between a dependent variable and the covariate independent variables and removes the variability from the dependent variable that can be accounted for by the covariates. Analysis of covariance models combines analysis of variance with regression analysis techniques. There are special extensions to ANCOVA calculations to estimate parameters for both categorical and continuous variables [35, 36]. However, ANCOVA models can also be calculated using multiple regression analysis using a design matrix with a mix of dummy-coded qualitative and quantitative variables [37].

RESULTS AND DISCUSSIONS

The results obtained for testing the materials for penetration force and deformation arrow is presented in table 2.

The processing is performed in the SPSS program (Statistical Package for the Social Sciences) using the stages and statistical tests specific to the ANCOVA regression model following several steps.

Systematization and processing of experimental data

An ANCOVA regression model is constructed with a nominal independent variable and a quantitative

	RESULTS OF THE EXPERIMENTAL DATA OBTAINED FOR PENETRATION FORCE AND DEFORMATION ARROW							
Fabric groups	Penetration force T (N)	Deformation arrow Δl (mm)	Fabric groups	Penetration force T (N)	Deformation arrow Δl (mm)	Fabric groups	Penetration force T (N)	Deformation arrow Δl (mm)
G1	985.80	32.60	G2	842.70	27.60	G3	732.50	18.90
	978.60	31.80		834.50	27.10		725.80	17.80
	981.20	31.90		828.90	27.50		729.40	16.80
	985.40	32.10		831.80	26.80		726.30	18.90
	973.70	31.30		837.50	27.50		730.50	19.00
	977.40	31.60		837.30	26.80		731.90	18.50
	969.70	32.10		840.40	28.10		733.70	18.70

variable in which: the dependent variable (Y) – the variation of the penetration force F (N); nominal independent variable – fabric group (G1 – 5 layers Kevlar, G2 – 5 layers Kevlar + 1 layer of metallic gauze, G3 – 5 layers Kevlar + 2 layers of metallic gauze; quantitative independent variable: deformation arrow, Δl (mm). Frequency distributions for the variation of the penetration force, T [N] depending on the studied fabric groups are represented in the Boxplot diagrams from figures 1–3.
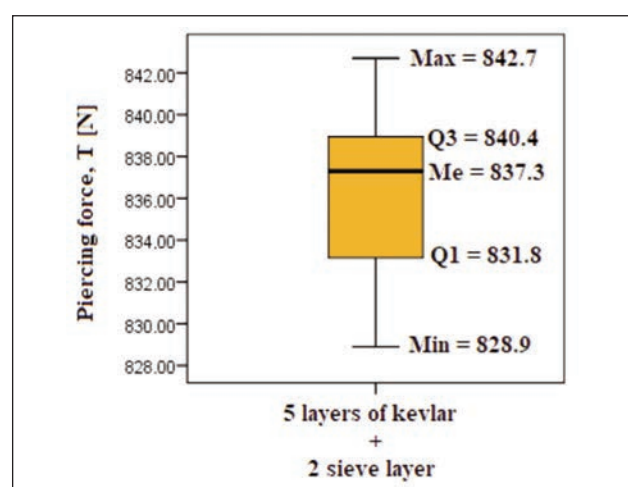
These diagrams include the most important statistical characteristics: minimum, maximum, median values, the lower quartile Q1 which delimits the smallest 25% of the measured values and the upper quartile Q3 which delimits the largest 25% of the measured values. A box plot (or box-and-whisker plot) shows the distribution of quantitative data in a way that facilitates comparisons between variables or across levels of a categorical variable. The box shows the quartiles of the dataset while the whiskers extend to show the rest of the distribution, except for points that are determined to be "outliers" using a method that is a function of the inter-quartile range.

Hypothesis formulation

H0 are no significant differences between the variation of the penetration force depending on the groups of fabrics studied and the deformation arrow.
H1: there are significant differences between the variation of the penetration force depending on the groups of fabrics studied and the deformation arrow.

Construction and interpretation of the regression model

Within the ANCOVA regression model, the nominal independent variable "fabric group" has 3 variants, so two dummy variables will be constructed. The reference variant (D1, D2=0) will be the one consisting of

Fig. 1. Boxplot diagram for group G1

Fig. 2. Boxplot diagram for group G2
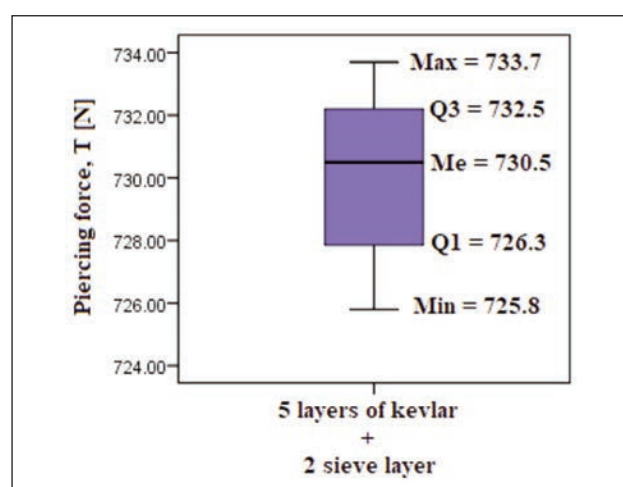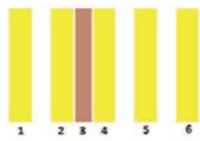
Fig. 3. Boxplot diagram for group G3

TRANSFORMING INTO DUMMY VARIABLES

Group	D1	D2	The position of the layers	Group	D1	D2	The position of the layers	Group	D1	D2	The position of the layers
G1	0	0	G1- 5 Kevlar layers	G2	1	0	G2- 5 Kevlar layers + 1 layer of metallic gauze	G3	0	1	G3- 5 Kevlar layers + 2 layers of metallic gauze

5 layers of Kevlar; therefore, all interpretations will be made in comparison to this category. The transformation into dummy variables is shown in table 3. The ANCOVA model is defined by the relation:

$$Y = \alpha_0 + \alpha_1 D_1 + \alpha_2 D_2 + \beta_1 X_1 + \varepsilon \quad (1)$$

Conditional average: $M(Y/D) = \alpha_0$; $D_1, D_2 = 0$; $M(Y/D) = (\alpha_0 + \alpha_2) + \beta_1 X_1$; $D_1 = 0, D_2 = 1$; $M(Y/D) = (\alpha_0 + \alpha_1) + \beta_1 X_1$; $D_1 = 1, D_2 = 0$.

The Levene's test is used to test the homogeneity of the variation within the model. Levene test result $F(2.18) = 1.807$, Sig. $= 0.193$ ($p < 0.05$) is statistically insignificant, therefore, the homogeneity condition of the variants is met. The effect of the nominal independent variable "fabric group" is significant, $F(2.17) = 410.790$, Sig. $= 0.000$, $p < 0.05$ and also, the effect of the covariate "deformation arrow" is significant, $F(1.17) = 2.676$, Sig. $= 0.020$, $p < 0.05$, as seen in table 4.

Also, the evaluation of the impact of the independent variables on the dependent variable based on the Type III analysis, shows that the probability F is much stronger for the fabric group ($F = 410.790$), compared to the tear deformation arrow ($F = 2.676$) on the variation penetration force.

The graph of the ANCOVA model is presented in figure 4, covariates appearing in the model are evaluated at the following values: deformation arrow = 25.8762 mm. The results show that the penetration force estimates for the three groups of fabrics are statistically related to the deformation arrow. Thus, as we introduce one or two layers of metallic gauze, the penetration force decreases in proportion to the deformation arrow.
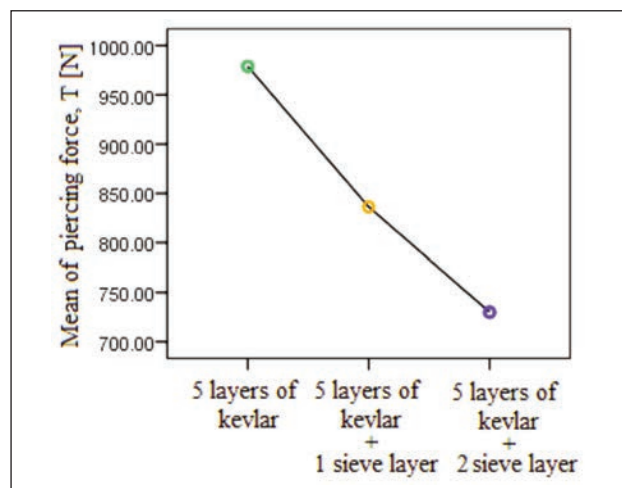
Fig. 4. ANCOVA chart for fabric groups

The coefficients of the ANCOVA model are calculated in table 4. The model estimates are: $\alpha_0 = 273.628$; $\alpha_1 = -40.037$; $\alpha_2 = 49.167$; $\beta_1 = 22,166$. The regression model is:

$$Y = 273.628 - 40.037 D_1 + 49.167 D_2 + 22.166 X_1 \quad (2)$$

Model interpretation:
a) $\alpha_0 = 273.628$, $D_1, D_2 = 0$, represents the average value estimated for the variation of the penetration force depending on the group of G1 fabrics and the deformation arrow;
b) $\alpha_0 + \alpha_1 = 273.628 - 40.037 = 233.591$ represents the average value estimated for the variation of the penetration force depending on the group of G2 fabrics and the deformation arrow;

TESTS OF BETWEEN-SUBJECTS EFFECTS

Source	Type III Sum of Squares	df	Mean Square	F	Sig.
Corrected Model	218291.452	3	72763.817	3553.18	0.000
Intercept	5546.617	1	5546.617	270.851	0.000
Fabric group	16824.733	2	8412.367	410.790	0.000
Deformation arrow	54.805	1	54.805	2.676	0.020
Error	348.135	17	20.479	-	-
Total	15331697.92	21	-	-	-

Table 5

MODEL COEFFICIENTS					
Model 1	**Unstandardized coefficients**		**Standardized coefficients**	**t**	**Sig.**
	B	Std. Error	Beta		
(Constant)	273.628	85.092	-	3.216	0.005
D1	−40.037	12.815	−0.191	−3.124	0.006
D2	49.167	36.769	0.227	1.337	0.029
Δl (mm)	22.166	2.663	1.228	8.323	0.000

c) $\alpha_0 + \alpha_2$ = 273.628 + 49.167 = 322.795 represents the average value estimated for the variation of the penetration force depending on the group of G3 fabrics and deformation arrow;

d) β_1 = 22.166 shows the variation of the penetration force for the fabrics from 5 layers of Kevlar in the conditions in which the deformation arrow increases.

Interpreting value Sig < 0.05 from table 5, it can be concluded that between the variation of the penetration force there are significant differences depending on the groups of fabrics studied and the deformation arrow (alternative hypothesis H1 is accepted).

Verification of the ANCOVA model involves a series of econometric modelling steps, such as: testing hypotheses on errors; homoscedasticity; normality; error autocorrelation and collinearity testing of independent variables.

a) Testing hypotheses on errors, $M(\varepsilon) = 0$ (zero error average)

H_0: $M(\varepsilon) = 0$; H_1: $M(\varepsilon) \neq 0$

The Student t test for errors (Unstandardized Residual), presented in table 6, is applied, from which it is observed that the value Sig. = 1 (p > 0.05), so the null hypothesis H_0 is accepted, whereby the average of the errors is 0.

b) Homoscedasticity, $V(\varepsilon_i) = \sigma^2$ (error variant is equal to dispersion)

H_0: the correlation coefficient is insignificantly different from 0 (null hypothesis of the Student's t test)

H_1: the correlation coefficient is significantly different from 0 (the null hypothesis of the Student's t test is rejected).

A nonparametric correlation test is applied between the estimated errors and the dependent variable, the Spearman correlation coefficient and the Student test are calculated for this coefficient, according to table 7. Because the values of Sig. of Student's t test for correlations: Penetration force T (N) – estimated errors

(0.084), D1 – estimated errors (0.242), D2 – estimated errors (0.443), deformation arrow – estimated errors (0.352) are greater than 0.05, the null hypothesis of the Student test is rejected, so the model is homoscedastic.

c) Normalcy of errors, $\varepsilon_i \sim N(0, \sigma^2)$

The testing of the normality of the error distribution is done with the non-parametric Kolmogorov-Smirnov test or by the graphical procedure in the form of a histogram. As can be seen from table 8, the value Sig = 0.970 is higher than the critical value p = 0.05, so the normality hypothesis H0 is accepted. From the error distribution, presented in figure 5 it is observed that the values are not normally distributed, they do not follow the distribution law described by the Gauss Laplace curve.

d) Error autocorrelation testing, cov (εi, εi)

H0: $\rho = 0$ (errors are not autocorrelated); H1: $\rho \neq 0$ (errors are autocorrelated)

The verification is done with the Durbin Watson test, according to table 9.
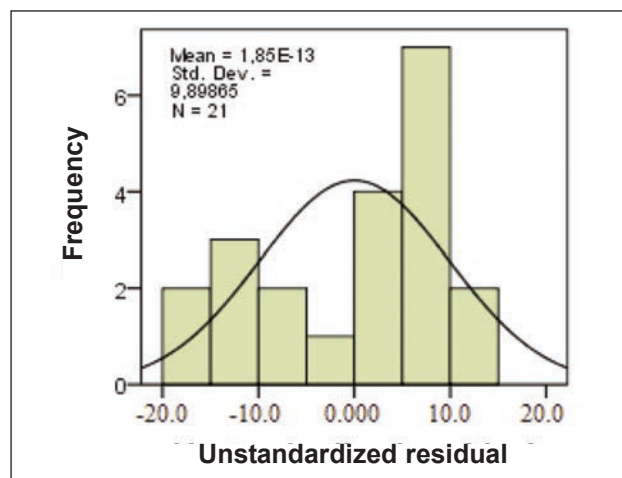
Fig. 5. Errors distribution

Table 6

STUDENT T TEST						
One-Sample Test	**Test Value = 0**					
	t	**df**	**Sig. (2-tailed)**	**Mean Difference**	**95% Confidence Interval of the Difference**	
					Lower	**Upper**
Unstandardized Residual	0.000	20	1.000	0.000	−1.8991	1.8991

SPEARMAN TEST FOR HOMOSCEDASTICITY HYPOTHESIS VERIFICATION						
Spearman's rho		Penetration force, T (N)	D1	D2	Deformation arrow	Residual for penetration force
Penetration force, T (N)	Correlation Coefficient	1.000	0.065	−0.817	0.945	0.312
	Sig. (1-tailed)	0.000	0.390	0.000	0.000	0.084
	N	21	21	21	21	21
D1	Correlation Coefficient	0.065	1.000	−0.555	0.138	−0.162
	Sig. (1-tailed)	0.390	-	0.005	0.276	0.242
	N	21	21	21	21	21
D2	Correlation Coefficient	−0.817	-0.555	1.000	−0.818	−0.033
	Sig. (1-tailed)	0.000	0.005	-	0.000	0.443
	N	21	21	21	21	21
Deformation arrow	Correlation Coefficient	0.945	0.138	−0.818	1.000	0.088
	Sig. (1-tailed)	0.000	0.276	0.000	-	0.352
	N	21	21	21	21	21
Residual for penetration force	Correlation Coefficient	0.312	−0.162	−0.033	0.088	1.000
	Sig. (1-tailed)	0.084	0.242	0.443	0.352	-
	N	21	21	21	21	21

KOLMOGOROV-SMIRNOV TEST		
One-Sample Kolmogorov-Smirnov Test		Standardized Residual for T (N)
N		21
Normal Parameters	Mean	0.0000
	Std.Dev	0.92195
Most Extreme Differences	Absolute	0.107
	Positive	0.074
	Negative	−0.107
Kolmogorov-Smirnov Z		0.491
Asymp. Sig. (2-tailed)		0.970

The value of the Durbin-Watson test DW = 2.091 is compared with the calculated value of the test (dl, du).

According to the literature, it is found that the value obtained is in the range (du, 4 − du), which leads to the acceptance of the null hypothesis (errors are not autocorrelated).

e) Testing the collinearity of independent variables

In practice, the identification of the collinearity of independent variables is done by different methods. Using the SPSS package, collinearity can be detected based on two indicators: Tolerance and VIF (Variance Inflation Factor), presented in table 10. In practice, it is considered that a VIF value > 10 indicates the presence of collinearity. If the tolerance indicator, TOL = 1 there is no collinearity, and if TOL = 0 we are in the extreme situation of perfect collinearity.

It is observed from table 10, that the VIF indicator has a high value between 4.410 and 25.797, which indicates

DURBIN WATSON TEST FOR ERROR AUTOCORRELATION TESTING					
Model	R	R Square	Adjusted R Square	Std. Error of the Estimate	Durbin-Watson
1	0.993[a]	0.986	0.983	13.57997	2.091

Note: [a] Test distribution is Normal.

TESTING THE COLLINEARITY OF INDEPENDENT VARIABLES COEFFICIENTS								
Model		Unstandardized Coefficients		Standardized Coefficients	t	Sig.	Collinearity Statistics	
		B	Std. Error	Beta			Tolerance	VIF
1	(Constant)	273.628	85.092		3.216	0.005		
	D1	−40.037	12.815	−0.191	−3.124	0.006	0.227	4.410
	D2	49.167	36.769	0.227	1.337	0.199	0.029	34.212
	Deformation arrow	22.166	2.663	1.228	8.323	0.000	0.039	25.797

that there is collinearity between the dummy variables D1, D2 and the quantitative independent deformation arrow variable, Δl (mm), used in the model.

CONCLUSIONS

The paper highlights the existence of significant differences between the variation of the penetration force in the function of the deformation arrow.

By analysing the presented data, it can be remarked that the use of G1 layers structure ensures the product a medium elongation, determined by a force and a pressure of low values, while the use of Kevlar layers combined with metallic gauze (G2 and G3 layers structure) generates similar results with the first one, but with significantly higher values in terms of puncture strength and pressure.

The ANCOVA model allows us to evaluate the homogeneity of a statistical population by separating and testing the effects caused by the factors considered.

Through Tests of Between-Subjects Effects, it is observed that the effect of the nominal independent variable "Fabric group" is significant, $F_{(2.17)}$ = 410,790, Sig. = 0.000, $p < 0.05$ and also the effect of the covariate "deformation arrow" is significant, $F_{(1.17)}$ = 2.676, Sig. = 0.020, $p < 0.05$. Interpreting the value of Sig < .05, it can be concluded that between the variation of the penetration force there are significant differences depending on the groups of fabrics studied (null hypothesis H0 is rejected). The properties of the estimators of the regression model parameters were verified through specific tests and allowed the construction of the ANCOVA model with a nominal independent variable and a quantitative independent variable. The ANCOVA model shows that the variation of the penetration force is significantly influenced of the nominal independent variable "fabric group", $F_{(2.17)}$ = 410,790, Sig. = 0.000, $p < 0.05$, as well as by the effect of the covariate „deformation arrow", $F_{(1.17)}$ = 2.676, Sig. = 0.020, $p < 0.05$.

REFERENCES

[1] Öberg, E.K., Dean, J., Clyne, T.W., *Effect of inter-layer toughness in ballistic protection systems on absorption of projectile energy*, In: Int. J. Impact Eng., 2015. 76, 75–82

[2] Yang, Y., Chen, X., *Investigation of energy absorption mechanisms in a soft armor panel under ballistic impact*, In: Text. Res. J., 2017, 87, 20, 2475–286

[3] Yang, Y., Chen, X., *Investigation on energy absorption efficiency of each layer in ballistic armour panel for applications in hybrid design*, In: Compos. Struct., 2017, 164, 1–9

[4] Zohdi, T.I., *Modeling and simulation of progressive penetration of multilayered ballistic fabric shielding*, In: Comput. Mech., 2002, 29, 1, 61–67

[5] Joo, K., Kang, T.J., *Numerical analysis of energy absorption mechanism in multi-ply fabric impacts*, In: Text. Res. J., 2008, 78, 7, 561–576

[6] Cunniff, M., Auerbach, M., Vetter, E., Sikkema, D.J., *High performance M5 fiber for ballistics/structural composites*, National Research Council (U.S.), The National Academies Press, 2004

[7] Cheeseman, B.A., Bogetti, T.A., *Ballistic impact into fabric and compliant composite laminates,* In: Compos. Struct. 2003, 35, 18, 161–173

[8] Armellino Jr., R.A., Armellino, S.E., *Ballistic Material for Flexible Body Armor and the Like*, US Patent No. 4522871, June 11, 1985

[9] Dunbavand, I.E., *Flexible Armor*, US Patent No. 4608717, September 2, 1986

[10] Harpell, G.A., Palley, I., Kavesh, S., Prevorsek, D.C., *Ballistic-resistant Fine Weave Fabric Article*, US Patent No. 4737401, April 12, 1988

[11] Medvedovski, E., *Ballistic performance of armour ceramics: Influence of design and structure*. Part 2, Ceram 2010, 36, 2117–2127

[12] Goncalves, D.P., de Melo, F.C.L., Klein, A.N., Al-Qureshi, H.A., *Analysis and investigation of ballistic impact on ceram-ic/metal composite armour*, In: Int. J. Mach., 2004, 44, 307–316

[13] Liu, S., Wang, J., Wang, Y., Wang, Y., *Improving the ballistic performance of ultrahigh molecular weight polyethylene fiber reinforced composites using conch particles*, In: Mater. Des., 2010, 31, 1711–1715

[14] Stopforth, R., Adali, S., *Experimental study of bullet-proofing capabilities of Kevlar, of different weights and number of layers, with 9 mm projectiles*, In: Def. Technol., 2019, 15, 186 -192

[15] Puran, S., Vikas, M., Priyawart, L., *Analysis of composite materials used in bullet proof vests using fem technique*, In: Int. J. Eng. Res., 2013, 4, 5, 1789–1796

[16] Barauskas, R., Abraitiene, A., *Computational analysis of impact of a bullet against the multilayer fabrics in LS-DYNA*, In: Int. J. Impact Eng., 2007, 34, 1286–1305

[17] Duan, Y., Keefe, M., Bogetti, T.A., Cheeseman, B.A., *Modeling the role of friction during ballistic impact of a high-strength plain-weave fabric*, In: Compos. Struct., 2005, 68, 331–337

[18] Ramaiaha, G., Chennaiaha, R., Satyanarayanarao, G., *Investigation and modeling on protective textiles using artificial neural networks for defense applications*, In: Mater. Sci. Eng. B, 2010, 168, 100–105

[19] Zelelew, T.M., Koricho, E.G., *Design and Analysis of Bullet Resistance Jacket Projectile Penetration: Reviews*, In: Mater. Sci. Eng., 2019, 8, 3, 1–5

[20] Stopforth, R., Adali, S., *Full metal jacket projectile penetration analysis of Kevlar only bulletproof vest*, In: Proceedings of 3rd International Conference on Composites, Biocomposites and Nanocomposites, 2018, South Africa, 98–106

[21] Glueck, D.H., Muller, K.E., *Adjusting power for a baseline covariate in linear models*, In: Stat. Med., 2003, 22, 2535–2551

[22] Avadanei, M., Dulgheriu, I., Radu, C.D., *Virtual prototyping design of bulletproof vests*, In: Industria Textila, 2012, 63, 6, 290–295

[23] Austin, P.C., *An introduction to propensity score methods for reducing the effects of confounding in observational studies*, In: Multivariate Behav. Res., 2011, 46, 3, 399–424

[24] Dulgheriu, I., Avadanei, M., Badea, S., Safta, I., *Experimental research on establishing the level of bullets protection for a ballistic protection structure*, In: Industria Textila, 2012, 63, 4, 198–203

[25] Lai, K., Kelley, K., *Accuracy in parameter estimation for targeted effects in structural equation modeling: Sample size planning for narrow confidence intervals*, In: Psychol. Methods, 2011, 16, 127–148

[26] Liu, X.S., *Sample size and the width of the confidence interval for mean difference*, In: Br. J. Math. Stat. Psychol., 2009, 62, 201–215

[27] Baguley, T., *Understanding statistical power in context of applied research*, In: Appl. Ergon., 2004, 35, 73–80

[28] Miller, G.A., Chapman, J.P., *Misunderstanding Analysis of Covariance*, In: J. Abnorm. Psychol., 2001, 110, 40–48

[29] Hristian, L., Ostafe, M.M., Manea, L.R., Apostol, L.L., *Study of Mechanical Properties of Wool Type Fabrics using ANCOVA Regression Model*, In: International Conference on Innovative Research (ICIR Euroinvent), Book Series: IOP Conference Se-ries-Materials Science and Engineering 2017, 209, 012075

[30] Engqvist, L., *The mistreatment of covariate interaction terms in linear mode analyses of behavioral and evolutionary ecology studies*, In: Anim. Behav., 2005, 70, 967–971

[31] Hristian, L., Sandu, A.V., Manea, L.M., Tulbure, E.A., Earar, K., *Analysis of the Principal Components on the Durability and Comfort Indices of the Fabrics Made of Core-coating Filament Yarns*, In: J. Chem., 2015, 66, 3, 342–347

[32] Singh, M., Bajpai, P., *Multiple Regression Analysis Using ANCOVA in University Model*, In: Int. J. Appl. Phys. Math., 2013, 3, 5, 336–340

[33] Manea, L.R., Hristian, L., Ostafe, M.M., Apostol, L.L., Sandu, I., *Analysis of Characterization Indexes for Worsted Fabrics Type Using Correlation Method as a Statistical Tool*, In: Rev. de Chim., 2016, 67, 9, 1758–1762

[34] Rutherford, A., *Anova and Ancova: A GLM Approach*, 2nd Edition Hoboken, NJ: John Wiley and Sons, 2011

[35] Muhammad, M., Li, N.-W., Muhammad, S.A., Muhammad, K.M., *Investigation of various factors affecting the coefficient of friction of yarn by using Taguchi method*, In: Industria. Textila, 2019, 70, 3, 211–215, http://doi.org/10.35530/IT.070.03.1555

[36] Hristian, L., Ostafe, M.M., Manea, L.R., Leon, A.L., *The study about the use of the natural fibres in composite materials*, In: Modtech International Conferince – Modern Technologies in Industrial Enginering IV, PTS 1–7, Book Series: IOP Conference Series-Materials Science and Engineering 2016, 145, 032004

[37] Haji, A., Nasiriboroumand, M., *Statistical study of the effect of metallic mordants on tensile strength of wool*, In: Industria Textila, 2018, 69, 6, 511–518, http://doi.org/10.35530/IT.069.06.1598

Authors:

IONUT DULGHERIU, SAVIN DORIN IONESI, MANUELA AVADANEI, LILIANA HRISTIAN,

EMIL CONSTANTIN LOGHIN, LILIANA BUHU, IRINA IONESCU

"Gheorghe Asachi" Technical University of Iasi, Faculty of Industrial Design and Business Management,
D. Mangeron, 29, 70050, Iasi, Romania
e-mail: idulgheriu@tuiasi.ro, mavad@tuiasi.ro, hristian@tuiasi.ro,
eloghin@tuiasi.ro, lbuhu@tuiasi.ro, iirina@tuiasi.ro

Corresponding author:

SAVIN DORIN IONESI
e-mail: dionesi@tuiasi.ro

Vegetable culture vs. climate change
Innovative solutions
Part 1. Research on the chemical analysis of Buzau white onion bulbs cultivated using diatomite and *Trichoderma*

VASILICA MANEA
CRISTINA BALAS
DUMITRU-MITEL TOMA
FLOAREA BURNICHI
DELIA JITEA

EMIL MIREA
ALEXANDRU-CRISTIAN TOADER
BOGDAN-GABRIEL STAICU
ANGELA DOROGAN

ABSTRACT – REZUMAT

Vegetable culture vs. climate change
Innovative solutions
Part 1. Research on the chemical analysis of Buzau white onion bulbs
cultivated using diatomite and *Trichoderma*

In the context of intense and forced industrialization, agricultural overexploitation and pesticide pollution, attempts are being made to find organic alternatives for fertilizing and herbicide crops and products with an insecticidal effect that does not give bio-resistance over time. Given the desire of people to consume organic products, there is an increasing need to expand ecologically grown areas in order to make them available to consumers. For this purpose, it was decided to carry out research on the chemical analysis of Buzau white onion bulbs, treated with diatomite and Trichoderma, correlating them with the impact on the plants under study. Among the experimental variants, the best polyphenol content was found in variant V2 treated with 52.5 g of diatomite/repetition, compared to the untreated control. The experiments took place within S.C.D.L. Buzau, in the pedoclimatic conditions of the area, the results being available for informing growers and consumers. The paper is part of a complex research project in which these are solutions to reduce the negative climate impact in agriculture, especially in vegetable crops. Conventional and unconventional, but as much as possible sustainable solutions, including textile structures, organic diatomite, eco-friendly equipment generates an innovative instrument vs. climate change effects in vegetable crops. Part 2 of this research presents the textile solution in the context of the approached topic.

Keywords: *diatomite, onion bulbs, Trichoderma spp., chemical analysis, textile nets for vegetable protection*

Culturi legumicole vs. schimbări climatice
Soluții inovative
Partea 1. Cercetări privind analiza chimică a bulbilor de ceapă albă de Buzău
cultivată utilizând diatomită și *Trichoderma*

În contextul industrializării intense și forțate, a supraexploatării agricole și a poluării cu pesticide, se încearcă găsirea unor alternative organice pentru fertilizarea și erbicidarea culturilor și a produselor cu efect insecticid care să nu genereze bio-rezistență în timp. Având în vedere dorința oamenilor de a consuma produse ecologice, este din ce în ce o mai mare nevoia de a extinde suprafețele cultivate ecologic pentru a le pune la dispoziția consumatorilor. În acest scop, s-a decis efectuarea de cercetări privind analiza chimică a bulbilor de ceapă albă de Buzău, tratați cu diatomită și Trichoderma, corelându-i cu impactul asupra plantelor studiate. Dintre variantele experimentale, cel mai bun conținut în polifenoli a fost găsit în varianta V2 tratată cu 52,5 g de diatomită/repetiție, comparativ cu martorul netratat. Experimentele au avut loc în cadrul S.C.D.L. Buzău, în condițiile pedoclimatice din zonă, rezultatele fiind disponibile pentru informarea cultivatorilor și a consumatorilor. Lucrarea face parte dintr-un proiect complex de cercetare în care acestea sunt soluții pentru diminuarea impactului climatic negativ în agricultură, în special în culturile de legume. Soluțiile convenționale și neconvenționale, pe cât posibil soluții durabile, incluzând structuri textile, diatomită organică, echipamente ecologice, generează un instrument inovator față de efectele schimbărilor climatice în culturile de legume. Partea a 2-a acestei cercetări prezintă soluția textilă în contextul subiectului abordat.

Cuvinte-cheie: *diatomită, bulbi de ceapă, Trichoderma spp., analize chimice, plase textile pentru protejarea legumelor*

INTRODUCTION

In the current context of the cultivated agricultural surfaces expanding in an ecological system, organic strategies for crops fertilization/herbicides alterna- tives and pathogens plant management by biological means [1], represents the most important direction as a friendly alternative environment strategy for sus- tainable agriculture. This global direction is extreme- ly important because about one-third of produced

crops are destroyed by pests and diseases [2]. In an attempt to reduce these inconveniences and to increase onion production, researchers and agricultural producers are in a permanent correlation research-development for suitable and effective as possible pest control management strategies. Most often synthetic fungicides are used to control fungal infections in onion crops. Because the onion bulb is affected by fungal pathogens in the soil, chemical reducing agents are used, such as Granosan, which is capable to decline fungal disease by 77% and leads to increased onion productivity with 106%, or carbendazim and antracol, which are very effective in controlling basal rot of onion [1].

Although the development of chemical pesticides is advanced, it was demonstrated a significant negative impact on the environment and population health [2, 3]. New strategies of non-pathogenic microorganism had been developed, that acts as a bio-control agent e.g., *Trichoderma spp.* [2]. This microorganism is safe for humans, highly effective, with multiple benefits against plant pathogenic fungi [1, 3] and also it is used to increase abiotic and biotic factors plant resistance [4]. This *Trichoderma* biological alternative to classic synthetic pesticides includes a wide range of species [3] that can be easily isolated, being found inaccessible sources, such as soil microflora of various ecosystems, agricultural fields, forests, and wetland areas in all climatic zones [4]. Horticultural researches demonstrated that *Trichoderma* species is a good plant growth promoter applied in many crops, especially in onion [5, 6], garlic (*Allium sativum*) [7], rice [8], potatoes and tomatoes cultures [9], beans, onions or peppers [4], providing major benefits in farming systems, such as the mitigation of biotic and abiotic stresses [4, 10].

Allium cepa (*Alliaceae*) represents a global economically important horticulture crop, due to its protective food and special nutritive value [11]. However, the onion white root and bulb are very vulnerable to pathogens factors, like fungal diseases, caused by the sclerotium-forming fungus *Sclerotium cepivorum* [7], or *Fusarium, Pythium, Rhizoctonia, Sclerotinia, Botrytis and Verticillium phatogens* [7] and also to foliar factors [1], that conduced inevitably to *Alliaceae* yield and quality reduction. This is the situation of many countries that are fighting this big problem, such as Brazil, where the onion production is not sufficient to fulfil internal demand, due to low productivity [7], or Nepal where the rise cultures are seriously affected by the climate and soil quality. In this context, *Trichoderma* inoculation as a seedling treatment can help to enhance rice production and productivity [10]. In India, where *Alternaria porri* (Ellis) Neerg. is one of the destructive onion diseases, more than 70% yield losses were reported. In this case, the inhibitory effect of *Trichoderma species viz., T. harzianum, T. pseudokoningii and T. virens* on mycelial growth and spore germination of *A. porri* were used [11]. *In vitro* studies were reported an efficient *Trichoderma* control by reducing the incidence of disease to 20–53%, using dry leaf biomass of

Withania somnifera in combination with *Trichoderma harzianum* by controlling onion basal rot disease [1]. Furthermore, the same microorganism could be a new biocontrol agent in the strategy concepts against some pathogen factors like *Fusarium oxysporum* and *F. solani* that damping-off of onion seeds, improving significantly the germination phenomena, by coating the seeds and spraying the seedbeds with a Burkina Faso native *Trichoderma* suspension [6]. On the other hand, studies on pathogens in rice crops treated with friendly herbicide showed that *Trichoderma* applied treatment increased the yields by 24%, compared with organic culture, and with 52% compared with non-organic one. The beneficial effect of *Trichoderma* treatment was different in intensity, depending on the variety, respectively 26–41% higher than classified crops [10]. This aspect is found to be very important from an economic point of view and especially for intelligent ecological management that will lead exclusively to significantly increased production yields. A friendly alternative for harmful chemical variants [12] in biological control of commercial crops is diatomite or diatomaceous earth. Reported data has shown an effective role as a fertilizing and insecticide agent. Diatomiceous earth and its compounds are considered conventional natural agents by desication comportment against insect pests [13].

This is a non-toxic material for crops and human health, with great environmental compatibility [12, 13]. Its effectiveness as a bio-agent is given by the nature of the chemical composition and by the source, respectively a silicon dioxide fossilized skeletons (up to 90%), alumina and ferric oxide [12]. In the recent years this inert natural insecticide powder [12, 13, 14] and its fungistatic effects [12] had spread to many agricultural crops affected by extern factors, such as *Spodoptera exigua* [13], *Rhyzopertha dominica, Sitophilus oryzae* (L.) (*Coleoptera Curculionidae*) [15]*, Sitophilus granaries* [14], nymphs of *Blattella germanica* [16], or *Trialeurodes vaporariorum* [17]. Diatomaceous earth as bioinput, fertilization agent was tested on important commercial crops like corn (*Zea mays*), bean (*Phaseolus vulgaris* L.), carrot (*Daucus carota* L.) and yellow potato (*Solanum phureja*) [17]. Studies have shown that the benefits of the crop are due to the combination of versatile diatomite with the presence of silica in the soil. So, the diatomite might be a very good bio-fertilizer depending on soil quality, respectively by water regimes and nutrient availability [18]. Until 2016, a few data regarding the availability of diatomite as fertilizing or insecticide agent in the horticultural areas of Romania are available. In this context, Thanassiou et al., in 2016, [15] performed a comparative study between Romanian and Greece diatomaceous earth, against *S. oryzae, R. dominica, T. castaneum* and *O. surinamensis,* observing the significantly better effects of Romanian diatomaceous earth (Patarlagele, Urloaia and Adamclisi sources).

In vitro efficacy was tested against PyriSec as a standard product. The test was conducted under a controlled climate and under natural feed (wheat grains) *Sitophilus granarius* L. (*Coleoptera: Curculionidae*) treatment, and the population's ability to reproduce was observed. Thus, after 60 days, the diatomaceous earth (Patarlagele source, Romania) has lockdown the insects' reproduction capacity with 100% efficiency, shortly after the administration. On the other hand, Urloaia and Adamclisi samples (Greece sources) had a block-level under 80% [14]. Therefore, the intensity effect of diatomaceous earth on agricultural crops pests is closely related to its behaviour and source. Bacterial diseases and *Fusarium proliferatum* represent a global problem that affects especially *Allium* genus (garlic, and more often onion crops). Onion bulb internal decomposition during maturation and curing, prior to harvest stages was observed. To reduce these inconveniences, diatomaceous earth-chlorine was used as a local onion culture treatment against pathogenic microorganisms [19]. The purpose of our research was to study the bio-fertilizer and herbicidal diatomite and *Trichoderma* treatments effect on white onion crops by the field cultivation technique.

The aim of the study consists in correlating the experimental data productivity and results/observations generated by the physic-chemical analyses of white onion products, with the impact and influence of the organic treatment applied, in relation to the pedoclimatic conditions of the Buzau area (Romania).

EXPERIMENTAL

Materials

In this study, there were used the following:
– white onion seedling (CSD biological category);
– covered solarium, S.C.D.L. Buzau type;
– granulated NPK-S 20/20/0-13 chemical fertilizer complex (Agropolic Chim., Bulgaria);
– diatomite suspension (CMC/diatomite powder);
– Vermorel pump type;
– Fusilade forte, Syngenta.

For all analysis performed, high purity reagents were used, and for the determination and studding of the parameters presented above, basic equipment was used, respectively a spectrophotometer, an analytical balance and a Memert oven.

Methods

The white onion culture was performed in the experimental field of S.C.D.L. Buzau. In 2019 this central location was the main Menuet bean forerunner culture area for diatomaceous earth crops experimental surface.

The culture was established on 1600 m^2, for these research experiments being allocated 10 furrows of 30 m length, modelled at 1.40 m and with a canopy opening of 94 cm. From this surface, on a length of 2.5 m on the ends and one furrow on the side, there were eliminations, in order to avoid the edge effect.

The white onion seedling was executed in a covered solarium.

When it had 55 days from emergence:
– the planting was done on furrows, 4 rows per furrow, grouped in pairs, with between 50–60 plants/each row of repetition;
– the planting scheme was 10 + 15 + 54 + 15 + 10 cm/furrow, which means about 220 plants/repetition – 7 m^2 and about 880 plants/variant – 28 m^2.

The planting step was done at 10 cm between plants/row, with twice per week drip irrigation, in the vegetation period. A rehearsal had a length of 5m and a width of 1.4 m, meaning 7 m^2. Each variant included 4 repetitions, totalling an area of 28 m^2.

A number of 5 experimental variants were established, as follows:
– V1, the untreated control;
– V2 treated with 52.5 g diatomite/repetition;
– V3 treated with 105.0 g diatomite/repetition;
– V4 treated with 210.0 g diatomite/repetition;
– V5 treated with *Trichoderma* T85-ICDPP collection, with radicular administration, respectively 2–3 granules per plant, in the planting phase.

In the 62th day of plant rise (May 2020), the solid diatomaceous earth was administered.

Specific technological protocols were performed, manual ploughing was performed (at the end of May), and at the beginning of June, the onion crop was sprayed with Fusilade/Galligan (1:1/ha).

In May-August 2020 period, 224 l/m^2 of precipitation were registered.

The granulated NPK-S 20/20/0-13 chemical fertilizer complex was mechanically administered on gutters, by a tractor and bunker cultivator, for a period of 18 days (in June 2020), respectively 55–65 kg/1600m^2.

A diatomite suspension, 8.3:1, was administered after emergence for 119 days, by plant manual spraying using a Vermorel pump type (33% or 3.3 l of diatomite suspension per plant, respectively for V2, V3, V4 samples).

Periodically the treatments for pathogens agents and fungal infections were performed (Fusilade forte – Goal 4F, 1:0.5/ha).

128 days after emergence, the onions formed yellow shirts in 70% of the crop, about 60% leaves dried and lay about 60%.

The entire onion crop was harvested after 115 days of planting, respectively 170 days after emergence. The production was weighed on repetitions and variants. An average of 10 bulbs per variant for physico-chemical studies and determinations, for both dehydrated leaves and fresh bulbs were selected.

For physico-chemical studies and determinations, ethanolic and aqueous extract onion bulbs and leaves were performed, according to Lee et al. [20] and Jiang et al. [21]. From onion leaf, water retention capacity and solubility index were performed according to Jiang et al. [21]; for aqueous and ethanolic onion leaf extracts, total polyphenol content, flavonoid content were performed according to Jiang et al. [21]. The parameters determined for the initial

onion bulb product were pH and the dry matter; for total initial onion bulb extract, the essential parameters were total polyphenol content, total flavonoid [21], reducing sugar content and nitrogen content/protein; for the ethanolic onion extract the determined parameters were also the total polyphenol and flavonoid content, following the same protocols.

RESULTS AND DISCUSSIONS

Onions are grown for both green and dried consumption as bulbs. In the present study, the production of consumption bulbs was evaluated in different experimental variants (figure 1). The production of consumption bulbs was evaluated in different experimental treatments and it was observed that the sample V3 with 105 g of diatomite at 7 m^2 administered, has the highest production value recorded, respectively 148.53 kg/28 m^2, compared to the untreated control V1, 123.99 kg/28 m^2 consumption bulbs.

Another variant of the study under observation was variant V5, where *Trichoderma* was administered. In this case, the bulbs production was superior to the control untreated sample V1, but inferior to the other variants, respectively 128.18 kg.

The production of onion bulbs of 5.30 kg/m^2, in the case of the V3 variant, treated with 105.0 g diatomite/7 m^2, was comparable to other studies where an average production between 2.71–8.65 kg/m^2 was reported (as t/ha 27.1–86.5) [22].
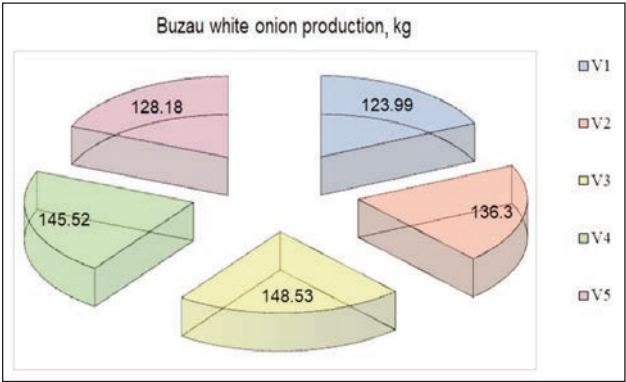

Fig. 1. The obtained white onion production (in kg) of consumption bulbs, in different experimental treatment, performed

The onion bulb pH value variation is presented in figure 2. The pH variation for the directly treated onion samples is essential, in order to establish the influence and product impact to applied treatment and also to study the experimental conditions product and productivity impact. It was observed that V1 control samples presented a lower pH value, above 5.06 ± 0.02, compared with the highest level over 5.25 ± 0.03, for V2 and V5 samples. Similar mean values of acidity (5.20 ± 0.01) were recorded for samples V3 and V4 samples.

It is known that onion has various very beneficial properties for our health, but a high acidity level can cause damage to the digestive system. The current

trend in nutrition is to consume the most basic foods, a context in which the results obtained in our study can lead in addition to increasing onion productivity and agricultural products of superior nutritional quality. So, it was observed that sample V2 is the most recommended variant with average productivity.
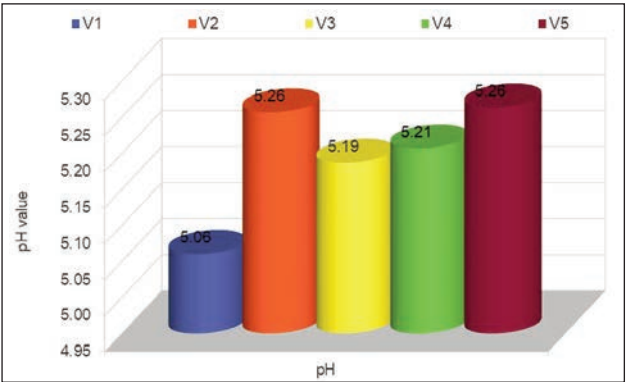
Fig. 2. The onion bulb extract pH value trend registered for all 5 culture types with differentiated treatment

Figure 3 presents the results obtained for fresh onion bulbs humidity studies by gravimetric assays. The fresh onion bulbs humidity analysis showed that the lowest diatomite concentration administrated to the V2 variant has a beneficial influence by high water content, a value compared to the highest level recorded for the sample treated with an almost double amount of diatomite (V3 samples).

The beneficial effect and impact on this sample are reflected and correlated with the lower acidity level determined. On the other hand, the amount of dry matter is the highest in control variant V1, 12.55 ± 0.1 g/100 g, and the smallest in V3 samples, respectively 10.61 ± 0.35 g/100 g. By extrapolation, the studies performed showed the lowest humidity, 87.45 ± 0.1 g/100 g, and the highest dry matter for the control untreated fresh onion bulbs, and the highest water content, 89.39 ± 0.3 g/100 g and a small dry matter in 105 g diatomite/7 m^2 applied treatment for V3 fresh bulb products, according to figure 3. In the scientific literature with a specific profile, the dry matter values

Fig. 3. The dry matter (DM) amount and water content (WC), expressed in g/100g pulp from fresh onion bulbs, for different treatment experimental samples

between 7.0–14.3 g/100 g fresh mass have been reported [22].

Total flavonoid contents of fresh and ethanolic extracts onion bulbs, obtained under different experimental conditions were performed [21].

The study and content analysis were performed both for the fresh onion bulb total extract and for ethanolic extract obtained, according to figure 4.

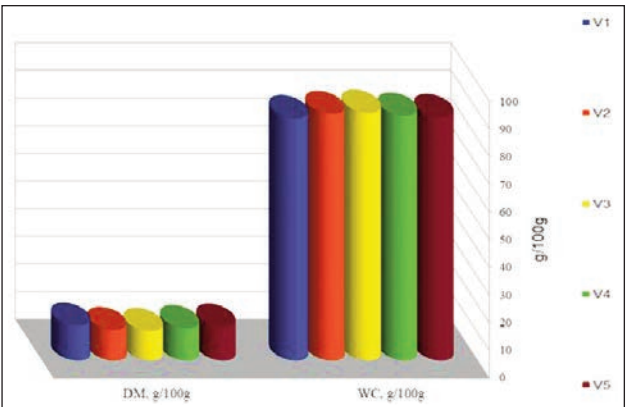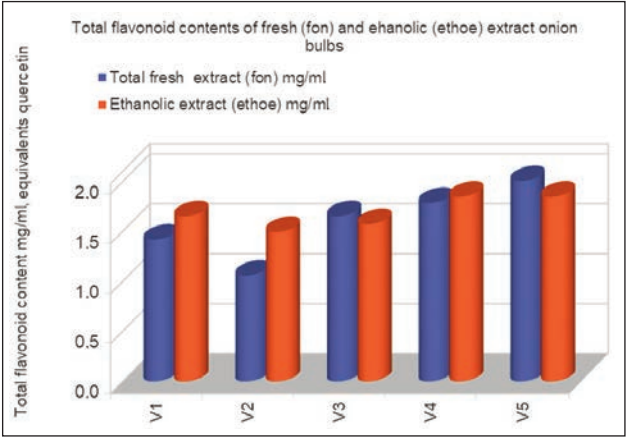Fig. 4. Total flavonoid contents of fresh (*fon*) and ethanolic (*ethoe*) extract onion bulbs, obtained under different experimental conditions

The experimental cultivation conditions showed an important impact concerning the flavonoid content. Therefore, the determinations performed for the total extract from fresh products showed a variable flavonoids content, directly dependent on the applied diatomite treatment. The higher applied diatomite concentrations were conducted to higher flavonoid content. This data is correlated with the water content trend determined. There is a significantly low content of flavonoid for products where diatomite treatment was minimal (case of V2 samples with 52.5 g diatomite/7 m^2 treatment, 1.059 ± 0.023 mg/ml total flavonoid content).

The *Trichoderma* suspension treatment applied demonstrated their efficacy, both for average productivity and for the quality of a superior product. As consequence, the data obtained showed the highest levels of flavonoids for the various V5, respectively 2.005 ± 0.076 mg/ml. Total flavonoid contents of ethanolic fresh bulb extract V4 and V5 samples were comparable, respectively 1.848 ± 0.06 mg/ml, and the lowest values were found also for V2 (1.496 ± 0.1 mg/ml), according to figure 4. The control V1 samples had a total flavonoid content at 1.653 ± 0.06 mg/ml, being thus reported a higher value compared to V2 (1.496 ± 0.1 mg/ml) and V3 onion samples (1.574 ± 0.2 mg/ml) (figure 5).

The white onion peel powder was also subjected to total flavonoid content determination, in quercetin eq. (mg/ml). As consequence, the number of flavonoids was highest in V5 *Trichoderma* treated, respectively 383.89 ± 0.03 mg/ml, followed closely by V4, 372.16 ± 0.03 mg/ml flavonoid content reported. All experimental variants had flavonoids higher values found in
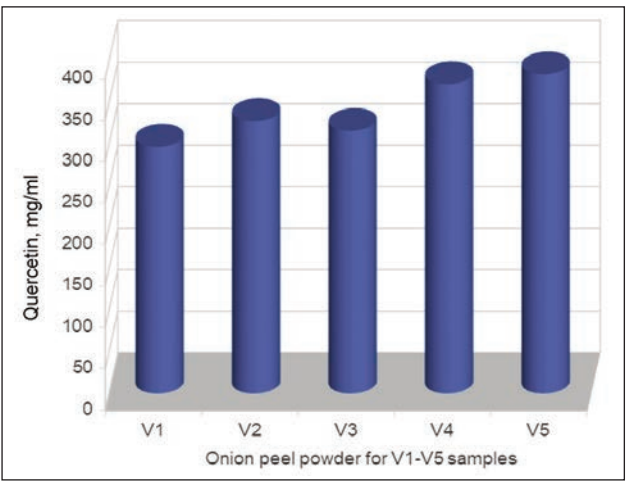
Fig. 5. Total flavonoid contents of fresh onion bulbs peel powder, obtained under different experimental conditions

onion peels, compared with the untreated control test V1 (296.69 ± 0.007 mg/ml), according to figure 6.

The polyphenols (in galic acid eq.) amount, extracted with ethanol, was found for the control V1 (0.834 ± 0.01 mg/ml), followed by variant V5 (*Trichoderma* treated) with 0.723 ± 0.009 mg/ml total flavonoid contents; the highest value was reported for V2, respectively 1.360 ± 0.007 mg/ml, according to figure 7.

Fig. 6. Total polyphenols contents of fresh (*fon*) and ethanolic (*ethoe*) onion bulbs, obtained under different experimental conditions
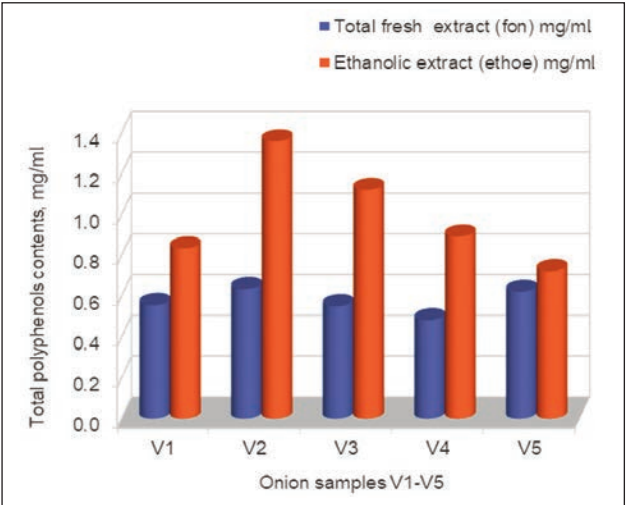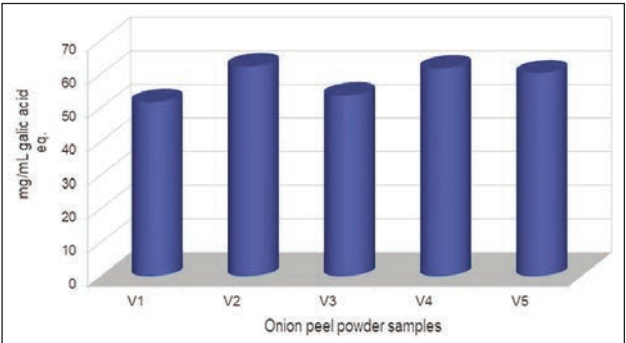

Fig. 7. Total polyphenols contents of fresh onion bulbs peel powder, obtained under different experimental conditions

In total fresh extraction, variant V4 presented the lowest amount of polyphenols (0.483 ± 0.005 mg/ml), control variant V1, 0.557 ± 0.01 mg/ml, and variant V2 had the highest value, respectively 0.635 ± 0.005 mg/ml, according to figure 6.

The number of polyphenols in onion peel powder, for products grown under different experimental conditions, the lowest level for control variant 51.685 ± 0.02 mg/ml, and the highest for V2 (62.355 ± 0.04 mg/ml), were found, as shown in figure 7.

CONCLUSIONS

The production of onion bulbs and their quality is strongly influenced by soil-climatic conditions and cultivation technology. Direct correlation with the number of nutrients administered, accompanied by additional water intake, under the conditions of predisposition to climate aridity and water-heat stress was found. It was reported a significant production increase for the V3 variant treated with 105 g diatomite/7 m^2, compared to the control variant. At the same time, the control has the highest amount of dry matter, which increases the storage period.

According to the results, the *Trichoderma* V5 sample had the highest flavonoids composition, both in the total and ethanolic fresh extract, followed by the variant V4 treated with 210 g diatomite/7 m^2. Also, for the ethanolic flavonoid fresh extract, the highest amount was determined for V5 onion samples. The number of total polyphenols, in both variant V2 peels powder and the ethanolic extract, was the highest reported.

The research will be further developed by using agro textiles to protect crops from the action of extreme weather events, ensuring plant vigour and optimal conditions for pollination and fruiting, which can result in significant increases in production. Another experiment included tests on the behaviour of agro textile materials as a support for seed germination and soil mulching, in a conventional or ecological system [23].

ACKNOWLEDGEMENTS

REFERENCES

[1] Akhtar, R., Javaid, A., *Biological Management of Basal Rot of Onion by Trichoderma harzianum and Withania somnifera*, In: Planta Daninha, 2018, v36:e018170507, 1–7, https://doi.org/10.1590/S0100-83582018360100009

[2] Nakkeeran, S., Renukadevi, P., Aiyanathan, K.E.A., *Exploring the Potential of Trichoderma for the Management of Seed and Soil-Borne Diseases of Crops*, In: Integrated Pest Management of Tropical Vegetable Crops, 2016, 4, Springer Science+Business Media Dordrecht 2016 R. Muniappan, E.A. Heinrichs (eds.), https://doi.org/10.1007/978-94-024-0924-6_4

[3] Cornea, C.P., Pop, A., Matei, S., Ciuca Voaides, M.C., Matei, M.A., Popa, G., Voicu, A., Stefanescu, M., *Antifungal Action of New Trichoderma Spp. Romanian Isolates on Different Plant Pathogens,* In: Biotechnol. & Biotechnol., EQ. XI Anniversary Scientific Conference,120 years of academic education in biology, 45 years Faculty of biology, 2009, 23, 766–770, https://doi.org/10.1080/13102818.2009.10818536

[4] Petrisor, C, Chireceanu, C., Chiriloaie-Palade, A., *Studii şi Cercetări Martie 2019. Biologie*, Universitatea ”Vasile Alecsandri” din Bacău SCSB, 2019, 28, 1, 55–58

[5] Petrisor, C, Paica, A., Constantinescu, F., *Influence Of Abiotic Factors on in Vitro Growth of Trichoderma Strains,* The publishing house of the Romanian Academy, 2016, Series B, 18, 1, 11–14

[6] Dabire, T.G, Bonzi, S., Somda, I., Legreve, A., *Evaluation of the Potential of Trichoderma harzianum as a Plant Growth Promoter and Biocontrol Agent Against Fusarium Damping-off in Onion in Burkina Faso*, In: Asian Journal of Plant Pathology, 2016, 10, 4, 49–60, https://doi.org/ 10.3923/ajppaj.2016.49.60

[7] Peter, W., Inglis, I.D., Sueli, C.M., Martins, I., Joao, B.T.S., Macedo, K., Sifuentes, D.N., Cleria Valadares-Inglis, M., *Trichoderma from Brazilian garlic and onion crop soils and description of two new species: Trichoderma azevedoi and Trichoderma peberdyi*, In: Plos one, 2020, 15, 3, 1–23, https://doi.org/10.1371/journal.pone.0228485

[8] Khadra, R.B, Uphoff, N., *Effects of Trichoderma seedling treatment with System of Rice Intensification management and with conventional management of transplanted rice*, In: Peer J., 2019, 7, e5877, https://doi.org/10.7717/peerj.5877

[9] Raut, I., Oancea, F., Santisima Trinidad, B.L., Calin, A., Constantinescu-Aruxandrei, M., Badea Doni, D., Arsene, M., Vasilescu, M.L., Sesan, G., Jecu, T.E., *Evaluation Of Trichoderma Spp. As A Biocontrol Agent Against Phytophthora Parasitica,* In: Scientific Bulletin. Series F. Biotechnologies, 2017, XXI, ISSN 2285-1364

[10] Ram, B.K., Uphoff, N., *Effects of Trichoderma seedling treatment with System of Rice Intensification management and with conventional management of transplanted rice*, In: Peer Journal, 2019, 7, e5877, 1–22, https://doi.org/10.7717/peerj.5877

[11] Prakasam, V., Sharma, P., *Trichoderma harzianum (Th-3) a Potential Strain to Manage the Purple Blotch of Onion (Allium cepa L.) Caused by Alternaria porri under North Indian Plains*, In: Journal of Agricultural Science, 2012, 4. 10, https://doi.org/10.5539/jas.v4n10p266

[12] Lupu, C., Delian, E., Chira, L., Chira, A., *New Insights Into The Multiple Protective Functions Of Diatomaceous Earth During Storage Of Agricultural Products*, In: Scientific Papers. Series A. Agronomy, 2018, LXI, 1, ISSN 2285-5785

[13] Ebodollahi, A., Sadeghi, R., *Diatomaceous Earth and Kaolin as Promising Alternatives to the Detrimental Chemicals in the Management of Spodoptera exigua*, In: Journal of Entomology, 2018, 15, 2, 101–105, https://doi.org/10.3923/je.2018.101.105

[14] Lupu, C., Manole, T., Chiriloaie, A., *Effectiveness Of Main Sources Of Diatomaceous Earth From Romania On Populations Of Sitophilus Granarius L. (Coleoptera: Curculionidae) Under Controlled Conditions*, In: Romanian Journal for Plant Protection, 2015, 8, 58–62, ISSN 2248 – 129X; ISSN-L 2248 – 129X.

[15] Athanassiou, G.A.C, Avallieratos, N.G.K., Chiriloaie, A.C., Assilakos, T.N.V., Fatu, V., Rosu, S.D., Iobanu, M.C., Udoiu, R.D., *Insecticidal efficacy of natural diatomaceous earth deposits from Greece and Romania against four stored grain beetles: the effect of temperature and relative humidity*, In: Bulletin of Insectology, 2016, 69, 1, 25–34, ISSN 1721-8861

[16] Hosseini, S.A, Bazrafkan, S., Vatandoost, H., Abaei, M.R., Ahmadi, M.S., Tavassoli, M., Shayeghi, M., *The insecticidal effect of diatomaceous earth against adults and nymphs of Blattella germanica,* In: Asian Pacific Journal of Tropical Biomedicine, 2014, 4, 1, S228–S232, https//doi.org/10.12980/APJTB.4.2014C1282

[17] Escobar, N., Espejo, J., Rodriguez, L., *WIT Transactions on Ecology and The Environment*, Environmental Impact II. WIT Press, 2014, 181, 409–419, https://doi.org/10.2495/EID140351

[18] Kollalu, S., Prakash, N.B., Meunier, J.D., *Diatomaceous earth as source of silicon on the growth and yield of rice in contrasted soils of Southern India,* In: Journal of Soil Science and Plant Nutrition, 2018, 18, 2, 344360, https://doi.org/10.4067/S071895162018005001201

[19] Shock, C., Feibert, E.B.G., Rivera, A., Saunders, L.D., In Shock CC. (Ed.) Oregon State University Agricultural Experiment Station, Malheur Experiment Station Annual Report 2017, Department of Crop and Soil Science Ext/CrS 159, 73–79

[20] Lee, K.A, Kim, K.-T., Kim, H. J., Chung, M.-S., Chang, P.-S., Park, H., Paik, H.-D., *Antioxidant activities of onion (Allium cepa L.) peel extracts produced by ethanol, hot water, and subcritical water extraction,* In: Food Sci. Biotechnol., 2014, 23, 2, 615–621, https://doi.org/10.1007/s10068-014-0084-6

[21] Jiang, G., Ramachandraiah, K., Wu, Z., Li, S., Eun, J.-B., *Impact of ball-milling time on the physical properties, bioactive compounds, and structural characteristics of onion peel powder*, In: Food Bioscience, 2020, 36, 100630

[22] Sekara, A., Pokluda, R., Del Vacchio, L., Somma, S., Caruso, G., *Interactions among genotype, environment and agronomic practices on production and quality of storage onion (Allium cepa L.) – A review*, In: Hort. Sci. (Prague), 2017, 44, 21–42, https://doi.org/10.17221/92/2015-HORTSCI

[23] Stroe, C.E., Sârbu, T., Manea, V., Burnichi, F., Toma, D.M., Tudora, C., *Study on soil burial biodegradation behaviour on polylactic acid nonwoven material as a replacement for petroleum agricultural plastics*, In: Industria Textila, 2021, 72, 4, 434–442, http://doi.org/10.35530/IT.072.04.1847

Authors:

VASILICA MANEA[1], CRISTINA BALAS[2], DUMITRU-MITEL TOMA[1],
FLOAREA BURNICHI[1], DELIA JITEA[2], EMIL MIREA[1], ALEXANDRU-CRISTIAN TOADER[1],
BOGDAN-GABRIEL STAICU[1], ANGELA DOROGAN[3]

[1]Vegetable Research and Development Station Buzau, V.R.D.S Buzau,
23 Mesteacanului Street, Buzau, Romania

[2]National Institute for Chemical Pharmaceutical Research and Development, ICCF,
112 Vitan Avenue, Bucharest, Romania

[3]National Research Development Institute for Textiles and Leather,
16 Lucretiu Patrascanu Street, Bucharest, Romania

Corresponding author:

VASILICA MANEA
e-mail: vasilicamanea.vm@gmail.com

Smart textiles for occupational safety health at oil stations and offshore platforms in the Black Sea

JAMAL KHAMIS
IOAN I. GÂF-DEAC
IOAN PETRU SCUTELNICU

MIHAELA JOMIR
ALEXANDRA GABRIELA ENE
IONUT ARON

ABSTRACT – REZUMAT

Smart textiles for occupational safety health at oil stations and offshore platforms in the Black Sea

The article shows that in order to develop smart textiles, elements of knowledge about the application part in the field are needed to create a model, to describe and propose how to obtain the information necessary to perform statistical analysis of data. The acquired results will serve in making feasible decisions of techno-medical-sanitation and sustainability through safety equipment. The experimental, scientific and practical contribution refers to the design of a model of "optimal sustainable techno-medical-sanitary equipment" by using smart textiles.
With the help of this model, it is possible to resort to parametric iteration/reiteration, aiming at the achievement, the value and qualitative fulfilment imposed to a general objective function of sustainable techno-medical-sanitary when smart textiles are used.
The developed model goes through further processing in "soft" information programming mode, and then, there will be the possibility and probability of its use as a calculation tool.

Keywords: textile industry, smart textiles, optimal sustainable medical technology, oil stations, offshore platforms

Textile inteligente pentru protecția sănătății lucrătorilor de la stațiile petroliere și platformele offshore din Marea Neagră

Articolul evidențiază faptul că, pentru dezvoltarea textilelor inteligente sunt necesare cunoștințe suplimentare în vederea creării unui model, pentru descrierea, obținerea și prelucrarea datelor în vederea efectuării analizei statistice. Rezultatele obținute vor fi utilizate în luarea unor decizii fezabile de salubritate tehnico-medicală și sustenabilitate, prin proiectarea și realizarea îmbrăcămintei de protecție. Contribuția experimentală, științifică și practică se referă la proiectarea unui model de „îmbrăcăminte tehnico-medical-sanitară", prin utilizarea textilelor inteligente. Cu ajutorul acestui model se poate utiliza iterarea/reiterarea parametrică, astfel încât să se obțină valorile și cerințele calitative impuse acestor tipuri de material, atunci când se utilizează textilele inteligente. Modelul dezvoltat va fi îmbunătățit în modul de programare a informațiilor „soft", acest lucru permițând utilizarea acestuia ca instrument de calcul.

Cuvinte-cheie: industria textilă, textile inteligente, tehnologie medicală durabilă, stații petroliere, platforme offshore

INTRODUCTION

At present, energy, including hydrocarbons, mainly participates in the energy mix and in the consumption of transport fuels. However, globally, energy is being resized, undergoing a "transitional" reconsideration.

The main directions of evolution in the distribution of petroleum products [1–3], with analytical emphasis on the area of human protection, labour, health, show that the average incidence rates of malignant neoplasms affecting hematopoietic and lymphoid tissues decrease with distance from the source of emission (for example, in the first 75 m in the vicinity of an oil distribution station), but depend fundamentally on the textile protective equipment used by workers.

There is no ideal situation in which a technical scheme for "air-steam inlet-fuel outlet" in an oil station or at the marine drilling wells to ensure the perfect fit [4–6]. Research in the field refers to descriptive statistical elements, binomial distribution elements or

Poisson distribution in micro-environments/microenvironments, in fuel distribution stations, fuels, in the area of drilling wells and spaces in their infrastructure. The participation of smart textiles in the defence of health is a fundamental way of action [7–10].

In fact, in order to develop smart textiles, elements of knowledge about the application part in the field are needed, to obtain a model, to describe and propose how to acquire the information necessary to perform statistical analysis of data, to reach results that are interpreted to serve to make feasible decisions of techno-medical-sanitation and sustainability through work clothing protection.

From a toxicological perspective, irregular biological events are recorded at petroleum distribution stations and also on offshore hydrocarbon platforms [5], indicating the effects of exposures. In essence, it is recommended that, starting from the major risks and dangers associated with petroleum products in exploration-extraction and distribution (highly flammable

products), protection operations, using smart textiles, be specific, special and safe.

RELATED LITERATURE

A World Health Organization report in 2014 points out that globally, due to handling, mishandling of petroleum products (including in the exploration-extraction perimeters) 2.3 million lives are lost and are affected properties worth over 4.5 billion euros. Volatile organic compounds are components of a heterogeneous group of chemicals that can cause adverse health effects (asthma, migraines, inflammation of the mucosa) and benzene is the characteristic of cancer risk [7, 8, 11].

The maximum allowed/maximum benzene content is regulated in Europe (Directives 2000/69/EC and 2008/50/EC). Evaluating the exposure of an organism, system or population/subpopulation to a hydrocarbon agent and its derivatives is a phase of the risk assessment process. [3]. There is always a scenario of exposures [2], through typical events or through potentially conscious, direct, negligent exposure [12, 13]. Identifying the type and nature of adverse effects marks the danger, which must also be assessed in the context of the risk assessment steps. The remedy, the incipient, immediate prevention remains the avoidance of contact with hydrocarbons and, especially, the avoidance of the use of gasoline as a degreaser and the accidental washing of hands, arms, etc.

In common practice, known as the standard for assessing the health risks caused by such exposure, the assessment, measurement of the presence and action of benzene, toluene, ethylbenzene and xylene (BTEX) is used. These components, once measured, complete the aggregate approach of quantifying the effects on exposure to the entire fuel/hydrocarbon. It is found that benzene has a carcinogenic effect and toluene [1], ethylene and xylene induce relatively non-carcinogenic health risks [14]. On the other hand, short-term exposure to gasoline is complementary to: i) skin irritation and ii) sensory dysfunction. They cause influences on the central nervous system (CNS), having as outputs conditions for fatigue, dizziness, headache, loss of coordination. All of these conditions are immediate, especially among genetically sensitive people.

According to the US Agency for the Registration of Toxic Substances and Diseases (ATSDR), there are more than 150 chemicals in gasoline, even in small amounts of benzene, toluene, xylene, ethylbenzene and traces of contaminants such as lead. Gasoline production is the result of process steps such as: i) chemical separation/fractional distillation, ii) molecular conversion/rearrangement and iii) final treatment. In some countries, leaded petrol has been banned (for example, in 2006 in South Africa) and its aromatic content has been increased from 34% to 40% (Octane Figure). In the US, the occupational safety and health standard for benzene is 3.2 mg/m^3 in an 8 hours shift. In Europe, the limit of benzene content is set at 3.2 mg/m^3 (1 ppm) in 6 hours TWA, and in South Africa, it is 16 mg/m^3 (5 ppm) in 8 hours of exposure. Prolonged exposure to benzene, even at low levels, under conditions of professional operation, induces the risk of DNA degradation/damage and leads to acute myeloid leukaemia or myelodysplastic syndrome [11].

EXPERIMENTAL WORK

Methods, classification and specific remarks

Our research aims at the network characterization of Petroleum Distribution Stations [8, 14], Offshore Platforms and intelligent textile systems recommended for use among workers. The experimental, scientific and practical contribution refers to the design of a model of "Sustainable Techno-Medical-Sanitary Optimum" {M(TMSD)} by using smart textiles. With the help of this model, it is possible to resort to parametric iteration/reiteration, aiming at the achievement, value and qualitative fulfilment imposed to a general objective function F (TMSD) of sustainable techno-medical-sanitary when using smart textiles.

The developed model continues to go through the processing in "soft" information programming mode, and later, there will be the possibility and the probability of its use as a calculation tool. The model has non-controllable values (*inputs*), transformation and obtaining controllable values (*outputs*), imposed for minimum costs and efficiency, safety, maximum sustainability (maximum techno-medical-sanitation for sustainability).

The {M(TMSD)}, model, which expresses the influence of the presence of smart textiles, has the potential for iterative and repetitive valences for all situations, cases of physical and chemical aggression, excessive temperatures, etc. from oil stations but also in other areas (for example, on offshore exploration-exploitation platforms in the Black Sea) [13, 15, 16], in a limited range (0,1). In the offshore area, we are dealing with the toxicity of elements dissipated from hydrocarbons, but also with extreme weather (winter, wind, frost, excessive sun exposure, etc.) which motivates the call for smart textiles to equip workers for protection.

The special attention paid to the variable $(TSMD)_{max}$, refers to the need to identify unsuitable situations in the system of distribution stations and on the Offshore Platforms of hydrocarbon-derived fuels. It is concluded that the optimal {(TMSD)}, for any variant, accompanies the "utility" but between "utility" and "optimal techno-medical-sustainable health" there can be disarticulations, different meanings (divergent increases/decreases). The use of smart textiles starts from the general framework and the achievement of comparative advantages, especially competitive in the field for efficiency, safety and sustainability.

Integrated interactive preventive model with probabilistic statistical testing for obtaining sustainable techno-medical-sanitary solutions by using intelligent textiles

Mathematical modelling requires the use of mathematical concepts and terms. [6]. A quantitative model for obtaining sustainable techno-medical-sanitary solutions using smart textiles aims at the graphic composition of the block scheme and, further, the corresponding equational formalization. The equations can be algebraic, transcendent and differential, integral or integro-differential which, through their formalizing role, can confirm some working hypotheses, of finding and interpreting. On this basis, the complex integrated interactive-preventive model with probabilistic statistical testing for obtaining sustainable techno-medical-sanitary solutions by using smart textiles is presented (figure 1).

In figure 1, the meanings of the notations are as follows: (ΔA) is impairments, (E) – oil exploitation/production (petroleum products), (Z_{pe}) – post-exploitation areas (oil/oil products in stations, offshore platforms), (A_s) – techno-sanitary impairments, (A_e) – techno-epidemiological (epidemiological) disorders, (OM) – Stations, Offshore platforms, (T_{sc}) – case study locations, (Z_{rn}^{ei}) – areas with oil resources of interest (Offshore Stations and Platforms) [7], M – management by using smart textiles, (C) – leadership through the use of smart textiles, (O_g) – organization by using smart textiles, (MC | IP) – complex interactive-preventive model with probabilistic statistical testing of the use of smart textiles, (S_i) – solutions (contributory/interactive part of the research) by using smart textiles. The advanced recommendation, on this occasion, is to emphasize the systemic and systematic concern for the inclusion of the aggregate covering parameter {[TMSD]} in the implicit, intrinsic, technical-functional configuration of technological flows in Petroleum Stations and Offshore Smart Textile Platforms. In this context, this mathematical construction is intended for the application extension by the subsequent realization of the computerized model, programmed, so that a specific software in the field is finally available.

Smart textiles are able to detect and react to changes in the environment. Some textiles react to external stimuli (chemical, electrical, thermal or otherwise) from the environment and provide practical results. We consider textile materials with the potential to collect, retain energy. Smart textiles, in turn, are becoming viable sources of energy. For example, the use of piezo-, pyro-, ferro- and dielectric materials in textiles induces the "intelligence" in question. However, methods are needed to manufacture different piezometric fabrics, in the context of the usual realization of woven, knitted and composite structures. In the already classical view, an intelligent system is an assembly that structurally articulates a sensor, a processor and an actuator, which manages control data. In general terms, we can speak of "portable electronics", respectively of functional fabrics. They can be used to:

• Thermal storage for temperature regulation. For example, including microcapsules with paraffin in the fabric structure, either by coating or by the spinning process, if the waxy material changes its phase on the solid-liquid-solid alignment, heat absorption and release are achieved. Such a temperature variation formalizes the microclimate in the comfort zone. In addition, if we are dealing with textiles that store and/or change shape under external stimuli and reach or return to their original shape, they show that temperature adjustments occur.
• Thermal reactions of textiles through variations in permeability. On this basis, the transition temperatures of a kinetic nature, related to molecular chains, are recorded.
• The colour of the textile changes due to an external stimulus. This transformation induces temperature variations and comfort adjustments. Photonics, in this case, refers to the aggregation of electrochromic materials (e.g., optical fibres, LEDs) with textile fabrics.

Some wires, made of textile material, represent supports for sensors, telecommunication, heating.
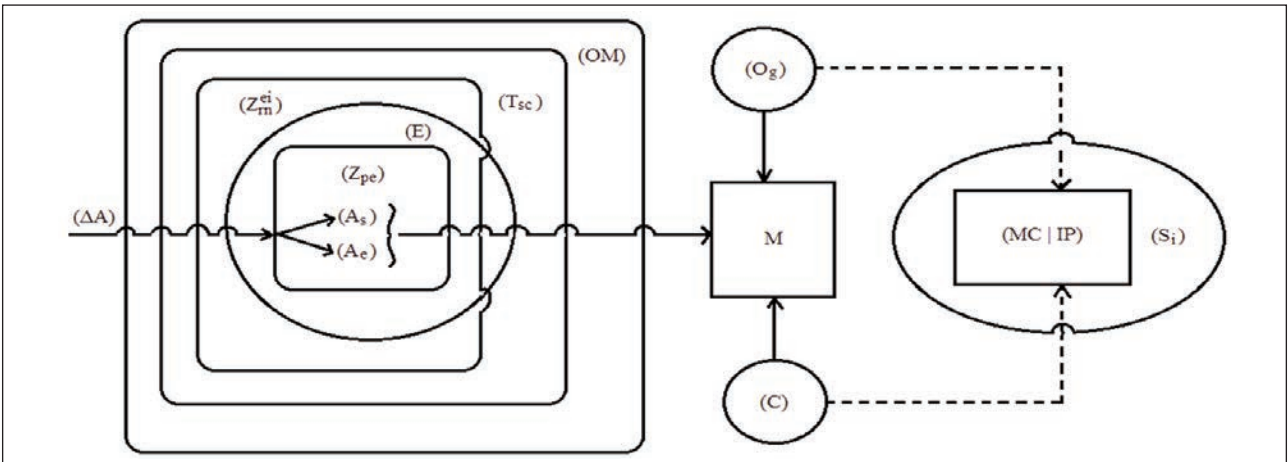

Fig. 1. Integrated interactive-preventive complex model with probabilistic statistical testing for obtaining sustainable techno-medical-sanitary solutions by using smart textiles [11]

Different textiles can be sensitive to stress, with instantaneous changes, becoming rigid or flexible to shocks. In this context, biomimetics can also be mentioned, representing similarities, similarities, imitations of biological reactions characterized by eco-natural properties (chameleonism). Smart textiles are components of protective textiles that increase overall socio-economic and health performance, sustainability [11].

RESULTS AND DEBATES

New characterization of intelligent/smart textile material in oil stations and offshore platforms

Textile-based triboelectric nanogenerators (T-TENGs) combine the functions of energy retention and self-powered detection with advantages of breathability and flexibility. This technological alignment is significant for the rapid progress in smart textiles because in the modern era the insistent requirements in the field are for versatility and multi-scenario practicability. In combination with fire-retardant conductive cotton fabrics, coated with polytetrafluoroethylene and a separator, a fire-retardant and environmentally friendly textile triboelectric nanogenerator (FT-TENG) is developed, which is equipped with fire resistance and special energy collection capabilities [9, 16]. As such, self-assembled layer-by-layer cotton fabrics have outstanding self-extinguishing performance.

In order to simply and efficiently increase the conversion capacity of portable thermoelectric textiles, a two-step in situ method is adopted. The fabrication of photo-thermo-electric textiles with a double surface takes place, one surface made of polypropylene fibres and another surface with a photo-thermal layer (PPy), respectively a thermoelectric layer (PEDOT). PPy is adapted to obtain temperature effects [15]. The PPy layer increases the photothermal conversion efficiency of the prepared fabric. The optimized photothermal fabric can improve the voltage generated from 294.13 to 536.47 µV under infrared light, and its power density is up to 13.76 nW/m². A flexible photothermal strip composed of prepared fabric, covered with Ag particles and textile substrates with low thermal conductivity, shows an output voltage of 2.25, 0.667 and 0.183 mV and output power of 0.7031, 0.0636 and 0.0049 nW under IR light (sunlight, respectively on the arm).

Photothermoelectric fabrics have the potential of a smart portable device for light conversion and wealth [12]. There are already textile sensors [4] for wireless monitoring equipment. The sensors, made entirely of textile, have the interface for data flow, their electronic storage and transmission potential.

In order to verify the proposed model, the specialists from INCDTP designed and created a woven fabric with the following functional, mounting and adjustment parameters (table 1). The programming scheme for the creation of smart textiles is presented in figure 2. To increase the breathability and flexibility functions of the smart textile, the woven fabric has been coated with polyurethane. The testing is still going on in order to minimize the errors of the model.

Table 1

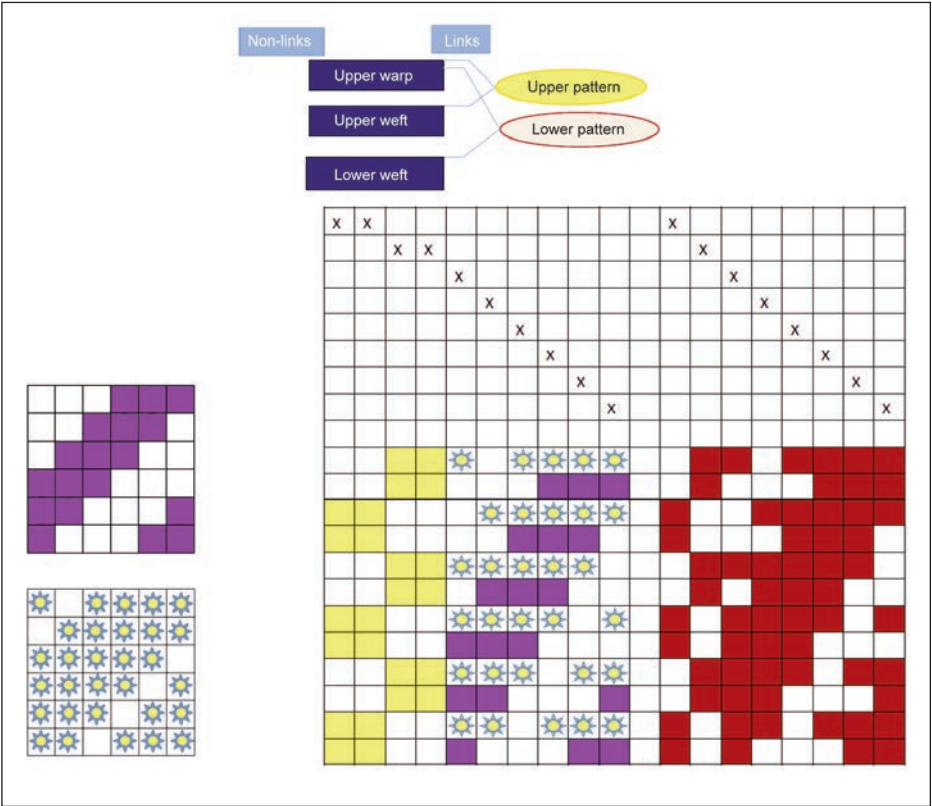| FUNCTIONAL AND MOUNTING PARAMETERS OF WOVEN FABRIC		
Parameters		**Data/Values**
Raw material	warp	100% PES
	weft	100% PES
Length density (dtex)	warp	83dtex/32fx1/850Z
	weft	110dtex/124f
Binding		weft semidouble with partial drawings D3/3 and D5/1
Warp density (yarns/10 cm)		420
Weft density (yarns/10 cm)		420
Width (cm)		175
Insertion speed (wm/min)		592
Index position		+1.5

Fig. 2. Programming scheme

CONCLUSIONS

We find that in the textile industry there is the possibility of exchanging information with the help of smart textiles, a property already considered revolutionary. Textile incorporation technologies are "smart composition" type responses, and "smart textile composite" type solutions show the new performance of fabrics. So, smart textiles can feel, react and adapt to environmental conditions. Therefore, clothing may become able to record, analyse, store, send and display data. The "new properties and utilities" type dimensions of smart clothing improve the comfort and performance of sustainable techno-medical-sanitary. General progress in the development of textiles by improving their functionality in relation to environmental conditions develops the textile market in the new global economy.

REFERENCES

[1] Adami, G., Larese, F., Venier, M., Barbieri, P., Lo Coco, F., et al., *Penetration of benzene, toluene and xylenes contained in gasoline through human abdominal skin in vitro,* In: Toxicol. Vitro., 2006, 20, 8, 1321–1330

[2] Boudet, C., et al., *Subjects adapt time-activity patterns during participation in a personal exposure assessment study,* In: Proceedings of the Annual Meeting of the International Society of Exposure Analysis (ISEA), Research Triangle Park, North Carolina, USA, 1997

[3] Burgherr, P., Hirschberg ,S., *Comparative assessment of natural gas accident risks,* Paul Scherrer Institut – PSI, January 2005

[4] Catrysse, M., et al., *Towards the integration of textile sensors in a wireless monitoring suit,* In: Sensors and Actuators A: Physical Volume, 2004, 114, 2–3, 302–311

[5] Daintith, T., Chandler, J., *Offshore petroleum regulation: theory and disaster as drivers for institutional change,* University of Western Australia / Advanced Legal Studies in London; Houston Journal of International Law, 6/7/2017

[6] Gazi, F., *Mathematical Modeling for Measures of Supply Chain Flexibility,* In: Journal of Mechanical Engineering, 2016, 45, 96, https://doi.org/10.3329/jme.v45i2.28977

[7] Gâf-Deac, I.I., *Analiza multicriterială la utilizarea raţională a resurselor naturale,* In: Revista Minelor, Bucharest, 2006, 11–12, 185–186

[8] Gâf-Deac, I.I, Scutelnicu, I.P., Bărbulescu, A., Khamis, J., Bubu, M.N., *Abordarea industrial-sistemică a extracției și valorificării substanțelor minerale utile,* Editura Scientific Publishing House, Bucharest, 2021, ISBN 978-606-95189-0-8

[9] Gâf-Deac, I.I, Scutelnicu, I.P., Sava, C., Bădău, A.-B., Bărbulescu, A., Rodica Hurloiu, L., Cioată, C., Reșetar, A., Pătraș, I., *Riscul ecologic post-exploatare pentru arealul costier maritim Dobrogea,* In: Revista pentru Dezvoltare Bazată pe Cunoaștere, București, 2015, 2, 18–24, ISSN 2393-2112 / ISSN-L 2393-2112

[10] Gonzalez-Flesca, N., Vardoulakis, S., Cicolella, A., *BTX concentrations near a stage II implemented petrol station,* In: Environmental Science and Pollution Research, 2002, 9, 169–174

[11] Khamis, J., *Economy and management of critical cases at the stations of distribution of petroleum products in Damasc, Syria,* Workshop 3: Knowledge, Innovation, Smart Development And Human Capital, The 6th International Conference, Economic Scientific Research – Theoretical, Empirical and Practical Approaches, ESPERA 2019, Bucharest, October 10 th–1 th, 2019

[12] Renwei, C., et al., *Flame-Retardant Textile-Based Triboelectric Nanogenerators for Fire Protection Applications*, In: ACS Nano, 2020, 14, 11, 15853–15863

[13] Scutelnicu, I.P., Khamis, J., Gâf-Deac, I.I., *Perspective comparative energetice: onshore –offshore,* Ed. Liberum Ideas, Bucharest, 2021, ISBN 978-606-95190-2-8

[14] Scutelnicu I.P., et al., *Super-Compact Structures of Quality Standards for Health and Security in the Sustainable Development of a Mining Basin in Romania,* In: IMPACT: International Journal of Research in Engineering & Technology, 2020, 8, 2, 11–22

[15] Xuefei, Z., et al., *Dual-Shell Photothermoelectric Textile Based on a PPy Photothermal Layer for Solar Thermal Energy Harvesting,* In: ACS Appl. Mater. Interfaces, 2020, 12, 49, 55072–55082

[16] Wang, S., Li, B., Liu, X., An, M., Zheng, L., Jiang, Z., *The Design of Intelligent production line for Clothing Industry,* In: 2020 IEEE 6th International Conference on Computer and Communications (ICCC*)*, 2020, 2403–2408

Authors:

JAMAL KHAMIS[1], IOAN I. GÂF-DEAC[2], IOAN PETRU SCUTELNICU[3], MIHAELA JOMIR[4], ALEXANDRA GABRIELA ENE[4], IONUT ARON[5]

[1]Ministry of Health, Parlaman st. - Nejmeh sq., Damascus, Syria

[2]Institute of National Economy "C. Kirițescu", Romanian Academy, 13 September St., 050711, Academy House, Bucharest, Romania

[3]Romanian Institute of Geology, Bucharest, Romania

[4] National Research Development Institute for Textiles and Leather, 16 Lucretiu Patrascanu, 030508, Bucharest, Romania

[5]University of Petroșani, 20 University St., Petroșani, Romania

Corresponding author:

MIHAELA JOMIR
e-mail: mihaela.jomir@incdtp.ro

Measuring the natural frequencies of knitted materials for protection against vibrations

MIRELA BLAGA   CRISTINA GROSU
NECULAI EUGEN SEGHEDIN

ABSTRACT – REZUMAT

Measuring the natural frequencies of knitted materials for protection against vibrations

In this study, the use of knitted structures as potential vibration isolators or parts of protective equipment is proposed. Four types of knitted structures were made from different yarns by varying the stitch depth. By combining these variables, a series of 48 patterns were tested for vibration isolation using the free vibration method to measure their natural frequencies. Knowledge of the natural frequencies of textiles is necessary when designing a material to protect it from vibration, in order to avoid the phenomenon of resonance that occurs when the excitation frequency of an external force overlaps with the natural frequency of the system. From the recorded values of the frequencies, it is possible to infer some properties of the knitted materials. The value of the natural frequency of any material gives information about the stiffness of the material. The higher the natural frequency, the more stiffness can be expected. The shape of the natural frequency curve is relevant to the material's ability to dampen vibrations. The smoother the shape, the higher the damping capacity of the material. The study shows that the yarn type and the structural parameters of the fabric affect the vibration behaviour. The tightness of the fabric is one of the most important variables affecting the level of natural frequencies of the material. This research is expected to support the development of knitted fabrics as good vibration isolators for humans by also showing their comfort level compared to alternative materials used so far.

Keywords: weft knitted structures, natural frequency, free vibration, raw materials

Măsurarea frecvențelor naturale ale materialelor tricotate destinate protecției împotriva vibrațiilor

În acest studiu, se propune valorificarea tricoturilor ca potențiali izolatori împotriva vibrațiilor sau ca părți componente ale echipamentelor de protecție. Cercetarea s-a efectuat asupra unui număr de 48 de variante de tricoturi, rezultate din tricotarea a patru structuri, fiecare fiind obținută din patru fire diferite și cu trei valori diferite ale adâncimii de buclare. În vederea caracterizării capacității de izolare a vibrațiilor, au fost măsurate frecvențele naturale ale tricoturilor, determinate prin metoda vibrațiilor libere. Cunoașterea frecvențelor naturale este necesară încă din etapa de proiectare a unui material, astfel încât acesta să poată oferi protecție la vibrații, evitându-se astfel fenomenul de rezonanță, care apare atunci când frecvența de excitație a unei forțe externe se suprapune cu frecvența naturală a sistemului. Valorile înregistrate ale frecvențelor naturale pot oferi informații privind anumite caracteristici ale materialelor tricotate, precum rigiditatea acestora. Cu cât frecvența naturală este mai mare, cu atât rigiditatea acestora este mai crescută. Forma curbei naturale de frecvență este relevantă pentru capacitatea materialului de a amortiza vibrațiile. Cu cât forma este mai aplatizată, cu atât capacitatea de amortizare a materialului este mai mare. Cercetarea arată că tipul de fire și parametrii structurali ai tricotului determină comportamentul acestuia la vibrații. Compactitatea tricotului este una dintre cele mai importante variabile, care influențează nivelul frecvențelor naturale ale acestuia. Această cercetare confirmă capacitatea de protecție a structurilor tricotate împotriva vibrațiilor, care, împreună cu nivelul ridicat de confort al acestora, pot constitui alternative ale materialelor utilizate până în prezent.

Cuvinte-cheie: tricoturi din bătătură, frecvențe naturale, vibrații libere, materii prime

INTRODUCTION

Vibration is a mechanical phenomenon that describes the physical energy of a vibrating object. Handling a vibrating instrument transfers the energy produced by the source to the body. The shocks generated by vibration gradually lead to physical discomfort, ranging from brief discomforts, such as kinetosis sourced from mild shocks to severe injuries, such as gangrene on the worker's fingers sourced from severe shocks [1, 2].

It has been found that the number of workers affected by occupational vibration exposure is high and varies in different countries depending on the industry. For example, it is estimated that 8–10 million workers in the USA are exposed to occupational vibration on a daily basis, while Eurofound reports that 20% of European workers are regularly exposed to vibration during at least ¼ of their working hours [3, 4].

To control the negative effects of vibration on the human body, two conditions are required: limiting the exposure time and using personal protective equipment (PPE), which acts as a damper by dissipating the energy generated by friction between internal components.

Recent studies have brought to light the ability of various textile fabrics as cushioning materials, which have also been shown to be superior in comfort and environmental friendliness to foam or rubber, which have been used abundantly in PPE construction in recent decades. Considering the high percentage of people who work with hand-held power tools, special attention has been given to the research of anti-vibration gloves so far.

LITERATURE REVIEW

A relevant number of patents disclose various models of anti-vibration gloves in which one or more layers are made of textile materials, particularly knitted fabrics, generally shielded with various impact-resistant materials, such as silicone protrusions, foam, nubs, or rubber cavities filled with compressed air. The most commonly used textile materials for patent models are cotton for the inner and core layers, high-performance yarns such as para-aramid, Kevlar or high-density polyethylene for the outer layer, and various elastic yarns to improve elasticity in the wrist or backhand areas of the glove [5–9].

Recent researches have investigated the vibration behaviour of various knitted spacer fabrics or new prototypes of gloves made of knitted materials by subjecting them to objective tests, namely air permeability, vibration isolation, compression or trial tests. Some of them were evaluated in comparison with various commercial anti-vibration gloves and obtained very good results. Polyester is the most commonly used raw material for anti-vibration knitted fabrics, especially for spacer fabrics. Nevertheless, few studies have aimed to investigate the influence of raw materials on the response to vibration. Seghedin et. al. found differences of (20–80) Hz between the responses of synthetic fabrics made from PES or PP and natural fabrics made from cotton or PAN [10]. In addition, a significant influence of the type of spacer yarn was found. In a group of warp knitted fabrics made of PES or PA yarns for the outer layers and mono/multifilaments from PES or monofilaments from PA as spacer yarns, the highest frequency level was found in the fabrics with monofilaments from PES as spacer yarns [11, 12]. Many other experiments investigated the vibration isolation performance of different knitted structures from PES, but the focus was on other features that affect this performance, such as fabric thickness, stitch density, spacer thread arrangement, or test direction [12–15]. Polyamide is the second option in raw materials for antivibration products. A prototype antivibration glove containing a spandex/nylon spacer fabric for the outer layers and polyester monofilament for the spacer yarn as the cushioning layer showed better performance than 3 other commercial antivibration gloves in wear tests and exposure to vibrations from a hammer drill [16]. Chen et al. investigated the vibration isolating effect of spacer fabrics with outer layers of nylon yarns or nylon/spandex yarns [17, 18]. No significant differences in damping performance were found for spacer fabrics with outer layers of 100% nylon yarn and nylon/spandex yarn [16]. However, better vibration isolation for spacer fabrics was achieved by the elastic yarn insertion technique, which consists of a feeding device attached to the side of the knitting machine, than the conventional method in which the elastic yarn is knitted together with the surface yarns. Yu et al. investigated the vibration isolation behaviour of spacer fabric with elastic insertion for the first time [19]. Based on the basic mechanical theory that to achieve good vibration isolation, it is necessary to reduce the dynamic stiffness of the isolation material to obtain small resonant frequencies during vibration, it was deduced that the use of thicker fabrics is strongly recommended for this purpose in the knitting field. In order to achieve a relatively high thickness without compromising flexibility, Chen applied a steam treatment to the weft-knitted spacer fabrics constructed with nylon and elastic yarns in the two outer layers. As a result, the elastic yarns shrank and the fabric became thicker [17].

High-performance yarns, such as Kevlar or Dyneema, have been used to provide gloves with anti-vibration, cut-resistant and fire-resistant properties for specialized applications. The samples in three-layer sandwich form consist of the top layer of 100% Kevlar or Dyneema, various spacer fabrics or silicone as the inner layer and 100% cotton fabric as the underlining. The samples with silicone or spacer fabric as the inner layer showed significant antivibration properties in the frequency range of 10–200 Hz, with the best damping performance in the range of 50–130 Hz. It was observed that the dexterity and hand comfort of the gloves increased significantly when the silicone layer was replaced with knitted spacer fabric [20].

Natural fibres, such as cotton, are widely used in the antivibration glove market because they offer higher comfort and warmth. Nevertheless, few studies have looked at their ability to reduce the transmission of vibrations. Most of these products consist of a normal glove knitted using conventional technologies with an anti-vibration layer applied to the palm, generally made of foam or rubber [21].

An innovative e-textile product designed to measure vibration has shown high performance after being evaluated under real vibration conditions by workers handling an electric drill. A textile dosimeter consisting of a small triaxial accelerometer incorporated into the core of a textile yarn was used to develop a vibration-measuring glove. Data acquisition was performed with a computer and data analysis was performed with Fast Fourier Transformation [22–24].

The experiments in this study aimed to investigate the influence of yarn type and fabric structural parameters on the performance of weft knitted fabrics in insulating against vibration.

MATERIALS AND METHOD

Tested materials

The studies were conducted with knitted fabrics of different yarns types, with a count 20/1 Nm: Cotton (CO), Polyester (PES), Acrylic and Polypropylene (PP). The selected knitted structures were: single jersey (SJ), interlock (I), sandwich 1 (SW1) and sandwich 2 (SW2) manufactured on electronic flat knitting machines, CMS 530 E6.2, Stoll. The knitted sections are listed in table 1.

For the present study, the stitch depth was set in three levels. The variation of the stitch depth was done by changing the position of the stitch cam using the NP values, which could be set in the knitting program of the M1 plus® software before manufacturing. The minimum and maximum values of the stitch depth were selected according to the machine gauge and the fabrics were defined as tight (NP=12.0), medium (NP=13.0) and loose (NP=14.0). Each structure was made from the four yarns with the three values of stitch density, resulting in a number of 48 samples in the experimental matrix that were subjected to analysis.

After knitting, the fabrics were relaxed in the dry state and the values of the fabric's structural parameters related to vertical density in cpc and horizontal density in wpc were determined. The mass per square meter (g/m²) was determined using an electronic balance (KERN ABT 320-4M) and the average of five measured values for each structure was calculated. Fabric thickness was measured using a Lab Mesdan device with a resolution of 0.01 mm under a compressive force of 10 cN/mm² in accordance with ASTM D1777-96(2019) Standard Test Method for Thickness of Textile Materials.

Testing method

To analyse the vibration behaviour of a system, it is important to determine its natural frequencies, which are free vibrations that occur when an elastic system is released from its equilibrium position. In the presence of frictional forces, the mechanical energy is dissipated and the vibration is damped by a certain number of cycles. The frequencies are independent of the initial conditions of the motion, so they are called natural frequencies of vibrations [25].

The dynamic performance of knitted fabrics has been studied by testing the dynamic behaviour of a piece of metal weighing 395 g and measuring 30×70×30 mm, attached directly to the surface with an adhesive [10–12, 26], while the textile material is attached to a heavy plate to avoid relative movements between the piece of fabric and the plate. Because the knitted fabrics are characterized by a highly anisotropic structure and different mechanical behaviour in various directions, for each sample the vibration was generated and measured along with three directions: walewise, coursewise and perpendicular on the fabric surface (figure 1).

The vibrations are measured with a PCB Piezotronics accelerometer and the signal is processed by a data acquisition system. The Frequency Spectrum Analysis is the basis of any diagnostic process that uses vibration measurement and consists of the signal decomposition into a sum of frequencies, each corresponding to a certain level of vibration, by applying Fast Fourier Transformation (figure 2).

Each curve consists of a certain number of waves, where the highest peak of the first wave in the horizontal direction is the natural frequency of the material, measured in Hz. The magnitude of the natural

Table 1

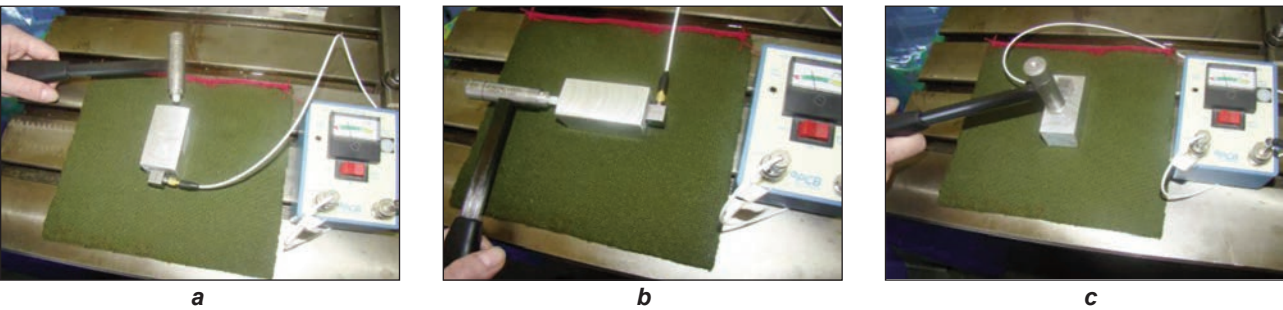| KNITTED STRUCTURE SECTIONS			
Single jersey (SJ)	Interlock (I)	Sandwich 1 (SW1)	Sandwich 2 (SW2)

a	b	c

Fig. 1. Measurement method of the natural frequencies [10]: *a* – walewise; *b* – coursewise; *c* – perpendicular
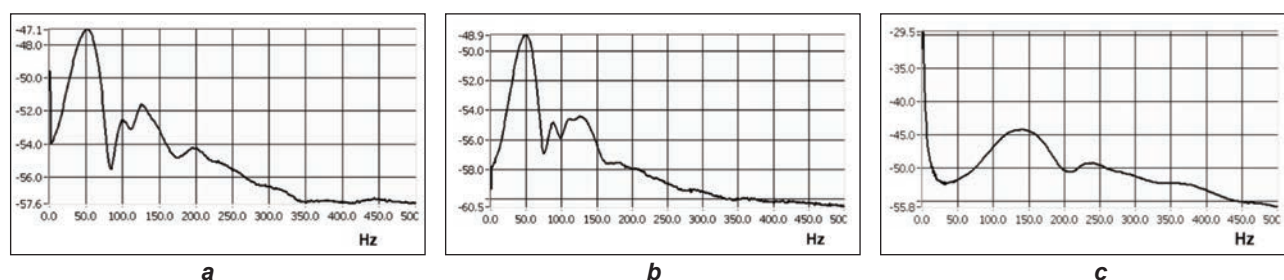
Fig. 2. Recorded natural frequencies of knitted fabrics: *a* – coursewise; *b* – walewise; *c* – perpendicular

frequency for each material provides information about its stiffness. The higher the natural frequency, the more stiffness is expected [26].

RESULTS AND DISCUSSIONS

Testing direction influence on fabric's natural frequencies

Knitting direction has been shown to affect some mechanical properties of knitted fabrics, therefore, it was considered in the present study to determine its effects. The experimental data of natural frequencies were analysed for each yarn type and structure. The example presented in figure 3 displays the four structures from PES and the frequency range for the three testing directions. The comparable frequency level of all fabrics in the transversal (38–58) Hz and longitudinal directions (40–59) Hz at low seismic weight, can be attributed to the vibrational mechanism, which in this case does not involve any movement or distribution of yarn within the structure. The highest values of the natural frequencies of the fabrics were recorded in the perpendicular direction (97–160) Hz, demonstrating the high stiffness of the system. The high ability to damp the vibrations well in this direction, is confirmed by the shape of the frequency curve with low peaks and a smooth profile (figure 2, *c*).
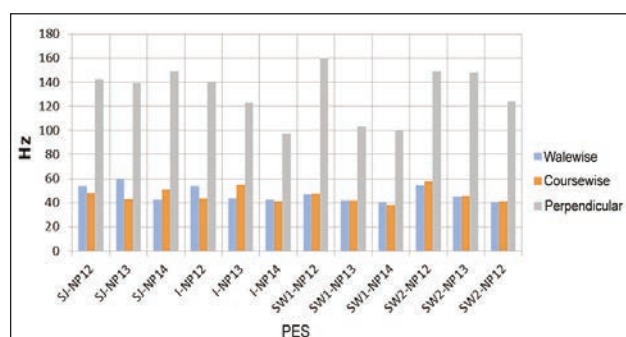

Fig. 3. Natural frequencies measured on different directions (Hz)

Yarn type influence on fabric's natural frequencies

Knitted fabrics made of natural and synthetic yarns have different values of the natural frequencies, regardless of their structure. The type of yarn affects the response of the fabrics in the dynamic tests. Knitted fabrics made of Acrylic, which imitate natural fibres, and of cotton have lower values of their natural

frequencies for all structures, all test directions and all stitch densities.

Analysis of experimental data selected for all fabrics in the perpendicular test direction, shown in figure 4, *a* and *b*, reveals a significant difference of (20–100) Hz between the frequencies of synthetic fabrics made of PES or PP and natural fabrics made of CO or PAN. The structure of natural yarns is made from staple fibres, their warm feel and soft handle indicate a less stiff knit and a lower level of natural frequencies. Synthetic yarns are very durable and mechanically resistant, and the knitted fabrics made from them are stiffer and have higher natural frequencies.

It can be observed the differences in the structures from different yarns. Single jersey has the highest stiffness when made from PP yarns, while interlock and sandwich fabrics are very stiff when made from PES. It can be assumed that the natural frequencies of fabrics for a particular knitted fabric can be controlled at the design stage by the raw materials used.

### Fabric tightness influence on fabric's natural frequencies

Stitch depth influences the value of the stitch length and the stitch density, which has a major impact on the characteristics of the knitted fabric, such as dimensional stability, weight, comfort, mechanical properties. On electronic flat knitting machines, the tightness of the knitted fabric can be adjusted by the position of the stitch cam (NP). The higher the NP value, the higher the stitch length, the looser the fabric. Under these circumstances, the data show that the natural frequency decreases with a higher NP, which is reflected in a lower stiffness of the fabric. In the case of PP (figure 5) and Acrylic fabrics (figure 6), all tested structures follow this tendency in the perpendicular direction. The exceptions are single jersey from PES (figure 3) and SW1-SW2 from CO (figure 7), which do not follow this rule.

Fabric thickness influence on fabric's natural frequencies

Fabric thickness can be a control parameter for fabrics where this parameter is evenly distributed on the surface. Fabrics with higher thickness and lower stiffness are recommended for vibration isolation [15]. In the diagram shown in figure 8, it can be seen that SW2 made of PES and PP is such a structure where the natural frequencies decrease with increasing thickness. The same is available for interlock from
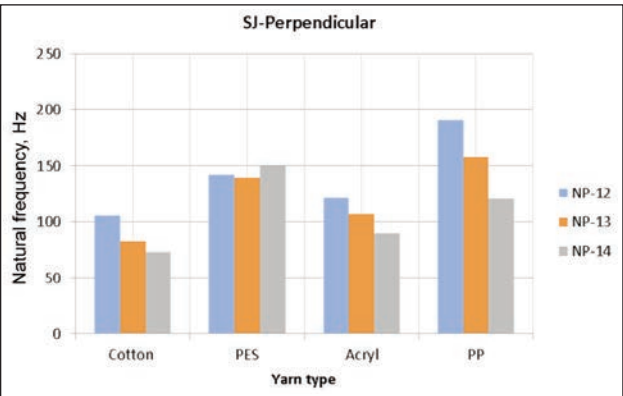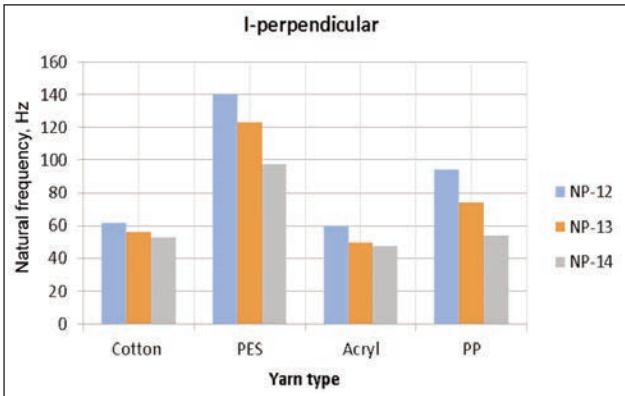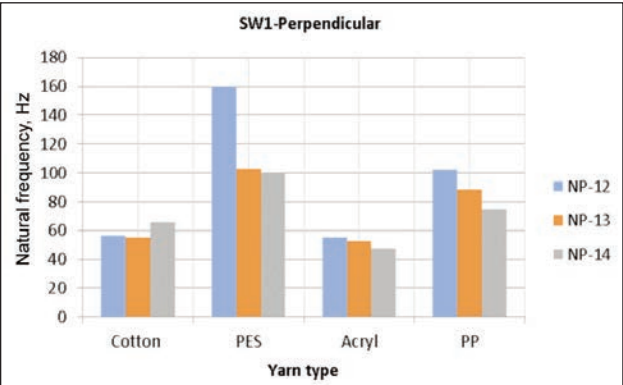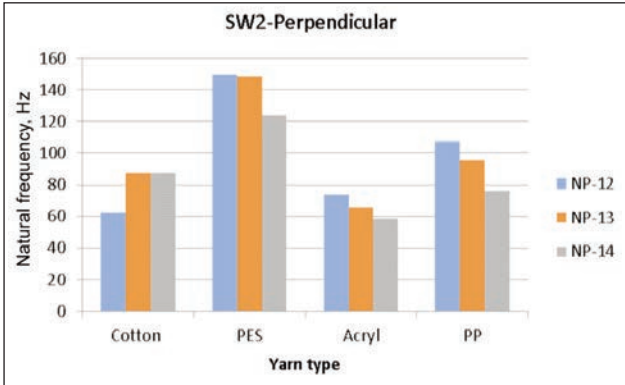
Fig. 4. Natural frequencies of knitted structures: *a* – Single jersey; *b* – Interlock; *c* – Sandwich 1; *d* – Sandwich 2
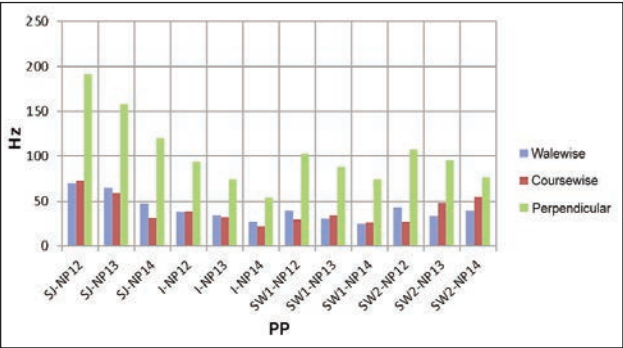
Fig. 5. Natural frequencies of PP fabrics
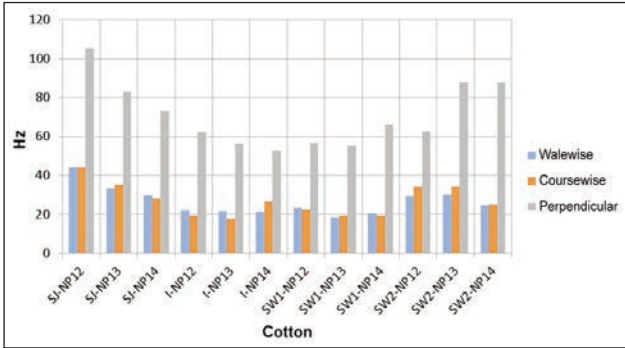
Fig. 7. Natural frequencies of CO fabrics
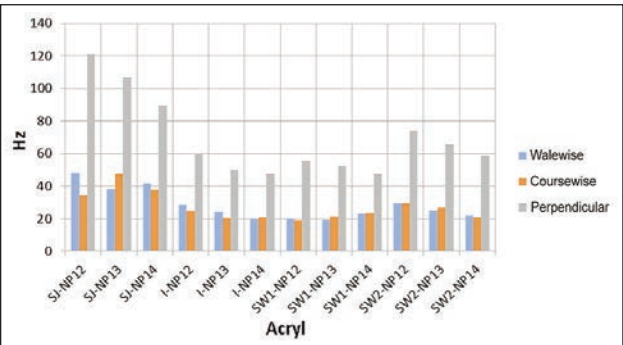
Fig. 6. Natural frequencies of Acryl fabrics

PES and Acrylic yarns and SJ from all yarns. SW1 shows a different behaviour due to its non-uniform thickness resulting from the structural connection of the two layers, creating thus a channelled structure.

CONCLUSIONS

Humans are exposed to vibrations in their activities from a variety of sources, whether from power tools or while riding in vehicles. The energy absorbed from these sources is emitted in the form of vibrations, some of which are transmitted to humans and can cause permanent occupational diseases, having also a negative influence on the worker's effectiveness and productivity [27].

The free vibration method, known in the field of mechanical engineering, was transferred by the authors to the textile field in order to test and characterize textile materials for potential vibration isolation applications.

Knowledge of the natural frequencies of textiles is necessary when designing a material to protect against vibration. Otherwise, resonance, a dangerous
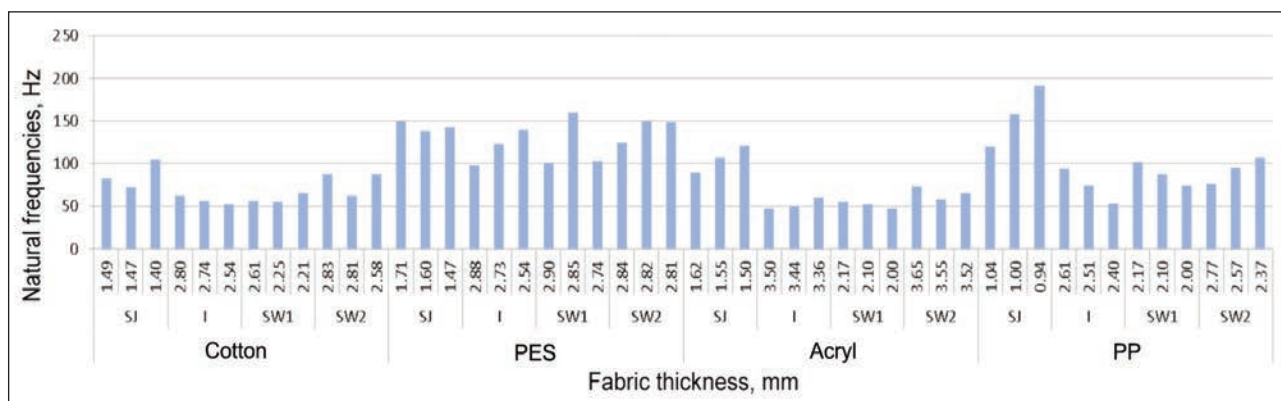
Fig. 8. Natural frequencies of various fabric's thickness

phenomenon that occurs during the use phase, may occur when the excitation frequency of an external force overlaps with the natural frequency of the system. This is the case, for example, with collapsed buildings during an earthquake, because the earthquake force overlaps with the natural frequencies of the building.

This study reports on an investigation of the natural frequencies of weft knitted fabrics made of different yarns determined by the free vibration method. The behaviour of four typical knitted fabrics, single layer and two layers, made of natural and synthetic yarns was experimentally investigated using a vibration test system that measures the frequency of a metallic mass attached to the fabric and excited by shock.

The results discuss the two main factors affecting the natural frequencies of knitted fabrics, namely the yarn type and the tightness of the fabric. The experimental data confirm that the selection of raw material is significant for the development of fabrics with controlled natural frequencies. Fabric tightness is a technological parameter that influences many properties of the produced structures, including the natural frequencies, as confirmed by this analysis.

In future research, the authors will present the design and fabrication of knitted fabrics tailored for a specific vibration isolation application. The particular requirements of the fabric's end use will determine what level of natural frequencies is desired. For example, the knitted fabric should have a different frequency range than the external system generating the vibrations to prevent their transmission. Thus, in the design phase, the structural and technological parameters to control the material properties must be defined.

The development of breathable and recyclable materials with good insulation performance is highly desirable as an alternative to polymer foams, rubbers, gels and air bladders. It was demonstrated that a thicker fabric with a lower stiffness has better vibration isolation performance due to its lower isolation frequencies [15].

As a design principle, a knitted fabric developed for antivibration purposes should be able to absorb energy efficiently while having sufficient stiffness to avoid collapse and an acceptable thickness to preserve the sense of touch and dexterity while performing tasks [18].

REFERENCES

[1] ISO-International Organization for Standardization, *ISO/WD 2631-1 Mechanical vibration and shock – Evaluation of human exposure to whole-body vibration – Part 1: General requirements,* 2001

[2] Canadian Centre for Occupational Health and Safety, Government of Canada, *Vibration,* 2021

[3] Eurofound, *Sixth European Working Conditions Survey – Overview report,* 2017

[4] Andrejiova, M., Pinosova, M., Badida, M., *Occupational Disease as the Bane of Workers' Lives: A Study of Its Incidence in Slovakia. Part 2,* In: International Journal of Environmental Research and Public Health, 2021, 18, 12990, 1–21, https://doi.org/10.3390/ijerph182412990

[5] Evich, K.O., Olegovna, S.M., *Russia Patent No. RU244337. Glove for protection hands from vibration,* 2012

[6] Gerhard, K., Joel, B., Romain, B., *France Patent No. WO2020094966. Vibration portection glove,* 2020

[7] Hughes, G., Hughes, J.C., *United States of America Patent No. US2015/0181955. Ambidextrous anti-vibration glove with impact and pinch point protection,* 2015

[8] Ok, K.J., *Korea Patent No. KR100487752. Glove for absorbing vibration, having vibration isolation structure contained within,* 2005

[9] Wei, C., *China Patent No. CN206565350. Vibration-absorbing mitten,* 2017

[10] Seghedin, N.E., Blaga, M., Ciobanu, R., *Weft knitted fabrics behaviour under dynamic testing,* In: Book of Proceedings of the 12th AUTEX World Textile Conference, 2012, ISBN 978-953-7105-44-0

[11] Blaga, M., Seghedin, N.E., Buhai, C., Chitariu, D., *Dinamic testing of the warp knitted spacer fabrics,* In: Proceedings of the 13th AUTEX World Textile Conference, 2013, ISBN 9783867803434 3867803439

[12] Blaga, M., Seghedin, N.E., *Knitted Spacer Fabrics Behaviour at Vibrations*, In: Journal of Textile Engineering & Fashion Technology, 2017, 3, 2, 602–608, https://doi.org/10.15406/jteft.2017.03.00092

[13] Liu, Y., Hu, H., *Vibration Isolation Performance of Warp-knitted Spacer Fabrics*, In: Proceeding of The Fiber Society 2011 Conference, 2011, 63–64, ISBN: 978-1-63266-644-4

[14] Liu, Y., Hu, H., *An Experimental Study of Compression Behavior of Warp-knitted Spacer Fabric*, In: Journal of Engineered Fibers and Fabrics, 2014, 9, 2, 61–69, https://doi.org/10.1177/155892501400900207

[15] Liu, Y., Hu, H., *Vibration isolation behaviour of 3D polymeric knitted spacer fabrics under harmonic vibration testing conditions*, In: Polymer Testing, 2015, 120–129, https://doi.org/10.1016/j.polymertesting.2015.09.003

[16] Sum, N.W., *Development of anti-vibration glove with weft knitted spacer fabrics,* BA Thesis, Institute of Textiles and Clothing, The Hong Kong Polytechnic University, 2013

[17] Chen, F., *A study of vibration behavior of weft-knitted spacer fabrics*, Doctoral Thesis, Institute of Textiles and Clothing, The Hong Kong Polytechnic University, 2015

[18] Chen, F., Liu, Y., Hu, H., *An experimental study on vibration isolation performance of weft-knitted spacer fabrics*, In: Textile Research Journal, 2016, 86, 20, 2225–2235, https://doi.org/10.1177/0040517515622149

[19] Yu, A., Sukigara, S., Masuda, A., *Investigation of Vibration Isolation Behaviour of Spacer Fabrics with Elastic Inlay*, In: Journal of Textile Engineering, 2020, 66, 5, 65–69. https://doi.org/10.4188/jte.66.65

[20] Palicska, K.L., Augusztinovicz, F., Szemeredy, A., Szucs, L., *Development and test of new knits of anti-vibration*, At: AUTEX2019 – 19th World Textile Conference on Textiles at the Crossroads, 2019

[21] Chainsaw Journal, *Anti-Vibration Glove Reviews – Worth Every Penny*, 2019, Available at: https://www.chainsawjournal.com/ [Accesed on September 2021]

[22] Riley, T.H., Dias, T., *The development of acoustic and vibration sensing yarns for health surveilliance*, In: Proceedings of the 25th International Congress on Sound and Vivration, 2018, 327–333

[23] Rahemtulla, Z., Riley, T.H., Dias, T., *Developing a Vibration-Sensing Yarn for Monitoring Hand-Transmitted Vibrations,* In: Proceedings, 2019, 32, 6, 1–4, https://doi.org/10.3390/proceedings2019032006

[24] Rahemtulla, Z., Riley, T.H., Dias, T., *Vibration-Sensing Electronic Yarns for the Monitoring of Hand Transmitted Vibration,* In: Sensors, 2021, 21, 8, https://doi.org/10.3390/s21082780

[25] Rades M., *Vibratii mecanice (Mechanical vibrations)*, Printech Publishing House, Bucharest, 2008

[26] Blaga, M., Harpa, R., Seghedin N.E., Marmarali, A., Ertekin, G., *Evaluation of the knitted fabrics stiffness through dynamic testing*, In: IOP Conf. Series: Materials Science and Engineering, 2018, 459, 012033, IOP Publishing, https://doi.org/10.1088/1757-899X/459/1/012033

[27] Mansfield, N.J, *Human response to vibration*, CRC Press, London, 2005

Authors:

MIRELA BLAGA[1], NECULAI EUGEN SEGHEDIN[1], CRISTINA GROSU[1,2]

[1]"Gheorghe Asachi" Technical University of Iasi,
56 D. Mangeron Street, 700050, Iasi, Romania

[2]National Research Development Institute for Textiles and Leather,
16 Lucretiu Patrascanu Street, 030508, Sector 3, Bucharest, Romania

Corresponding author:

MIRELA BLAGA
e-mail: mblaga@tex.tuiasi.ro

Textile structures for limiting the effects of maritime and fluvial disasters

ALEXANDRA GABRIELA ENE
MIHAELA JOMIR

GEORGETA POPESCU
CATALIN GROSU

ABSTRACT – REZUMAT

Textile structures for limiting the effects of maritime and fluvial disasters

Water is essential for the lives of humans, animals and plants, while representing an indispensable resource for the economy, and its management goes beyond national borders. Water pollution with oil residues affects both surface water and groundwater; its consequences on the organoleptic properties of water, aquatic fauna and flora are particularly damaging for all ecosystems and their biodiversity.

Mechanical recovery of the pollutant provides, according to the international norms, the limitation of the polluted surface and the concentration of the pollutant in order to recover and store the water-hydrocarbon mixture, with limits related to the agitation of the marine/fluvial environment and distance from the intervention base to the polluted area. The choice of blocking/storage systems must take into account several factors, such as type and amount of pollutant recovered, the flow of recovery units, area of use, hydro-weather conditions in the field, mode of transport and mode of location in terrain.

This study presents the constructive solutions for the dams made of textile materials, used in case of disasters in the maritime and fluvial area.

Post-processing of data, performed with the help of IBM multiplatform software suite, highlighted the variation intervals of the structural parameters for 7 composite materials differentiated by: location, mass, raw material, thickness and thermal resistance.

These composites were the basis for computer-aided designs of 14 experimental models (EM), differentiated by the dimensions used, the materials of the floats, the skirt and the area of use (maritime from 4bf to 10 bf or fluvial).

Keywords: *3D simulation, CAD, digitized technology, woven fabrics, design engineering, pattern*

Structuri textile pentru limitarea efectelor dezastrelor maritime și fluviale

Apa este esențială pentru viața oamenilor, a animalelor și a plantelor, reprezentând, în același timp, o resursă indispensabilă pentru economie, iar gestionarea sa depășește frontierele naționale. Poluarea apei cu reziduuri petroliere afectează atât apele de suprafață, cât și pe cele subterane, acest gen de poluare a devenit ubicuitar, iar consecințele ei asupra proprietăților organoleptice ale apei, faunei și florei acvatice sunt deosebit de nocive și durabile.

Recuperarea mecanică a poluantului prevede, conform normelor internaționale, în primul rând limitarea suprafeței poluate și concentrarea poluantului în vederea recuperării și stocării amestecului apa-hidrocarburi, desigur cu limite legate de: starea de agitație a mediului marin/fluvial și distanța de la baza de intervenție la zona poluată. Alegerea sistemelor de blocare/stocare trebuie să țină cont de mai mulți factori, cum ar fi: tipul și cantitatea de poluant recuperate, debitul unităților de recuperare, zona de utilizare, condițiile hidro-meteo din teren, modalitatea de transport și modalitatea de amplasare în teren.

Lucrarea prezintă soluțiile constructive pentru barajele realizate din materiale textile, utilizate în caz de dezastre atât în zona maritimă, cât și în cea fluvială. Postprocesarea datelor, realizată cu ajutorul multiplatformei IBM a evidențiat intervalele de variație ale parametrilor structurali pentru cele 7 variante de materiale compozite diferențiate prin: zona de amplasare, masa, materie primă, grosime și rezistența termică. Aceste materiale compzite au constituit baza proiectării CAD a 14 modele experimentale, diferențiate prin: tipo-dimesiunile utilizate, materialele textile din componența flotorilor, jupei și arealul de utilizare (maritime de la 4bf până la 10 bf sau fluvial).

Cuvinte-cheie: *simulare 3D, CAD, tehnologie digitizată, țesături, inginerie asistată, tipar*

INTRODUCTION

Water pollution with oil residues is a very important problem; it is difficult to prevent and remedy, and it affects both surface water and groundwater. Pollution of the marine environment with hydrocarbons is a worrying phenomenon, which has taken an unprecedented scale since the 1960s. The sources and causes of pollution have multiplied year by year in proportion to the emergence and proliferation of risk factors, especially between the 1970s and the 1980s. Incidents in drilling, extraction, transport, transfer operations, loading/unloading, refining, storage, etc. have generated imminent risks, given the dangerous properties of oil and petroleum products. In addition, marine oil pollution may be caused by acts of war against shore-side oil installations [1, 2]. The choice of separation and storage systems must take into account several factors, such as the type and amount of recovered pollutant, the flow of recovery units,

area of use, hydro-meteorological conditions in the field, mode of transport and mode of location/placement.

The floating element is in the form of a continuous "curtain" and consists of:
• the freeboard that follows the shape of the wave;
• the skirt that does not allow the pollutant to move in the water and is fixed under the floating element;
• auxiliary systems for fixing the floating elements to each other, maintaining the floating element and the extended skirt in a horizontal position (ballast and chaining), coupling elements.

To describe the phenomena that arise when the fluid is isolated from a floating structure that delimits a mixture (e.g., water and hydrocarbons in open space) and to be able to clearly predict the efficiency of the gravitational storage-separation system, it is necessary to take into account the theories regarding the type of wave, the shape of the seabed and the dimensions of the floating superstructure [3].

Starting from the fundamental theory of system construction, the theories of Fluid Mechanics were studied, which allowed the determination of potential equations for small-amplitude waves and the equilibrium equations for the trochoidal waves (unde multi-direction Gerstner wave with solutions for the Stokes waves).

These led to the conclusion that, for the realization of water-hydrocarbon mixture separation-storage systems, textile structures with a mass of 180 m^2 – 400 g/m^2, thicknesses of 0.2–0.5 mm and thermal resistance of 0.071 m^2K/W (for the balance heat flow in summer or in the situation when it passes from the inside to the outside, during winter) must be used [4, 5].

The structural analysis performed was based on the theories of continuous media mechanics. In other words, the textile structure was considered a continuous, impermeable environment that fills a certain area of space, so that in each of its geometric points, there is a material point of the environment. The woven textiles under analysis contain cotton, polyester (PES), polyamide (PA) and polyamide 6.6 (PA6.6) yarns, with tenacity values of min. 0.60 N/tex and max. 12.4 N/tex, loop resistance of min. 100 N, knot strength of min. 80 N.

The calculation and simulation were performed using the finite element method (FEM), establishing the values of the constituent elements for mesh and the real exploitation conditions of the marine environment (the state of agitation of the sea at 4bf, 6bf, 7bf and 10bf, which implies a wind speed of 11–55 kt (20–102 km/h), wave height from 1.5 m to 12 m and distributed pressures starting with 1500 N/m^2 and increasing up to 12000 N/m^2, respectively).

Thus, by using the solver included in the IBM multi-platform software suite for computer-aided design (CAD), computer-aided manufacturing (CAM) and computer-aided engineering (CAE), the visualization of the phenomena that take place on the composite structure (displacement under dynamic pressure,

Von Mises stress – nodal values and translational displacement vector) was possible, so the dimensions of the floating elements and of the skirts could be determined, which constitute modular experimental models of the whole directing-storage-separation of water-hydrocarbon mixtures system architecture [5, 6].

MATERIALS AND METHOD

Textile structures used for the development of the experimental models

The results obtained following the use CAD/CAM/CAE techniques allowed the design and development of composite structures for the realization of the experimental models (EM) (table 1).

Constructive solutions for the experimental models of floating elements

The constructive solutions for the floating elements, the dimensions of the patterns that will be modelled and simulated using a specialized program – Optitex Pattern Making PDS software (EFI Optitex) – from INCDTP, as well as the developing technology of the 14 experimental models, are presented below.

EM01 and EM02 - use: marine environment and fluvial area
• Float construction shape: straight circular cylinder;
• Float dimensions: bases – circles with a diameter of 300 mm, length of 900 mm;
• Float material type: C4 and C5;
• Float colour: EM01 (C4) and EM02 (C5);
• Skirt construction shape: rectangle, dimensions 900 mm × 800 mm;
• Skirt material type: C2;
• Skirt colour: EM01 (C2) and EM02 (C2);
• Float closure mode: 20 mm wide Velcro tape placed at 180° from the skirt;
• Assembly method: the joint of the circles of a straight circular cylinder with the rectangle is a French seam, finished on the outside with a 2 mm pin stitch. When joining the skirt with the floating cylinder, the grosgrain is added in order to increase the resistance of the seam.

The rectangular skirt has the sides finished by 10 mm double folding edge and the lower edge has a channel with a height of 30 mm for the insertion of the chain/ballast. On the diameter of the cylinder bases are applied on one side the Velcro - loop and on the other side the Velcro hook that allows the cylinders to be fastened, in order to be able to lock the cylinders between them and capture the oil fractions.

EM03 and EM04 - use: marine environment and fluvial area
• Float construction shape: straight circular cylinder;
• Float dimensions: bases – circular surfaces with a diameter of 600 mm, length of 1200 mm;
• Float material type: C1;
• Float colour: EM03 and EM04 (C1);
• Skirt construction shape: rectangle, dimensions 1200 mm × 1100 mm;

Table 1

COMPOSITE STRUCTURES DESIGN DATA AND CHARACTERISTICS		
Composite structure	**Design data/Identification EM**	
C1	Fibrous composition	100% cotton
	Width	140 cm
	Weave	Basket weave
	Finishing type	polyurethane (PU) film coating
	Colour	Khaki
C2	Fibrous composition	45%/55% PES/PA
	Width	150 cm
	Weave	Rep weave
	Finishing type	PU impregnation
	Colour	Orange
C3	Fibrous composition	45%/55% PA6.6/PES
	Width	150 cm
	Weave	Rep weave
	Finishing type	PU impregnation
	Colour	Purple
C4	Fibrous composition	100% PA6.6
	Width	150 cm
	Weave	Plain weave
	Finishing type	PU film coating
	Colour	White
C5	Fibrous composition	100% PES
	Width	150 cm
	Weave	Plain weave
	Finishing type	PU film coating
	Colour	Green
C6	Fibrous composition	100% PES
	Width	140 cm
	Weave	Basket weave
	Finishing type	PU film coating
	Colour	Grey
C7	Fibrous composition	100%PES
	Width	150 cm
	Weave	Rep weave
	Finishing type	PU film coating
	Colour	Turquoise

- Skirt material type: C1 and C2;
- Skirt colour: EM03 (C2) and EM04 (C1);
- Float closure mode: 20 mm wide Velcro tape placed at 180° from the skirt;
- Assembly method: the joint of the circles of a straight circular cylinder with the rectangle is a French seam, finished on the outside with a 2 mm pin stitch. When joining the skirt with the floating cylinder, the grosgrain is added in order to increase the resistance of the seam. The rectangular skirt has the sides finished by 10 mm double folding and the lower edge has a channel with a height of 30 mm for the insertion of the chain/ballast. On the diameter of the cylinder bases are applied on one side the Velcro - loop and on the other side the Velcro hook that allows the cylinders to be fastened, in order to be able to lock the cylinders between them and capture the oil fractions.

EM05 and EM06 - use: marine environment and fluvial area
- Float construction shape: straight circular cylinder;
- Float dimensions: bases – circular surfaces with a diameter of 300 mm, length of 900 mm;
- Float material type: C3 and C6;
- Float colour: EM05 (C3) and EM06 (C6);
- Skirt construction shape: rectangle, dimensions 900 mm × 800 mm;
- Skirt material type: C3;

- Skirt colour: EM05, EM06 (C3);
- Assembly method: the joint of the circles of a straight circular cylinder with the rectangle is a French seam, finished on the outside with a 2 mm pin stitch. When joining the skirt with the floating cylinder, the grosgrain is added in order to increase the resistance of the seam. The rectangular skirt has the sides finished by 10 mm double folding edge and the lower edge has a channel with a height of 30 mm for the insertion of the chain/ballast. On the diameter of the cylinder, bases are applied 250 mm wide grosgrain tapes that allow the cylinders to be fastened, in order to be able to lock the cylinders between them and capture the oil fractions.

EM07 and EM08 - use: marine environment and fluvial area
- Float construction shape: straight circular cylinder;
- Float dimensions: bases – circular surfaces with a diameter of 600 mm, length of 1200 mm;
- Float material type: C1 and C5;
- Float colour: EM07 (C1) and EM08 (C5);
- Skirt construction shape: rectangle, dimensions 1200 mm × 1100 mm;
- Skirt material type: C2 and C1;
- Skirt colour: EM07 (C2) and EM08 (C1);
- Assembly method: the joint of the cylinder (skirt with float) is made through a French seam and on the outside the fixing seam at a 2 mm distance from the edge. When joining the skirt with the float, the grosgrain was added in order to increase the resistance of the seam. The skirt has the sides finished by a double folding of the edge and fixing by sewing, and the lower edge has a channel with a height of 30 mm for the insertion of the chain/ballast. On the diameter of the cylinder, bases are applied 250 mm wide grosgrain tapes that allow the cylinders to be fastened, in order to be able to lock the cylinders between them and capture the oil fraction.

EM09, EM10 and EM11 - use: marine and fluvial harbours
- Float construction shape: frustum
- Float dimensions: large base with a diameter of 530 mm, small base with a diameter of 100 mm;
- Float material type: C3, C4 and C7;
- Float colour: EM09 (C3), EM10 (C7) and EM11 (C4);
- Skirt construction shape: rectangle, placed on the diameter of the large base, dimensions of 530 mm × 510 mm;
- Skirt material type: C3, C4 and C7;
- Skirt colour: EM09 (C3), EM10 (C7) and EM11 (C4);
- Assembly method: the large base of the circle of the frustum cone is assembled through a French seam followed on the outside by a 2 mm pin stitch. The small base of the frustum consists of 2 overlapped circles, stitched together, and on the diameter of the small circle was applied 50/60 mm grosgrain tape. To cover and reinforce the edge of the small circle of the frustum 25 mm einfas tape /grosgrain tape was added. A loop of 100 mm folded length grosgrain tape with the 20 mm width was added over the wide grosgrain tape. Through this loop, a cable tape will be inserted to hold the frustums between them in order to achieve the system of blocking and capturing the oil fractions. On the side of the cone trunk, a waterproof zipper with a length of 360 mm was stitched.

EM12, EM13 and EM14 - use: marine environment and fluvial area
- Constructive shape of the float: straight circular cylinder;
- Float 1 dimension: bases – circular surfaces with a diameter of 300 mm, length of 1200 mm;
- Float 1 material type: C2 and C3;
- Float 1 colour: EM12 (C3), EM13 (C3) and EM14 (C2);
- Float 2 and 3 dimensions – submerged elements: bases – circular surfaces with a diameter of 300 mm, length of 1200 mm;
- Float 2 and 3 material type: C2, C4 and C3;
- Float 2 and 3 colours: EM12 (C2), EM13 (C4) and EM14 (C3);
- Constructive skirt shape: rectangle, dimensions of 1000 mm × 1200 mm;
- Skirt material type: C1, C6
- Skirt colour: EM12 (C6), EM (C6) and EM14 (C1);
- Assembly method: the 20 mm wide grosgrain tape was applied along the cylinder length of the submerged elements, and the submerged elements were stitched together to reinforce the stitching.
2 overlapping tapes of 300 mm length each (grosgrain) were applied on the film-coated side of the float and on the film-coated side of the submerged elements. 20 mm length of each end of the grosgrain tape is reinforced. To increase the resistance of the seams, 20 mm of reinforcing grosgrain tape is applied on the inside of the float and on the submerged elements. When joining each skirt with each float, the 20 mm wide grosgrain tape was added in order to increase the resistance of the seam. The skirt has the sides finished by a double folding edge and the lower edge has a channel with a height of 30 mm for the insertion of the chain/ballast. On the diameter of the floating cylinder, the grosgrain tapes were added, which allow the cylinders to be attached to each other to achieve the system of blocking and capturing oil fractions. 1070 mm length waterproof zippers were applied on each base of the cylinder.

RESULTS

CAD design of the experimental models

Using the modules included in the program, the changes made to the patterns were transferred to the virtual model. In addition, using Optitex 3D, the following data was obtained:
- the visualization in the virtual 3D mode of the experimental models created as 2D patterns;
- the analysis of how the changes made on 3D models affect 2D patterns;

Fig. 1. Workflow for transforming into 3D samples of EM01–EM014

• the direct transition from concept to virtual 3D model with all aspects related to the fully defined product (material properties and their behaviour) [7].

The workflow for taking over 2D models and transforming them into 3D samples is shown in figure 1.

Design stages EM01–EM14

I. Construction of the 2D pattern, with the help of the integrated PDS software (figures 2 and 3).

II. Establishing the positions of the parts in the virtual plan, of assembly lines and placement of accessories (zippers, Velcro, carbines, ballast), assembly and placement lines, assigning materials and colours. The obtained elements for all 14 experimental models are shown in figure 4.

III. 3D simulation, verification and correction of possible nonconformities and visualization of the experimental models (through two windows simultaneously: PDS and 3D) (figures 5 and 6).

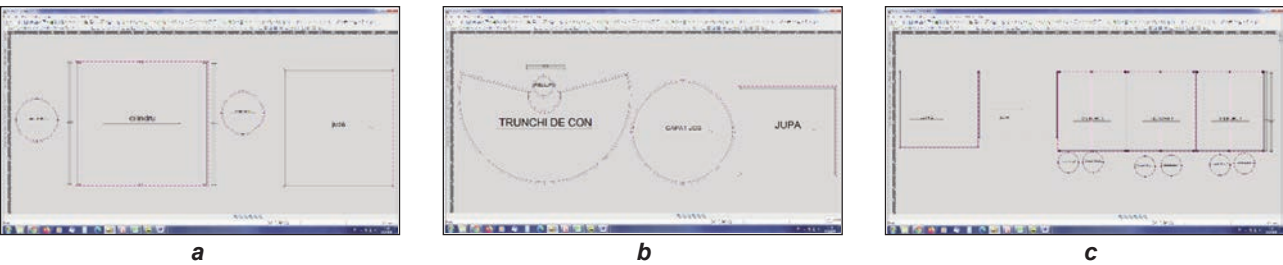

a   b   c

Fig. 2. Design of the patterns for: a – EM01–EM08; b – EM09–EM11; c – EM12–EM14
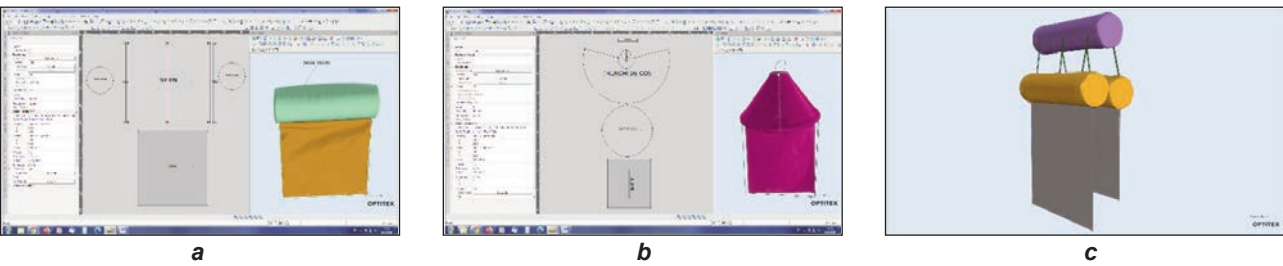

a   b   c

Fig. 3. Insertion of the determining parameters values of the materials for:
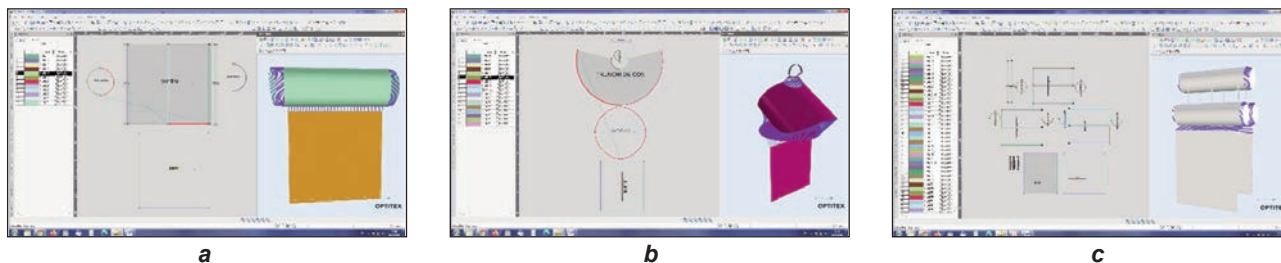a – EM01–EM08; b – EM09–EM11; c – EM12–EM14

Fig. 4. Establishing the assembly seams between the parts of the experimental models:
a – EM01–EM08; *b* – EM09–EM11; *c* – EM12–EM14
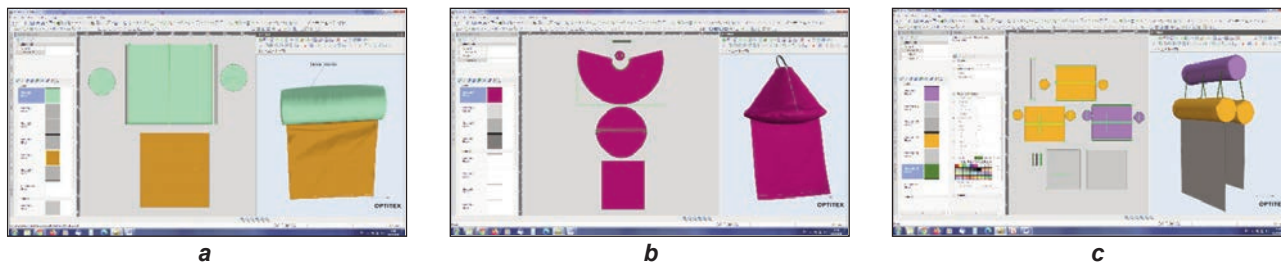
Fig. 5. 2D print and 3D virtual model of the experimental models: *a* – EM01–EM08; *b* – EM09–EM11; *c* – EM12–EM14
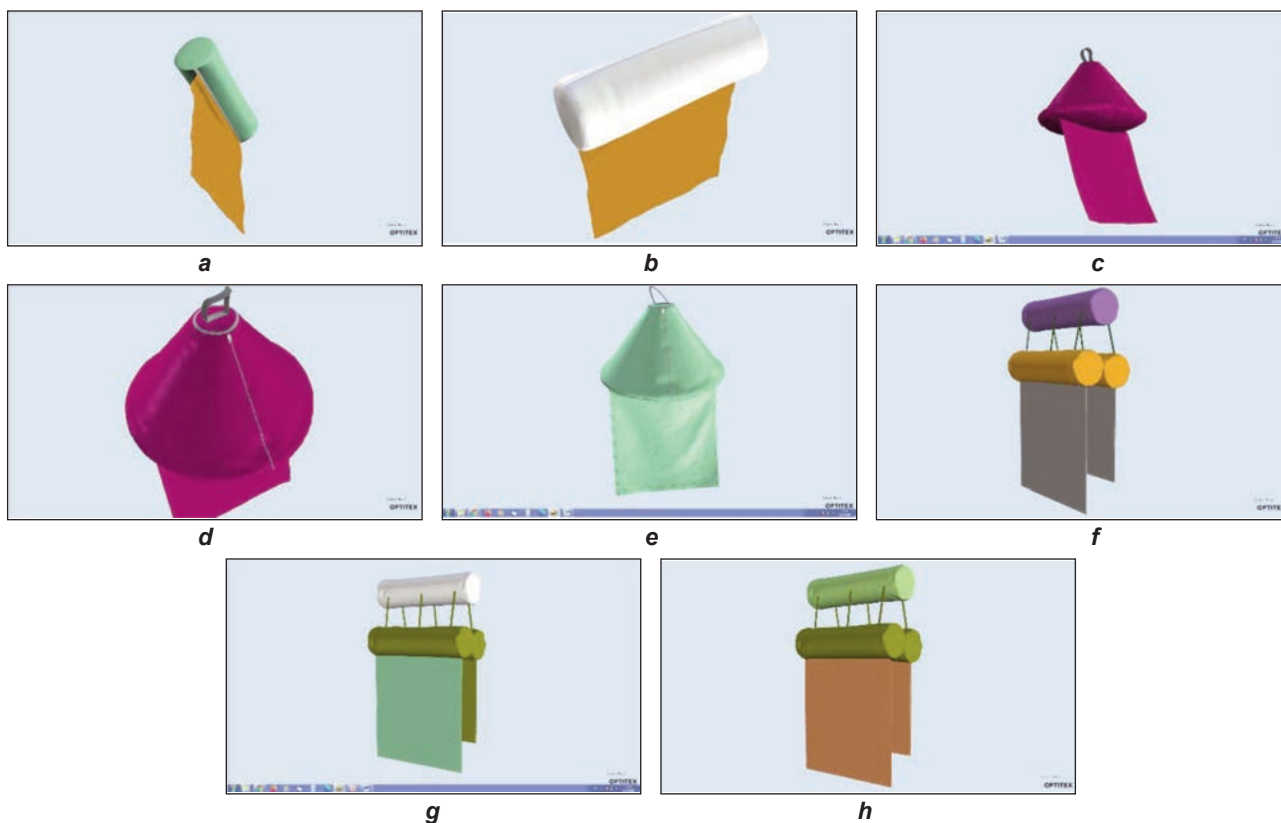
Fig. 6. 3D simulation for: *a* and *b* – EM01–EM08; *c, d* and *e* – EM09–EM11; *f, g* and *h* – EM12–EM14

The 14 experimental models were made in the sampling room from Design and Anthropometry Department within INCDTP, using as technological equipment the simple sewing machine, seam 301, the joining of the elements being made with 20 mm grosgrain or, depending on each case, Velcro or zipper. For the structure fastening of EM09 – EM11, a special sea waterproof zipper was used.

CONCLUSIONS

The 14 experimental models that have been designed vary depending on size, material and pattern in order to meet the requirements of the marine and fluvial environment. The EMs meet several requirements imposed by the exploitation in real conditions of use, such as the concentration on a strictly delimited area of oil residues, distance from the

intervention base to the polluted area, the state of agitation of the marine environment.

The use of CAD/CAM/CAE techniques allowed the design and development of 7 composite structures identified as C1–C7, which were used to make the experimental models EM01–EM14.

The combination of woven fabrics for different dimensions of floating elements and skirts was made in order to verify the dimensional stability of the composite material, resistance to solar radiation, resistance to large temperature variations and resistance to sea agitation (4bf–10bf).

The CAD design made using the Optitex software allowed the visualization of the patterns created for each experimental model. All 14 experimental models were assembled within the pilot station of INCDTP, using the provided equipment. The developed experimental models will be tested at the berth in the Port of Constanta, Romania and at the embankment in the Port of Galati, Romania.

ACKNOWLEDGEMENTS

REFERENCES

[1] Basco, D., *Pneumatic barriers for oil containment under wind, wave, and current conditions,* In: International Oil Spill Conference Proceedings, 1971, 1, 381–391, https://doi.org/10.7901/2169-3358-1971-1-381

[2] Popescu, D.M., Nistoran, D.E, *Poluarea apelor de suprafata cu lichide petroliere,* Ed. Printech Bucuresti, 2010

[3] Popescu, D.M., *Studiul evolutiei interfatei a doua fluide imiscibile vascoase cu aplicatie la poluarea cu petrol produsa pe curgerile cu suprafata libera*, Universitatea Politehnica Bucuresti, 2008, 145–154

[4] Hendrickx, R., *Maritime Oil Pollution: an Empirical Analysis*, Shifts in Compensation for Environmental Damage, Springer, Part of the Tort and Insurance Law book series (TIL, volume 21), 2007, 243–260, Available at: https://link.springer.com/chapter/10.1007/978-3-211-71552-9_7 [Accessed on May 2021]

[5] Akyuz, E., Ilbahar, E., Cebi, S., Celik, M., *Maritime Environmental Disaster Management Using Intelligent Techniques,* Intelligence Systems in Environmental Management: Theory and Applications, Part of the Intelligent Systems, Reference Library book series (ISRL, volume 113), 2017, 135–155

[6] *Erosion Pollution*, Available at: https://www.erosionpollution.com /oil_booms.html [Accessed on May 2021]

[7] *Optitex software guide*, Available at: https://help.optitex.com [Accessed on May 2021]

Authors:

ALEXANDRA GABRIELA ENE, MIHAELA JOMIR, GEORGETA POPESCU, CATALIN GROSU

National Research Development Institute for Textiles and Leather,
16 Lucretiu Patrascanu, 030508, Bucharest, Romania

Corresponding author:

MIHAELA JOMIR
e-mail: mihaela.jomir@incdtp.ro

Indigenous intelligent materials for the textile field

SABINA OLARU   MARIANA BEZDADEA

ABSTRACT – REZUMAT

Indigenous intelligent materials for the textile field

The present work reflects an area of cutting-edge research, bioengineering and industrial microbiology, emphasising the new physiognomy of macromolecular chemistry, supramolecular chemistry. Membranes are advanced materials whose specificity manifests itself in order, organisation, structural stability, and functional stability, explaining their own character of separation and selectivity.

A hypothesis finds applications in a variety of fields. The more numerous and diverse these fields are, the higher the probability that this hypothesis applies.

The aim of the paper is to present applications of polyurethane membranes in the textile industry by integrating them into garment structure and also in wastewater purification. The proposed membrane technology is innovative and will be of fundamental economic importance in the coming years.

Keywords: membranes, textile, advanced materials, wastewater

Materiale indigene inteligente pentru domeniul textil

Materialul prezentei lucrări reflectă un domeniu de cercetare de vârf, bioingineria, microbiologia industrială, subliniind noua fizionomie a chimiei macromoleculare, chimia supramoleculară. Membranele sunt materiale avansate care prezintă specificitatea manifestată prin: ordine, organizare, stabilitate strucurală, stabilitate funcțională, explicând caracterul lor propriu de separare și selectivitate.

O ipoteză își găsește aplicații în cele mai diferite domenii. Cu cât aceste domenii sunt mai multe și mai variate, cu atât probabilitatea valabilității ipotezei respective este mai mare.

Scopul lucrării este acela de a prezenta aplicațiile membranelor poliuretanice în industria textilă, prin includerea lor în structura vestimentară, dar și în purificarea apei uzate. Tehnologia membranară propusă este una inovatoare și constituie o miză economică reală în anii viitori.

Cuvinte-cheie: membrane, textile, materiale avansate, apă reziduală

INTRODUCTION

Chemical science is based on the biological world by an axiom of existence: the simple fact that biological systems exhibit the fantastic complexity of structures and functions that the molecular universe can provide. Molecular recognition, self-assembly, and information transfer play an important role in the formation of artificial systems that mimic the behaviour of life.

Supramolecular chemistry is the "chemistry beyond the molecule" that produces more complex entities that arise from the combination of chemical species bound by intermolecular forces. Supramolecules (membranes) are characterised by the spatial arrangement of their compounds through the architecture of the superstructure and the nature of the intermolecular bonds that compose them.

In this way, advanced materials can be obtained that are endowed with properties reminiscent of the five senses [1]: specificity (mind), selectivity (understanding), stability (opinion), order (imagination), and organisation (feeling).

Supramolecular compounds can form membranes that provide the ability to separate healthy cells from microbes and viruses, allow transport and separation processes and are of particular importance in various fields: technology, chemistry, physics, biology, medicine, geochemistry, hydrology, agronomy, ecology, nutrition, etc. [2–4].

INDIGENOUS POLYMERIC MEMBRANES

The term membrane is a Latin word meaning coating, shell or sheet. In 1890, Pfeffer mentioned the cell surrounded by the membrane (cell membrane coating), but also the behaviour of the membrane as a universal barrier [1]. Thus, according to a rather simple definition cited by Spriggs, the membrane is a device in the form of a usually thin film that acts as a physical barrier between two fluids and allows some degree of permeability between them. The definition is incomplete and needs to be extended by specifying the factors that affect the behaviour of the membrane [1].

Mariana Bezdadea [5, 6] considers that membranes are gel-like synergistic colloidal systems with a specific supramolecular architecture, i.e., an associative and steric arrangement of hydrophilic and hydrophobic micro and macro phases that perform the same
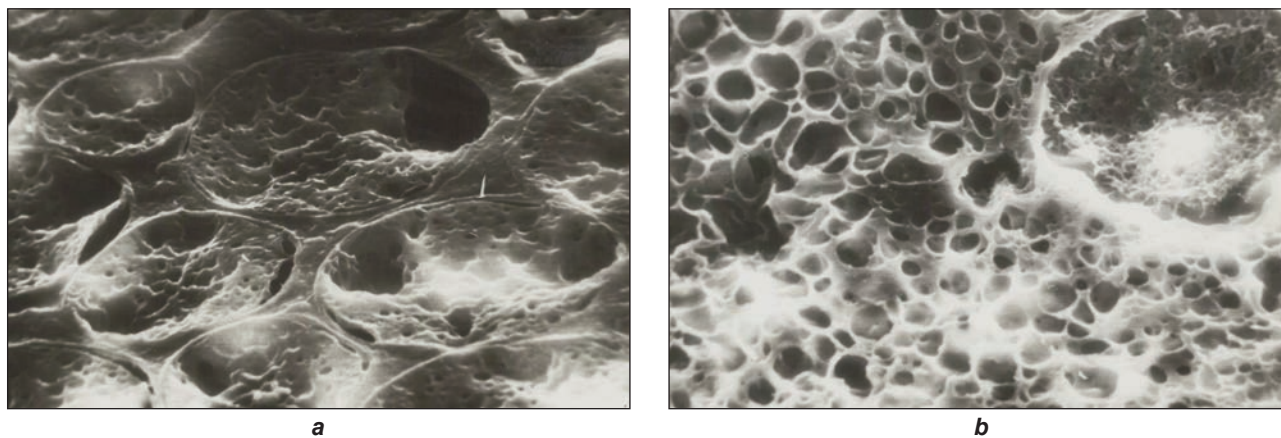
Fig. 1. Scanning electron microscopic images for polyurethane (PU) UF-MF membrane (×3000):
a – glossy side; *b* – the matte side [1]

function and consist of hexagonal helical shapes compatible with spherical or cylindrical structures, which explains the presence of the pore system. In addition, membranes are mimetic systems that artificially or synthetically reproduce the properties and functions of a biological system, combining order with action (imperative of biological systems) [2–4, 7–9].

A chronology of important information in the study of supramolecular chemistry is: in 1982, Mariana Bezdadea with the doctoral thesis "Matrix polymerisation" [3], in 1987 the Nobel Prize of J.M. Lehn, in the same year 1987 independently of J.M. Lehn, Mariana Bezdadea interferes with the book "Matrix polymerisation (template) - biotechnology" [2]. In the following years [10–13], J.M. Lehn and co-workers pointed out that reactivity and catalysis are the fundamental features of the functionality of supramolecular systems, as molecular receptors carrying suitable groups that can complex the substrate under conditions of stability, selectivity and speed [14, 15]. In 2013 [16], J.M. Lehn pointed out the importance of adaptation through order, organisation, and reinforcement of self-assembly of components accessing functions such as training, knowledge, and learning during dynamic transformations and changes. Mariana Bezdadea noted the same adaptation through order, organisation, and self-organisation of components in the fabrication of membranes made of polyvinyl acetate (PVAc), polyurethane (PU), and polystyrene (PS) [1–9].

The "guest" molecules: vinyl acetate monomer or another polymer (PU), are activated on the one hand by the donor function exerted by the electron pair of the oxygen of the OH groups of the polysaccharide "host", an "electron pressure" and on the other hand by an "electron depression" due to the established hydrogen bonds. The "host" or molecular sieve, matrix, or template is both a donor and an acceptor. Thus, the "attraction/repulsion" mechanism of bifunctional catalysis exerted by the molecular sieves studied provides for the action of OH groups on one side and hydrogen bonds on the other [1–3].

In the mechanism of formation of asymmetric polyurethane (PU) membranes, the cellulose matrix serves as an orientation surface and produces an "induced adaptation", and the "lock and key" theory here is reminiscent of the model of enzymatic catalysis.

The polyurethane (PU) ultrafiltration membrane shows larger ellipsoidal or spherical macro phases on the glossy side (figure 1).

The structural-functional asymmetry of cross-linked or non-crosslinked polyurethane membranes reflects their rectifying property, which brings them closer to biological membranes. The rectification phenomenon is based on an asymmetry of the existing structure and energy barriers on the two sides of the membranes [1].

APPLICATIONS OF INDIGENOUS MEMBRANES IN INDUSTRIAL PRACTICE

In general, one can imagine a pyramid of membrane applications. At the top is a small amount of valuable, separate, purified products, while at the base of the pyramid are recovered substances with a low price and very high demand. Not surprisingly, most biotechnology activities are located at the top of the pyramid. The closer we get to the top of the pyramid, the more stringent the purity requirements become. This purity is the key cost factor. For example, up to 80% of the cost of obtaining therapeutic proteins is attributable to the extraction and purification processes (figure 2).
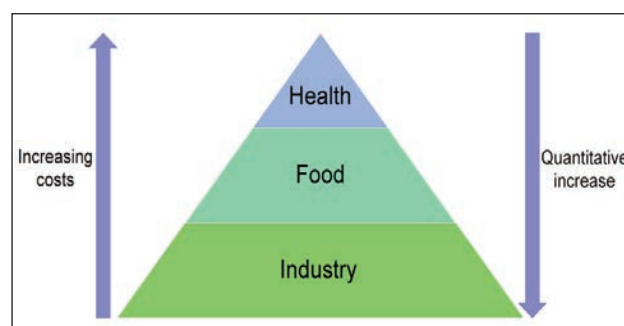

Fig. 2. Overview of membrane applications [1]

Process with indigenous polyurethane membrane in the advanced textile field

Smart textiles are used in a wide range of fields: protective equipment, sportswear, special clothing – recommended for medical treatments, such as bandages in the field of blood circulation, protection – for unstable climatic conditions or clothing that responds to temperature variations of the human body, protective equipment for places with poor visibility and/or firefighters. Advanced textiles show a special behaviour, modifying their properties under the action of an external factor [17, 18]. Materials with special properties can also be produced using membranes.

Information technology, biotechnology and nanotechnology are some of the development directions that influence the production of smart or advanced textiles, materials that can respond to specific stimuli.

In this context, both the physicochemical properties and the sanogenetic physiological indicators of a series of indigenous polyurethane membranes (PU) were studied in comparison with an imported membrane (polyamide) and a textile fabric (polyester). Studies on the flexibility and elasticity of indigenous polyurethane membranes indicate the need to use them in a suitable composite material [1].

The following materials were used: indigenous polyurethane membranes (PU) I3 and I4 non-cross-linked and I8 cross-linked [6, 19], Pall polyamide membrane (import/produced by Pall Corporation, USA) and polyester fabric.

The methods of material analysis were as follows:
* *Morphological structure* of the membranes was observed with a Tesla B.S. 300 electron microscope.
* *Porosity* (ε,%) is the fraction of the volume of the membrane not occupied by the polymer, calculated according to the following formula:

$$\varepsilon = n\pi r^2 \qquad (1)$$

where *n* is the number of pores per cm^2 and *r* is the radius of the pore.
* *Pore size* (*r*, μm) of the membranes used was determined by the Bubble Point method.
* *Permeability for distilled water* (*P*, m/h) was determined on a vacuum ultrafiltration and microfiltration laboratory apparatus (UF-MF), with a front module (homemade device).
* *Vapour permeability* (μ, g/m$^2 \cdot$h) was measured by determining the mass loss by evaporation of the liquid (distilled water) using a Herfeld beaker according to GB/T 12704-91.
* *Air permeability* ($P_{a\Delta p}$, m^3/min$\cdot$m^2) is defined by the volume of air transmitted per unit time and per unit area of the material and was measured with a measuring system FX 3350 – Dynamic Air Permeability Tester, according to ASTM method D737-75.
* *Thermal conductivity* (λ, kcal/m$\cdot$h$\cdot$°C) was determined by measuring the heat flux that flows through the product when placed in a temperature gradient, using a Shirley Tog Metre system.
* *Hydrophilicity* (%) was determined by determining the rate of capillary rise on samples sized following STAS 6146-87.

* *Hygroscopicity* (%) is the property of absorbing or releasing moisture in the form of vapours; it determines the sorption/desorption process, determined according to STAS 12749-89.
* *Flexibility* of the membranes used in comparison with a textile material was expressed in relative units, *H*% of the reference value, and determined on a Flexometer type FF 20 – Metrimpex, on samples, dimensioned according to STAS 8392-80; the flexibility *H* was defined by the ratio between the area under the variation diagram of the bending angle when increasing the free end of the sample by 10 mm and the area corresponding to the maximum flexibility (standard – absolutely flexible):

$$H = A/A_{abs} \cdot 100 \ \% \qquad (2)$$

* *Total germ content* was determined by the membrane method, according to STAS 3001-91.

Regardless of the destination, the structure of the garment must allow continuous or near-continuous air exchange, even when special treatments are applied. The ability to absorb and retain moisture depends on hydrophilicity and hygroscopicity, which in turn depend on the capillary system and porosity (number of pores – places not occupied by the polymer), pore size and their distribution. The ability to absorb and release water vapour to the atmosphere (hygroscopicity) depends on the affinity for water molecules of the functional groups in the OH<COOH<NH$_2$<OCONH polymer chain. The convective permeability (under the influence of an external force) to distilled water for the ensemble membrane/textile material is influenced and directed by the type of membrane structure.

Table 1 shows that the porosity of the membrane mainly influences the permeability to distilled water. Thus, the lowest permeability values are registered for polyurethane membranes I4 and Pall membrane 0.062 m/h and 0.88 m/h, respectively. In these membranes, where the pore size is minimal 0.91 μm and 0.78 μm respectively, the porosities are comparable, 44% and 49.05%, respectively, while in polyurethane membranes I3 and I8, with comparable and larger average pore size 4.17 μm and 3.24 μm, respectively different values of permeability for distilled water are recorded 6.05 m/h and 1.57 m/h, respectively.

The membrane/textile material ensemble shows changes in distilled water permeability values, compared to the textile material permeability, of 6.57 m/h. The lowest value, namely 0.06 m/h, was observed for the ensemble membrane I4 (PU)/textile material.

In general, there is a decrease in distilled water permeability values, from 6.57 m/h for the textile material to 0.06 m/h for the membrane I4/textile material ensemble, 0.42 m/h for the membrane I8/textile material ensemble, 0.24 m/h for the Pall membrane/textile material ensemble, and an increase to 7.89 m/h for the membrane I3/textile material ensemble. These differences confirm the importance of the link between the structural properties of the membrane and its final application.

Membrane/ material	Porosity ε (%)	Pore size r (μm)	Number of pores on cm^2 n (pores/cm^2)	Permeability to distilled water P (m/h)	Permeability to distilled water of ensemble membrane/textile material P* (m/h)
			PHYSICO-CHEMICAL CHARACTERISTICS OF POLYURETHANE MEMBRANES I3, I4, I8, PALL MEMBRANE AND POLYESTER TEXTILE MATERIAL		
I3	70.38	4.17	1.28	6.05	7.89
I4	44.00	0.91	16.92	0.062	0.06
I8	65.27	3.24	1.98	1.57	0.42
Pall	49.05	0.78	25.67	0.88	0.24
Textile material	74.56	14.60	0.11	6.57	-

Note: P* represents the permeability to distilled water of membranes and textile material.

SANOGENETIC PHYSIOLOGICAL INDICATORS OF POLYURETHANE MEMBRANES, COMPARED TO PALL MEMBRANE AND A TEXTILE MATERIAL (POLYESTER)

Membrane/ material	Vapour permeability μ (g/m^2·h)	Air permeability $P_{a\Delta p}$ (m^3/min·m^2)	Thermal conductivity λ (kcal/m·h·ºC)	Hydrophilicity h (cm/sec.)	Hygroscopicity (%)	Flexibility H (%)		
						L	T	D
I3	17.68	0.125	0.0104	0.28	2.3	5.05	15.38	14.22
I4	7.77	0.070	0.0060	0.17	0.6	60.00	61.40	62.20
I8	13.23	0.075	0.0065	0.14	2.9	32.30	29.40	29.70
Pall	14.71	0.05	0.0113	0.12	0.9	15.33	24.38	2.66
Textile material	21.7	50	0.0095	0.02	16.2	9.33	38.10	24.70
Standard quality limits	1–50	0.166	0.01–0.05	0.2 at ½ h for cotton	8 for cotton 14 for wool 0.4 for polyester	-	-	-

Table 2 shows the sanogenetic physiological indicators air permeability $P_{a\Delta p}$, vapour permeability μ, thermal conductivity λ and hydrophilicity h for the studied polyurethane membranes and for the Pall membrane, in comparison with textile material.

Table 2 shows that all membranes are hydrophilic (the reference value is 0.2 cm/sec). It is also clear from the values of thermal conductivity λ between 0.006 kcal/m·h·ºC and 0.01 kcal/m·h·ºC that the membranes fall into the group of thermal insulation materials. All membranes have very low values for air permeability.

This property is specific to waterproof materials (wind or raincoats), for which the quality limit is 0.166 m^3/min·m^2. In addition, the membranes are vapour permeable, provided they are airtight (the quality limits vary widely, between 0 and 50 g/m^2·h).

The I4 polyurethane membrane has a vapour permeability of 7.77 g/m^2·h, which is close to that of a waterproof material that is considered control and for which the following properties have been determined:
• thermal conductivity, λ = 0.0148 kcal/m·h·ºC;
• vapour permeability, μ = 7.18 g/m^2·h;
• air permeability, $P_{a\Delta p}$ = 0.166 m^3/min·m^2.

Flexibility determinations indicate structural uniformity and a low degree of cross-linking, affecting advanced materials' physiological, functional, and technical properties. Membrane I4 with the lowest degree of cross-linking has the highest flexibility value of 60%, but also structural uniformity in the three directions longitudinal (L), transverse (T), diagonal (D), the values for H,% are very close. Membrane I8 is less flexible (H, 30%), but has a uniform structure.

The ability of the textiles to absorb moisture from the body, combined with their thermal insulation capacity and air permeability, should create a feeling of comfort in an adverse environment. In fact, the feeling of comfort results from the balance between the energy generated and the exchange with the environment; this is done by the garment which is a component of the environment, an addition of protection. The values from table 2 show that the studied membranes could be extended to create composite garment structures (textile and membrane) intended for disposable clothing for medical personnel.

All membranes are hygroscopic within the specific limits of polyester and cotton in combination with synthetic or man-made fibres.

Vapour permeability is characteristic of an effortless state (up to 20 g/m^2·h) for polyester fabrics [20]. Low air permeability values do not affect product quality since vapour permeability, hydrophilicity, hygroscopicity, and thermal insulation are within normal limits.

Polyurethane membrane I4, which has the smallest pore radius (0.91 µm), the lowest porosity (44%), the largest number of pores per cm^2 (16.92/cm^2), and the lowest permeability to distilled water (0.062 m/h) compared to the other two polyurethane membranes, can be used by unconventional methods high-frequency current welding, ultrasonic welding, laser welding and can be extended to produce specific composite materials.

Polyurethane membranes belong to the group of heat-insulating materials and the group of waterproof materials; they can ensure the expansion of their use for special clothing products. For the disposable clothing of medical personnel, it was necessary to test the disinfecting properties of PU and Pall membranes.

Table 3 shows the results obtained according to STAS 3001-91, Membrane Method. It can be observed that the total number of germs/ml of permeate decreases drastically for membranes I3 and I4, which can be used as components of some clothing structures, disposables for doctors since they have disinfecting properties. The indigenous polyurethane membranes I3 and I4 show a considerable reduction in the total number of germs/ml in ultrafiltrated water, from 5 germs/ml in drinking water to 1 germ/ml in ultrafiltrated solution. Polyurethane membrane I8 did not show the same spectacular decrease, and Pall membrane recorded 0 total germs/ml in the ultrafiltrate. The use of polyurethane membrane I4 for disposable medical clothing is currently under investigation.

Table 3

DISINFECTANT CHARACTERISTICS OF POLYURETHANE AND PALL MEMBRANES FOR ULTRA- AND MICRO-FILTRATION

Membrane	Total number of germ/ml; 37°C initially	Total number of germ/ml; 37°C from permeate
I3	5	1
I4	5	1
I8	5	4
Pall	5	0

Membrane I3 exhibits some asymmetry (different morphological structure on both sides, different pore openings, negative charge mainly on one side and positive on the other) [19]. The positive charge generated on the skin surface attracts the negative charge of the active membrane side, and the posterior side of the membrane carries the positive charge, resulting in mutual cancellation of charges.

Membrane I4 is the most uniform and flexible. The flexibility in the three directions L, T, D is very close with values around 60%, in contrast to I3 and Pall membranes and the textile material. It can be concluded that the polyurethane membrane I4 has the following characteristics:
• is more flexible;

• is structurally uniform;
• has a fine membrane structure;
• has a higher ratio between soft and hard than the other native membranes;
• has physiological, functional and technical properties close to those of a modern textile material.

Process using indigenous polyurethane membrane for the unconventional treatment of wastewater from the textile industry

For environmental and economic reasons, wastewater is one of the significant environmental issues [21–23]. It is estimated that industry consumes nearly 20% of the world's available freshwater, and the textile industry consumes 4% of all freshwater extraction globally [24]. We could estimate that 2/3 of the dye mass used in a textile company ends up in a wastewater treatment plant or a river [1].

Wastewater and improperly treated water are discharged into rivers, contributing to excessive pollution. Textile processes thus pollute the environment by consuming large amounts of water and discharging residues into nature that can pollute the air, the water, and the soil. For example, processing one kilogram of textile material requires 100 litres of water, 15–20 kw/h of energy, and 5 kg of oxygen, which are used to generate thermal energy. The following wastes are generated: 60–70 g of sludge, 30–40 g of textile waste, 7 kg of CO_2, 400 g of slag (combustion of coal).

In textile cleaning, there are few cost-effective experiences so far. An interesting project would be the one that would allow the coupling: biological treatment - membrane separation (figure 3).

A technological process for wastewater quality correction using polyurethane membranes was studied [25, 26]. Four indigenous polyurethane membranes and one Pall membrane were used, and three types of membrane transport and three different membrane structures were recorded. The membrane techniques used were ultrafiltration and microfiltration (UF-MF).

The indigenous polyurethane membranes A, S1A, S2A, S3A and the Pall membrane were experimentally characterised by: porosity (%), degree of swelling for distilled water (g/g), density ρ (g/cm^3), by the pycnometer method, permeability for distilled water P (m/h), the pore size of the membrane, by the Bubble Point method (table 4) [26].
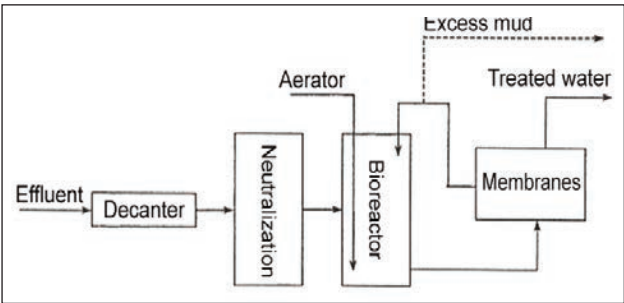

Fig. 3. Coupling scheme: biological-membrane separation [23]

Membrane	Pore diameter φ (µm)	Density ρ (g/cm^3)	Thickness $\delta m \cdot 10^6$ (m)	Porosity ε (%)	Degree of swelling (g/g)	Permeability to distilled water P^* (m/h)
			CHARACTERISATION OF THE USED MEMBRANES			
A	3.36	7.7	85	65.6	1.90	11.23
S1A	1.85	4.8	22.5	63	1.69	0.31
S2A	1.56	1.98	61.61	58.14	1.38	0.70
S3A	5.09	8.5	12.26	63	1.72	2.20
Pall	0.5	1.78	43.96	77.4	3.44	1.88

Note: *Permeability to distilled water, at UF-MF at 20°C, in vacuum 40–60 mm Hg.

Membrane/ substance	Organic substances (SO) (mg KmnO$_4$/l)	Total hardness D_T (°G)	Permeability $P \cdot 10^2$ (m/h)	Diffusion coefficient $D \cdot 10^6$ (m^2/h)	Performance (m^3/h)
		EXPERIMENTAL DATA WITH UF-MF OF WASTEWATER*			
A	37.92	7.61	1.06	0.90	29.95
S1A	47.00	7.39	0.37	0.08	10.45
S2A	28.44	8.28	0.88	0.54	24.90
S3A	50.56	9.40	0.55	0.06	15.54
Pall	12.64	9.98	1.26	0.55	35.60
Cationic resin	55.36	8.96	-	-	-
Anionic resin	52.18	8.40	-	-	-
Wastewater	37.97	24.08	-	-	-

Note: * Working conditions 20°C, vacuum 40–60 mm Hg, membrane surface 0.0030 m^2; Perfomance=permeability coeficient ·surface, in m^3/h.

The wastewater's ultra- and microfiltration were performed with a front filtration module in a laboratory unit. To improve the degree of demineralisation, UF-MF was repeated.

Organic matter (mg KMnO$_4$/l) was determined according to STAS 7587-96, and total hardness was expressed in German degrees (°G). Scanning microscopic images were obtained using a Tesla B.S. 300 electron microscope.

Membrane A was found to have a performance close to that of the Pall membrane: 29.95 m^3/h and 35.6 m^3/h, respectively (table 5).

Organic matter is best retained by the Pall membrane. With repeated UF-MF and 10 times larger active surface area (on industrial module), membrane A and membrane S2A show a drastic percentage decrease for organic matter and total hardness (table 6). Less significant differences occur for membranes S1A and S3A.

Membrane S2A has the lowest density of 1.98 g/cm^3 and has a loose structure explained by the removal of macromolecular chains after cross-linking.

The different behaviour of the indigenous membranes, A and SA, shows a higher degree of cross-linking than those of the SA series. Scanning electron microscopy images show different conformational supramolecular structures (figure 4) [1].

Membrane	Decreasing D_T (%)	Decreasing SO (%)
	REPEATED UF-MF OF WASTEWATER	
A	33	45
S$_1$A	18	9
S$_2$A	34.8	41.2

Figure 4 shows the non-cross-linked membrane A and the cross-linked membrane S2A with the two surfaces: active and posterior. The microscopic images show an advanced degree of asymmetry in the native membranes. The Pall membrane is symmetrical.

Ion exchange resins respond well to demineralisation but do not retain organic matter (table 5). The Pall membrane performs better in reducing D_T and organic matter (table 5).

The indigenous membranes A and the membranes of the series SA reach the degree of potability of the wastewater; however, with repeated UF-MF there is a drastic decrease in the content of organic substances and a better degree of demineralisation.

In order to correct the quality of industrial effluents, the possibility of removing traces of Cu^{2+} by mycelization with sodium lauryl sulfate was also studied. The
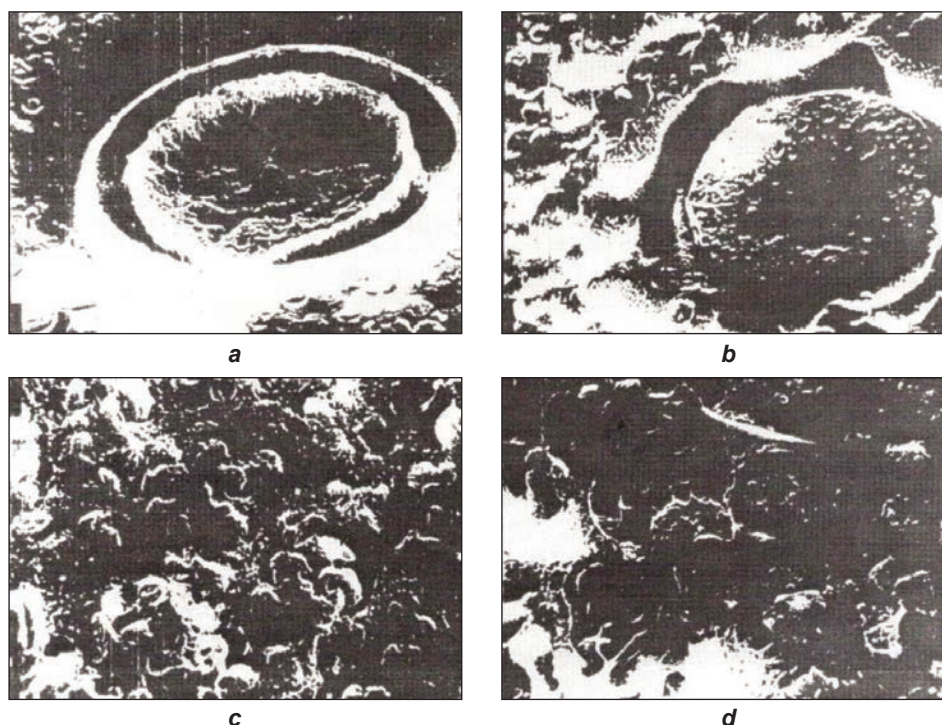
Fig. 4. Scanning electron microscopic images on the non-crosslinked polyurethane membrane A and the polyurethane membrane cross-linked with zeolite S2A:
a – cross-linked membrane, active surface [x1800]; *b* – non-crosslinked membrane, active surface [x1800]; *c* – reticulated membrane, posterior surface [x3000]; *d* – non-crosslinked membrane, posterior surface [×3000]

separation process was based on micellar solubilisation, followed by the well-known ultrafiltration process MEUF (micellar enhanced ultrafiltration), a micellar intensification of ultrafiltration. By using surfactants at a critical micelle concentration where their molecules form micellar associations, this technique has successfully removed both the metal ion and the organic solution from wastewater [27].

CONCLUSIONS

This work reflects the physiognomy of supramolecular chemistry, dynamic chemistry given by the lability of non-covalent interactions. We are dealing with chemical dynamics, and supramolecular chemistry has the possibility of expressing molecular and supramolecular dynamical diversity. The new paradigm is selection through the dynamics of constitutional diversity, which responds to internal pressures and external factors to explain adaptability.

The hydrophilic/hydrophobic, flexible/rigid, amorphous/crystalline, soft/hard scales that occur in the structure of membranes depend on the type of hydrogen bonds and Van der Waals bonds that occur between their micro and macro phases.

Membranes find their application in the textile field by being integrated into the garment structure, which must at all times be a favourable environment for the absorption of moisture and other harmful emanations from the body.

The tests and determinations carried out highlight the properties of the membranes analysed, for which the following is noted:

- Polyurethane membrane I4 has sanogenetic physiological indicators comparable to those of water-proof material.
- The flexible behaviour, shown with high values in the three directions L/T/D, allows extending the use of the polyurethane membrane I4 in the form of composite material for the disposable clothing of the medical personnel.
- The disinfecting properties of polyurethane membranes I3 and I4 are highlighted by the decrease in the total bacterial count in ultrafiltration and microfiltration of drinking water [21, 28, 29].

The textile industry is polluting due to chemical processing. For example, textile raw materials, by-products, technologies, and machinery in the textile industry contain significant pollutants. The proposed membrane technology is innovative and will have real economic significance in the coming years.

Finally, a new purification technique is defined: micro- and ultrafiltration (MF-UF), a technique for the recovery and reuse of wastewater. A and SA series indigenous polyurethane membranes can be used to achieve the degree of potability of wastewater.

To conclude this review of the main applications of membranes produced with original methods, it is emphasised in the textile field that new horizons are opening in supramolecular chemistry [30, 31].

REFERENCES

[1] Bezdadea, M., Olaru, S., *Chimie supramoleculară aplicată – Membrane (Biotehnologie)*, Ed. Oscar Print, Bucharest, 2018

[2] Bezdadea, M., *Polimerizare matricială (replică) – Biotehnologie*, Ed. Științifică și Enciclopedică București, 1987

[3] Bezdadea, M., *Polimerizarea matricială*, Doctoral thesis, Polyethnic Institute of Iași, 1982

[4] Bezdadea, M., *Biomimethics effects during formation of membranes*, In: Roum. Biotechnol Lett., 2006, 11, 4, 2851–2863

[5] Bezdadea, M., *Use of Glycidyls in the Modification of Polyurethane Membrane Strcutures*, In: International Conference Speciality Polymer Supramolecular Aspects of Polymer Synthesis and Polymer Structure, Mainz, Germany, 1991

[6] Bezdadea, M., Savin, A., Ciobanu, G., *Use of glycidyls in the modification of polyurethane membrane structures,* In: Polym. International., 1993, 32, 407, https://doi.org/10.1002/pi.4990320412

[7] Simionescu, C., Bezdadea, M., Patent RO no. 84569, 1984

[8] Bezdadea, M., Grigoriu, G., Patent RO no. 91260, 1987

[9] Neacșu I., Mariana Bezdadea, Rev. Roum. Chim., 1987, 32, 8, 749

[10] Balaban, T.S., Goddard, R., Linke-Schaetzel, M., Lehn J.M., *2-aminopyrimidine directed self-assembly of zinc porphyrins containing bulky 3,5-di-tert-butylphenyl groups*, In: J. Am. Chem. Soc., 2003, 125, 14, 4233-4239, https://doi.org/10.1021/ja029548r

[11] Drahoňovský, D., Lehn, J.M., *Hemiacetals in dynamic covalent chemistry: formation, exchange, selection, and modulation processes*, In: J. Org. Chem., 2009, 74, 21, 8428–8432

[12] Folmer-Andersen, J.F., Lehn, J.M., *Thermoresponsive Dynamers: Thermally Induced, Reversible Chain Elongation of Amphiphilic Poly(acylhydrazones),* In: J. Am. Chem. Soc., 2011, 133, 28, 10966–10973, https://doi.org/10.1021/ja2035909

[13] Hafezi, N., Lehn, J.M., *Adaptation of Dynamic Covalent Systems of Imine Constituents to Medium Change by Component Redistribution under Reversible Phase Separation*, In: J. Am. Chem. Soc., 2012, 134, 30, 12861–12868, https://doi.org/10.1021/ja305379c

[14] Lehn, J.M., *Supramolecular Chemistry – Scope and Perspectives Molecules, Supermolecules, and Molecular Devices (Nobel Lecture)*, In: Angew. Chem., 1988, 100, 91–116

[15] Lehn, J.M., *Cryptates: inclusion complexes of macropolycyclic receptor molecules*, In: Pure Appl. Chem., 1978, 50, 9-10, 871–892, http://dx.doi.org/10.1351/pac197850090871

[16] Lehn, J.M., *Perspectives in Chemistry – Steps towards Complex Matter*, In: Angew. Chem. International, 2013, 52, 10, 2836–2850, https://doi.org/10.1002/anie.201208397

[17] Ul-Islam, S., (Ed.), Butola, B.S., (Ed.), *Advanced Textile Engineering Materials*, Wiley, ISBN: 978-1-119-48785-2, September 2018

[18] Saber, D., Abd El-Aziz, K., *Advanced materials used in wearable health care devices and medical textiles in the battle against coronavirus (COVID-19): A review*, In: Journal of Industrial Textiles, 2021, https://doi.org/10.1177/15280837211041771

[19] Bezdadea, M., Mitu, S., Cârâc, S., *Possibilities of using indigenous polyurethane membranes on special apparel*, In: Industria Textilă, 2004, 55, 4, 263–266

[20] Mitu, S., *Confortul şi funcţiile produselor vestimentare*, Ed. Gh. Asachi, Iasi, 1993

[21] Martinetti, R., Sainctavit, L., L'Industrie Textile, 1997, 1288, 49–52

[22] Moreau J., L'Industrie Textile, 1995, 1264, 59

[23] Martinetti R., Sainetavit L., L'Industrie Textile, 1998, 1300, 46

[24] Ellen McArthur Foundation, *The New Textiles Economy Report*, 2017, Available at: https://ellenmacarthur foundation.org/a-new-textiles-economy [Accesed on November 2020]

[25] Bezdadea, M., Filipescu, F., *The impact of indigenous membranes with dyestuff*, In: Industria Textilă, 2000, 51, 3, 196

[26] Bezdadea, M., Teslariu, M., Tivadar, A., Marin, S., Vârlan, C., *The nonconventional treating of the finishing plant effluents*, In: Industria Textilă, 2003, 54, 1, 36

[27] Zavastin, D.E., Creţescu, I., Bezdadea, M., *Study of separative performances, of a cellulose acetate-polyurethane blend membrane for the treatment of some phenolic aqueous solutions*, In: J. Env. Protect. Ecol., 2012, 13, 2, 497–505

[28] Simionescu, C.I., Bezdadea, M., Chemical Abstracts, 1985, 80, 133908a

[29] Bezdadea, M., Mitu, S., Cârâc, S., *The Study Of New Special Materials Used Against Pathogenic Agents*, In: Industria Textila, 2006, 57, 4, 261–266

[30] Pollack, G.H. (Ed.), Chin, W.-C. (Ed), *Phase Transitions in Cell Biology*, Springer, ISBN: 978-1-4020-8650-2, 2008

[31] Pollack, G.H, Cameraon, I.L., Wheatley, D.N., *Water and the Cell*, Springer, ISBN: 101-4020-4926-9, 2006

Authors:

SABINA OLARU[1], MARIANA BEZDADEA[2]

[1]National Research Development Institute for Textiles and Leather,
16 Lucretiu Patrascanu Street, 030508, Bucharest, Romania

[2]"Gheorghe Asachi" Technical University of Iasi, 56 D. Mangeron Street, 700050, Iasi, Romania

Corresponding author:

SABINA OLARU
e-mail: sabina.olaru@incdtp.ro